# Space Truck DSE 2019

## Group 4

Designing a mission that allows students to perform experiments in space by 2020

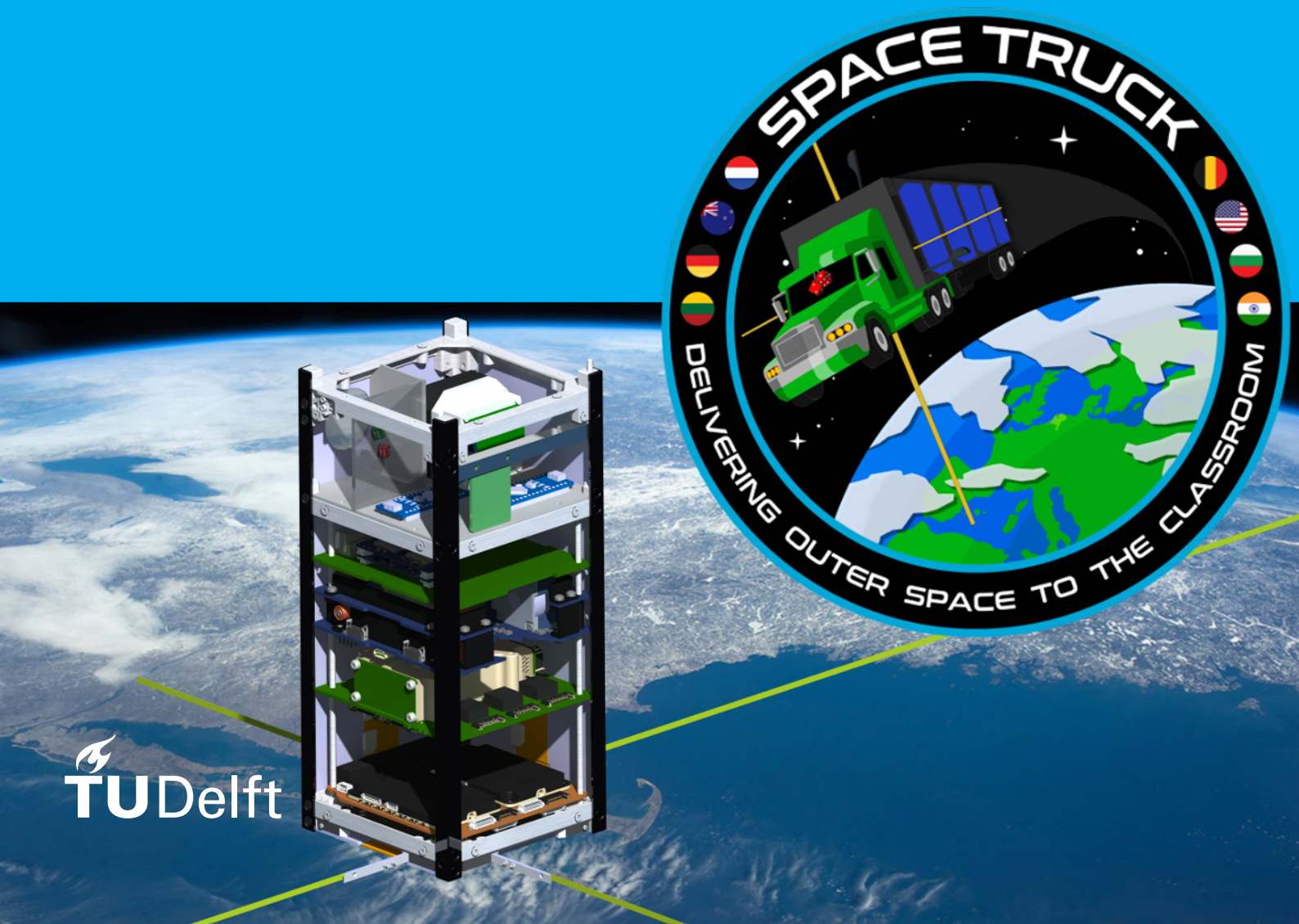


TU Delft

# Space Truck DSE 2019

## Designing a mission that allows students to perform experiments in space by 2020

by

Andrew Spekreijse
Iliyan Kermedchiev
Johan Monster
Klaas Meinke
Mel Costa
Moritz Schwarze
Simonas Stasevičius
Tim Burgers
Tuur Baldewijns

To complete the Design Synthesis Exercise at
the Delft University of Technology, Faculty of Aerospace Engineering
to obtain the degree of Bachelor of Science

# Acknowledgements

The group would like to express their deep gratitude to their tutor, Chris Verhoeven, who has been instrumental in realizing this project. We would also like to thank our coaches Mario Coppola and Diana Olejnik for providing us feedback on our reports and helping us with the vital project management aspect of the project.

The group would also like to extend their gratitude to many industry experts for their patient guidance, enthusiastic encouragement and useful critiques of the design. To begin with, we would like to thank Stefano Speretta for sharing his extensive knowledge on many subsystems from thermal control, to structures and computing. Next we would like to thank Heinz Stoewer for reviewing our design concepts and giving valuable feedback on our mission architecture. Our grateful thanks are also extended to Edwin Hakkenes, for his advice has been very helpful when designing the Computing and Data Handling subsystem, to Prem Sundaramoorthy, whose advice has been very insightful and to Saullo Castro, for his insight regarding the design of the payload. In addition, Sam Spekreijse has been helpful in understanding and selecting the computer bus protocol. We would also like to thank Rob Hamann, Wouter Weggelaar and Bert Monna for providing us feedback on our design.

We would also like to extend our gratitude to the VSV, especially Casper Dek and Didier van der Horst for their help, to Hyperion Technologies for sponsoring this project and Geert Henk Visser for providing us with practical advice on satellite projects, as well as to ISIS for their help and for answering various CubeSat questions.

# 1

# Executive Overview

## Introduction

The Vliegtuigbouwkundige Studievereniging (VSV) 'Leonardo da Vinci' has decided to develop and build a CubeSat in preparation for its 75th anniversary in 2020. The main goal of this ambitious project is to give school children in the Netherlands access to space. The CubeSat is to be designed and tested by students from the TU Delft and shall be ultra-reliable in case of payload failure, facilitating two payloads. One payload will be designed for primary school children and the other for high school students. In order to achieve compatibility between the payload and the satellite bus, an interface is implemented based on the plug-and-play concept yielding a system that is able to handle multiple types of payloads. Due to its high payload variance and robustness, the project is given the name "Space Truck". The mission need statement based on the VSV is: *"The VSV plans to increase the general enthusiasm for technology and space travel among children in the Netherlands"* [1]. The DSE part of the exercise consists of performing the preliminary design of the satellite and its mission objective in an academic setting. The project objective statement is formulated as: *"Design a mission that allows students to perform experiments in space by 2020."*

## Market Analysis

The primary objective of the mission is to bring space to the class rooms and thus school involvement is a major concern. In order to participate, a school has to offer the NLT module, as well as possess a FunCube Dongle Pro+ and a tabletop antenna. The equipment is a one time investment in the range of 150 Euros.

After conducting an extensive market research it can be found that the concept of modularity is not fully exploited and that there is a market share which can be taken over. However, due to a tight deadline the concept of modularity is only partially applied and it should be further developed in the following generations. Detailed information can be found in chapter 3.

The Return On Investment (ROI) for this project is educational. Research shows that approximately 114,992 school-going children will get benefit from this project. With total project costs around €426,320 , the cost per user is €3.91. This cost would reduce to €1.37 per user if this design is reused for a new satellite, which is highly likely. For context, the weighted average amount the Dutch Government spends on primary and secondary school education per year is €9,811 per student.

## Design Concepts

When the design of the Space Truck began, three concepts were established with each being optimized for a different payload configuration. The first configuration focuses on simplicity of the bus hosting two low power payloads. The second configuration strives for high payload power hosting 2 high-power or 4 low-power payloads. Finally, the third configuration aims for high reliability by introducing redundancies, enabling 2 medium-power payloads.

## Detailed Design Overview

[1] https://vsv-satellite.com/?page_id=52&lang=en [Retrieved on 22.05.2019]

### Astrodynamics

The Space Truck is designed as a multipurpose bus suited for many missions in Low Earth Orbit. As a starting point for design, an orbit range is defined. The Space Truck is designed to be suitable for all orbits within this range.

There are two limiting factors for the orbit range. First, to limit in-orbit lifetime to a maximum of 25 years, as requested by the IADC space debris mitigation guidelines, the maximum orbit altitude is reduced to 600 km. Secondly, in order for a Space Truck to be operable from the Netherlands, the inclination must be enough such that the orbit passes overhead. As such, the updated orbit range for which the Space Truck is designed is from 300 to 600 km altitude, with orbit inclinations between 52 and 128 degrees.

For the defined orbit range, the appropriate orbital parameters are calculated. Their maximum and minimum values are identified, so that various subsystems of the spacecraft can be sized based on the worst case scenario. This data can be found in Table 5.6. In addition, the sensitivity of altitude, inclination, and launch year to the orbital lifetime are investigated. Delaying the launch date will lead to a shorter orbital lifetime. A more in-depth discussion can be found in chapter 5.

### Structures

The structure that is chosen for the satellite is the ISIS 2U Long Stack. This structure was chosen because the manufacturer is located in Delft, it is easy to access different subsystems during and after assembly and the structure is a good fit for the Space Truck concept since it has 1.5U volume for the bus subsystems and 0.5U volume for the payload. 0.5 U is considered sufficient for student built experiments that can fly in the Space Truck. The payload being designed for this iteration of the satellite is easily able to fit. Any additional structural elements must be made of Aluminium 7075 or 6061-T6 since these materials have a similar thermal expansion coefficient to the deployer that the satellite will be inside during launch.

### Payload

The payload for the satellite will consist of two different modules. Both modules will be connected to the OBC through an Arduino Nano, such that the Plug and Play concept is applied. One of the modules will be used to answer questions that primary school children asked during a contest which was held among multiple primary schools across The Netherlands. The second payload will provide additional data for a module in a high school course called ”Earth Observation & Satellites”, in which students analyse satellite data. The primary school module will be inspired by the question: ”Can you play rock paper scissors in space?”. The idea of the concept that is developed is to take a picture of two floating dice, which would have pictures of a rock, paper or scissors on its sides, with a window in the background facing the Earth. In this way children can play a game with the satellite since the position of the dice will change over time. The dice will be locked up in a compartment such that they will always stay in the field of view of the camera. More details about the primary school module can be found in section 9.3. The high school module will consist of a commercial off-the-shelf long wave infrared camera. This camera has been chosen because the existing satellite that provides data for the high school course does not supply data on temperature. The camera is relatively simple to implement since commercial off-the-shelf options are available. More details on the high school payload module are given in section 9.4.

### Telemetry

The communications subsystem provides the means to ”talk” or exchange information with the satellite. It is done through modulated radio waves. The on-board communications hardware consists of two Gomspace AX100 transceivers and an ISIS crossed VHF/UHF dipole antenna. One transceiver is tuned to UHF amateur frequency band, the other to VHF. The UHF transceiver is used for transmission only and the VHF transceiver is always receiving. This dual configuration allows for a full-duplex link, whereas a single AX100 is capable of half-duplex only. This is done mainly to have ceaseless reception capability, which ensures the spacecraft can always be controlled. The commands will be sent from the TU Delft ground station on the amateur VHF band. Telemetry can be received with the FunCube Dongle Pro+ on the amateur

UHF frequencies. The use of amateur radio bands will be justified by publishing the telemetry decoding instructions online and also possibly implementing a digipeater to be used by radio amateurs. The telemetry data packets will adhere to the Cubesat Space Protocol and will implement multiple data integrity methods. A detailed description of the physical link and data packets can be found in chapter 10.

### Electric Power System

The electric power system provides the necessary power to all the other systems. Due to the fact that the orbit is unknown and the payload module aims to be modular, the power available to the system is highly likely to be a limiting factor. The most viable power generating source is solar cells. In order to produce a sufficient amount power with non-deployable 2U-size solar panels, the satellite should be oriented such that two of the side panels are illuminated by the Sun. Furthermore, if the bottom in addition to the side panels, is illuminated at an optimal angle, available power increases by 5%. To account for the incidence angle, the effective area is calculated using the principle of superposition. The optimal angle such that the solar irradiance illuminates only the side panels is at an incidence angle ($\xi$) of 45°. Furthermore, in order for the Sun to also illuminate the bottom panel, the additional incidence angle is $\psi = 19.47°$ for the side panels and $90° - \psi$ for the bottom panel. Taking into account life and inherent degradation, and the overall EPS efficiency and assuming a worst case orbit at 300 km results in the mean orbit power generated to be 2.97 W. The altitude of 300 km is the worst case since it has the greatest eclipse time as a ratio of the full orbital period for the range of orbits given in chapter 5. The power module is selected so that it can facilitate the solar panels as well as provide the necessary output voltage and current. In addition, the power module also consists of a 32 Wh battery back, which can provide up to 20 W at a nominal voltage of 5 V. More detailed analysis can be found in chapter 11.

### Attitude Determination and Control

The Attitude Determination and Control System stabilizes and points the spacecraft to a certain target location. The considered configuration for this design is the Hyperion iADCS 200 including a inertial measurement unit (IMU), a 3-axis magnetometer (MTM), 3 magnetotorquers (MTQ), 3 reaction wheels (RW) and 6 sun sensors. The MTQs can be utilized for coarse pointing, detumbling, momentum dumping and stabilization while the RWs provide fine pointing, higher turn rates and stabilization. In chapter 14 a first order estimate is provided regarding the disturbance torque magnitudes for different heights and the effective performance of the considered MTQs and RWs. The smallest available RWs were found to provide sufficient slew rates to turn the CubeSat 180° in about 20 s around the largest axis of inertia. Moreover it provides limited stabilization for the satellite of at least a few minutes per orbit. The ADCS shall be able to provide 5 operational modes: idle condition, detumbling, target-pointing, sun-pointing and momentum dumping. The pointing modes can be activated and deactivated by the OBC, while detumbling and momentum dumping are performed by the ADCS automatically. A more detailed description and analysis can be found in chapter 14.

### Thermal Control

The thermal control system is responsible for maintaining the temperature of the spacecraft's components within their operational ranges. By looking at the operational temperature ranges of the different components and applying a 10 $°C$ margin, a design range from 0 $°C$ to 30 $°C$ is established. A simplified thermal model is made that simulates the spacecraft orbiting the earth. The model assumes that the spacecraft has a uniform temperature. This model is then used to determine what coatings are required to maintain the spacecraft's temperature. It was found that if all sides of the spacecraft are covered with solar cells except for the area of the payload aperture, that the temperature can be maintained passively by applying aluminized kapton tape to the rest of the exposed surfaces. The resulting temperature over the given range of orbits then ranges from -6.33 $°C$ to 31.5 $°C$. Although this is outside the design range, the assumptions made in the thermal model are conservative and the temperatures that will actually be experienced are likely to be less extreme due to the fact that during the simulation the specific heat capacity is estimated to be a lower value, which results in greater thermal

variation due to the lesser thermal inertia. Furthermore, the design limits are driven by two components in particular; the ADCS and the ArduCam. By including electrical heaters to make sure components do not undercool and heat sinks to make sure components do not overheat, the temperature requirements for all components can be met. More details on the thermal design can be found in chapter 12.

### Command and Data Handling

The Command and data Handling (CDH) system is responsible for the communication of systems on the spacecraft as well as scheduling tasks and processing information received/generated by the spacecraft. the On Board Computer (OBC) is the main hub which facilitates system communication. The main communication bus protocol used between all systems and the OBC is UART using a RS-485 electrical standard. Not all systems support RS-485, therefore RS-232, UART is used for one system and I2C is used for antenna deployment. The OBC used is the CP400.85 Processing Platform, sponsored by Hyperion Technologies. This OBC supports a Linux based operating system, drawing typically 0.55W and has a ARMv7 500MHz processor with 512MB of volatile memory storage and up to 7.5GB of non-volatile radiation protected storage. Through its companion board, up to seven UART connections are supported, ample for this spacecraft.

### System Integration

For the fully integrated system, it is found that the chosen components can be accommodated in the mass and height budget. The power budget of the Space Truck takes into account the basic functionality which consists of heater operation during eclipse, OBC operation and ADCS sun pointing. On top of this, the power budget takes into account the power required for three attitude changes. This is enough to point the spacecraft towards the sun when it comes out of the eclipse as well as point the spacecraft towards a target and back. The power budget also allows for 15 minutes of transmission. The budget then has sufficient power to allow the payload to use 500 $mWh$ per orbit. The more detailed spacecraft characteristics can be found in subsection 15.1.2.

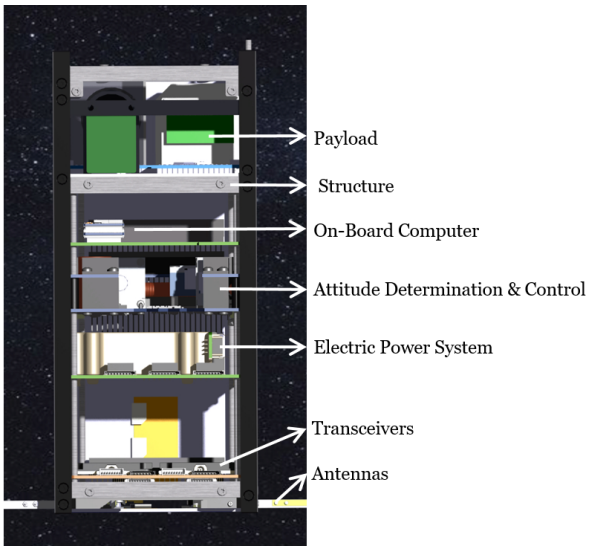


Figure 1.1: The subsystems of the Space Truck

The functionality of the spacecraft has been divided into four main modes; initialization mode, idle mode, nominal mode and safe mode. On power up, all the spacecraft systems go into initialization mode and go through a routine to get them ready for operation, including connecting to the OBC. Once the subsystems have completed there initialization procedure, they go into idle mode. In idle mode they maintain there basic functioning like maintaining temperature and sending housekeeping data. When ground commands are received or when tasks are scheduled, the corresponding commands get send to the connected subsystems. If

a severe error is detected, the spacecraft will go into safe mode where it sends down its status and waits for ground input.

## Risk Management Overview

Risk management is a evolving process as seen in chapter 16, which begins with identification of potential risks, assessment and finally planning mitigation processes to avoid them. The approach towards risk management, in terms of the various steps taken and methods used to identify and manage risk are discussed in section 16.1. First, two studies about in-orbit spacecraft and CubeSat failures are analysed in section 16.2. This gives insights into common failure modes, subsystems and components with high failure rate. This helped identify critical subsystems, components and parts prone to failure. It was found that gyroscopes, solar arrays, control processors and payload modules have higher failure rate than other components. It also identifies subsystem failures which have higher probability of leading to Loss Of Mission (LOM). It was found that failures in power subsystem, structure and payload module have a higher chance of leading to LOM. From the study about CubeSat failures, it was found that about 45% of CubeSat could not be contacted after deployment. This makes it hard to identify the type of failure that occurred leading to an unresponsive CubeSat. It was also found in this study that most of these non-contacted CubeSats were university projects with low budgets, tight time schedule and inadequate system level testing. In section 16.3, Fault tree analysis (FTA) is used to identify faults and failures that could occur in components and subsystems which contribute to loss of mission (LOM). The failures are scored in terms of likelihood (L) and consequence (C) to arrive at the risk score which is the multiple of the two. The rationale for the L and C scores are explained for each failure. For each risk, a mitigation idea or strategy is put forth. It was found that some initial design choices or ideas had to be changed as the new risks were identified. The half-duplex TTC system was changed to full-duplex system so as to not risk single point of failure (SPOF). The choice of non-deployable solar panels was also made to avoid the risk of LOM due to deployment failure. Some other risks with high scores, found in the EPS, CDH and payload module were evaluated and mitigated. All risks are then re-evaluated in terms of their likelihood and consequence, after risk-mitigation and new risk scores were defined. The risk map and the post-mitigation risk map as seen in Figure 16.9 depict how the risk changed as a result of mitigation strategy.

## Sustainable Development Strategy

The Sustainable Development Strategy used is reflected in the design in four different ways. First, the product itself is designed to be both a versatile and reusable platform. This is because it can operate in a variety of different LEO orbits, and accommodate many payloads, both on a software and a hardware level. Secondly, the sustainability aspect is reflected in the selection of commercially off-the-shelf (COTS) components. Thirdly, it should be considered to offset the emmisions caused by the launch vehicle. Finally, sustainability can be addressed by managing the orbital lifetime of the satellite such that it will not become space debris. This affects the design in two ways: First, the design space is shrunk in order to ensure that the Space Truck deorbits within 25 years. Secondly, a de-orbiting mode is included in the software, which reduces the orbital lifetime by decreasing the satellite's ballistic coefficient. An analysis of the de-orbiting mode's performance can be found in subsection 5.4.4.

## Operations and Logistics

In chapter 19, the logistics of the Space Truck concept are investigated. It shows the Space Truck market on a higher level in the form of a flow diagram. Logistics of a Space Truck mission is also shown in this chapter. It shows the stages of the Space Truck after orbit insertion to end of life.

## Future Development Plan

The period after the DSE is split up into three phases: Transition, Detailed Design and Test & Manufacturing.

In the transition phase, the design will be checked by a group of industry experts that will give feedback on the design from the DSE. Next to this, a new team is set up to work on this project in the academic year 2019/20. The new team will consist of a core team as well as a support team. Additionally, internships are arranged at some of the sponsoring companies during which several parts of the detailed design will be done. In section 21.1, the transitional phase is described in more detail.

Two of the most important parts to be completed in the detailed design phase are the writing of the software and designing the Primary School payload module. The software that need to be written is mostly for the OBC and the communications system. The structural parts of the Primary School module need to be further analysed and additional models need to be made. An in-depth description of detailed design phase is provided in section 21.2.

In section 21.3 the manufacturing, assembly, integration and test (MAIT) phase is explained. At the beginning, it can be split into two separate activities that can run in parallel, prototyping and testing the payload and performing flat bed testing on the bus subsystems. The payload must be thoroughly designed and tested since none of the components are commercial off the shelf, validated components. In order to do this a mock structure is constructed and the payload is fully assembled inside and several standard tests are performed. These issues are not critical for the bus subsystems such as the antenna, ADCS and on-board computer. What is considered more critical with these systems is interfacing, the field in which most university built satellites fail. In order to mitigate this risk, the subsystems should be electronically connected and tests should be performed and operations simulated to discover possible glitches.

Once the payload and bus have separately been verified to function, they can be brought together for a system-wide test. First, a flat-bed test should be performed and finally the spacecraft can be assembled by sliding the components on the stack rod, assembling the payload in the payload bay and attaching the antennas and solar panels. Finally, the fully integrated satellite must undergo a series of tests including a mechanical shock test, a vibration test, a thermal cycling test, a vacuum test and a radiation test. It is still to be decided by the VSV whether a separate qualification and flight module will be built.

## Conclusion

This report is a product of a two-fold mission. First, it is the VSV's plan to launch an educational and commemorative CubeSat satellite into space in 2020, with the goal of *"increasing the general enthusiasm for technology and space travel among children"*. On the other hand, the mission of this DSE is a subset of VSV's mission, and concerns the preliminary design of this satellite and its payloads. The project objective statement of this DSE is to *"design a mission that allows students to perform experiments in space by 2020"*. A secondary objective of this project is to design a satellite bus that is both versatile and robust, suited for multiple LEO missions.

The outcome of this design phase aligns with the DSE project objective. The payload module implementation side is made accessible to students by its use of common protocols and hardware, and the overall design of the bus is kept simple, to make sure the development can be realized in time. Regarding the VSV's mission, the Space Truck design is versatile, paving the way for future student CubeSat missions on the same platform, beyond the VSV's launch next year. This accessibility serves to involve children and young students with applications in space, hoping to nurture an enthusiasm for space-related technology and bringing outer space closer to the classroom than ever before.

# Contents


1 Executive Overview 2

2 Introduction 15

Part 1: Project Definition

3 Market Analysis 17
- 3.1 Education . . . 17
- 3.2 Publicity . . . 17
- 3.3 Modularity . . . 18
- 3.4 Implications on Final Design . . . 18
- 3.5 Return On Investment . . . 18

4 Requirements 20

Part 2: Design

5 Astrodynamics 27
- 5.1 Orbit Generalisation . . . 27
- 5.2 Orbit Characteristics . . . 28
- 5.3 First Order Lifetime Estimations . . . 29
- 5.4 GMAT Lifetime Estimation . . . 30
- 5.5 Orbit Generalisation Revisited . . . 34
- 5.6 Launch Vehicle Considerations . . . 35

6 Design Concepts 36
- 6.1 Method . . . 36
- 6.2 Concepts . . . 36

7 Trade-Off Summary 40
- 7.1 Trade-Off Method . . . 40
- 7.2 Trade-Off Criteria and Weights . . . 40
- 7.3 Trade-Off Results . . . 41
- 7.4 Trade-Off Sensitivity . . . 42

8 Structures 44
- 8.1 Primary Structure . . . 44
- 8.2 Verification . . . 44
- 8.3 Material Characteristics . . . 45
- 8.4 Payload Adapter Plate . . . 45

9 Payload 47
- 9.1 Payload Restrictions . . . 47
- 9.2 Payload-OBC Connection . . . 48
- 9.3 Primary School Payload . . . 48
- 9.4 High School Payload . . . 56
- 9.5 Final Design Payload Module . . . 57

10 Communications 59
- 10.1 Physical Layer . . . 59
- 10.2 Data Link Layer . . . 63
- 10.3 Transmission Schedule . . . 65
- 10.4 Verification . . . 66

11 Electrical Power System 67
11.1 Power Sources . . . 67
11.2 Power Module . . . 69
11.3 Electric Block Diagram . . . 69
11.4 Verification . . . 70
11.5 Fail-Safe . . . 71

12 Thermal Control System 72
12.1 Thermal Requirements . . . 72
12.2 Preliminary Thermal Model . . . 72
12.3 Preliminary Results for the Thermal System . . . 75
12.4 Final Thermal Control System Design . . . 77

13 Command and Data Handling 78
13.1 Requirements for the System . . . 78
13.2 OBC Options . . . 78
13.3 Payload Controller Selection . . . 79
13.4 Protocol Selection . . . 81
13.5 Intra-Spacecraft Communications . . . 82
13.6 Software . . . 82
13.7 Sensitivity Analysis . . . 82

14 Attitude Determination and Control 84
14.1 Concepts and Hyperion Sponsorship . . . 84
14.2 Trade-Off . . . 84
14.3 Control Behaviour and Validation . . . 85
14.4 Control Operations for ADCS . . . 90
14.5 Sensitivity Analysis . . . 90

15 System Integration 92
15.1 System Characteristics . . . 92
15.2 Spacecraft Layout . . . 94
15.3 Functional Flow Diagram . . . 95
15.4 Functional Breakdown Structure . . . 102

Part 3: Design Evaluation

16 Risk Management 105
16.1 Approach . . . 105
16.2 Spacecraft and CubeSat Failure Statistics . . . 106
16.3 Risk Analysis and Mitigation . . . 108
16.4 Risk Map . . . 114

17 Compliance Matrix 115

18 Reliability, Availability and Safety Characteristics 118
18.1 Reliability . . . 118
18.2 Availability . . . 118
18.3 Safety . . . 118

19 Operations and Logistics 120

20 Sustainable Development Strategy 123

Part 4: Post DSE

21 Future Development Plan 125
21.1 Project Design and Development Logic . . . 125
21.2 Detailed Design Phase . . . 127
21.3 Manufacturing, Assembly, Integration and Test . . . 129

22 Cost Breakdown 136
23 Conclusion 137
Bibliography 138
A Appendix A: Engineering Drawings 141
B Appendix B: GMAT Simulation Input Parameters 142
C Appendix C: Gantt Chart 143
D Appendix D: Individual Contributions 146

# List of Symbols

## List of Greek Symbols

| Symbol | Parameter | Unit |
|---|---|---|
| $\alpha$ | Absorptivity | - |
| $\xi$ | Superimposed incidence angle of solar arrays on the 2 side panels | $deg$ |
| $\psi$ | Incidence angle of solar arrays on projection of the side panels | $deg$ |
| $\beta_{eclipse}$ | Eclipse angle | $deg$ |
| $\varepsilon$ | Satellite elevation angle | $deg$ |
| $\lambda$ | Earth Latitude | $deg$ |
| $\mu$ | Earth Gravity constant | $(k)m^3 \cdot s^{-2}$ |
| $\rho$ | (Atmospheric) Density | $kg \cdot m^{-3}$ |
| $\tau$ | Orbital period | $min$ |
| $\tau_{day}$ | Time in sunlight during one orbital period | $min$ |
| $\tau_{eclipse}$ | Time in eclipse during one orbital period | $min$ |
| $\tau_{pass}$ | Time the satellite is in view during one passing | $min$ |
| $\phi$ | Geocentric semi-angle | $rad$ |
| $\omega$ | Angular velocity | $rpm$ |
| $\dot{\omega}$ | Angular acceleration | $rad \cdot s^{-2}$ |
| $\omega_{ES}$ | Orbital angular velocity | $rad \cdot s^{-1}$ |
| $\omega_{11}$ | Fundamental natural frequency | $rad \cdot s^{-1}$ |

## List of Latin Symbols

| Symbol | Parameter | Unit |
|---|---|---|
| $A$ | Area | $m^2$ |
| $A_{ref}$ | Reference area | $m^2$ |
| $a$ | Albedo coefficient | $-$ |
| $a$ | Length of the sides of a square plate | $m$ |
| $a_{drag}$ | Atmospheric drag acceleration | $m \cdot s^{-2}$ |
| $B$ | Ballistic Coefficient | $kg \cdot m^{-2}$ |
| $C$ | Heat capacity | $J \cdot kg^{-1} \cdot K^{-1}$ |
| $C_D$ | Drag coefficient | $[-]$ |
| $C_{mn}$ | Vibrational Amplitude | $m$ |
| $C_R$ | Coefficient of reflectivity | $[-]$ |
| $c$ | Circle of Confusion (CoC) | $mm$ |
| $c_m$ | Center of mass | $m$ |
| $c_p$ | Center of pressure | $m$ |
| $D$ | Electro-magnetic Dipole Moment | $A \cdot m^2$ |
| $D$ | Plate Stiffness | $J \cdot m^2$ |
| $D_f$ | Furthest distance of acceptable sharpness | $mm$ |
| $D_n$ | Nearest distance of acceptable sharpness | $mm$ |
| $d$ | Distance between antennas | $m$ |
| $E$ | Young's modulus | $N \cdot m^{-2}$ |
| $E_b$ | Received energy per bit | $J$ |
| $F$ | Receiver noise | $dB$ |
| $f$ | Frequency | $m$ |
| $f$ | Focal distance | $mm$ |

| Symbol | Parameter | Unit |
|---|---|---|
| $f_{n_{long}}$ | Natural frequency in longitudinal direction | $Hz$ |
| $f_{n_{lat}}$ | Natural frequency in lateral direction | $Hz$ |
| $G$ | Gravitational constant | $m^3 \cdot kg^{-1} \cdot s^{-2}$ |
| $G_a$ | Albedo flux | $W \cdot m^{-2}$ |
| $G_r$ | Receiving antenna gain | $dB$ |
| $G_s$ | Direct solar flux | $W \cdot m^{-2}$ |
| $G_t$ | Transmitting antenna gain | $dB$ |
| $h$ | Orbit altitude from earth's surface | $km$ |
| $h$ | Thickness of a square plate | $m$ |
| $H$ | Hyperfocal distance | $mm$ |
| $I$ | Geometric moment of inertia | $m^4$ |
| $I_{x,y,z}$ | Mass moment of inertia along respective axis | $kg \cdot m^2$ |
| $i$ | Orbit inclination angle | $deg$ |
| $K_{max}$ | Maximum kinetic energy | $J$ |
| $k$ | Boltzmann constant | $W \cdot Hz^{-1} \cdot K^{-1}$ |
| $L$ | Length | $m$ |
| $L_a$ | Transmission path loss | $dB$ |
| $L_l$ | Transmitting circuit loss | $dB$ |
| $L_{po}$ | Polarization mismatch loss | $dB$ |
| $L_{pr}$ | Receiving antenna pointing loss | $dB$ |
| $L_{pt}$ | Transmitting antenna pointing loss | $dB$ |
| $L_r$ | Reception feeder loss | $dB$ |
| $L_s$ | Free-space loss | $dB$ |
| $M$ | Earth Magnetic Field Constant | $T \cdot m^3$ |
| $M_E$ | Earth Mass | $kg$ |
| $m$ | Mass | $kg$ |
| $N$ | Aperture Size (F-number) | $-$ |
| $N_0$ | Noise spectral density | $W \cdot Hz^{-1}$ |
| $P$ | Signal power | $W$ |
| $q_I$ | IR radiation | $W \cdot m^{-2}$ |
| $Q$ | Net emitted heat | $W$ |
| $Q_{internal}$ | Internally dissipated heat | $W$ |
| $R$ | Orbit radius | $km$ |
| $R_E$ | Radius of earth | $km$ |
| $R_b$ | Bit rate | $bit \cdot s^{-1}$ |
| $r_{orbit}$ | Orbit radius | $km$ |
| $s$ | Focus Distance | $mm$ |
| $s$ | Slant range | $km$ |
| $T$ | Torque | $N \cdot m$ |
| $T_a$ | Disturbance torque due to aerodynamic drag | $N \cdot m$ |
| $T_m$ | Disturbance torque due to magnetic flux | $N \cdot m$ |
| $T_o$ | Reference noise temperature | $K$ |
| $T_r$ | Amplifier noise temperature | $K$ |
| $T_s$ | System noise temperature | $K$ |
| $V_{circ}$ | Orbital velocity(circular orbit) | $m \cdot s^{-1}$ |
| $W(x, y)$ | Shape Function | $m$ |

# List of Abbreviations

| Abbreviation | Meaning |
|---|---|
| ADCS | Attitude Determination and Control System |
| AOCS | Attitude and Orbital Control System |
| ASM | Attached Sync Marker |
| BER | Bit error rate |
| bps | Bits per second |
| CAD | Computer Aided Design |
| CAN | Controller Area Network |
| CCSDS | Consultative Committee for Space Data Systems |
| CDH | Command and Data Handling |
| CoC | Circle of Confusion |
| Comms | Communication system |
| COPUOS | Commitee of the Peaceful Uses of Outer Space |
| COTS | Commercial-Off-The-Shelf |
| CRC | Cyclic Redundancy Check |
| CS | Spacecraft |
| CSP | Cubesat Space Protocol |
| DOD | Depth-of-Discharge |
| DoF | Depth of Field |
| DSE | Design Synthesis Exercise |
| EM | Electromagnetic |
| EMF | Earth Magnetic Field |
| EoM | End of Mission |
| EPS | Electric Power System |
| ESA | European Space Agency |
| FEC | Forward Error Correction |
| FoV | Field of View |
| FR4 | Flame Retardant 4 |
| FTA | Fault Tree Analysis |
| GMAT | General Mission Analysis Tool |
| GMSK | Gaussian Minimum Shift Keying |
| GPS | Global Positioning System |
| HMAC | Hash-based Message Authentication Code |
| IADC | Inter-Agency Space Debris Coordination Committee |
| IARU | International Amateur Radio Union |
| IGRF | International Geomagentic Reference Field |
| IR | Infrared Radiation |
| ITU | International Telecommunications Union |
| I2C | Inter Integrated Circuit |
| LEO | Low Earth Orbit |
| LHCP | Left Hand Circular Polarization |
| LOM | Loss Of Mission |
| LOX | Liquid Oxygen |
| MAIT | Manufacturing, Assembly, Integration and Test |
| MMOI | Mass Moment of Inertia |
| MTQ | Magnetotorquer |
| NTR | Dutch Public Broadcaster |
| NTL | Nature, Technic and Life (High School Course) |

| Abbreviation | Meaning |
|---|---|
| OBC | On-Board Computer |
| OOSA | Office for Outer Space Affairs |
| OS | Operating System |
| PA | Pointing Accuracy |
| PCB | Printed Circuit Board |
| PK | Pointing Knowledge |
| PnP | Plug and Play |
| RAM | Random-Access Memory |
| RDP | Reliable Data Protocol |
| RF | Radio Frequency |
| RHCP | Right Hand Circular Polarization |
| ROI | Return On Investment |
| RS | Recommended Standard |
| RS | ReedSolomon |
| RW | Reaction Wheels |
| RTOS | Real-Time Operating System |
| SDRAM | Synchronous Dynamic Random-Access Memory |
| SMA | SubMiniature version A |
| SMAD | Space Missions Analysis and Design |
| SNR | Signal to noise ratio |
| SPI | Serial Peripheral Interface |
| SRP | Solar Radiation Pressure |
| SSA | Side-side-angle |
| STR | Star Tracker |
| TRL | Technology Readiness Level |
| TTC | Telemetry, Tracking and Control |
| TU | Technical University |
| UHF | Ultra High Frequency |
| URCB | Ultra Reliable CubeSat Bus |
| USB | Universal Serial Bus |
| UART | Universal Asynchronous Receiver-Transmitter |
| VHF | Very High Frequency |
| VSV | "Vliegtuigbouwkundige studievereniging", Study society of Aerospace Engineering |
| WBS | Work Breakdown Structure |
| WFD | Work Flow Diagram |
| XTEA | eXtended TEA (Tiny Encryption Algorithm) |

# 2
# Introduction

2020 will be the 75$^{th}$ anniversary of the "Vliegtuigbouwkundige Studie-Vereniging" (VSV) 'Leonardo da Vinci'. The VSV is the study association of all aerospace engineering students at the Faculty of Aerospace Engineering (Lucht- en Ruimtevaarttechniek) at Delft University of Technology (TU Delft). To celebrate its 15$^{th}$ Lustrum, students came up with the idea to launch a satellite to celebrate the occasion.

## Project Context

TU Delft has as of the time of publication, sent two satellites into space, namely Delfi-C3 and Delfi-n3Xt, two 3U CubeSats as the first two satellites designed and built by Dutch universities. The next satellite expected to launch is Delfi-PQ, a 3U PocketSat. All these satellites are unique and testing/demonstrating something which was uncommon during their conception. A CubeSat designed, built and tested by students is no longer unique. As a result, the idea for this satellite is to be the first satellite that brings the ideas of school children to space. For this reason, the main goal of this project is *"increasing the general enthusiasm for technology and space travel among children"*[1]. Moreover, this satellite will be designed so the spacecraft bus can easily allow different payloads to be attached, allowing for shcool children, students and researchers to put their ideas in space without having to design, develop and test a full spacecraft. The satellite, planned for 2020, will contain the following two payload modules:

- One payload will contain an experiment that will answer a question asked by primary school pupils.
- The other payload will contain an experiment whose data high school students can analyse and learn from.

This is a an ambitious project to finalise before the end of 2020. The Dutch Space Industry has become highly involved in helping realise this project's completion through sponsoring of hardware, providing technical experience and testing facilities. This report is the sum of the work done over nine weeks by a group of nine students, creating the top level design for this CubeSat. This work was done within the framework of the final year project, the Design Synthesis Exercise (DSE) required to obtain the BSc. in Aerospace Engineering from TU Delft.

## Project Objectives

Therefore, the work presented in this report majorly concerns the preliminary design of the satellite bus, and the two accompanying payloads for the VSV's mission. This report's authors are acting as contractors to the VSV and their main objective is to make the design suitable to their requirements. As such, the project objective statement of this DSE is: *"Design a mission that allows students to perform experiments in space by 2020"*.

A subset of this objective was to build the satellite such that it would not only be able to perform this mission, but would be versatile enough to be an Ultra-Reliable CubeSat Bus (URCB). This URCB would then be able to perform many missions in Low Earth Orbit with a variety of payloads. Thus, a goal of this design is to be flexible and modular, such that the CubeSat bus may be used in the future for different payloads.

[1] `https://vsv-satellite.com/` [Retrieved on 20-06-2019]

## Report Structure

The report can be separated in the following main parts, the first part (chapters 3 through 6) provide an overview on the project definition in which the project objectives, market analysis and the requirements are discussed. Chapters 6 through 16 are concerned with detailed design of the satellite and the different subsystems. Chapter 16 provides an overview of the final design. In the third part (chapter 17 through 21), the design will be evaluated and the sustainable development strategy is presented. In the consecutive part (chapters 22 and 23), the future development plan for after the DSE and the financial breakdown of the project are discussed. In the last chapter, the final conclusions are drawn.

# 3
# Market Analysis

This chapter consists of the market analysis of the Space Truck project. The objective of the chapter is to define and establish the market environment for the services that the satellite can provide. The environment is derived from the main stakeholder: VSV 'Leonardo da Vinci', and its objective for the project. Unlike ordinary analysis, where the competitive cost, the volume of the market and the future markets are inspected, this analysis focuses on the implications of the market on the final design and the project in general. Furthermore, a cost breakdown is done for the project and can be found in chapter 22.

The first section of the chapter concerns the involvement of schools. In the next section, the publicity and media coverage plan of the VSV are discussed. The next section discusses the concept of modularity in the design and the long run advantages that come with it. Following there is a section about the pros and cons of having system sponsored at such early design stages as well as the effect that they have on the design. The last section discusses in detail the return on investment.

## 3.1. Education

The primary objective of the mission is to bring space to the classrooms, or in other words to educate. Therefore, involving schools should be a major concern. It would be simple for schools to participate in the project since every high school which offers the NLT module should be able to join the project. The VSV has provided a link[1] which displays that more than 100 schools would be able to participate in the project, provided they have a FunCube dongle pro plus and a tabletop antenna. The cost of the equipment is affordable as it is a one time investment in the range of 150 euro, which can be covered by the budget of the NLT module. All the information that is needed such as the payload manual and the manual to set up the equipment will be made available online on a website. In addition, every radio amateur would be able to receive the satellite data, provided the fact that the satellite transmits when they are in range.

## 3.2. Publicity

Publicity of the project is instrumental for its success. Achieving good media coverage is essential as the VSV's objective is to get every component of the satellite sponsored and publicity would attract potential sponsors. The VSV has several strategies to achieve publicity and media coverage. Currently they are relying on meetings with companies and the DSE Symposium. In the later stages they are planning to create media events for every milestone of the project such as for the design conclusion, testing, shipping to the launcher, launch, deployment and operational life. In addition, they are planning to contact the media outlets TU Delta, the NTR, "het Klokhuis" and "het Jeugdjournaal". Furthermore, a future plan is to use professionals to raise awareness and attract media attention to the project.

Publicity is also one of the main reasons for companies like ISIS and Hyperion to sponsor components for the project. In addition. the payload ideas are provided by primary and high school students, as well as the fact that the actual mission objective is to provide data which will be used in schools for teaching. The project is highly focused on education and therefore it has potential to attract publicity. Another leading reason for sponsorship from big companies is to gain flight heritage for their components. Furthermore building and launching a complete

[1] https://betavak-nlt.nl/nl/p/vereniging-nlt/ledenoverzicht/ [Retrieved on 20.6.2019]

satellite is too expensive for a company to do alone. However, when several companies are each contributing with a component, as well as the fact that the satellite is designed by students, it would make it more affordable.

## 3.3. Modularity

After conducting an extensive market research it can be found that the concept of modularity in the design is not fully exploited in the market and thus there is a huge market share in the CubeSat business, which can be taken over. However, due to the tight deadline and the objective to launch the satellite by the end of 2020, the idea of plug-and-play and modularity is overlooked to a certain extent. In addition, this would be the first satellite in series and it is developed by students, therefore the first mission should definitely be a success so that the possibility of the project being shut down subsequently is minimized. Nevertheless, the design is still as modular as possible since a modular satellite would be the first step to make space available to students. The satellite is designed for a range of orbits and the aim is to make the payload module as interchangeable as possible. All of this would serve as a support to simplify the design of the next prototype, where the concept of a modular design would be further developed.

## 3.4. Implications on Final Design

The market situation of the Space Truck project influences the final design significantly. The imposed constraints and requirements drive the design of the satellite. On one hand, a prime example for a positive influence is the sponsorship of the Attitude Determination and Control System (ADCS) and the On-Board Computer (OBC) from Hyperion. It is helpful to have defined systems at such an early stage, and be able to design around them, as this shrinks the design space for the other systems by leaving only compatible components. Moreover it also discards payload ideas which cannot be supported by the ADCS or OBC. On the other hand, the market carries drawbacks such as the fact that the VSV has selected the payload ideas only several weeks prior to the deadline, which makes it particularly challenging to implement in the design and adjust it.

## 3.5. Return On Investment

Attempting to quantify the Return On Investment (ROI) for educational projects is not as straightforward compared to financial sector investments as the returns are not as easily quantifiable monetarily. Hence a non-financial return metric must be used meaning the ROI is not strictly financial. [17] defines ROI for education using Equation 3.1. For the purposes of this simple analysis, only school aged children from the Netherlands will be the main focus for the education benefits from this project. This is because while the idea for this system is so it can be used by a large number of schools, the first mission is the highest cost one and therefore the worst case situation.

$$ROI = \frac{(Increase\ in\ Student\ Learning)x(Number\ of\ Students\ Helped)}{(Amount\ spent)} \tag{3.1}$$

As ”Increase in Student Learning” cannot be determined as a number, Equation 3.1 shall be taken as ”Cost per Student” (which will be compared to current costs spent on education per student in the Netherlands, allowing a somewhat useful, relative cost comparison). If this cost is deemed to be positive, it will be ”multiplied” by the the potential educational benefit (somewhat subjectively decided on).

Starting with the amount spent per student, the total approximate costs for this project are summarised in Table 3.1. It is important to note that most of this cost will not result in an outlay of tender.

The ”Number of Students Helped” can be very large. As the design of the cubesat supports the use of FUN Cube+ dongles (see chapter 10), in theory *all* students interested in the Netherlands can be reached. For the purposes of this analysis, only primary and secondary

Table 3.1: Table summarizing the costs involved in the project. Numbers are for sub parts (such as individual systems costs in "Hardware Costs") are not given for confidentiality reasons.

| What | Cost in Euros | Comments |
|---|---|---|
| Opportunity cost of Engineering students | 292,320 | Based off a wage of 20 per hour with a total of 14,616 hours expected to be spent overall on the project. |
| Hardware Costs | 134,000 | Current approximation of total hardware costs from the VSV |
| Testing Costs | 23,000 | Estimation of the cost for testing from the VSV |
| Total Cost | 426,320 | |

students following NLT will be considered. According to the CBS, there are around 1,427,500 primary school students in the Netherlands [2]. Taking a conservative percentage of these students, assuming there is sufficient media attention for this project, at least 5% of students are reachable, meaning at least 142,750 primary students will get value out of this project. The number of secondary schools offering the NLT modal in the Netherlands is 184 [3](in both HAVO and VWO), with 652 schools in the Netherlands in total [4]. There are 340,198 HAVO/VWO students in the Netherlands where the total school population at 968,197 [5]. Assuming the ratio of HAVO/VWO schools to total schools in the Netherlands is the same as the same as the ratio to HAVO/VWO students to total students in the Netherlands, the total number of schools who offer HAVO/VWO is 229 schools. Using the inverse of this number, times the number of HAVO/VWO students, multiplied by the number of schools offering NLT number, multiplied the ratio of all students who do the *Nature and Technology* profile ( 0.16, calculated using data from [6]) gives the number of student who follow the NLT modal, and therefore get use from this project as about 43,717 students. This means the total number of students who will get use from this program is 114,992 students.

This results in a ”cost per student” of 3.91 euros. Compared to the (weighted) average of what is spent on school aged children per year in the Netherlands, €9,811 (calculated from [7]. This is a very low cost, relatively speaking.

Increase in student learning is subjective to quantify. Given this, education in STEM fields can be abstract for school aged children but all hands-on applications from STEM is beneficial for students [43]. As this project is providing semi-live data to students, it is more ”tangible” than data presented in books. Given the education from this project complements/can replace less-tangible STEM classroom activities, it is deemed that the increase in student learning is positive.

Taking these factors in to consideration, the cost per student is small both in terms of physical cost and relative cost (as compared to overall education expenditure) with a positive impact on education, the Return On Investment for this project is overall very positive.

It should be noted that the numbers presented here are rough and not as accurate as would be possible with more data. The perspective on acceptable cost ratios and educational benefits are also subjective and preliminary and to be more determined, review studies should be done. Additionally, the cost numbers used have been for the flight in 2020. If this design was to be used again (which it is designed for), the cost for engineering would be comparatively nothing as no additional would need to be done, reducing the cost per student to 1.37 euros ceteris paribus.

[2] https://longreads.cbs.nl/trends17-eng/society/figures/education/[Retrieved on 20-06-2019]
[3] https://betavak-nlt.nl/nl/p/vereniging-nlt/ledenoverzicht/[Retrieved on 20-06-2019]
[4] https://opendata.cbs.nl/statline/#/CBS/nl/dataset/03753/table?dl=1063F[Retrieved on 20-06-2019]
[5] https://statline.cbs.nl/StatWeb/publication/?PA=80040ned[Retrieved on 20-06-2019]
[6] https://www.ocwincijfers.nl/.../key-figures-education/keyfigures-education-2016.pdf[Retrieved on 20-06-2019]
[7] https://longreads.cbs.nl/trends17-eng/society/figures/education/[Retrieved on 20-06-2019]

# 4

# Requirements

This chapter lists the requirements which have been derived from the top level requirements given in the project brief. The requirements are split up into general requirements, performance and operational requirements, and requirements on each individual subsystem. These requirements are based off the project description provided by the VSV.

## Top Level Requirements

| ID | Requirement | Comment |
|---|---|---|
| SC-GEN-1010 | The SC shall not exceed 2.5 kgs | |
| SC-GEN-1020 | The SC bus shall only be comprised of flight proven hardware | |
| SC-GEN-1030 | The SC bus shall only be comprised of flight proven hardware combinations (discarded) | Discarded due to payload considerations |
| SC-GEN-1040 | The SC bus shall be operable within 300 km to 600 km orbital height range | |
| SC-GEN-1050 | The SC bus shall adhere to the CubeSat standard | |
| SC-GEN-1060 | The SC bus shall allow attachment of the payload | |
| SC-GEN-1070 | The SC shall comply with all relevant legal requirements | Dependent on satellite insurance and operation regulations in the Netherlands |
| SC-GEN-1080 | The SC shall be certified using tbd certification standards before flight | Dependent on launch provider specifications |
| SC-GEN-1090 | The SC shall be certifiable before May 2020 | |
| SC-GEN-1100 | The SC shall not exceed a size of 3U | |

## Performance and Operational Requirements

| ID | Requirement | Comment |
|---|---|---|
| SC-GEN-2010 | The SC bus shall remain operable up to a radiation level of 5 krad | Based on a 5-year mission simulation at 600 km in SPENVIS |
| SC-GEN-2020 | The operational temperature range of the bus shall be between 0 and 30 degrees Celsius (discarded) | Redundant requirement (Compare to system temperature ranges) |
| SC-GEN-2030 | The SC bus shall maintain operability of the payloads up to 5 krad | Based on a 5-year mission simulation at 600 km in SPENVIS |
| SC-GEN-2040 | The SC shall implement at least the following modes:<br>• Safe mode<br>• Nominal operation mode<br>• Initialization | |

## Power Management System Requirements

| ID | Requirement | Comment |
|---|---|---|
| SC-PMS-1010 | The power management system shall be able to generate sufficient watts during the day for fully charging batteries and nominal SC operations | To power all system and charge the batteries |
| SC-PMS-1020 | The power management system shall supply a maximum of 2 watts peak power to the payload | Maximum power available to the payload after nominal SC operations are consuming their nominal power |
| SC-PMS-1030 | The power management system shall be able to provide the SC systems with electrical power sufficient for their required operation during eclipse periods | |
| SC-PMS-1040 | The power management system shall be able to store enough electrical energy to operate the satellite during eclipse periods | Given SC-PMS-1030 |
| SC-PMS-1050 | The power management system shall prevent power surges to other systems | |
| SC-PMS-1060 | The power management system shall prevent electrical back flow between the power management system and subsystems | |
| SC-PMS-1070 | The power management system shall update the CDH system with the state of power consumption in watts once per clock cycle | Keeps updates consistent and simple |
| SC-PMS-1080 | The power management system shall remain operable up to a radiation level of 5 krad | Based on a 5-year mission simulation at 600 km in SPENVIS |
| SC-PMS-1090 | The power management system shall remain operable between a 0 and 30 degrees Celsius range within the SC bus | The expected temperature range inside the SC over an orbit |
| SC-PMS-1100 | The power management system shall be able to go into its safe mode when commanded to | |
| SC-PMS-1110 | The power management system shall remain operable outside eclipses in the event of a battery failure | To ensure the satellite is at least diagnostic-able in case of battery failure |

## Thermal System

| ID | Requirement | Comment |
|---|---|---|
| SC-THRM-1010 | The thermal system shall provide the CDH system with the SC bus system temperatures when requested | |
| SC-THRM-1020 | The thermal system shall measure the temperature of the SC bus with a range of $\pm 1$ degree Celsius | Low fidelity data to allow sufficient information for temperature control systems |
| SC-THRM-1030 | The thermal system shall remain operable up to a radiation level of 5 krad | Based on a 5-year mission simulation at 600 km in SPENVIS |
| SC-THRM-1040 | The thermal system shall remain operable between -12 and 42 degrees Celsius | Expected operational temperature range of the SC bus $\pm 12$ degrees (40% of operational range) for unexpected temperature fluctuations |
| SC-THRM-1050 | The thermal system shall be able to maintain the the designed for temperature range of the battery | To maintain battery optimal temperature range, as specified the EPS provider |

## Structures System

| ID | Requirement | Comment |
|---|---|---|
| SC-STR-1010 | The SC structure shall withstand all the expected structural loads generated on a launch | So the SC does not get crushed or falls apart |
| SC-STR-1020 | The SC structure shall withstand all the expected vibration loads generated on all reasonably expected launchers | So the SC does not fail during launch |
| SC-STR-1030 | The SC structure shall not allow movement of internal systems from their assembled place | |
| SC-STR-1040 | The SC structure shall not allow movement of the payloads from their assembled place | |
| SC-STR-1050 | The SC structure shall enable system components to move when those components are intended to do so | |
| SC-STR-1060 | The SC structure shall remain operable between a 0 and 30 degrees Celsius range within the SC bus | The expected temperature range inside the SC over an orbit |
| SC-STR-1070 | The SC structure shall perform as designed up to a radiation level of 5 krad | Based on a 5-year mission simulation at 600 km in SPENVIS |
| SC-STR-1080 | The SC structure shall allow attachment of the payload | |
| SC-STR-1090 | The SC structure shall have a longitudinal natural frequency of greater than 60 Hz | The highest natural frequency occur at launch |
| SC-STR-1100 | The SC structure shall have a lateral natural frequency of greater than 60 Hz | The highest natural frequency occur at launch |

## Attitude Determination and Control System

| ID | Requirement | Comment |
|---|---|---|
| SC-ADCS-1010 | The ADCS shall be able to determine the spacecraft attitude around all 3 dimensional axes with an accuracy of at least 3 degrees | Conservative estimation after research |
| SC-ADCS-1020 | The ADCS shall be able to determine the angular velocity of the SC with an accuracy of $\pm$ 0.5 degrees per second around all 3 dimensional axes | |
| SC-ADCS-1030 | The ADCS shall update the CDH system with attitude information at least every 0.1 seconds | |
| SC-ADCS-1040 | The ADCS shall be able to receive commands from the CDH system | |
| SC-ADCS-1050 | The ADCS shall be able to rotate the SC 180 degrees in 2700 seconds around all 3 dimensional axes | The slew rate is needed to maintain solar cells in the correct orientation |
| SC-ADCS-1060 | The ADCS shall be able to point the SC in a given direction with an accuracy of 5 degrees | Required accuracy for power generation |
| SC-ADCS-1070 | The ADCS shall have full control over the SC angular velocities over all 3 dimensional axes up to a maximum rotational velocity of 500 degrees per second | |
| SC-ADCS-1080 | The ADCS shall remain operable up to a radiation level of 5 krad | Based on a 5-year mission simulation at 600 km in SPENVIS |
| SC-ADCS-1090 | The ADCS shall remain operable between a 0 and 30 degrees Celsius range within the SC bus | The expected temperature range inside the SC over an orbit |
| SC-ADCS-1100 | The ADCS shall be able to go into its different operational modes when commanded to | |

## Communication System

| ID | Requirement | Comment |
|---|---|---|
| SC-COM-1010 | The comms shall be able to receive 9,600 bits per second from the TU Delft ground station | Sending rate from the ground station |
| SC-COM-1020 | The comms shall be able to send 15,360 bits per second to mission operations | Bit rate needed to send house keeping data and minimum generated payload data |
| SC-COM-1030 | The comms system shall work with a supply DC voltage of 5V | Supply voltage is 5V |
| SC-COM-1040 | The comms system shall be working nominally with a receiving SNR of greater than 7.8dB | Link budget estimation from the transmitter datasheet (threshold value) |
| SC-COM-1050 | The comms system shall send signals with a signal power of at least 1 watt | |
| SC-COM-1060 | The comms system shall receive signals with a signal power of at least tbd watts | Redundant requirement (compare to SC-COM-1070) |
| SC-COM-1070 | The comms system shall be able to communicate with the TU Delft ground station | |
| SC-COM-1080 | The comms system shall have a sending bit error rate of no more than 1E-5 bits from ground stations | Acceptable bit error rate from literature |
| SC-COM-1090 | The comms system shall be able to receive data from the TU Delft ground station | |
| SC-COM-1100 | The comms system shall be able to send data to the TU Delft ground station | |
| SC-COM-1110 | The comms system shall have a receiving bit error rate of no more than 1e-5 BITS from the TU Delft ground station | Acceptable bit error rate from literature |
| SC-COM-1120 | The comms system shall remain operable up to a radiation level of 5 krad | Based on a 5-year mission simulation at 600 km in SPENVIS |
| SC-COM-1130 | The comms system shall remain operable between a 0 and 30 degrees Celsius range within the SC bus | The expected temperature range inside the SC over an orbit |
| SC-COM-1140 | The comms systems shall be able to go into its different operational mode when commanded to | |
| SC-COM-1150 | The comms system shall be sending signals receivable by fun-cube pro+ dongles | This will be needed so students and amateurs can get access to semi-live data from the SC |
| SC-COM-1160 | The comms system shall always have its radio receivers on when there is sufficient power available | No command to shut down the receivers, they can only not work when the power available in the spacecraft is insufficient to power them |

## Command and Data Handling System

| ID | Requirement | Comment |
|---|---|---|
| SC-CDH-1010 | The CDH system shall be able to execute a command within a range of two seconds of the scheduled execution time | |
| SC-CDH-1020 | The CDH system shall be able to pre-schedule all commands up to 2 days before they occur | |
| SC-CDH-1030 | The CDH system shall be able to communicate with all other mission critical SC systems | |
| SC-CDH-1031 | The CDH system shall we able to send and receive information from the comms system | |
| SC-CDH-1032 | The CDH system shall we able to send and receive information from the ADCS | |
| SC-CDH-1033 | The CDH system shall we able to send and receive information from the payloads | |
| SC-CDH-1034 | The CDH system shall we able to send and receive information from the power system | |
| SC-CDH-1035 | The CDH system shall decode all uplink transmissions in nominal operation mode | |
| SC-CDH-1040 | The CDH system shall be able to store up to 2 Gb of data | To store Linux Debian distribution on the OBC as well as, code for SC operations and storing data generated from the SC |
| SC-CDH-1060 | The CDH system shall remain operable up to a radiation level of 5 krad | Based on a 5-year mission simulation at 600 km in SPENVIS |
| SC-CDH-1070 | The CDH system shall remain operable between a 0 and 30 degrees Celsius range within the SC bus | The expected temperature range inside the SC over an orbit |
| SC-CDH-1080 | The CDH system shall produce diagnostics information when non-nominal conditions in the payload occur | |
| SC-CDH-1090 | The CDH system shall be able to provide the payload with navigation data | |
| SC-CDH-1100 | The CDH system shall be able to provide the payload with attitude data | |
| SC-CDH-1110 | The CDH shall have a safe mode | |
| SC-CDH-1120 | The CDH shall be able to go into its safe mode when commanded | |
| SC-CDH-1130 | The CDH shall receive and acknowledge all commands from SC systems | |
| SC-CDH-1140 | The CDH system shall process the data from other SC systems in nominal operation mode | |
| SC-CDH-1150 | The CDH system shall encode all downlink transmissions in nominal operation mode | |
| SC-CDH-1160 | The CDH system shall use encrypted or otherwise secured command system | To prevent unauthorised commands being implemented on the spacecraft |

## Payload

| ID | Requirement | Comment |
|---|---|---|
| SC-PAY-1010 | The payload shall consists of at least two modules | |
| SC-PAY-1020 | If one module fails for mechanical reasons, the other module shall not be affected | |
| SC-PAY-1030 | If one module fails for electrical reasons, the other module shall not be affected | |
| SC-PAY-1040 | If one module fails for thermal reasons, other modules shall not be affected | |
| SC-PAY-1050 | If one module fails for command related reasons, the other module shall not be affected | |
| SC-PAY-1060 | If one module fails for data handling reasons, the other module shall not be affected | |
| SC-PAY-1070 | The payload shall function using the supplied SC bus voltage | |
| SC-PAY-1080 | The payload shall remain operable up to a radiation level of 5 krad | Based on a 5-year mission simulation at 600 km in SPENVIS |
| SC-PAY-1090 | The payload shall remain operable between a 0 and 30 degrees Celsius range within the SC bus | The expected temperature range inside the SC over an orbit |
| SC-PAY-1100 | The payload shall support a data connection to the CDH system | The CHD provides the data and communication links between the comms system and the payload |
| SC-PAY-1130 | The payload shall not exceed a size of 1U | |
| SC-PAY-1140 | During the pre-cursor flight, both modules small be education modules | |
| SC-PAY-1150 | The payload shall be verifiable without the SC bus | |
| SC-PAY-1160 | The payload shall be testable without the SC bus | |
| SC-PAY-1170 | The payload shall be certifiable without the SC bus | Dependent on launch provider specifications |

# 5
# Astrodynamics

An important mission parameter for space missions is the region of space that the to be designed spacecraft will inhabit. The choice of orbit has a large impact on many different aspects of the spacecraft. Section 5.1 briefly discusses what orbit range was considered for the design of the spacecraft, and how this range was established. The various orbital characteristics of this range are discussed in section 5.2, with lifetime estimations being treated separately in section 5.3. These lifetime estimations are further refined in section 5.4. The results affect the chosen orbit range and shrink the established orbit range, which is discussed in section 5.5. Finally, as a launch vehicle has yet to be chosen, section 5.6 outlines some considerations that help with launcher choice.

## 5.1. Orbit Generalisation

Since the choice of orbit impacts the spacecraft design, one of the first things that has to be established is what orbit the Space Truck will inhabit. However, for the design of the spacecraft, an orbit range rather than a single orbit was chosen. The reason for this is twofold.

Firstly, at the time of writing, no launch vehicle has yet been chosen, and so the orbit after launch is still uncertain. Even CubeSat launches come at significant cost, and as a free launch opportunity may come up by chance, it makes sense to design the CubeSat such that it can perform its mission in a variety of orbits.

Secondly, the philosophy behind the Space Truck implies that it by itself must be versatile enough to support different missions, which may be in different orbits. Therefore, it is sensible to design the Space Truck with a range of orbits in mind. In addition, this allows for a significantly more reusable CubeSat bus design, which is in line with the team's sustainable development strategy.

To determine the best orbit range to design for, a statistical method was used on data entries from an online CubeSat database[1]. The first observation that could be made from this data is that the large majority of CubeSats was injected into a circular orbit, with merely 14.1% of successfully launched CubeSats inhabiting a non-circular orbit. Hence, it was decided that for baseline design, only circular orbits would be considered. The remaining data set then consisted solely of 952 CubeSats with circular orbits. Their altitude and inclination angle were subsequently plotted in a bubble graph (see Figure 5.1), which revealed that many CubeSat orbits are clustered around two main orbits.

A box was drawn around these two main points, such that many datapoints would be included. The rationale for doing so was that by designing for many historical CubeSat missions, the CubeSat bus design would be robust and versatile, able to perform adequately on many different future CubeSat missions. The chosen orbit range is represented by the indicated area in Figure 5.1. It includes all inclination angles, though there have been no known missions that have had an orbit inclination of more than 100°. The lowest altitude that will be considered is 300 km, and the highest is 700 km. Within the chosen design space, 96.9% of circular CubeSat orbits from the data set are represented.

[1] www.nanosats.eu/#database[Retrieved on 03-05-2019]

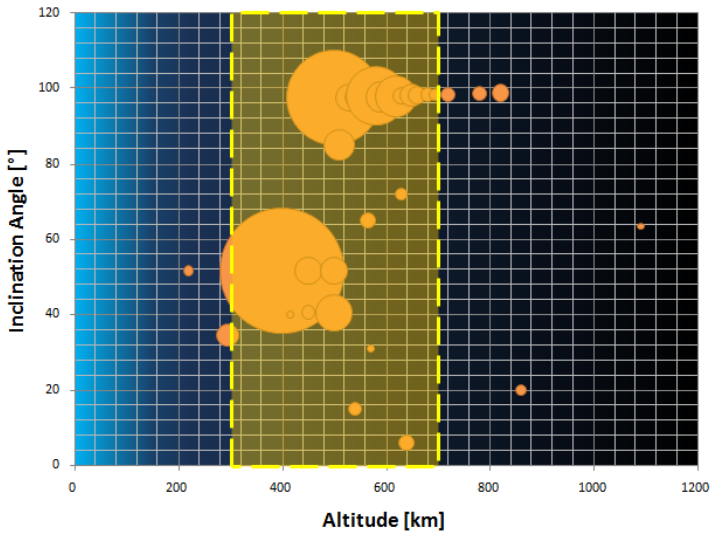


Figure 5.1: Chosen area on the altitude-inclination plane. $h \in [300, 700]; i \in [0, 120]$

## 5.2. Orbit Characteristics

Generalizing the orbit into a domain of altitude ($h$) and inclination angle ($i$) means that many of the other orbit parameters, such as velocity and eclipse time, will be domains. To ensure that the Space Truck design suffices for all considered orbit values, it is important to know where the worst cases are located, and design for those. The orbit parameters were calculated using first order methods as discussed in Fortescue [31], which will be briefly described below:

### Orbital Period and Velocity

Since all relevant orbit are presumed circular, velocity can be found using Kepler's Third Law:

$$\tau = 2\pi\sqrt{\frac{r_{orbit}^3}{\mu}} = 2\pi\sqrt{\frac{r_{orbit}^3}{GM_E}} \tag{5.1}$$

where $r_{orbit}$ is the orbit radius and $\mu$ is the gravitational constant of the larger body, in this case Earth ($\mu_{Earth} = 3.986 \cdot 10^5 [km^3 s^{-2}]$).

Next, orbital velocity can be found from Equation 5.2

$$V_{circ} = \sqrt{\frac{\mu}{r_{orbit}}} \tag{5.2}$$

### Eclipse Properties

For eclipse times and angles, it is assumed that Earth's shadow is a cylinder. Some sources suggest that since Earth's shadow cone has a top angle of 0.53° [41], for LEO satellites, the impact of ignoring penumbral effects is minimal. Then, for circular orbits, the eclipse angle $\beta_{eclipse}$ can be found using Equation 5.3.

$$\beta_{eclipse} = arcsin(\frac{R_E}{R_E + h}) = arcsin(\frac{R_E}{r_{orbit}}) \tag{5.3}$$

The eclipse period for each orbit case can then be found from Equation 5.4.

$$\tau_{eclipse} = \frac{2\beta_{eclipse}}{360°}\tau \tag{5.4}$$

### Ground Visibility

Furthermore, the visibility time of a satellite during a direct pass $\tau_{pass}$ can be found using Equation 5.5

$$\tau_{pass} = 2\phi/\omega_{ES} \tag{5.5}$$

Here $\phi$ is the geocentric semi-angle, and $\omega_{ES}$ the orbital angular velocity. $\phi$ is a function of the satellite's orbit and the satellite elevation $\varepsilon$, according to Equation 5.6.

$$\phi = -\varepsilon + arccos(\frac{R_E}{R_E + h}cos(\varepsilon)) \tag{5.6}$$

A typical value for the satellite elevation is 5°, and so this is used. The orbital angular velocity is found using Equation 5.7.

$$\omega_{ES} = \sqrt{\omega_E^2 + \omega^2 - 2\omega_E\omega cos(i)} \tag{5.7}$$

This still requires two inputs. $\omega_E$ is a known constant of $7.3 \cdot 10^{-5}$, and $\omega$ may be found for circular orbits using the following approximation:

$$\omega_{circ} = 631(R_E + h)^{-3/2} \tag{5.8}$$

All terms are now defined, and so $\tau_{pass}$ can be found. Lastly, the slant range $s$ can be found from using the previously defined parameters and Equation 5.9.

$$s = (R_E + h)\frac{sin(\phi)}{cos(\varepsilon)} \tag{5.9}$$

### Results

After performing the aforementioned calculations, the minimum and maximum values for each orbit parameter were found, as well as their locations on the $(h, i)$-plane. The results can be found in Table 5.1.

Table 5.1: Orbit characteristics for the chosen $(h, i)$-domain

| | Min value | Location min | Max value | Location max |
|---|---|---|---|---|
| $V$ [km/s] | 7.508 | h=700 | 7.730 | h=300 |
| $\tau$ [s] | 5423 | h=300 | 5917 | h=700 |
| $\tau$ [min] | 90.4 | h=300 | 98.6 | h=700 |
| $\beta_{eclipse}$ [deg] | 64.3 | h=700 | 72.8 | h=300 |
| $\tau_{eclipse}$ [min] | 35.2 | h=700 | 36.5 | h=300 |
| $\tau_{day}$ [min] | 53.8 | h=300 | 63.4 | h=700 |
| $s$ [km] | 1499 | h=300 | 2562 | h=700 |
| $\tau_{pass}$ [s] | 389.2 | h=300, i=90 | 747.4 | h=700, i=0 |

## 5.3. First Order Lifetime Estimations

One parameter that is of great interest when considering any satellite mission is the orbital lifetime. Orbit lifetime may vary greatly depending on orbit. The book Space Mission Analysis and Design (SMAD) provides a coarse method for orbit lifetime estimation [23]. This method takes orbit altitude, solar activity, and ballistic coefficient. In this report, the ballistic coefficient definition is based on that of [23], namely:

$$B = \frac{m}{C_D A_{ref}}\left[\frac{kg}{m^2}\right] \tag{5.10}$$

Where $m$ is the object mass, $C_D$ the object drag coefficient, and $A_{ref}$ the reference area with respect to the freestream. The method of [23] has merely two options for solar activity; High solar activity and low solar activity. The ballistic coefficient also has two options, namely 50 $kg \cdot m^{-2}$ and 200 $kg \cdot m^{-2}$.

The ballistic coefficient of the Space Truck can be calculated using the aforementioned definition of Equation 5.10. Several sources suggest that for CubeSats, a $C_D$ of 2.2 will yield the best results in the absence of more accurate data [30], [39]. If $A_{ref}$ is then assumed to be equal to a 2U sidepanel (0.02 $m^2$), and the mass is presumed to be 2.5 $kg$, then according to Equation 5.10, the approximated ballistic coefficient is 56.8 $kg \cdot m^{-2}$ This results in the lifetime values in the second row of Table 5.2.

Because future Space Truck missions may take place during active or inactive solar periods, it is best to design for the worst case. This is when solar activity is high, as thermospheric drag then becomes most severe [23]. However, the upcoming mission of the VSV is scheduled for the end of 2020. The transition between solar cycle 24 and 25 is scheduled to occur halfway throughout 2020 [32]. This can also be seen in Figure 5.2.

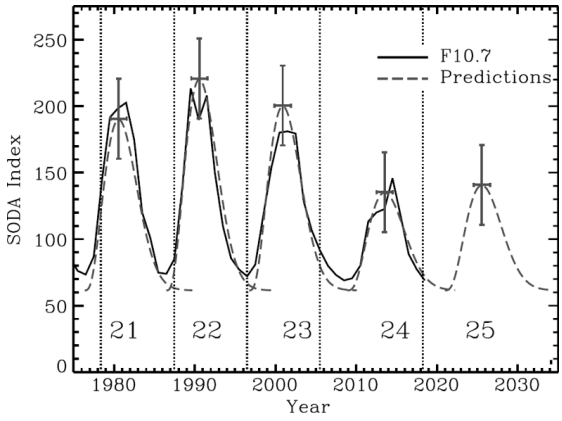


Figure 5.2: Predicted and actual SODA index of several solar cycles [32]

This means that 2020 is marked by a particularly low solar activity, which typically results in a lower atmospheric density experienced by satellites, which in turn may increase satellite lifetime substantially. As a result, taking the value corresponding to low solar activity estimation may be more representative of the 2020 mission. Therefore, for first order lifetime estimation, both the low and high solar activity values are displayed in Table 5.2.

Table 5.2: Orbit lifetime in days for the estimation method of SMAD

| Altitude h [km] | 300 | 400 | 500 | 600 | 700 |
|---|---|---|---|---|---|
| Lifetime [days]; Solar Low | 55 | 511 | 953 | 1,613 | 12,883 |
| Lifetime [days]; Solar High | 14 | 83 | 270 | 941 | 12,355 |

At this point, it is worth mentioning that the described method of orbital lifetime estimation from SMAD may be insufficiently accurate. First, it ignores a number of important variables, such as inclination, and for other variables it is not clear whether they were included in the analysis, such as third body effects or solar radiation pressure. Secondly, some input variables are rather coarse, given that only two values can be picked for solar activity, which may vary greatly during the mission, and ballistic coefficient, which for the current design is close to, but not equal to 50. Lastly, [23] mentions that its values were obtained from software package $SatLife$, but some research turned up that very little validation data is available for this software, requiring the use of another orbit calculation tool to validate the obtained data.

## 5.4. GMAT Lifetime Estimation

In order to improve the existing analysis of orbit lifetime, a second method was employed. There are a number of orbit calculation software packages available online, such as STK, GMAT, FreeFlyer, and the TUDAT library. NASA's GMAT was chosen for the analysis, as it is free, rich in features, and generally well-documented and verified. This means that as a tool, GMAT will not need to be verified. The official SMAD validation & verification document contains more detailed information about the used verification methods [37].

### 5.4.1. Simulation Approach

To obtain a clear image of the variety of orbit lifetimes the designed Space Truck could see, the following approach was taken. As orbit lifetime depends on both altitude and inclination, the orbital lifetime needs to be assessed whilst both varying independently. However, as some of the simulations could run for up to 7 hours, yielding a single orbit lifetime envelope, it remained important to pick important orbits that would represent the effect of $h$ and $i$ on lifetime well.

Using the GMAT simulation tool, three things were investigated:

1. The sensitivity of orbital lifetime to altitude and inclination
2. The sensitivity to launching the Space Truck in 2020, 2021 and 2022, respectively
3. The potential effect of an ADCS-driven deorbiting mode

The GMAT software requires a number of input parameters, both for its satellite model, but also for the numeric propagator that is used to perform the simulations. Appendix B provides an overview of the input parameters that were used for the orbit lifetime estimations relevant to the Space Truck design. The launch date were varied to account for delays in the assembly, testing and launch phases.

### 5.4.2. Lifetime Sensitivity to Altitude and Inclination

First, the orbital lifetimes were simulated for orbits with altitudes of 300 km through 700 km, in steps of 100 km, and inclination angles of 0°, 51.6°, and 90°. 51.6° was chosen as opposed to 45° because many CubeSats have an orbit with that inclination, and therefore it is of additional interest (the regularly frequented ISS orbit is at 51.6°, and many CubeSats are deployed from there). The goal of this analysis was to observe the sensitivity of orbit lifetime to both orbit altitude and inclination.

The lifetime simulations for altitudes of 700 km were terminated after running for around 20 hours, after which the propagator would be computing orbit properties around 2065. The reason for early termination is twofold. Firstly, the simulations were cut short because the simulation software would experience significant slowdowns, increasing the computation time of obtaining additional data to an unacceptable extent. Secondly, the data beyond this point is of much less use. Not only is the geomagnetic and solar activity only modelled up until 2044, resulting in more inaccurate results beyond this year, but the simple notion that the orbit lifetime is much greater than 25 years is much more useful than knowing the exact lifetime of such an orbit. This is because international space debris mitigation treaties dictate that LEO satellites must remain in orbit no longer than 25 years. This will be touched upon in section 5.5 in more detail.

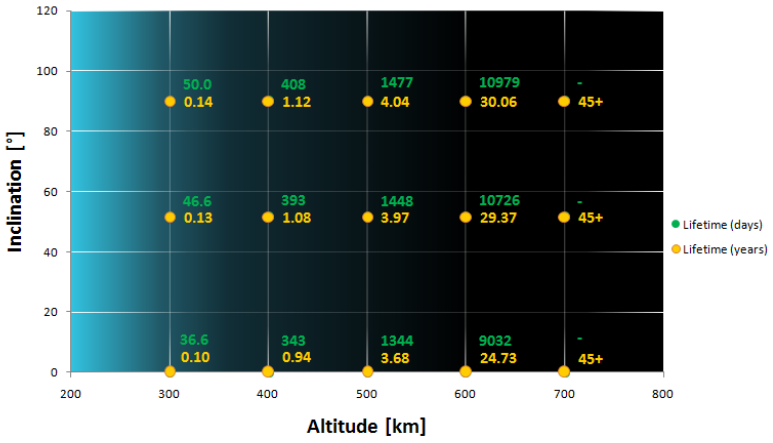


Figure 5.3: Orbit lifetime estimations in days and years for various CubeSat orbits on the $h, i$-plane. All values obtained with GMAT.

Table 5.3: Orbit lifetime in days for various estimation methods, altitudes and inclinations

| Altitude h [km] | 300 | 400 | 500 | 600 | 700 |
|---|---|---|---|---|---|
| Method of SMAD, solar low | 55 | 511 | 953 | 1,613 | 12,883 |
| Method of SMAD, solar high | 14 | 83 | 270 | 941 | 12,355 |
| GMAT ($i = 0°$) | 36.6 | 343 | 1,344 | 9,032 | 16,500+ |
| GMAT ($i = 51.6°$) | 46.6 | 393 | 1,448 | 10,726 | 16,500+ |
| GMAT ($i = 90°$) | 50.0 | 408 | 1,477 | 10,979 | 16,500+ |

The resulting orbital lifetimes can be found in Figure 5.3, as well as in Table 5.3. A number of things are of note.

- First, the lifetime values obtained from GMAT are much more similar to the low solar activity values obtained from SMAD [23] than the high solar activity values. This is as expected, as 2020 is expected to experience very low solar activity [32]. However, the values start to significantly diverge for orbit altitudes of 500 km and higher. There could be a variety of reasons for this, but it is difficult to say why exactly there is such a large disparity, as not many details are known about the exact method that SMAD employs.
- Inclination has a notable impact on orbit lifetime, increasing it by as much as 36% (comparing GMAT values only). The most likely reason for this is the large difference density distribution in Earth's atmosphere. Atmosphere regions directly above the equator will experience higher densities than regions at the poles, due to relative distance to the sun. Highly inclined orbits experience this thicker region of atmosphere less frequently, whilst low inclination orbits spent most of their time there. There are other effects that may contribute, such as atmosphere oblation.
- Finally, it is of note that some the lifetimes of orbits at 600 km already are past 25 years[1], suggesting that without any way to affect orbit course, the Space Truck should not be launched into such an orbit.

### 5.4.3. Sensitivity to Launch Year

In the previous analysis, the effect of inclination on orbit lifetime was investigated. However, it is also of interest to know how orbit lifetime is affected if the Space Truck is launched later than 2020, because the predictions indicate that solar activity will increase after 2020. Such a situation may occur if the development of the Space Truck is delayed at any point, or there are no available launchers in 2020. To this end, the following simulations were run. For two mission types, one lasting 90 days and one lasting a full year, the orbit lifetimes were simulated for various orbit inclinations. This was then repeated for 2021 and 2022. The results can be found in Figure 5.4 and Table 5.4. The goal of this analysis was to observe the sensitivity of orbital lifetime to launch year and inclination.

Table 5.4: Required orbit altitudes in km for a mission of either 90 or 365 days for various years and various inclinations

| Inclination [°] | 0° | 30° | 51.6° | 90° |
|---|---|---|---|---|
| 90 day mission in 2020 | 331 | 328 | 325 | 323 |
| 90 day mission in 2021 | 348 | 345 | 341 | 339 |
| 90 day mission in 2022 | 362 | 358 | 354 | 352 |
| 365 day mission in 2020 | 404 | 401 | 413 | 410 |
| 365 day mission in 2021 | 436 | 425 | 420 | 419 |
| 365 day mission in 2022 | 444 | 440 | 436 | 449 |

From the data, one can observe that the required orbit altitude to maintain a fixed mission duration increases from 2020 on. This is as expected, as solar activity is expected to increase from 2020 on, as seen in Figure 5.2, decreasing lifetime. For example, for a mission duration of one year, an orbit range of just over 400 km will suffice if the satellite is launched in 2020, whilst if it is launched just two years later, the required orbit altitude will have to be over 450

[1] 25 years equals 9131 days

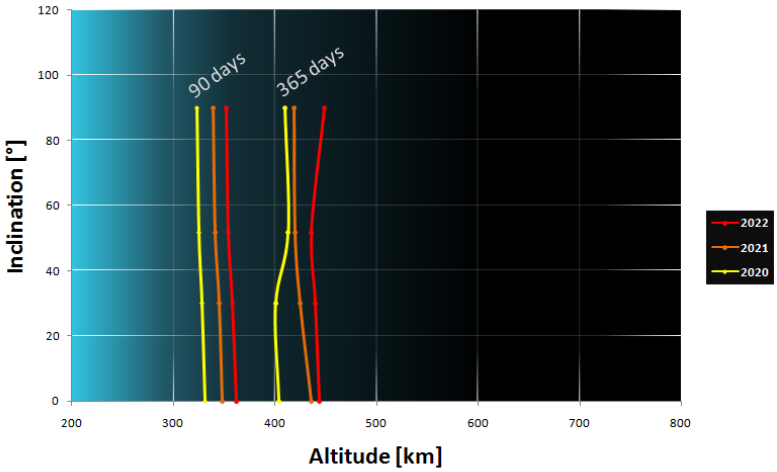


Figure 5.4: Required orbit altitudes for a mission of either 90 or 365 days for various years.

km. In conclusion, the planned 2020 is favourable for short-term lifetime, as even low altitude orbits remain in orbit for much longer than regularly. However, the same reason, deorbiting within the available 25 years becomes more difficult. If the launch window is delayed, deorbiting becomes less critical, but especially for short missions, mission lifetime suffers as a result.

### 5.4.4. Sensitivity to Drag Area

The current design of the Space Truck does not have any active orbit control capability, and as such cannot actively deorbit itself at the end of its lifetime. However, since there will be an active ADCS module on board, the satellite will have the capability to rotate itself such that drag is maximized. The effective area that the free stream "observes", here notated as $A_{ref}$, is then no longer 0.02 $m^2$, but 0.02827 $m^2$. Since GMAT accepts $A_{ref}$ as an import parameter, another analysis was done to get an estimate of what kind of effect this configuration would have on orbital lifetime. In other words, the goal of this analysis was to observe the sensitivity of orbit lifetime to a change in drag area. The results of this analysis can be found in Table 5.5.

Table 5.5: Effect of increasing the freestream reference area on satellite lifetime [days]

| Altitude h [km] | 300 | 400 | 500 | 600 |
|---|---|---|---|---|
| $i = 51.6°$, $A_{ref} = 0.02\ m^2$ | 46.6 | 393 | 1,448 | 10,727 |
| $i = 51.6°$, $A_{ref} = 0.02827\ m^2$ | 32.8 | 299 | 1,161 | 5,868 |
| Relative effect on lifetime | -29.6% | -24.0% | -19.8% | -45.3% |

The results of the analysis show that changing the freestream area $A_{ref}$ may have a dramatic impact on mission lifetime, but it varies significantly with orbit altitude. The general trend is that the higher the orbit altitude, the less effect the proposed deorbiting mode has. This is expected, because as a satellite get further away from Earth, the air density decreases quickly, making drag forces only a minor influence at higher altitudes.

However, this trend is broken by the simulated datapoints at 600 km altitude. Here, the increase of $A_{ref}$ brings about a 45.3% reduction in orbit lifetime. The decay envelopes of these datapoints have been plotted in Figure 5.5. From the figure can be seen that the red curve travels through two solar cycles, generally around 11 years each, after which it starts the typical decline pattern that eventually results in deorbit. However, the blue curve can be seen going through one solar cycle, losing more altitude than the red curve, and experiences so much drag throughout the second solar cycle that it deorbits entirely.

As such, it may be that high reduction in orbital lifetime for the 600 km orbit is a result of the particular interaction with the solar activity, rather than a generalised case for orbits at this altitude. Another reason why these figures may be optimistic is that $C_D$ has remained

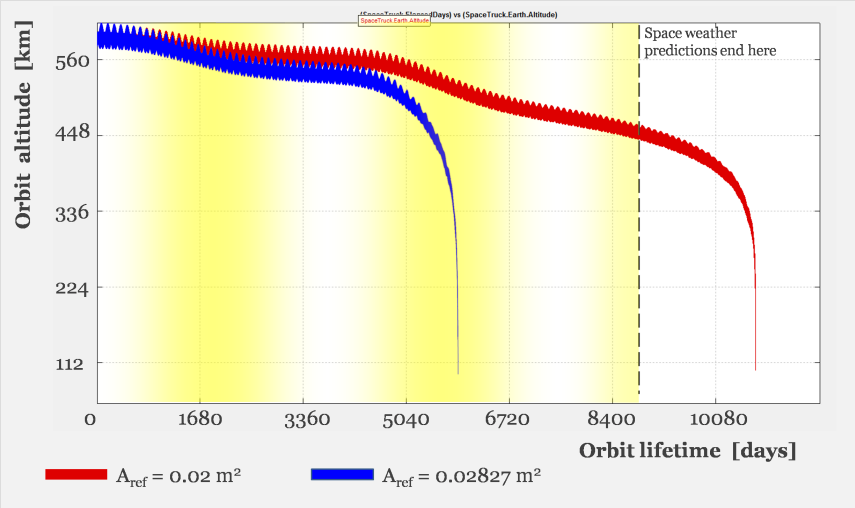


Figure 5.5: Simulated effect of the increase of the freestream area $A_{ref}$ in deorbiting mode. The orbit altitude is 600 km, the orbit inclination is 51.6° and the launch year is 2020. The projected intensity of solar cycles has been represented in yellow.

constant throughout this analysis, whilst in reality, this value may fluctuate enough to affect the outcome. The obtained results should therefore not be treated as anything but coarse estimations. During detailed design, a more detailed analysis may be done to more accurately address these issues.

## 5.5. Orbit Generalisation Revisited

At the beginning of this chapter, there is a brief description of the chosen orbit range for which the Space Truck is designed. It is decided that the Space Truck would be capable to support its payloads for orbit altitudes between 300 and 700 km, and for all inclinations. However, as the design process progressed, two issues came up to challenge this design choice.

### 5.5.1. Upper Lifetime Limit

According to this membership document from UN's Office for Outer Space Affairs[2] (OOSA), The Netherlands is a member of the Commitee of the Peaceful Uses of Outer Space (COPUOS). This means that The Netherlands fully adheres to several international space debris mitigation guidelines, among which are those of the Inter-Agency Space Debris Coordination Committee (IADC). These guidelines specify that for LEO satellites, a maximum lifetime of 25 years is appropriate [7]. However, the lifetime analysis in the previous section yielded that for a satellite launched into a 700 km orbit may be in orbit for well over 45 years. As the current Space Truck design has no active orbit control, the only way to adhere to this international guideline is to shrink the design space such that the Space Truck is not in danger of remaining in orbit for longer than 25 years. As the exact altitude boundary may vary depending on solar activity, some flexibility must be allowed for this constraint.

### 5.5.2. Operability Limit

National Space Law[3] in The Netherlands decrees that one can only operate a spacecraft by being a licensed operator. However, if the satellite is owned by a Dutch operator, it also must be operated from Dutch soil. For this to work, the satellite must pass over Dutch soil at some point. Yet, if the Space Truck is launched in a low inclination orbit, it may never pass over The Netherlands. By defining the orbit design space such that the satellite will definitely pass over The Netherlands, this problem can be alleviated.

[2] http://www.unoosa.org/documents/pdf/spacelaw/sd/Netherlands.pdf [Retrieved on 12-06-2019]
[3] http://www.unoosa.org/oosa/en/ourwork/spacelaw/nationalspacelaw/netherlands/space_activities_actE.html [Retrieved on 19-06-2019]

### 5.5.3. Revised Orbit Range

With these two things in mind, the orbit range defined in section 5.1 can be revised into a more appropriate design space. This range will be defined as follows:

- All altitudes between 300 and 600 km
- All inclinations between 50° and 130°

The new orbit range is also depicted in Figure 5.6. For the aforementioned reasons, it provides a better basis from which to design the satellite. Therefore, during detailed design, these constraints should be used in place of the ones mentioned at the beginning of the chapter. In accordance, the values in Table 5.1 were updated to reflect these changes. The updated parameters can be found in Table 5.6.

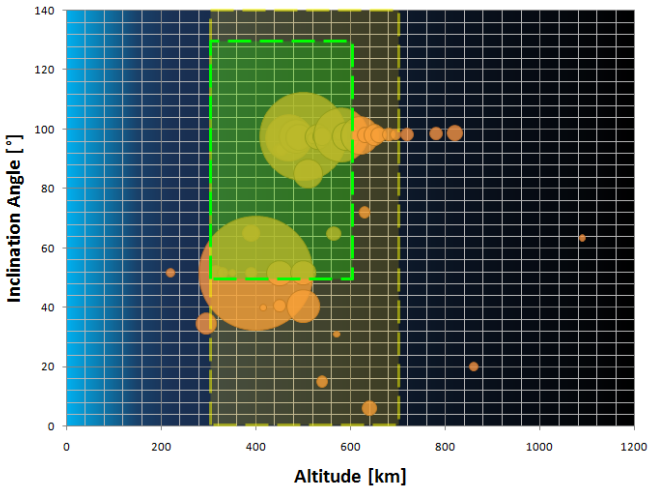


Figure 5.6: Revised area on the altitude-inclination plane. $h \in [300, 600]; i \in [50, 130]$

Table 5.6: Updated orbit characteristics for the chosen orbit range

| | Lowest value | Location low | Highest value | Location high |
|---|---|---|---|---|
| $V$ [km/s] | 7.562 | h=600 | 7.730 | h=300 |
| $\tau$ [s] | 5423 | h=300 | 5792 | h=600 |
| $\tau$ [min] | 90.4 | h=300 | 96.5 | h=600 |
| $\beta_{eclipse}$ [deg] | 66.1 | h=600 | 72.8 | h=300 |
| $\tau_{eclipse}$ [min] | 35.4 | h=600 | 36.5 | h=300 |
| $\tau_{day}$ [min] | 53.8 | h=300 | 61.1 | h=600 |
| $s$ [km] | 1499 | h=300 | 2328 | h=600 |
| $\tau_{pass}$ [s] | 389.2 | h=300, i=90 | 653.0 | h=600, i=50 |

## 5.6. Launch Vehicle Considerations

At the time of writing this report, no launch vehicle has yet been chosen. This section contains a few consideration that can be used to help with that investigation. The first criterion of a suitable launch opportunity is that the injection orbit lies within the orbit range as described in Figure 5.6. If not, the lifetime of the mission may be longer than 25 years, so that it will no longer comply with the IADC space debris mitigation guidelines. In addition, the spacecraft may be unable to be operated from Dutch soil. For operation from a ground station in Delft, which is at 52° latitude, an orbit inclination between 50° and or more is desired.

In case a launch opportunity presents itself, the injection orbit can be propagated in a program like GMAT to assess its suitability. The analysis done in this chapter looks at orbit inclination, altitude, and launch time as variables, but these are all fixed for a given launch opportunity. With these values fixed, one can easily find other orbit characteristics, such as pass frequencies, which will be essential in the final sizing of the communication system. Lifetime can then also be more accurately assessed. This analysis is important in particular if the injection orbit is an elliptical orbit, because these orbits were scoped out of the preliminary design analysis.

# 6
# Design Concepts

This chapter describes the initial concepts that were created. First, the methodology of how the concepts are obtained is explained. Then the design option tree which generates the three concepts is shown together with the tables of the concept's characteristics.

## 6.1. Method

In order to create the three concepts, it is decided to optimize different important criteria for the design. These criteria are simplicity, power and reliability.

Simplicity is important because it reduces the amount of work to be done to complete the project. Since the satellite is student designed and built, the practical knowledge of the workers is low for a satellite project. Combining this with the ambitious timeline of launching in the year 2020, means that many man-hours will be needed to fulfill the mission. The project becoming much longer than intended or even not being completed at all, are large risks. In order to minimize this risk, so that the amount of required man-hours does not exceed the amount of available man-hours, the simplicity of the design is maximized. This also leaves more time for the important tasks of verification and validation.

Power is critical to facilitate high data transmission rates and pointing knowledge/accuracy for the payload. It enables good communication with the satellite and allows for a larger design space for the individual payloads. Optimizing for power however, can lead to a degradation of reliability and an increase in required spacecraft mass which would reduce the mass available for the payload. Moreover, the design complexity is expected to increase resulting in a higher risk of the deadline not being met.

Finally, the criteria that is optimized to create the third concept is reliability. The reliability of the satellite is very important as failure of one payload should not affect the other payloads or the bus. Considering the CubeSat Bus is meant to be an "Ultra-Reliable CubeSat Bus" the importance of reliability in the design is stressed.

A design option tree which outlines the different concepts can be seen in Figure 6.1.

## 6.2. Concepts

In this subsection the three concepts are described. The structure and thermal subsystems are constants across each design and are therefore not discussed here.

### 6.2.1. Concept 1

For the first design, which is designed for maximum simplicity, the simplest components which, nonetheless, ensure the functioning of the bus and payload are chosen. The satellite has solar panels on all sides as well as on the bottom. The top is left free for an aperture so that the payloads can be exposed to their environment if necessary. No active ADCS is used and only a magnet is placed inside to align the satellite with Earth's magnetic field. Sun sensors are used, along with solar panel data to give a rough estimate of the satellite's attitude, which can aid in analysing experiment data. A simple, low power computer from ISIS is used. The telemetry system is a GomSpace AX100U UHF transceiver and an Endurosat UHF antenna. UHF is used as it is simple, reliable and cheap. However, the data downlink is low, a maximum of 19.2 kbps, assuming unlimited bandwidth.

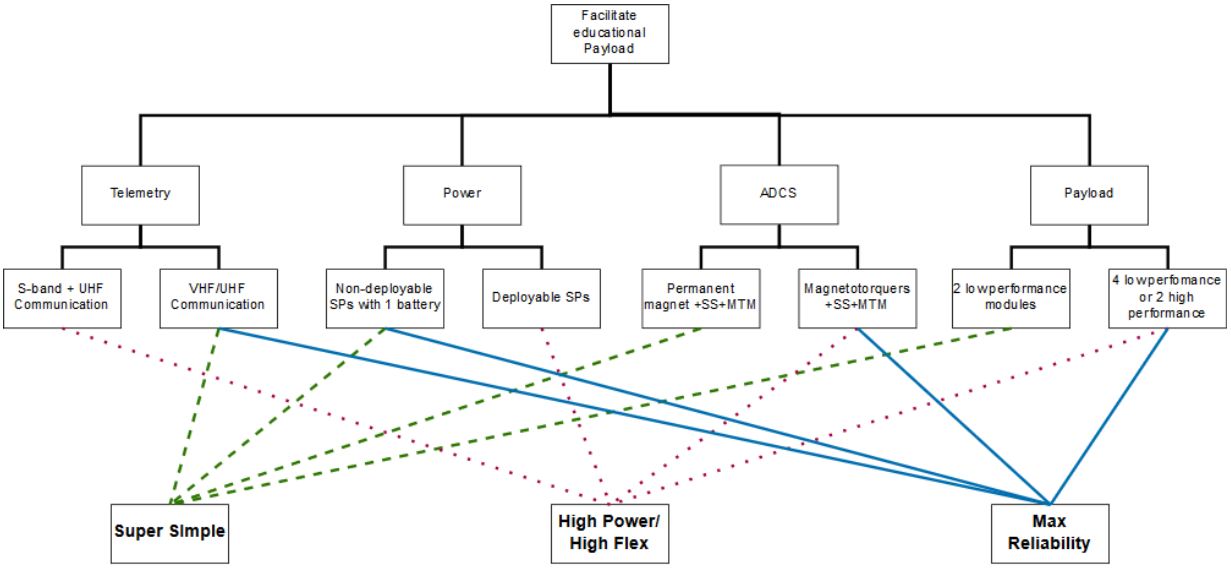


Figure 6.1: Design (Concept) Option Tree (SS: Sun Sensor, MTM: Magnetometer, SP: Solar Panel)

The budgets of the first concept can be seen in Table 6.1. One can see that mass is not an issue. The payloads could exceed one kilogram without the satellite passing the mass limit of 2.5 kilograms. The stack height is also not a issue. The limiting factor for payloads on this satellite will be data downlink and power, as only 290 mW are available. This concept is very sensitive with respect to power. If the power production of the solar panels decreases by only 16% or the subsytems draw 300 mW power more than expected, there is no power left for the payload, which might be considered a mission failure.

Table 6.1: Concept 1: Maximum Simplicity. Overview of the selected subsystems.

| | Description | Power [W] | Stack Height [cm] | Mass [g] | Cost [EUR] |
|---|---|---|---|---|---|
| ADCS | Sun sensor, solar panel (for attitude determination) and magnet (for passive alignment with Earth gravitational field) | 0.3 | 2 | 100 | 8,000 |
| Computer | ISIS onboard computer, 4000MHz ARM9 processor | 0.5 | 1.24 | 94 | 4,400 |
| Power | 4 side solar arrays + 1 on the bottom, 1 Lithium polymer battery | 0 | 2.7 | 445 | 18,400 |
| Structure | ISIS 2U | 0 | 0 | 400 | 4,000 |
| Telemetry | Gomspace AX100U software configurable UHF transceiver + Endurosat UHF antenna | 0.43 | 0.65 | 110 | 9,000 |
| Thermal Control | Tape, heat sinks, electric heaters | 0.25 | 0 | 20 | 120 |
| Sum | | 1.48 | 6.59 | 1169 | 43,920 |
| Total available | | 1.77 | 21.19 | 2500 | - |
| Available for payload | | 0.29 | 14.6 | 1331 | - |

### 6.2.2. Concept 2

The second design optimizes the power production by using deployable solar panels. The solar panels fold out from the sides and are pointed towards the Sun using the active ADCS of the satellite. The excess energy is stored in a lithium ion battery. A Pumpkin space board is used

Table 6.2: Concept 2: Maximum Power. Overview of the selected subsystems.

| | Description | Power [W] | Stack Height [cm] | Mass [g] | Cost [EUR] |
|---|---|---|---|---|---|
| ADCS | Sun sensors, Magnetometer, Inertial Measurement Unit and Magnetorquers | 2 | 4 | 320 | 25,000 |
| Computer | BeagleBoneBlack(BBB) board from Pumpkin space. 1GHz processor | 2.5 | 1.45 | 71 | 5,000 |
| Power | 4 deployable side solar arrays + 1 on the bottom, 1 Lithium polymer battery | 0 | 4.7 | 1090 | 27,800 |
| Structure | ISIS 2U and extra structure for payloads | 0 | 0 | 469 | 4,000 |
| Telemetry | IQ SpaceCom HiSPiCO S Band Transmitter + IQ Wireless S-band patch antenna + nanoavionics UHF Digital Radio SatCOM UHF + ISIS CubeSat turnstile antenna system | 1.74 | 2.9 | 290 | 20,600 |
| Thermal Control | Tape, heat sinks, electric heaters | 0.25 | 0 | 20 | 120 |
| Sum | | 6.49 | 13.05 | 2260 | 82,520 |
| Total available | | 12.79 | 21.19 | 2500 | - |
| Available for payload | | 6.30 | 8.14 | 240 | - |

for the on-board computer. The telemetry system of this concept uses the S-band bandwidth using a transceiver and antenna from the company IQ. This gives a maximum data rate of 1.6 Mbps, 14 times greater than using the GOMspace UHF transceiver. Because of the stack height of the components, the payloads will not fit into the ISIS 2U structure and hence an additional structure needs to be used. This could be done by asking for a custom 2.5U structure, similar to the 2U long stock configuration.

The budgets of this concept are summarized in Table 6.2. Due to the fact that this concept is the most advanced one, it is also the most expensive one at a cost of 82,520 Euros. This does not include testing and integration since testing will be sponsored and the integration is performed by unpaid students [1]. However, the man-hours needed, especially for this concept, should not be underestimated as students need to be willing to do this work for free, and the amount of man-hours available could, as a result, be limited. The power budget of this satellite is much higher than that of Concept 1, as is to be expected since it has deployable solar panels pointing actively towards the Sun. The payloads will not be limited by power or data consumption. However, the mass of the bus is already very high. If the mass budget of the 2.5 kg is to be respected, only 240 g can be allocated to the payloads, without taking contingency into account. This means that this concept is quite sensitive with respect to mass. For example, if later in the design the total mass of the spacecraft, excluding the payload, is found to increase by 10%, the available mass for the payload would decrease to 14 $g$ which is insufficient to have a reasonably sized payload. Although mass is not a killer requirement, this is not preferred as it will increase launch cost, potentially over-budget.

### 6.2.3. Concept 3

The third concept is designed with high reliability in mind. The initial approach was to optimise reliability by means of redundancy. In order to implement this, many redundant components are introduced. The satellite will consist of double the amount of Sun sensors as well as magnetometers for attitude determination. Magnetorquers are chosen because they do not have

[1] However, the project is supervised by tutor and coaches which are being paid. These costs are not taken into consideration

Table 6.3: Concept 3: Maximum Reliability. Overview of the selected subsystems. Note that for the power budget, the power is given positive if the subsystem produces power and negative if it consumes power. The sum of the power is thus the power available for the payload

| | Description | Power [W] | Stack Height [cm] | Mass [g] | Cost [EUR] |
|---|---|---|---|---|---|
| ADCS | Sun sensors x2, Magnetometer and Magnetorquers | 1.3 | 1.5 | 200 | 22,000 |
| Computer | Endurosat On board computer x2. ARM Cortex M7 version, 216Hz per board | 0.34 | 2.5 | 116 | 5,800 |
| Power | 4 side solar arrays, 1 Lithium polymer battery | 0 | 3 | 652 | 16,800 |
| Structure | ISIS 2U | 0 | 0 | 400 | 4,000 |
| Telemetry | Gomspace AX100U software configurable UHF transceiver x2 + Endurosat UHF antenna | 0.43 | 1.3 | 219 | 18,000 |
| Thermal Control | Tape, heat sinks, electric heaters | 0.25 | 0 | 20 | 120 |
| Sum | | 2.32 | 8.3 | 1607 | 66,720 |
| Total available | | 2.997 | 21.19 | 2500 | - |
| Available for payload | | 0.677 | 12.89 | 893 | - |

moving parts and are very reliable. There are also two GOMspace UHF transceivers and two EnduroSat on-board computers for redundancy. Many of the subsystems are similar to the simple option (Concept 1) but have redundancy. The overall power provided by the power system increases compared to Concept 1, since there is an active ADCS which means the solar panels can be actively pointed at the Sun. In this concept, the solar panels cover all the sides and bottom of the satellite.

In Table 6.3 it can be seen that there would be 0.68 W available to the payload if Concept 3 is chosen. The payloads would have available weigh more than a kilogram, similarly to Concept 1. The stack height of the components fits comfortably into a 2U structure, leaving space (0.5 U) for the payloads. Finally, the cost of this system sits between that of Concept 1 and Concept 2 at 67,000 Euros.

It is important to note that even though the third concept is designed with high reliability in mind, the implementation is found to not be optimum. After a discussion with industry experts, it is realized that these extra layers of redundancy also make the spacecraft more complex. This complexity has the potential of decreasing the spacecraft's reliability.

# 7

# Trade-Off Summary

In order to compare the concepts presented in chapter 6 and choose one of them, a trade-off was performed. A summary of this trade-off is described here. In section 7.1, the method which was used for the trade-off is described. In section 7.2 the trade-off criteria and weights are given along with the rationale behind them. The results are then described in section 7.3 and a sensitivity analysis of the trade-off is given in section 7.4.

## 7.1. Trade-Off Method

To determine what trade-off method to use, it is important to note that the issue of choosing a concept was considered too complex to be solved by a formula. For this reason, a qualitative method was selected over a quantitative one.

The trade-off is performed by making a trade summary table in which the columns correspond to the different concepts and the rows correspond to the different trade criteria. The height of each row is set proportional to the weight of the corresponding criteria. The cells are then given a color dependent on how well the concepts score for given criteria. Cells are colored green if the concept is excellent and exceeds the requirements for the specific criteria, blue if it meets the requirements, yellow if there are some correctable deficiencies and red if the concept has considerable deficiencies.

Once the cells have all been graded, i.e., colored, the winner of the trade-off can be determine visually by comparing the overall color of the columns corresponding to the different concepts.

## 7.2. Trade-Off Criteria and Weights

The criteria used to compare the concepts are complexity, performance, reliability, cost, sensitivity and sustainability.

The complexity of the design is important to take into consideration as the Space Truck is set to launch in 2020. A complex design would increase the development time and as a result might not be feasible given the set deadline. Because this deadline is quite important, it was decided to assign a high weight to this criteria. The weight for the complexity criteria is 0.3.

The Space Truck is meant to support multiple payloads made by different customers. As these customers rely on the correct functioning of the Space Truck, reliability is a very important criteria. Also, considering the Space Truck is a mission demonstrator the failure of this mission would increase the likelihood of the project not being continued. Therefore, the reliability criteria has been given a high weight of 0.2. This is, however, lower than the weight of the complexity criteria. This is due to the fact that it is difficult to reduce the complexity once a design concept has been chosen. The reliability on the other hand, can be increased quite easily by choosing components with flight heritage and/or by testing the design.

The performance is related to the resources available for the payload. As the Space Truck should be as versatile as possible it is desirable to keep the performance high. However, considering that the Space Truck is a demonstrator, the reliability is considered more important. Therefore, the weight for the performance criteria is chosen to be 0.15. Furthermore, the performance criteria is split up into four sub-criteria: payload mass, payload power, data rate and pointing accuracy. As it is impossible to have a payload unless a sufficient amount of mass and power is available, these sub-criteria are considered the most important and each make up 35% of the performance criteria. Having a large data rate would allow the payload to send more

data through and as a result is also quite important. Thus, the data rate sub-criteria makes up 20% of the performance criteria. Pointing accuracy is also taken into account, making up 10% of the performance criteria. Its low weight is due to the fact that the Space Truck is not necessarily required to have a payload that requires pointing. However, as having a better pointing accuracy would widen the possible payloads, it is still taken into account.

The Space Truck being a university satellite, the cost involved is quite important. However, as a lot of parts and services are likely to be sponsored, the overall cost will likely be decreased by a substantial amount, regardless of the design. The cost criteria has therefore been given a weight lower than that for performance. The weight for the cost criteria has been set at 0.15.

When small changes in major design parameters result in large changes in the design, the design is considered to be sensitive. For this trade-off, the main design parameters for which sensitivity is considered are mass and power. If a concept is more likely to go over the mass limit, it may become infeasible due to there not being enough mass left for the payload. Likewise, if the power is likely to greatly decrease due to small design changes, there might not be enough power left for the payload, rendering the design infeasible. Therefore, a less sensitive design is desirable. The sensitivity criteria has been given a weight of 0.15 as it is considered on par with performance and cost.

Sustainability is important to keep in consideration in any design. However, due to the fact that the sustainability considerations for the different design concepts are quite similar, this criteria has been given the lowest weight of 0.05.

## 7.3. Trade-Off Results

The scores are given based on intuition and by comparing the different concepts. The results have been summarized in Table 7.1 for the performance subcriteria and in Table 7.2 for the main criteria.

Table 7.1: The trade summary table summarizing the results of the trade-off for the performance criteria for the different design concepts

| | Maximum simplicity | Maximum power | Maximum reliability |
|---|---|---|---|
| Payload Power | B Low payload power | VG Very high payload power | G High payload power |
| Payload Mass | VG Very high payload mass | VB Very low payload mass | G High payload mass |
| Data Rate | G Low data rate | VG Very high data rate | G High data rate |
| PA | VB No pointing | Very high pointing accuracy VG | G High pointing accuracy |
| Peformance | B Bad | B Bad | G Good |

Table 7.2: The trade summary table summarizing the results of the trade-off for the different design concepts

| | Maximum simplicity | Maximum power | Maximum reliability |
|---|---|---|---|
| Complexity | VG No deployables Passive ADCS Simple layout | VB Deployable panels Active ADCS S Band antenna | B No deployables Active ADCS Complex Layout |
| Performance | B See Table 7.1 | B See Table 7.1 | G See Table 7.1 |
| Reliability | VG Too simple to fail | B Higher likelyhood of failure due to complexity | G Reliable due to redundant systems However, complex so not excellent |
| Cost | VG 43,920 EUR | B 82,520 EUR | G 66,720 EUR |
| Sensitivity | G Power sensitive | B Very high mass sensitivity | VG Low sensitivity |
| Sustainability | B No de-orbit | G De-orbit pointing | G De-orbit pointing |

For the first concept both the performance and the sustainability are lacking. The lack of an active ADCS causes a decrease in available power since the satellite is not able to point towards the Sun, and thus performance is decreased. Since the satellite is not able to point, the CubeSat is not able to actively increase its surface area in case the satellite should be de-orbited. The other concepts have an active ADCS and thus they will de-orbit faster, as explained in chapter 20. Since the first concept uses simple components which are designed to be too easy to fail, it gets an excellent score for reliability. This concept also performs excellently for the criteria of cost, since no complex and thus expensive components are required. The

power available for the payload is limited and thus a small change in the design can lead to significant effects for the payload. If the power used by the subsystems, not including the payload, increases too much, the available power may be insufficient to support the payload. Hence, the first concept is quite critical to power. Since this is the only parameter that scores high in the sensitivity analysis it is still sufficient.

The second concept maximizes available power, so it is able to support payloads that require a lot of power and have a high data rate. However, since the mass available for the payload is very limited, this automatically limits the use of high performance payloads. The second concept is rated insufficient for reliability, cost and sensitivity. Since this concept uses more complex subsystems it has a higher chance of failure. The deployable solar panels and implementation of an S-band antenna increase the complexity of the design to a great extend. The second concept therefore scores very poorly on the complexity criteria. Since the mass left over for the payload is relatively small, it has a high sensitivity, as explained in subsection 6.2.2. The cost for this concept is the highest of all concepts by a significant margin. Therefore, it has the worst score.

The third concept was intended to maximize the reliability of the bus by adding redundancy for essential subsystems. However, it was later realized that this would complicate the design and as a result, might decrease the reliability. Since the design freedom for the payload is not very limited by any of the parameters assigned to performance it is given a sufficient score. This automatically makes the payload less sensitive for small changes and thus a high score is assigned to sensitivity. Cost is lower than that for the second concept, yet higher than the cost for the simple design concept. The third concept thus has a score for the cost criteria to reflect this. The third concept has no deployable solar panels or other complex systems but due to the complexity added by the redundancy, it is still given an insufficient score.

By visually inspecting Table 7.2, it becomes obvious that the best design concept is the one that maximizes simplicity. Therefore, this concept is selected for further design activities.

## 7.4. Trade-Off Sensitivity

In order to assess the sensitivity, different methods are applied. Firstly, the bias of different grading schemes is investigated and then the impact of the removal of one criteria or a variation in the respective weights is studied.

Different grading schemes are utilised to quantify the criteria and simplify the comparison. The three grading schemes discussed are ascending scores (0,1,2,3), logarithmic scores (0,1,10,100) and positive and negative scores (-2,-1,1,2). In addition averaging of the scores can be applied to compare the grading schemes. For the positive and negative scheme the largest difference in relative grading is found while the scattering is significantly smaller for the other two schemes.

The impact of a high score is increased for a logarithmic and positive and negative scheme. This is favourable to have better distinguishable results, but may also create the risk of excluding concepts that are similarly suitable.

From the variation in weights the criticality of the criteria can be assessed. The criteria can be divided into three categories: critical effect, strong effect and marginal effect. Critical refers to one option becoming significantly better compared to the previously preferred option. A strong effect means that two concepts become approximately equally favourable while marginal effects do not cause a significant change in trade-off outcome. It should be mentioned that the criticality of a criteria does not only depend on its weight. If the grading difference is small the effect is decreased. If the factor strongly favours or downgrades an option its importance increases. Due to this phenomena the effect of cost is for example reduced while it increases for sustainability.

For each of the criteria, the sensitivity has been investigated by varying the criterias weight and the concepts scores. The results were then summarized in Table 7.3. When looking at Table 7.3, it can be concluded that the sensitivity of the trade-off criteria is reasonable. Nevertheless the difference between weight and impact for power and cost can be balanced to increase the impact of cost for the trade-off. The criticality analysis was in this case performed for the positive/negative grading scheme and it can be assumed that the impact of certain criteria shift

for different grading schemes as the difference decreases.

Table 7.3: Criteria categorization and weights

| Criteria | Effect | Weights |
|---|---|---|
| Complexity | critical | 0.3 |
| Reliability | critical | 0.2 |
| Power | marginal | 0.0525 |
| Sustainability | marginal | 0.05 |
| Cost | strong | 0.15 |
| Mass | marginal | 0.0525 |
| Sensitivity | strong | 0.15 |
| Data Rate | marginal | 0.03 |
| PA | marginal | 0.015 |

# 8 Structures

The structure of the satellite has the role of holding all other components in place and providing the necessary stiffness such that the satellite can survive all loads during its lifetime, mainly those during launch. The structure is comprised of a primary structure which holds the other bus subsystems and the payload adapter plate, designed for the payload to sit on. Both are verified to withstand launch loads.

## 8.1. Primary Structure

When choosing the primary structure, three different companies that sell 2U structure are considered, ISIS from Delft, Pumpkin Space from San Francisco and Clyde Space from Glasgow. ISIS offers two 2U structures, the traditional one and the Long Stack (LS), as does Pumpkin Space who offers a skeletonized and a solid version of their structure. Clyde Space offers one 2U-sized structure. The criteria that were considered during the trade-off were layout, cost, location of company, mass and material.

The outcome of the trade-off was to choose the ISIS 2U LS. As can be seen in Figure 8.1, this structure has a preferable layout for the Space Truck concept, providing 53 mm for the payload at the top, as well as a stack height of 144 mm for the bus subsystems. ISIS structures are designed so that all subsystems can be easily accessed during and after assembly. This structure has a mass of 198 g, including stack rods. [1]

The full trade-off between the different structures can be found in the Midterm Report [13]. GTM Advanced Structures, the company that manufactures structures for ISIS, has generously offered to sponsor the project.

Figure 8.1: The ISIS 2U Long Stack

## 8.2. Verification

Although the ISIS 2U Long Stack has flight heritage since 2017, [2] verification is performed to ensure the structure can survive the necessary load environments. This is done by analyzing the

[1] https://www.isispace.nl/wp-content/uploads/2016/02/ISIS-CubeSat-Structures-Brochure-v1.pdf [Retrieved on 09-05-2019]

[2] https://www.isispace.nl/product/2-unit-long-stack-cubesat-structure/ [Retrieved on 21-06-2019]

CAD drawings of the ISIS 2U LS. In order to find an approximation of the moment of inertia, the structure is simplified as four beams at the corners of the structure. Only the Steiner's terms are considered, giving a moment of inertia of $I = 4A \cdot 0.05^2$. The total cross sectional area is taken to be four times the area of one of the corner beams. It is assumed that the center of mass is located at the geometric center. In order to find the natural frequency of the structure, it is modelled as a spring with a mass at the end. The equations used are given in Equation 8.1 and Equation 8.2, where $E$ is the E-Modulus, $A$ is the cross sectional area, $L$ is the length, $m$ is the mass and $I$ is the moment of inertia and all values are given in S.I. Units.

$$f_{n_{long}} = \frac{1}{2\pi}\sqrt{\frac{EA}{Lm}} \tag{8.1}$$

$$f_{n_{lat}} = \frac{1}{2\pi}\sqrt{\frac{3EI}{L^3 m}} \tag{8.2}$$

Because of the crude moment of inertia and spring model, very conservative values are used for the mass and length of the satellite. Requirement SC-GEN-1010 from chapter 4 specifies that the satellite mass shall not exceed 2.5 kg, so this mass is used. Requirement SC-GEN-1100 specifies that the satellite shall not exceed a size of 3U, meaning that the longest possible dimension is 34 cm. As a conservative estimate, the mass is considered to be centered around $L = 0.34$ m. The result of this analysis is that the lowest natural frequency of the structure is 118 Hz, in the lateral direction.

In the Baseline Report, it is found that the most critical natural frequency requirement is given by the Polar Satellite Launch Vehicle (PSLV) which requires that the longitudinal natural frequency is greater than 60 Hz, which is easily fulfilled by this design [12]. It should be noted that the orientation of the CubeSat in the launcher is unknown, so the strictest natural frequency requirements applies to all axes.

## 8.3. Material Characteristics

According to the CubeSat standards[3], there are two materials that are recommended for structural elements, Aluminium 7075 and 6061-T6. These two materials are recommended because they have similar expansion coefficients to CubeSat deployers. Their material characteristics can be found in Table 8.1. Aluminium 7075 is stiffer and has a significantly higher yield and ultimate strength. Although it's density is higher than that of Aluminium 6061-T6, it is decided to use Al 7075 for the construction of additional elements due to these superior material characteristics.

Table 8.1: Properties of Aluminium 7075 [4] and 6061-T6 [5], the two recommended alloys for CubeSat structures.

| Property | Al 7075 | Al 6061-T6 |
|---|---|---|
| Yield Strength | 503 MPa | 276 MPa |
| Ultimate Strength | 572 MPa | 310 MPa |
| Shear Strength | 331 MPa | 206 MPa |
| E-Modulus | 71.7 GPa | 68.9 GPa |
| Density | 2.81 g/cc | 2.7 g/cc |
| Poisson's Ratio | 0.33 | 0.33 |

## 8.4. Payload Adapter Plate

In order to separate the payload from the bus, a payload adapter plate is designed. The design of the bus is meant to be able to support a variety of payload options according to the Space Truck concept. The mass allocated to the payload in the budget is 500 g. Thus, this will be

[3] http://org.ntnu.no/studsat/docs/proposal_1/A8%20-%20Cubesat%20Design%20Specification.pdf[Retrieved on 21-06-2019]
[4] http://asm.matweb.com/search/SpecificMaterial.asp?bassnum=MA6061T6 [Retrieved on 21-06-2019]
[5] http://asm.matweb.com/search/SpecificMaterial.asp?bassnum=MA7075T73[Retrieved on 21-06-2019]

the mass of the payload in a worst case scenario. The worst case distribution of this mass for a modal analysis is as a point in the center of the plate.

In order to analyze the modal properties of the plate, the deflection of the plate in response to a point force is found. In Chapter 11 of "Demystifying Numerical Models", the Navier solution to the bending of a simply supported square plate is given by Equation 8.3. [22] Here, $D$ is the plate stiffness, $F$ is the point force, $L$ is the length of the sides of the plate, $t$ is the thickness, $w_{max}$ is the maximum deflection and $v$ is the Poisson's Ratio and all units are given in S.I. units.

$$w_{\max} \approx 0.01160\frac{FL^2}{D} \qquad D = \frac{Et^3}{12\,(1-v^2)} \tag{8.3}$$

The CubeSat has a base of 10x10 cm so the length is set to $L = 0.1$ m. By dividing the deflection by the force applied, the spring constant can be found to be $k = 5.55 \cdot 10^{13}t^3$. Using the equations for the natural frequency of a spring with a mass at the end (Equation 8.4) and setting the mass to 0.5 kg and the natural frequency to 60 Hz, a plate thickness of 1.09 mm is found. In accordance with aerospace standards, a safety factor of 1.5 is used to arrive at a plate thickness of 1.6 mm.[6]

$$k = \frac{F}{w_{max}} = \frac{D}{0.0116L^2} \qquad f_n = \frac{1}{2\pi}\sqrt{\frac{k}{m}} \tag{8.4}$$

It must also be calculated whether the plate can withstand shear forces that occur during launch. The maximimum launch loads that are stated for the Vega rockets and the Falcon 9 in their online user manuals are 7 g and 8.5 g respectively. [7] [8] The launch loads for the PSLV are not known since the user's manual is not published online. Taking a conservative value of 15 g for the maximum launch acceleration and multiplying by the maximum mass of the payload, 0.5 kg, a force of 73.5 N is found. The shear strength of Al 7075 is 331 MPa. The force of the payload would have to act across a length of 0.14 mm in order to shear through a 1.6 mm thick plate. This is four orders of magnitude smaller than the length of the plate, which is considered acceptable.

The calculations performed in order to size the plate are verified by comparing to the thickness to that of other subsystems. The ADCS has a mass of 400 g, which is in the same order of magnitude as that of the payload. The thickness of the aluminium plate which the ADCS sits on is also 1.6 mm, so this is considered sufficient evidence that the calculations are performed correctly.

An engineering drawing of the payload adapter plate can be found in Appendix A. Holes have been drilled at the appropriate locations to bolt the plate to the primary structure. Using CATIA and a density of 2.81 g/cm$^2$ a mass of 42 g is calculated for the payload adapter plate.

[6] https://ntrs.nasa.gov/archive/nasa/casi.ntrs.nasa.gov/20140011147.pdf [Retrieved on 21-06-2019]
[7] https://www.spacex.com/sites/spacex/files/falcon_users_guide.pdf [Retrieved on 21-06-2019]
[8] http://www.arianespace.com/wp-content/uploads/2015/09/Vega-Users-Manual_Issue-04_April-2014.pdf [Retrieved on 21-06-2019]

# 9 Payload

The payload for this mission will consist of two modules that will be focused on education. For one of the modules, primary school children from The Netherlands were asked to send in ideas of what the satellite should do in space. The deadline for sending in the ideas and questions was on the 17th of May 2019. One of those ideas is selected and a payload will be designed that will answer that question. The primary school module will be discussed and designed in section 9.3.

The second educational payload module will consist of a sensor that can provide data which can be analysed by high school children in a course that focuses on doing calculations on satellite data which is called "satellieten en aardobservatie" (Satellite and Earth Observation)[28]. The course currently uses the data of the Copernicus satellite program which focuses on earth observation. This will be supplemented by data from the second educational payload [13]. The second educational module will be further discussed in section 9.4.

During the design of the education payload modules, the DSE group worked together with the educational department of the VSV that is responsible for the implementation of the satellite in the educational program. The VSV was updated by weekly meetings where they gave the DSE group feedback on the progress of the design of the payload. Since the concepts of the payload were communicated to the DSE group on the 21st of May 2019, the DSE group had limited time to do the preliminary design and the detailed design of the payloads. Further design of the payload is necessary and the plans for after DSE are presented in chapter 21.

For future missions, the payload will be fully isolated from the satellite bus such that people can make their own payload module which has to adhere to some constraints. The payload will then adhere to the plug and play concept in which the payload can be plugged into the spacecraft bus and will be fully operational. A data sheet has been made in which these requirements and constraints for a payload module. It can found in Table 15.5. The payload module can then be tested separately from the bus. This procedure is further explained in chapter 19.

## 9.1. Payload Restrictions

The payload modules have some restrictions that influence the choice of the different options for both the primary school and the high school module. The available resources that the bus provides to the payload are summarized in Table 9.1. The available volume for the payload is split up into two sections of 100 x 50 x 50 *mm* and the mass is split up into 250 gram modules. If there is still a gap in the size and mass budget for one payload, it can still be used for the other payload. The power and data rate are not driving requirements for the payload design. If the combined payloads exceed the set limit for the data or power requirement, the time that the payload is operational can be decreased and be made compatible with the data and power budgets.

Table 9.1: Resources available for the combined payload modules

| Mass [gram] | Volume [mm] (l x w x h) | Data available per pass [kB] | Power available per orbit [mWh] | Pointing accuracy available [degrees] | Voltage [V] | Micro controller |
|---|---|---|---|---|---|---|
| 500 | 100 x 100 x 50 | 4000 | 500 | 1 - 5 | 3.3/5/unregulated | Arduino Nano |

## 9.2. Payload-OBC Connection

The payload needs to be connected to the OBC, since the payload modules are not able to process the data to send it to the transceiver. Another advantage of connecting the payload to the OBC is that the OBC can perform some debugging of the payload when necessary. There are several options to connect the payload to the OBC. Three different options are shown in Figure 9.1

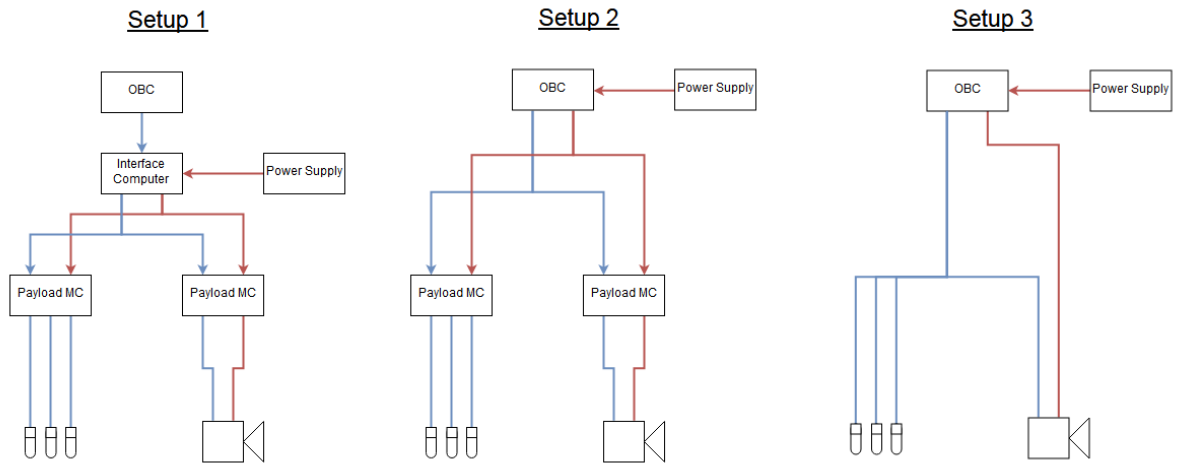


Figure 9.1: Payload-OBC connection options (the payload on the left shows three sensors and on the right a camera module)

Set up three shows a direct connection between the payload and the OBC. An advantage of a direct connection is that there are less points of failure present in the system. However, the concept of using a modular (Plug and Play) payload implies that different instruments can be connected to the Space Truck and then the bus can interpret the data without re-programming the OBC to be compatible with a new instrument. Since the plug and play concept of the payload is not supported by using the third setup, this option is discarded. Setup 2 uses a micro controller in between the payload and the OBC. This creates the opportunity to program the micro controller to make the total payload module (instrument + micro controller) compatible with the OBC. In the first set up, an extra interface computer is added between the micro controller of the payload and the OBC. The initial idea was that the interface computer performed some debugging on the payload when non-nominal conditions occurred in the payload. However, the OBC that is included in the final design has the processing capability to perform the debugging on the OBC itself. The interface computer thus becomes unnecessary for the design of the system. It will also increase the points of failure of the system and make the connection more complex then needed and thus this option was discarded. The payload will be connected to the OBC via a micro controller. For this design, an Arduino Nano will be used as a micro controller. The full trade-off can be found in section 13.3.

## 9.3. Primary School Payload

As described in the introduction of the chapter, the Primary School Payload will answer one or multiple questions from the primary school children. In this section, the concepts for this module are presented and one of the concepts is selected for a more detailed design.

### 9.3.1. Analysis of the Concepts

A preliminary selection of the questions was made in which the feasibility of the design was taken into account. Questions that were obviously not feasible or were too focused on individual children were discarded e.g. ”Can I bring my teddy bear in the satellite”. The DSE group and the VSV wants to use this module to also inspire other primary school children in space and

not only one individual.

After the first selection round, the feasibility of the remaining question was analysed and some questions that could be answered using the same instrument were grouped. Three different concepts were selected that could answer the remaining questions: IR sensor(s)/camera, Dice concept and an camera. All three concepts were further researched and the advantages and development challenges were identified.

### IR sensor(s)/camera

Either an IR sensor or IR camera can be used to answer the following questions of the primary school children.

- What is the temperature of the moon?
- Is it cold in space?

An IR camera has the advantage over the sensor, because it directly provides an visual image that shows the data. The image helps the children in understanding what the data means [18]. A challenge that occurs when trying to measure objects in space is that the temperature range of the objects in space are often not covered by the temperature range that the instruments are able to detect. The cold temperatures of both the dark side of the Moon (average -173 °C [1]) and the vacuum of space (average -270 °C [2]) can not be measured with COTS sensors and instruments that fit in the size of that is assigned to the payload module[16].

An additional challenge occurs when researching the field of view of the instrument needed to measure the temperature of the moon. From the earth's surface, the full moon is 0.5° [3]. This means that the instrument needs either a high resolution or a small field of view angle. This often increases the size of the lens that is attached to the instrument. An overview of the identified advantages and challenges can be found in Table 9.2

The second question can also be answered by providing some temperature data of several subsystems of the satellite itself. The different subsystems that are able to provide temperature data can be found in [REF to thermal section table? If it will be there...]

Table 9.2: Advantages and development challenges for the IR sensor/camera

| Advantages | Development challenges |
|---|---|
| - COTS options available | - Needs pointing accuracy |
| - Availability to answer more questions | - Limited measurable temperature range |
| - Space for redundancy (with sensors) | - High resolution necessary (for moon pointing) |

### Dice concept

One of the primary school children asked the following question:

- Can you play rock paper scissor in space?

After a discussion with the VSV, it was decided that the payload would produce some pictures in which this question can be answered and eventually a game could be played with the satellite. Several concepts were made, but after a discussion with some experts[4] and the VSV one concept was selected based on the feasibility of the design. The selected concept to answer this question is visualized in Figure 9.2. In this module there is a camera that is pointing towards two floating dice that are in a separate section. The camera and the dice are separated by a window such that the dice are not able to leave the field of view or hit the camera and the micro controller. An additional window is present at the outside of the satellite such that a picture can be taken from the dice floating in the box with earth in the background. The rock, paper and scissors sign are

[1] https://www.space.com/18175-moon-temperature.html[Retrieved on 02-06-2019]
[2] https://sciencing.com/temperatures-outer-space-around-earth-20254.html[Retrieved on 02-06-2019]
[3] https://lco.global/spacebook/using-angles-describe-positions-and-apparent-sizes-objects/[Retrieved on 04-06-2019]
[4] Dr. Ir. Chris Verhoeven of the department of microelectronics of the TU Delft and Dr. Stefano Speretta of the Aerospace Engineering Faculty of TU Delft

visible on the sides of the dice. The dice have a different color to make a distinction between the two. The camera takes pictures of the floating dice and a winner can then be identified.

The advantages and development challenges can be found in Table 9.3. A more detailed design where all these challenges are addressed and possible solutions are provided, can be found in subsection 9.3.4.

Table 9.3: Advantages and development challenges for the dice concept

| Advantages | Development challenges |
|---|---|
| - Easy for children to visualise and understand<br>- New concept<br>- Children are interested in games | - Extensive testing and verification due to free moving parts<br>- No COTS options for total module<br>- Getting both the dice and earth in focus |

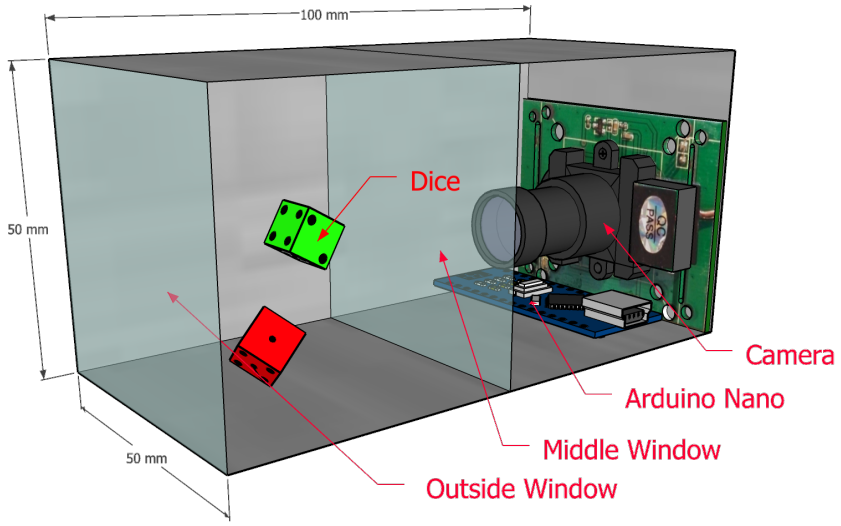


Figure 9.2: Preliminary sketch of the dice concept

### Camera

With a camera module the following questions from the primary school children can be answered:

- How does the blood moon look from space?
- How does a hurricane look from space?
- Can the satellite measure how many cm the moon is?

The questions considering taking pictures of the moon result in the same challenges for the resolution and field of view occur as described in subsection 9.3.1. To answer the questions focused on the moon, an accurate model of the orbital trajectory needs to be uploaded and the satellite need to be able to point to the moon with a sufficient accuracy such that the moon is visible in the picture. The model is required to know at which point in time the satellite needs to point the camera to the moon. With the model and the pointing accuracy, a possible solution to implement the hurricane question in the payload is to up link the coordinates of where hurricanes are predicted to be in the near future and then the satellite knows when to point to the earth surface to take a image of the hurricane. An overview of the advantage and challenges of this concept is presented in Table 9.4.

Table 9.4: Advantages and development challenges for the camera module

| Advantages | Development challenges |
|---|---|
| - COTS options available<br>- Availability to answer more questions | - Needs pointing accuracy<br>- High resolution necessary (for moon pointing) |

### 9.3.2. Selection of the Primary School Module

The different concepts were presented to the VSV and after a discussion with the DSE group, both parties agreed that the feasibility of dice concept need to be further researched during the last weeks of the DSE. This concept was chosen because the children could get in contact with space through playing a simple game. This also has never be done on a satellite, which is not the case for the other two options. A back-up option will also be researched in case the dice concept ends up to be infeasible. The back-up option is discussed in subsection 9.3.6.

### 9.3.3. Implementation of the Dice Concept

The idea of the dice concept is that pictures would be available every day, preferably multiple times per day, however, this is highly dependent on the amount of passes the satellite makes above The Netherlands. The two dice would have a different color and the children can than select a color and the satellite will send a picture in which the orientation of both dices is shown. Some complications that can occur and possible solutions for it can be found in subsection 9.3.5. Another possible idea is to only place one dice in the compartment such that the children can play against the satellite. The payload will be designed for two dice since this requires more complexity in the design (eg. for the illumination of the dice described in Figure 9.3.4). The payload module designed for two dice will also be compatible for one dice.

To visualize how the module will operate, a flow diagram is made, which can be found in Figure 9.3. Software will be used to check if the dice have moved since the last picture and thus different sides of the dice are visible. It will also check if only one side of both dice is visible. A threshold is set to accept pictures with a range of orientations for both dice. This checks if one dice is not hidden behind the other. The ADCS will be used if the dice did not move with respect to the last picture that was taken. The slew rates, that can be found in Table 14.2, which can be achieved with the ADCS are relatively high and can thus be used to ”shake” the dice.

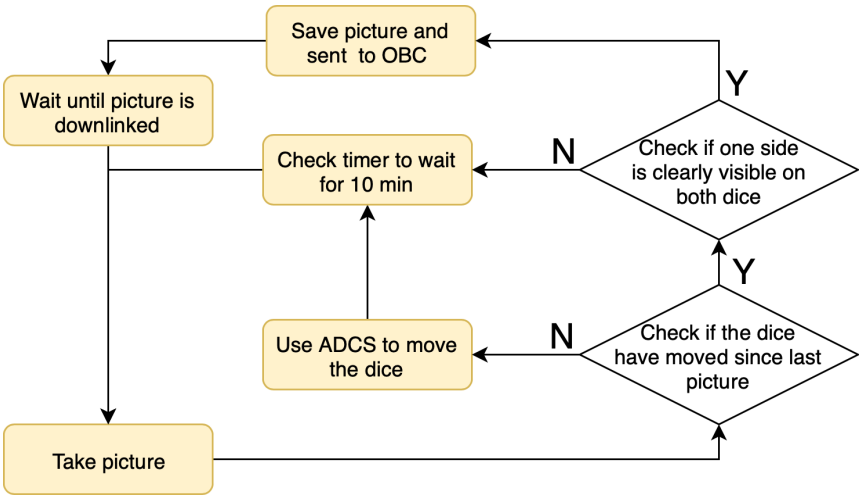


Figure 9.3: Flow diagram of the operations of the dice concept

### 9.3.4. Dice Concept Design

The dice concept is broken down into parts that can be analysed separately. Each of the parts the design challenges will be identified and possible solutions will be discussed. All the elements are summed up below. During the selection of all the different elements, the size and the mass are considered such that the total payload module still meets the requirements specified in section 9.1.

- Camera + Lens
- Flash
- Dice
- Window
- Support Structure

### Camera + Lens

Before the camera and the lens are selected, the specifications that are required are identified. First, the concept requires that both the dice and earth are in focus. This implies that the Depth of Field (DoF) of the camera needs to start at the first possible location where the dice can be located and end at infinity. The DoF is dependent on the type of sensor of the camera and the aperture size, focal length and focus distance of the lens. It also depends on the Circle of Confusion (CoC) that is selected. The CoC is defined as "how much a point needs to be blurred in order to be perceived as unsharp" [5]. A small CoC means that the DoF is increased since a larger depth of the picture is perceived as sharp. The average digital camera has a standard circle of confusion between 0.005 up to 0.03 mm [6]. The DoF of the camera can be calculated using an online calculator [5]. For the relevant equation refer to the validation and verification part. When all the variable described above are quantified, the calculator calculates the nearest and furthest distance of acceptable sharpness (respectively $D_n$ and $D_f$). The difference between these to parameters is defined as the DoF.

The nearest distance of acceptable sharpness must thus be smaller than the first possible location of the dice to the lens to get the dice in focus. This distance is determined by the length of the lens and camera combined and the position where the window between the dice compartment and the camera is located. Decreasing the volume of the dice compartment by moving the middle window further from the camera, will allow the camera to require a larger nearest distance of acceptable sharpness. However, an increase in the length of the camera and lens set up will decrease the allowable distance. These two influences thus need to be balanced to find a solution. Both the dice also need to be in the Field of View (FoV) of the camera. The required FoV is also determined by the distance between the end of the lens and the middle window.

As a next step, a combination of possible cameras and lenses were researched and a solution has been found where both the DoF and the FoV meet the set requirements. The combination of a 2MP ArduCAM mini[7] with a 1.3 MM Computar lens [8] lead to a feasible design. The main advantage of the ArduCAM over other camera modules was the compatibility of the camera with the Arduino Nano. The important parameters of both the camera and the lens are presented in Table 9.5.

Table 9.5: The specifications of the ArduCAM and the lens combined

| Mass [g] | Size [mm] l x w x h | Power [mW] | Resolution [MP] | Data per picture [kB] | Aperture size | Focal length [mm] | Sensor-size [inch] | FoV [degree] |
|---|---|---|---|---|---|---|---|---|
| 37.2 | 33 x 24 x 34 | Normal: 350<br>Low: 100 | 2 | 200 | F/2.8 | 1.3 | 1/4 | H: 151.0<br>V: 117.6 |

When the focus distance of the camera is set to 40 mm and the circle of confusion at 0.015 mm, the camera is able to achieve a $D_n$ of 20 mm and a $D_f$ at infinity. Which means that the distance from the lens to to the middle window should be at least 20 mm to get both the dice and earth in focus. To get the full dice compartment in the FoV of the camera, the lens needs to be at a minimum distance of 22 mm from the middle window. Thus to meet both the requirements on the DoF and FoV, the middle window will be located 22 mm from the lens of the camera.

Verification & Validation To verify the calculations from the online DoF calculator, Equation 9.1, Equation 9.2 and Equation 9.3 are used.

$$H = \frac{f^2}{Nc} + f \qquad (9.1) \qquad D_n = \frac{s(H-f)}{H+s-2f} \qquad (9.2) \qquad D_f = \frac{s(H-f)}{H-s} \qquad (9.3)$$

[5] https://www.cambridgeincolour.com/tutorials/depth-of-field.htm[Retrieved on 12-06-2019]
[6] https://www.dofmaster.com/digital_coc.html [Retrieved on the 13-06-2019]
[7] http://www.arducam.com/arducam-mini-released/ [Retrieved on the 13-06-2019]
[8] https://www.vision-dimension.com/en/lenses/mini-lenses-s-mount/fisheye/computar-s-mount-lens-h1328kp/213 [Retrieved on the 13-06-2019]

In these formulas, $H$ is the hyperfocal distance [9] in $mm$, $f$ is the focal distance in $mm$, $N$ is the f-number (aperture size), $c$ is the CoC in $mm$, $s$ is the focus distance in $mm$. The default CoC of the DoF calculator is found to be 0.0015 mm. Using this value for CoC in the equations, the same results were found.

To validate the equations and the online calculator, a small experiment was set up to visualize the DoF of the camera and lens, which can be seen in Figure 9.4. A similar sized camera and lens were used for this experiment [10]. The specifications of the camera and lens were used to calculate the DoF. The position of the dice was used to measure the DoF in the experimental set up. The calculated DoF matched the DoF of the experimental set up reasonably well. Since $D_n$ and $D_f$ can not be quantified from the Figure 9.5, no numerical value for the DoF of the experiment can be given.


Figure 9.4: Top view of the experiment to validate the DoF calculations

Figure 9.5: Picture from the camera that was used in the experiment

### Windows

For the both the middle and the outside window two different materials were considered. Both Quartz and Fused Silica are used in space application such as lenses for instruments or the windows for ISS and the Apollo missions [36]. Both materials are used because of they are highly resistant against thermal shock. The main difference between the two materials is that Quartz is made from crystalline silica and Fused Silica is composed of a non-crystalline silica glass [11]. This lowers the transmission in the UV-spectrum for Quartz compared to Fused Silica. This makes Quartz the best option for the windows, because it protects the components inside the payload from UV-light.

An additional idea for the outside window is to use it as a lens if the furthest distance of acceptable sharpness did not reach infinity. If after testing the camera and the lens the sharpness of object located at ”infinity” appears to be a blurry, an additional lens from Quartz can be used for the outside window.

A critical point in the structural design of the payload is the physical connection between the middle window and the outside window with the aluminum parts. Some of the available options are bolting, gluing and welding. Welding is known to be an effective connection between quartz and aluminium. One should weld for 40 minutes at 893 K [12]. Additional sizing and shaping of the windows need to be done after the DSE.

### Flash

A flash is necessary to illuminate the visible side of the dice from the camera perspective. Objects in space are only illuminated when hit directly by a source of light. Since the outside window will be pointed towards earth, the light that will be visible on the picture will come from the albedo reflecting from the earth. However, this will only light the dice from the back side and thus an additional flash is needed to light the other side of the dice. An estimate for the luminous flux of the albedo for the payload module can be estimated. The solar radiation from the albedo effect equals 410 $\frac{W}{m^2}$ [27]. The maximum area that can be illuminated by the albedo

[9] Hyper focal distance is the minimum distance from the camera at which all the object after that distance can be brought into acceptable sharpness

[10] https://www.foxtechfpv.com/fh18c-520tvl-wide-voltage-mini-camera.html[Retrieved on 16-06-2019]

[11] https://abrisatechnologies.com/2012/10/fused-silica-vs-quartz/ [Retrieved on 15-06-2019]

[12] https://www.tandfonline.com/doi/pdf/10.1080/09507118709449362[Retrieved on 12-06-2019]

light is restricted by the size of the outside window, which is 0.0007 $m^2$. This value needs to be multiplied with the luminous efficacy of albedo. However, no value of this can be found, so a to make a very conservative estimate the luminous efficacy of direct sunlight was taken, which equals 93 Lumen per Watt [27]. This results in a maximum amount of 27 lum received as back light. There is no ratio between front and back light known at which the quality of the picture will be acceptable. This thus needs to be determined by experiment. If that is tested, a LED can be selected which produces the right amount of flash needed. Due to the short operational time of the flash, the power used by it can be neglected [15].

Two LEDs are necessary to light both dice. The LEDs can not be placed along the center line of the lens without obstructing the view and thus there will be a offset of the LED with the center line of the lens. This means that it is possible that one die is obstructing the light from the LED for the other die that is located at the back of the compartment. If at least 2 LEDs are used which are placed somewhere above and below the lens, the volume that is in full shadow will be relatively small. One draw back of placing the LED in the camera compartment is that the reflection of the flash on the Quartz can lead to imperfections on the picture. This can be tested by performing a experiment with the camera set up.

### Dice

The materials looked at for the dice must have elastic properties, so as not to disintegrate or cause damage to other parts of the CubeSat. Some of the flight worthy elastomers used in spacecrafts in the past are: Flouroelastomers, Nitrile rubber and Silicone rubber.

Table 9.6: The properties of the different types of elastomers considered for dice

| Elastomer | Outgassing (%) | Density (g/cc) | Cost (US $/kg) | Temperature (Celcius) | Properties |
|---|---|---|---|---|---|
| Flouroelastomer | 0.07 | 1.81 | 13.72 | -15 to 200 | Used to make O-rings, more inert |
| Nitrile rubber | 1.06 | 1 | 2.50 | -25 to 120 | Less resistant to atomic oxygen and ozone |
| Silicone rubber | 0.1-1 | 1.06 | 2.50 | -55 to 200 | Ozone protected, and UV protected |

The temperatures mentioned in Table 9.6 is the temperature range at which the material does not lose its stable properties and remains intact. Since the density of the materials are less than 2 grams per cubic centimeter, its comparative mass with respect to the cube sat is very low. For the size of the dice, three sizes were considered: 5 mm, 7mm or 10mm (a standard dice is 10-11 mm). When a physical experiment was done as seen in Figure 9.5, 5 mm dice were seen as too small for the setup in order to get a clear picture and could increase the complexity of the manufacturing, where as 11 mm dice that are seen in the picture were too big for the compartment. That is the reason the 7 mm dice was selected. Another concern noticed in this concept is the behaviour of the dice during launch. A preliminary analysis is performed between the options of having free floating dice and having them docked till orbit insertion. A docking system for the dice is complex to design and has mechanical parts, which adds to risk. It adds to weight, needs to be tested specifically which would add to development cost and also adds to the time budget. For a free floating concept, the dice can be assumed to be soft and elastic enough not to damage the CubeSat because of launch and vibrational loads, and this will be further analysed in the next subsection (Support Structure). If the free floating dice pass the pre-launch tests, it can be used. Whereas for a docked concept, its releasing mechanism will cost a lot to validate. In all the renders and sketches from the dice concept, normal dice were used for simplicity. The dice that will be used in for this concept will have signs of rock, paper and scissor on the sides.

### Support Structure

A payload adapter plate is designed in section 8.4. The plate is designed for all feasible payloads the Space Truck could service in space. For this specific payload a further support structure is required to hold it in place. All elements discussed in this section are represented in Figure 9.6 and engineering drawings are included in Appendix A.

In order for the ArduCAM to be orientated perpendicular to the payload adapter plate so that it can take pictures of the dice, structurally sound mounting holes are required on the side of the payload bay. These are provided by the means of a beam which is attached to two of the beams of the primary structure. A L-beam is chosen as this shape is lightweight while providing

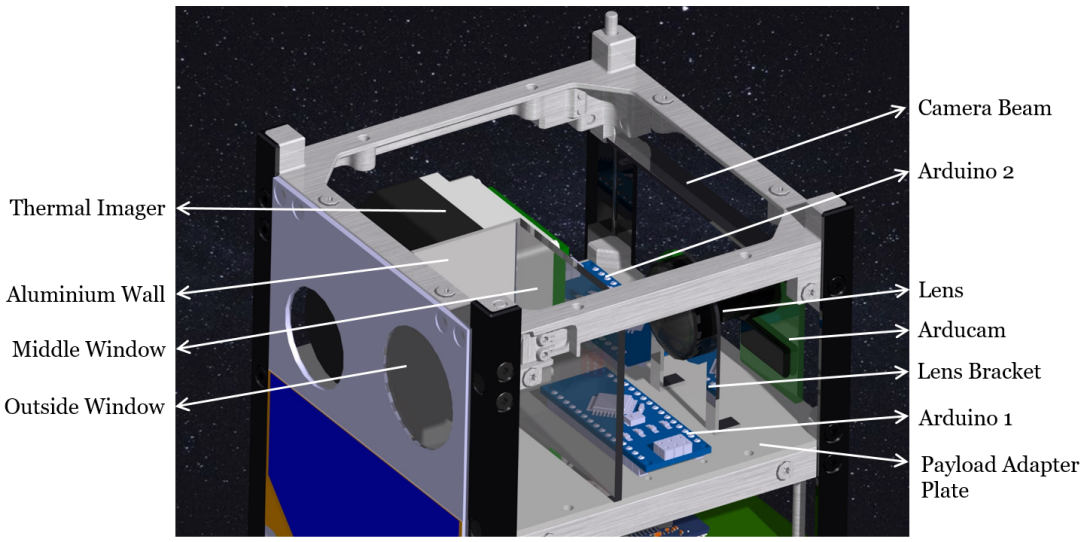


Figure 9.6: The layout of the payload with labels for the different parts labelled.

stiffness in all directions, an important consideration since the orientation of the CubeSat in the launcher is not known. The bottom of the Arducam can be attached to the payload adapter plate using solder or glue to minimize vibrations.

A more sturdy solution is needed for the lens. They extend more than 30 mm from the camera beam and weigh 17 g. In order to minimize longitudinal vibrations and loads a lens bracket is placed around the lens with two legs which are attached to the bottom of the payload bay. This solution allows the launch loads to be absorbed in axial stress of the bracket rather than bending stresses in the lens, which make the structure stiffer and less prone to failure.

To mount the Arduino Nanos in the payload bay, holes are drilled in the payload adapter plate. The mounting pattern is in imperial units and can be found online [13]. The size of the mounting holes is 0.07 inches (1.778 mm). Since a bolt which fits through this size hole should be bought in Europe it is decided to use 1.75 mm bolts and thus the holes in the plate are this size.

Verification In order to verify that the walls can withstand the impact of dice, the maximum kinetic energy they could reach is calculated. The maximum velocity that the dice could achieve is when it resonates with the maximum frequency of the launcher. The velocity of the dice will then be equal to 4.2 $m/s$. Using this number and the mass of the dice, the maximum kinetic energy ($K_{max}$) is calculated.

Next, the fundamental natural frequency for the aluminium walls is calculated using Equation 9.4 in which the plate stiffness,$D$, is calculated using Equation 8.3, $\rho$ is the density in $\frac{kg}{m^3}$, $a$ is the sides of the plate in $mm$ and $h$ is the thickness of the plate in $mm$ [8]. After this, the vibrational amplitude of the plate ($C_{mn}$) is calculated by substituting Equation 9.5 in the Equation 9.6, in which $W(x,y)$ is the corresponding shape function for the fundamental natural frequency of the plate.

The vibrational amplitude of the aluminium plates was found to be an order of $10^8$ smaller than the thickness of the plates, thus the effect can be neglected. This calculation was verified by inserting problem 9.6 from "Thin Plates and Shells" and the same result was found [8]. [14]

$$\omega_{11} = \frac{2\pi^2}{a^2}\sqrt{\frac{D}{\rho h}} \tag{9.4}$$

$$W(x,y) = \sum_{m=1}^{\infty}\sum_{n=1}^{\infty} C_{mn} \sin\frac{m\pi x}{a} \sin\frac{n\pi y}{b} \tag{9.5}$$

[13] https://www.mouser.com/pdfdocs/Gravitech_Arduino_Nano3_0.pdf[Retrieved on 16-06-2019]

[14] Dr.ing. S. Giovani Pereira Castro from the Aerospace faculty of the TU Delft provided the necessary reference to do the calculations

$$K_{\max} = \frac{\omega^2}{2} \iint_A \rho h W^2(x,y) \mathrm{d}x\mathrm{d}y \tag{9.6}$$

### 9.3.5. Further Challenges

To test if the payload module can withstand the vibrational loads from the launcher, a model needs to be made in which these vibrations are simulated. Since this might be too complex, a test set up can be made in which the launch vibrations are simulated. However, this could increase the testing costs. A trade-off for the most efficient way to test the payload needs to be made.

The movement of the dice inside the satellite need to be simulated to see how often the ADCS is needed to move the dice. Since the dice do not experience the drag that the satellite experiences, the orbital velocity of the dice and the satellite will differ [24].

Another challenge that can occur is during the vibrational test of the integrated satellite. Since there are free moving dice inside the satellite the results that come out of the vibrational test will differ slightly every time it is tested. However, since the mass of the dice is very small compared to the mass of the satellite, this effect might be neglectable, but further research is needed to test this.

### 9.3.6. Back-Up Option

The dice concept needs to be further designed and tested and this adds risk to the project, so a back-up option needs to be selected. Since the High School payload module already exists of a IR camera, which will be discussed in subsection 9.4.2, the camera concept that is introduced in subsection 9.3.1 can be chosen. The camera can be used to answer the questions from the primary school children. Additionally, the images taken from the satellite can be used in primary schools to teach the children geography. The children can try to find where on the globe the satellite took the picture such that children playfully learn geography. COTS camera modules are available and thus one can be selected according to the requirements set in section 9.1.

## 9.4. High School Payload

As an effort to introduce high school students to space and its applications, a study module is being introduced which comprises of orbital mechanics, satellites and subsystems, different types of instruments and their measurements, space debris, etc. TROPOMI is one of the instruments discussed as a part of this module along with its data. This payload is meant to compliment this data in a smaller scale.

Tropospheric Monitoring Instrument(TROPOMI) is capable of mapping the entire atmosphere on a daily basis. It is used to study atmospheric composition, by comparing light reflected by the atmosphere to direct sunlight. The instruments are sensitive to different wave lengths of light from infrared to ultraviolet [15]. In the infrared region, short wave infrared(SWIR) is measured by TROPOMI whereas long wave infrared(LWIR) is not. Two of the many suggestions provided by high school teachers were instruments capable of measuring albedo or infrared emission of the earth's surface.

### 9.4.1. Albedometer

Albedo is defined as the ratio of the amount of light reflected by a surface without being absorbed, to the amount of light received by the surface[16]. In order to estimate the reflectance of earth's surface, every point on earth must be observed from all angles for reflected light, which is impossible [26]. The current model of earth's albedo is based on long term data collection from both satellites and ground based observation systems with some assumptions and approximations. There is a lot of post data processing which involves use of cloud mask, atmospheric corrections for the reflected light absorbed by the atmosphere, anisotropic corrections, etc[26].

[15] http://www.tropomi.nl/over-tropomi/how-tropomi-works/?lang=en[Retrieved on the 12-06-2019]
[16] https://climate.ncsu.edu/edu/Albedo[Retrieved on the 12-06-2019]

With a cubesat carrying low resolution instruments working on limited power and link budget, it can be safely assumed that an albedometer is not a feasible option.

### 9.4.2. LWIR Camera

Long wave infrared radiation is emitted by an object itself, unlike short wave infrared radiation which like visible radiation is either reflected or absorbed by an object. LWIR detectors(uncooled) are made of materials like vanadium oxide(VOx) and amorphous silicon(a-Si). The spectrum is visualised in Figure 9.7.

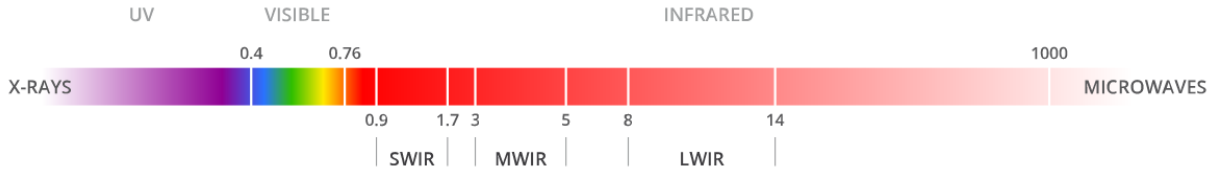


Figure 9.7: Electromagnetic spectrum[17]
in $\mu m$

Many earth observation satellites carry LWIR cameras as a payload. These are designed and developed for the very purpose of space application. Given the available resources and time schedule of the CubeSat, it is not feasible to develop a LWIR camera from scratch. Some LWIR cameras are available which would fit within the cost, size and mass budget of the CubeSat, but they are not flight proven or even made for space application. Most sensors dealing with light or electromagnetic radiation are sensitive to damage due to UV rays. With enough UV shaded lens and radiation shielding for the electronics, this risk can be reduced. The choice of the current LWIR camera is based on a similar camera being used as a payload in Phoenix CubeSat[18] which is to be launched in October, 2019. If the mission is successful, then the use of this particular camera for the mission can be validated. The size, mass, and link budget restrictions on the payload module drives the camera and lens, and their specifications are seen in Table 9.7. It must be mentioned that any part of the camera cannot be air tight. If necessary these compartment must be ventilated by a small hole so as to allow the air to escape while launch. If not, there could be a expansion of air causing an explosion, which could be small but can damage the Cubesat. In Figure 9.8, the ground coverage of a single picture taken by the LWIR camera at an altitude of 400 $km$ can be seen.

Table 9.7: Specifications[19]
of LWIR camera and lens

| Model Name | Temperature Measurement Range [degree] | Mass [g] Camera + Lens | Cost [US$/] | Camera size [mm] | Lens size [mm] | FOV [degree] | Coverage @400km [km] |
|---|---|---|---|---|---|---|---|
| FLIR tau 2 | -40 to 550 | 70 | 8,000 | 45x45x30 | 29 dia, 19 length | 32 x 26 | 250x195 |

## 9.5. Final Design Payload Module

The final layout of the Primary School and High School module is shown in Figure 9.9. The total mass of the Primary School module adds up to approximately 200 grams. The High school module only weights 70 grams, excluding the material to attach the IR-camera to the structure. The payload adapter plate weight approximately 40 grams. The total mass for the payload section thus adds up to 310 grams. An additional 190 grams can thus be used to increase the structure supporting the payloads if necessary. A close up of the final layout for the primary school module is shown in Figure 9.10.

[17] https://www.opto-e.com/resources/infrared-theory[Retrieved on the 12-06-2019]
[18] http://phxcubesat.asu.edu/[Retrieved on the 12-06-2019]
[19] https://www.oemcameras.com/flir-tau-2-640-19mm-thermal-imaging-camera-core.htm[Retrieved on the 13-06-2019]


Figure 9.8: Ground coverage of FLIR tau 2 camera with 19mm lens at an altitude of 400km

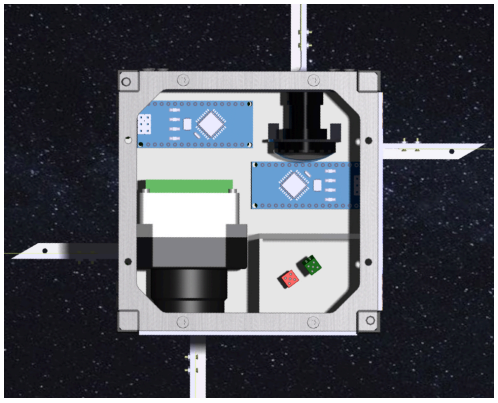

Figure 9.9: Catia render of the top view of the paylaod section

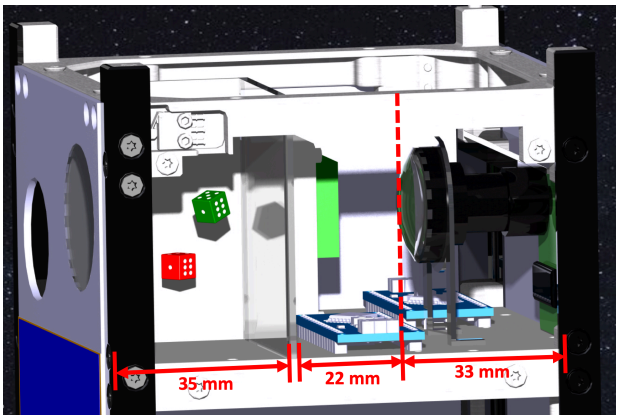


Figure 9.10: Catia render of the side view of the primary school payload module

# 10
# Communications

The communications system will allow remote control of the spacecraft and information retrieval from it. Both will be done by transmitting electromagnetic (EM) waves carrying digital data. Information from the satellite is interesting to several parties: the participating schools, the makers of the satellite, and radio amateurs along with other interested hobbyists. The schools, which are the target audience of this mission, care about the payload data, as it contains their proposed experiments. The satellite team would like to know the detailed state of the satellite as well as the payload data. Radio amateurs are people generally interested in receiving radio signals sent from space, so they would be curious about a routine satellite beacon, but payload data and/or messages from other people would be especially interesting. Thus, licensed radio amateurs will possibly be able to send messages to the satellite to use it as a relay station. Commanding of the satellite will be done using the TU Delft ground station by qualified professionals. A schematic illustration of the satellite communications is shown in Figure 10.1.

## 10.1. Physical Layer

Establishing a physical link between the ground and the spacecraft requires producing a compatible signal that is strong enough. The main obstacles are noise and distortion caused by external environment and imperfect electrical circuitry. The information carrying wave has to be distinguishable in the presence of this noise, thus the signal-to-noise ratio is a defining parameter in assessing the link quality.

The basic hardware components required for a one way link are a transmitter, a transmitting antenna, a receiving antenna and a receiver. For two-way communications the same set of hardware is required for both directions. The transmitter and receiver are often integrated into a single transceiver apparatus. Since commercial off-the-shelf components have to be used, available options from ISIS, IQ Spacecom, GomSpace, Satlab, Endurosat, Pumpkin space, NanoAvionics, Clyde Space, Astronautical Development, Antenna Development Corporation were considered. The GomSpace AX100 software-defined radio transceiver is chosen to serve as the on-board transmitter and receiver mainly because of it's power efficiency of 3.201 W, which is lower than its competitors. For a detailed trade-off the reader is referred to the mid term report [13].

The switch-based half-duplex architecture of the AX100 means constantly switching between the transmitter and receiver [2]. However, after a detailed technical risk assessment in section 16.3, it is decided that it is desirable to always have the receiver turned on. This prevents a situation where the satellite is stuck with a turned off receiver and no way to receive commands, not even a command to turn the receiver back on. The switch is also an element that is susceptible to wear and has accounted for CubeSat failures in the past. Thus, a decision is made to go for full-duplex communications architecture.

Since it is desirable to keep the power consumption and other characteristics of the AX100 it is decided to use two transceivers working simultaneously: one always kept on receive mode and the other for transmission. This facilitates a full-duplex link, the receiver is never switched off and redundancy is introduced in the system. GomSpace state that this configuration is possible [2].

Initially, a single Endurosat UHF turnstile CubeSat antenna was to be used for both transmission and reception. However, two different frequency bands need to be used for downlink

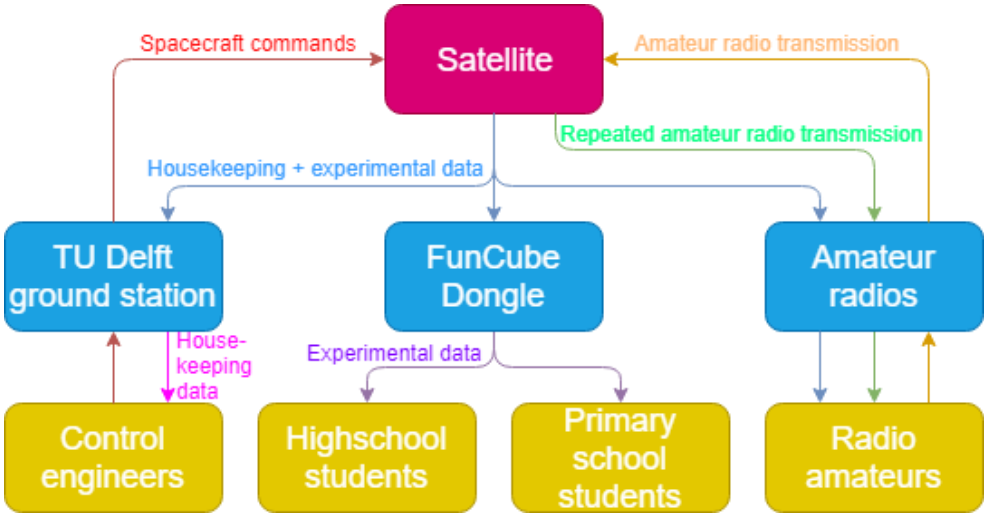


Figure 10.1: Communication flow diagram

and uplink in the full-duplex case. The second transceiver is therefore tuned to VHF and needs an additional antenna. Another turnstile antenna at the other side of the satellite was first considered, but taking into account problems with interference and the big losses that come with circular polarization mismatch, the ISIS crossed dipole antenna tailored for UHF/VHF full-duplex communications is chosen instead. The downside is a less omnidirectional, donut shaped radiation pattern that has blind spots in the axial direction of the dipole, however, these are partly compensated by the resonant effect of the satellite structure, see Figure 10.4. The dipoles produce linearly polarized waves, whereas the turnstile antennas would produce circular polarization. The worst polarization loss when receiving a circularly polarized wave with a linearly polarized antenna is -3 dB, irrespective of the wave's sense. However, using, for example, a right hand circularly polarized (RHCP) antenna to receive left hand polarized (LHCP) waves comes with a penalty of about -20 dB [35]. If a RHCP antenna is flipped over it produces LHCP waves, therefore the polarization of transmission from the ground station would have to be matched to the spacecraft orientation, introducing significant inconvenience. Opting for a linearly polarized dipole antenna therefore makes communication with the satellite simpler.

As mentioned, the TU Delft ground station will be used to send commands to the satellite on the VHF band. For easy reception of telemetry by the schools, the Funcube Dongle Pro+ receiver is proposed [13]. It comes in the form of a portable USB stick with a standard SMA female antenna port. This allows receiving the data from the satellite with only a computer and a table top antenna. A software package has to be running on the computer and the antenna should be circularly polarized for best reception, as explained before. A linear antenna is also possible, but it's orientation would have to be adjusted to match that of the linear EM wave. Some cheaper dongles are available on the market as well, however the sensitivity and noise performance of the Funcube dongle were found to be much superior, therefore it is highly recommended.

### 10.1.1. Link Budget

To ensure that the downlink and uplink can be successfully established, a link budget is calculated. It shows the received signal to noise ratio, based on which, the bit error rate can be estimated. The link budget is estimated using Equation 10.1, taken from [42] and modified to include additional factors, namely $L_{pt}$, $L_{po}$ and $L_r$.

$$\frac{E_b}{N_0}[\text{dB}] = P - L_l + G_t - L_{pt} - L_a - L_s - L_{po} + G_r - L_{pr} - L_r + 228.6 - 10\log_{10} R_b - 10\log_{10} T_s \quad (10.1)$$

$E_b$ is received energy per bit, $N_0$ is the noise spectral density, $P$ is signal power generated by the transmitter, $L_l$ is the transmitter-to-antenna line loss, $G_t$ is the transmitting antenna gain, $L_{pt}$ is the transmitting antenna pointing loss, $L_a$ is the transmission path loss, $L_s$ is the free-space

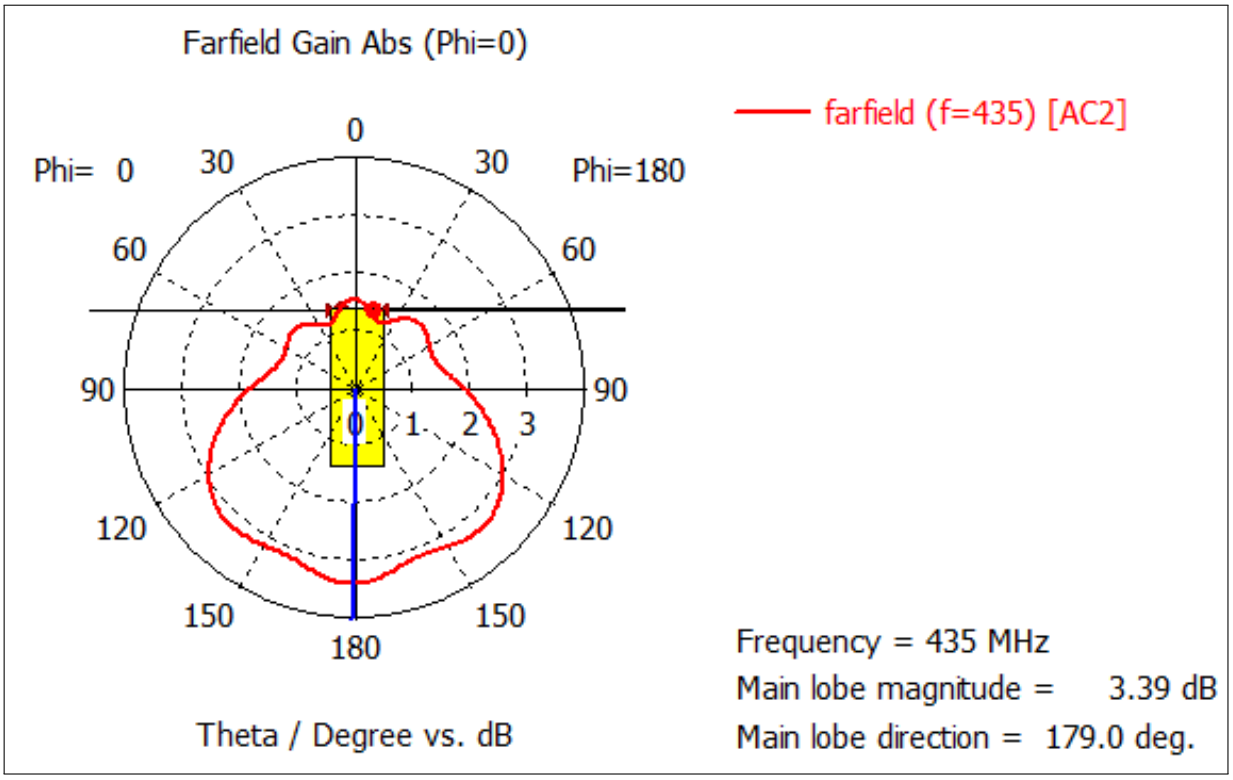


Figure 10.2: ISIS UHF dipole polar radiation plot

loss, $L_{po}$ is polarization mismatch loss, $G_r$ is the receiving antenna gain, $L_{pr}$ is receiving antenna pointing loss, $L_r$ is the reception feeder loss, all in [dB], except $R_b$ is the bit rate in [bit/s] and $T_s$ is the system noise temperature in [K].

### 10.1.2. Downlink

The downlink is analysed for different orbital altitudes in the range 300 - 600 km, considering 5 different spacecraft orientations and corresponding antenna gains: nadir, 45°, 90°, 135°, and 180°. The antenna gains are estimated using radiation pattern diagrams for the crossed UHF/VHF dipole configuration on a 3U Cubesat provided by ISIS through personal correspondence. They can be seen in Figure 10.2 and Figure 10.3. The downlink frequency in the provided diagrams is taken to be 435 MHz.

The constant factors that are used in the link equation for downlink analysis are listed in

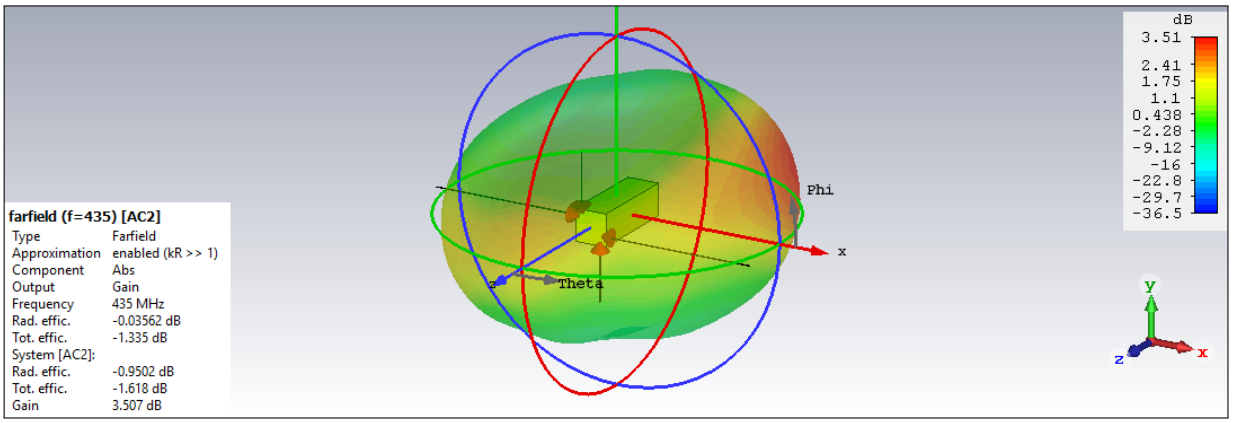


Figure 10.3: ISIS UHF dipole 3D radiation plot

Table 10.1

| Factor | Value | Comment |
|---|---|---|
| $P$ | 30 dBm | Typical output power of the AX100U [2] |
| $L_l$ | 0.5 dB | Transmission line losses [2] |
| $L_{pt}$ | 0 dB | Transmitting antenna pointing loss [2] |
| $L_a$ | 2.5 dB | 2.1 dB atmospheric loss + 0.4 dB ionospheric loss + 0 dB rain loss [2] |
| $L_{po}$ | 3 dB | Spacecraft-to-ground antenna polarization loss [2] |
| $G_r$ | 0 dB | A conservative assumption |
| $L_{pr}$ | 0 dB | Assuming an omnidirectional ground antenna |
| $L_r$ | 0.5 dB | Reception feeder loss [2] |
| $T_s$ | 544.23 K | Antenna noise temperature + cable noise temperature + amplifier noise temperature |

Table 10.1: Downlink budget factors

The free-space loss is calculated using the formula $L_s[\text{dB}] = 20\log_{10}(d) + 20\log_{10}(f) - 147.55$, where $d$ is the distance between antennas in [m] and $f$ is the frequency in [Hz]. The receiving antenna gain $G_r$ is assumed 0 dB to be conservative, allowing the recipients to use a simple omnidirectional antenna without satellite tracking functionality. Thus, the ground station antenna pointing loss $L_{pr}$ is also taken as 0 dB. The receiving system noise temperature consists of antenna noise temperature, cable noise temperature and amplifier noise temperature. A conservative estimate for antenna noise at 435 MHz is 150 K and 35 K for the cable noise [42]. The amplifier noise temperature is calculated using the formula $T_r = T_0 \cdot (F - 1)$, where $T_0$ is a reference temperature taken to be 290 K and $F$ is the receiver noise figure [6]. The typical noise figure from the specifications of the Funcube Dongle Pro+ is used[1], which is 3.5 dB at 435 MHz. This gives an amplifier noise temperature of 359.23 K, which gives a total system noise temperature $T_s = 544.23$ K. The bit rate $R_b$ is a setting in the transmitter, thus it is left as a variable in this analysis. GMSK modulation is assumed with convolutional coding, which can be decoded with a bit error rate of about $10^{-5}$ if $E_b/N_0 > 7.8$ dB [2].

For each altitude the maximum beam angle that intercepts the Earth, measured from the nadir pointing axis, is calculated by considering a right triangle, where the RF beam is one cathetus, Earth's radius $R_e$ is the other cathetus and spacecraft's distance from the center of the earth $R$ is the hypotenuse. Then, the maximum beam angle is given by $\theta_{max} = \sin^{-1}\left(\frac{R_e}{R}\right)$. For 600 km orbit $\theta_{max} = 66.05°$, for 500 km $\theta_{max} = 68°$ and for 300 km $\theta_{max} = 72.75°$. Five spacecraft orientation cases were analysed separately, assuming that the same spacecraft axis remains pointing nadir during a single pass. The antenna gain is tabulated with the corresponding beam angles from 0 to $\theta_{max}$ on both sides of the nadir axis. Then, for each angle-gain pair the link budget is calculated, by plugging in the corresponding antenna gain and calculating the slant range for the beam angle. The slant range is calculated by solving a SSA triangle using the law of sines. After tabulating the $E_b/N_0$ for each angle it becomes clear approximately at what beam angles the signal diminishes to less than 7.8 dB. The total coverage arc is calculated for these angles by using two triangles to find the angles from the earth's center to the edges of coverage and multiplying by the Earth's radius. The spacecraft's travel distance is calculated by multiplying $R$ by the same angles and finding the orbital velocity $v_o \approx \sqrt{GM/R}$, where $G$ is the gravitational constant, $M$ is the mass of the earth and $R$ is the distance between the spacecraft and the center of the earth. A calculation example for the symmetric nadir case for 600 km is given in Table 10.2.

Other orientations and altitudes were analysed analogously for GMSK modulation, 435 MHz. The results for the optimal bit rates for each case are shown in Table 10.3.

### 10.1.3. Uplink

A conversation with Stefano Speretta, one of the designers of the TU Delft ground station, revealed that the station offers a UHF antenna with a gain of 15 dBi and transmitted power of 100 W, with maximum losses of 1.5 dB. Therefore, 50 dBm is taken as transmitted power $P$, 1.5 dB as transmission line losses $L_l$ and 15 dBi as the antenna gain $G_t$. 0.5 dB is taken

[1] `http://www.funcubedongle.com/?page_id=1201` [Retrieved on the 17-05-2019]

| nadir | | 9600bps | 12000bps | 19200bps |
|---|---|---|---|---|
| beam angle [deg] | gain [dBi] | $E_b/N_0$[dB] | $E_b/N_0$ [dB] | $E_b/N_0$ [dB] |
| 0 | 3.39 | 19.11 | 18.14 | 16.10 |
| 15 | 3.2 | 18.60 | 17.63 | 15.59 |
| 30 | 3.25 | 17.61 | 16.64 | 14.60 |
| 40 | 3.3 | 16.46 | 15.49 | 13.45 |
| 42.5 | 3.3 | 16.07 | 15.10 | 13.06 |
| 45 | 3.3 | 15.65 | 14.68 | 12.64 |
| 60 | 3 | 11.42 | 10.45 | 8.41 |
| 64 | 2.8 | 9.30 | 8.33 | 6.29 |
| 68 | 2.7 | 4.41 | 3.44 | 1.40 |
| for GMSK | BER 1E-05 at 7.8dB | | | |
| max angle [deg] | | 65.22 | 64.43 | 61.15 |
| coverage arc [km] | | 2907.30 | 2711.06 | 2155.36 |
| contact time [min] | | 6.86 | 6.39 | 5.08 |
| max Mbits received | | 3.95 | 4.60 | 5.86 |

Table 10.2: 500 km nadir downlink analysis

| altitude | orientation | bit rate | Mbits received |
|---|---|---|---|
| 600 km | nadir | 19200 bps | 5.50 |
| 600 km | 45° | 19200 bps | 5.07 |
| 600 km | 90° | 19200 bps | 4.98 |
| 600 km | 135° | 19200 bps | 4.51 |
| 600 km | 180° | 19200 bps | 4.32 |
| 500 km | nadir | 19200 bps | 5.86 |
| 500 km | 45° | 19200 bps | 5.36 |
| 500 km | 90° | 19200 bps | 5.28 |
| 500 km | 135° | 19200 bps | 5 |
| 500 km | 180° | 19200 bps | 4.61 |
| 300 km | nadir | 19200 bps | 5.29 |
| 300 km | 45° | 19200 bps | 5.14 |
| 300 km | 90° | 19200 bps | 5.07 |
| 300 km | 135° | 19200 bps | 4.91 |
| 300 km | 180° | 19200 bps | 4.59 |

Table 10.3: Maximum Mbits transferred per passing for multiple scenarios

for the transmitting antenna pointing loss $L_{pt}$ [2] and 2.5 dB for the atmospheric losses $L_a$ [2]. Worst case altitude of 600 km and elevation angle of 5°were taken for the free-space loss $L_s$, which results in 153.39 dB. The ground-to-spacecraft antenna polarization loss $L_{po}$ is taken to be 3 dB [2]. The worst case antenna gain of -20 dBi is taken for $G_r$ (see Figure 10.4 and Figure 10.5). Since the worst case gain is taken, antenna pointing loss $L_{pr}$ is 0. Reception feeder loss $L_r$ is taken to be 0.2 dB [2]. The bit rate $R_b$ is assumed to be 9600 bps [2] and the receiving system noise temperature $T_s$ is specified as 234 K [2]. GMSK modulation is assumed with convolutional coding, which can be decoded with a bit error rate of about $10^{-5}$ if $E_b/N_0 > 7.8$ dB [2]. This results in an $E_b/N_0$ of 19 dB, which gives a link margin of 11.2 dB which should suffice for a successful command reception at all times.

## 10.2. Data Link Layer

The communications are planned to be carried out in the amateur satellite UHF and VHF bands. Usage of these frequencies requires some benefit for the radio amateur community. Firstly, the telemetry of the satellite has to be unencrypted and instructions on decoding the telemetry have to be made publicly available. Secondly, one way to make the CubeSat serviceable for the amateur radio operators is to include a repeater functionality. With the two digital radios

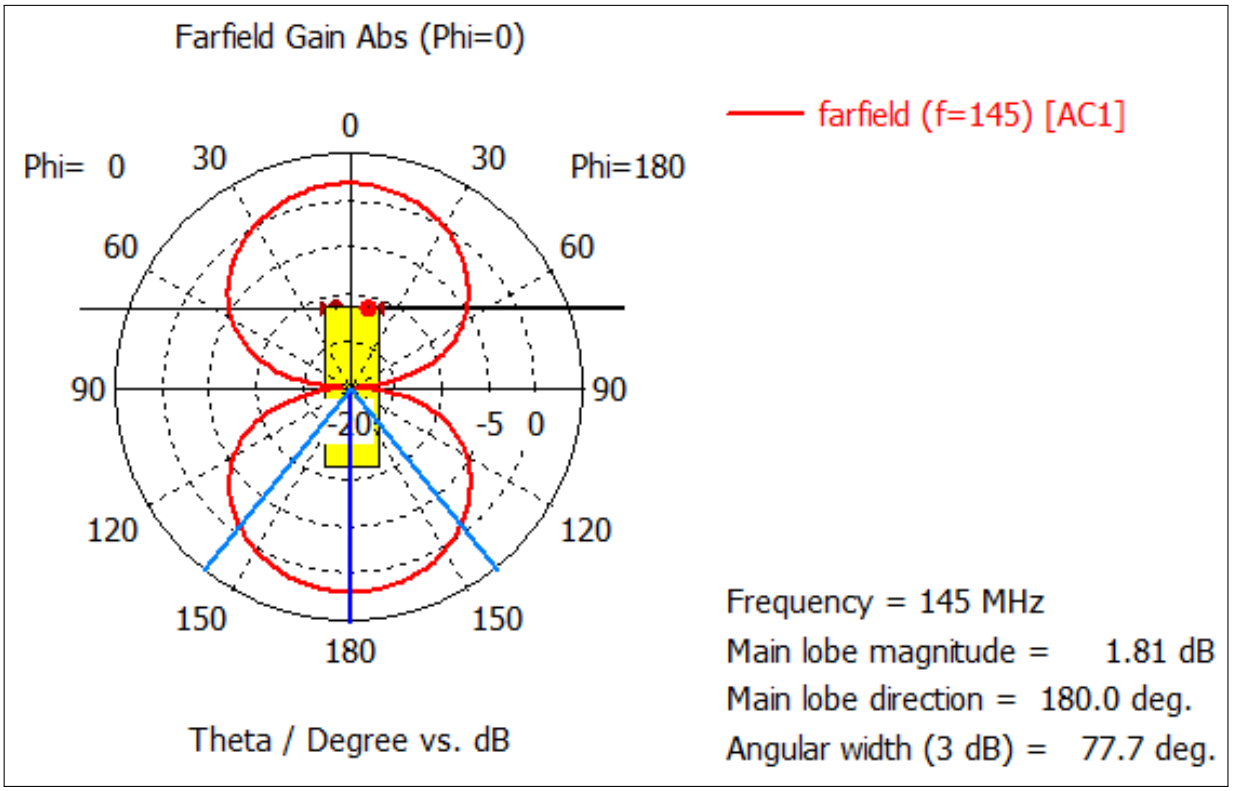


Figure 10.4: ISIS VHF dipole polar radiation plot

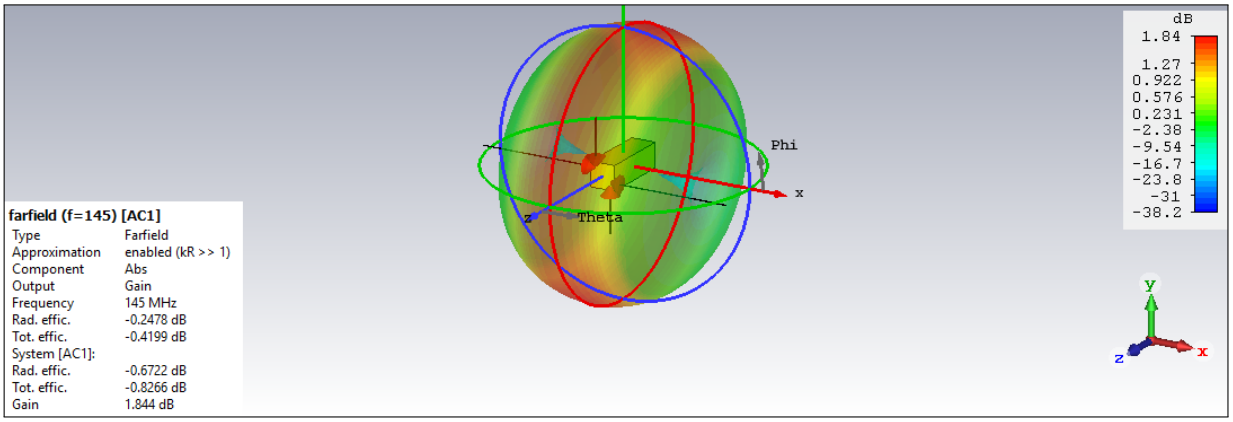


Figure 10.5: ISIS VHF dipole 3D radiation plot

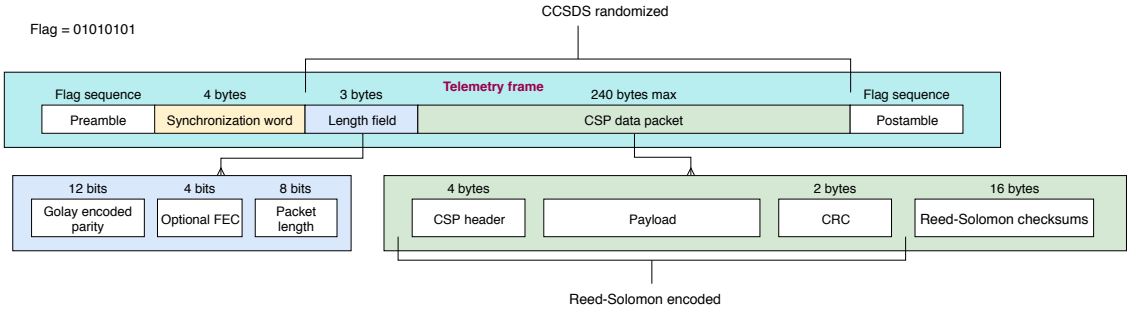


Figure 10.6: Telemetry frame structure

onboard a digipeater mode can be implemented.

The AX100 implements a protocol stack called Cubesat Space Protocol (CSP). The protocol is based on a 32-bit header containing both transport and network-layer information. On Daniel Estévez's EA4GPZ / M0HXM webpage[2] there is a detailed telemetry description of the GOMX-3 satellite, which also uses the AX100 and CSP. Based on it, some information about the header is extracted. It contains priority, source, destination, destination port, and source port fields, as well as a reserved field and single bit HMAC, XTEA, RDP, CRC fields. The priority field has 2 bits and therefore allows to specify 4 levels of priority, the value 2 being normal priority. The source field contains a 5-bit address of the subsystem that sent the packet, in GOMX-3, for example, an address value 1 is assigned to the OBC, 4 to the ADCS and 5 to the COMMS. The destination address and port for beacon transmission are set to 10 and 30. The source port field is indicative of the type of packet, port 1 for example corresponds to ping reply. HMAC stands for Hash-based Message Authentication Code, XTEA for eXtended TEA (Tiny Encryption Algorithm), RDP for Reliable Data Protocol and CRC for Cyclic Redundancy Check. The four last fields indicate if these methods are being used.

A 32-bit Attached Sync Marker (ASM) along with a Golay encoded variable length field are implemented in the AX100. This constitutes a 4 byte (32 bit) synchronization word marking the beginning of the frame. This is considered quite lengthy and thus provides good synchronization. [5] A 3 byte Golay length field follows. It consists of 12 Golay encoded parity bits, 4 optional FEC bits and 8 bits specifying the packet length. The parity bits allow up to 3 bit errors to be corrected in the length field. The variable length data field comes next with a 240 byte maximum. Reed Solomon (223,255) Forward Error Correction (RS) is applied to the data field, which costs 16 bytes per frame. [5] HMAC will be used to add 4 byte hashsums to the commands that will allow the satellite to authenticate, as well as verify the integrity of the messages. CCSDS randomization is another feature offered by the transceiver that costs no bytes. It is a standard randomization procedure recommended by The Consultative Committee for Space Data Systems (CCSDS) wherein an exclusive-OR operation is applied to the bits of the data stream and corresponding bits of a standard pseudo-random sequence. [20] This is applied mainly to make sure the signal has sufficient bit transition density, in other words, it prevents long sequences of just ones or just zeros, which could cause the decoder to lose synchronization. [20] From this information the rough structure of a typical telemetry frame is extrapolated, shown in Figure 10.6. The exact length of the data packet, as well as the settings and the precise structuring of the frame will have to be determined when programming and testing the transceiver.

## 10.3. Transmission Schedule

The current resource budget (subsection 15.1.1) allocates in total about 15 minutes for transmission per orbit. There are mainly two types of telemetry frames that can be anticipated: a beacon containing housekeeping data and payload data frames. The housekeeping data are

[2] https://destevez.net/2016/05/decoding-packets-from-gomx-3-modulation-and-coding/ [Retrieved on 19/6/2019]

mainly voltage levels, currents, temperatures and other relevant satellite status indicators. These can be easily fitted in the 220 bytes that are available for data in a single frame or less, when RS and HMAC are employed. Litsat-1's satellite status field, for example, takes up 106 bytes. Therefore, assuming a 256 byte housekeeping frame and a bit rate of 19.2 kbps it takes about 0.1 seconds to transmit it. Therefore, during a 5 minute pass, if a beacon frame is transmitted every 10 seconds it will take up just 3 seconds of transmission time and the rest of the 297 seconds can be used to transmit payload data frames. That would amount to 5.7 Mbits of payload data frames. A transmission schedule update can always be sent as a command to the spacecraft, thus it remains quite flexible and can be optimized for different needs in-flight.

## 10.4. Verification

The link budget calculations are done using an Excel sheet, which is verified by comparing with an example link budget found in the AX100's datasheet [2]. When identical inputs are used the excel tool produced identical results, therefore the formulas are verified to be correct. Satellites that use the same components serve as a verification for the design. Funcube uses a UHF/VHF crossed dipole antenna and the Funcube dongle to receive the signals, thus it serves as verification for the downlink. The fact that only flight-proven components are used, verifies that they work in space environment. As of November 23, 2018 the AX100 has flown on 9 CubeSats, 2 of which, ExAlta-1 (CA03) and qbee (SE01), are educational university satellites downlinking on UHF amateur band[3]. Further, The Missouri University of Science and Technology Satellite Research Team incorporates two AX100 radios operating on UHF and VHF amateur radio bands to facilitate a full-duplex link and prevent "accidental transmitter locks" on their Missouri-Rolla Satellite[4] [4]. This verifies the reasoning behind this configuration.

[3] `https://www.klofas.com/comm-table/table.pdf` [Retrieved on 23/6/19]
[4] `http://web.mst.edu/~mrsat/subsystems/communications.html` [Retrieved on 24/6/19]

# 11
# Electrical Power System

The Electrical Power System (EPS) provides the required power to the other subsystems. The main components of the power system are the power sources and the power module. The primary parameters which drive the design are the average and peak electrical power requirements. They size the power generation system, the energy-storage system given the eclipse period and the Depth of Discharge(DoD), and the power-processing and distribution equipment.

## 11.1. Power Sources

Photovoltaic solar cells are preferred for low power missions since they are well-known and reliable. Furthermore they have much higher specific power, affordable specific cost, unlimited fuel availability and carry minimum risk compared to both static and dynamic power sources and to fuel cells. In addition, solar cells are optimised for Earth orbiting spacecraft. Key design parameters include: the spacecraft configurations, the required peak and average power, illumination, and orientation[42]. From the preliminary estimations done during the baseline and the midterm phases of the project, power was a constraint [12][13]. Furthermore, the two payloads that are designed for the VSV are still in early design stages, therefore the power generated should be maximised to satisfy the needs of all the systems as well as to allow for interchangeable payloads, according to the modularity concept.

The final design has a structure with a 2U size as mentioned in chapter 7. In chapter 3 it is mentioned that the VSV's objective is to have all of the components of the spacecraft sponsored. During a stakeholder meeting held by the VSV, it was mentioned by the CEO of GTM that solar cells from Airbus might be integrated into solar panels. However, as of yet there are no concrete agreements or confirmation from the VSV and therefore a trade-off will be made consisting of the panels offered by the leading companies. Table 11.1 represents four of the companies that offer high efficiency solar panels which produce the highest possible power. The table does not include the panels offered by GTM since they would be custom-made and there is no available information on specifications. In addition, Pumpkin Space is considered, since their solar panels produce significantly less power and therefore would not be included in the trade-off.

Table 11.1: Parameters for different COTS solar panels

| Provider/Name | Power [W] | Voltage [V] | Mass [g] | Cost [EUR] |
|---|---|---|---|---|
| EnduroSat 2U Solar Panel [1] | 4.8 | 4.66 | 80 | 3000 |
| ISIS 2U Solar Panel [2] | 4.6 | 3 (5 and 8 on demand) | 100 | 3500 |
| GOMspace 2U Solar Panels [3] | 4.6 | 4.8 | 114 | NA |
| DHV 2U Solar Panel [4] | 4.8 | 4.8 | 100 | 4000 |

In terms of orientation and configuration, there are two primary design options to choose from. The first option is to have the satellite oriented towards the Sun such that two of the side panels are illuminated. In this concept the power production is optimized, however the

[1] https://www.endurosat.com/products/cubesat-solar-panels-x-y/ [Retrieved on 17-06-2019]
[2] https://www.isispace.nl/product/isis-cubesat-solar-panels/ [Retrieved on 17-06-2019]
[3] https://gomspace.com/shop/subsystems/power/p110-solar-panel.aspx [Retrieved on 17-06-2019]
[4] https://www.cubesatshop.com/product/cubesat-solar-panels/ [Retrieved on 17-06-2019]

orientation is constrained. The second orientation option is when the Sun illuminates two side panels and the bottom panel. The power production would be higher, however, the increase is highly dependent on the incidence angles and thus the constraint on the orientation would be the driving parameter for the orientation of the spacecraft.

### 11.1.1. Trade-Off

All of the aforementioned solar panels consist of triple-junction solar cells and are space qualified. Most of the parameters such as size, voltage and efficiency are identical which makes the trade-off significantly more complex. There are small performance differences which can be used as a criteria.

The most convenient option of the solar panels is arguably EnduroSat. They produce more power for the same size, while also being lighter, cheaper and a detailed data sheet for the panels is made publicly available. Furthermore, it is possible to use both the panels and power module from EnduroSat which would ensure that the two components are compatible and the interaction between them would be verified by the company itself. One drawback that should be noted is that EnduroSat does not currently produce 2U panels and a custom made one might not be possible. Nevertheless connecting two 1U panels in parallel should yield minimum losses. Compared to these, the panels of both GOMspace and DHV are inferior. They are significantly heavier, more expensive and provide less information. Therefore, the latter two options can be discarded.

Last but not least, the ISIS panels have a number of advantages. The company is based in Delft and has already agreed to spare resources to help the project, which makes it easier to get hands-on familiarity with the components and get technical support if necessary. Moreover ISIS produces 2U panels and similar to EnduroSat, a power module. Although the panels produce less power, they are more efficient compared to the EnduroSat ones.

### 11.1.2. Final Choice

The solar panels and the power system of the different companies are made of the same materials. Therefore the power systems are interchangeable. Currently, the ISIS solar panels are considered advantageous compared to all the other solar panels. However, if EnduroSat would produce 2U panels, they should also be considered due to their superior characteristics and detailed documentation.

The payload ideas are defined at a later stage into the project and are still being developed. Furthermore, both the ADCS and the OBC are sponsored by Hyperion and not all specifications are currently known. Therefore it is not possible to verify whether the EPS is compatible with the different systems. As a result the solar panels and power module from EnduroSat are not entirely discarded as options.

As previously stated, the power generated should be maximised in order to supply enough power for the payloads as well as to provide a healthy margin. In order to produce the maximum amount of power, the satellite should be oriented such that two side and the bottom panels are all simultaneously pointing at the Sun. The maximum power production is found by deriving with respect to the optimum incidence angle, first for the two side panels and subsequently for the plane of their projection and the bottom panel.

$$(A_{2U}\cos\xi + A_{2U}\cos(\frac{\pi}{2} - \xi))' = 0 \tag{11.1}$$

The first angle is at which the solar irradiance falls onto the side panels. Equation 11.1 represents how to calculate the optimal value, which is when the two side panels are at $\xi = 45°$. In addition, this is also the optimum angle if the satellite is operating in the first power option, where the Sun illuminates only two side panels. The second angle is with respect to the orthogonal of the projection of the side panels and the bottom panel.

$$((\sqrt{2}A_{2U})\cos\psi + A_{1U}\sin(\frac{\pi}{2} - \psi))' = 0 \tag{11.2}$$

Solving Equation 11.2 results in the optimal incidence angle being $\psi = 19.47°$, and $90° - \psi$ with respect to the orthogonal of the projection and the bottom panel respectively. The incidence

angle would cause a decrease in power, however, as the area is effectively increased it would result in a net increase of 50% compared to only one side panel pointing at the Sun and a 5% increase compared to when two sides are pointing at the Sun. In order to design for redundancy there should be solar panels on all sides of the satellite beside a 0.5U surface which is reserved as an aperture for the payloads.

Before creating the power budget, the albedo also has to be taken into consideration as its effect usually cannot be ignored. Solar cells typically do not absorb wavelengths longer than $2\mu$m and since the Earth radiates at longer wavelengths, which peak at 10 $\mu$m and only $4 \cdot 10^{-8}$% of the energy is shorter than 2 $\mu$m the Earth absorbed solar irradiance which is radiated back is ignored[5]. In order to approximate the contribution of the albedo several assumptions are made. First, the average Earth reflectivity is 30%[27]. Then, only 50% of the Earth is reflecting light, which is based on a cosine function, whose average is $2/\pi$. Finally, distance losses account for another 8.8%, assuming a 300 km orbit. The orbital altitude is chosen as it has the greatest eclipse time as a ratio of the full orbital period for the range of orbits given in chapter 5. Taking into account all the factors, results in a contribution of about 0.29 W which is almost 11% increase.

The budget of the two configurations is presented in Table 11.2. The power budget calculation includes a life degradation rate of 0.98, an inherent degradation of 0.77 and an overall EPS efficiency of 0.8 and it is calculated for an orbit of a 300 km altitude. As specified in section 11.1 the first option is when two side panels are illuminated by the Sun and the second is when the bottom panel is illuminated in addition to the side panels. All of the orientation modes originate from the same configuration and therefore the overall mass and cost are the same - 475 g and 18500 euro respectively.

Table 11.2: Electric Power System design budget

| Orientation mode | Mean Power Generated with Albedo [W] | Mean Power Generated without Albedo [W] |
|---|---|---|
| Free tumbling | 1.97 | 1.82 |
| Option 1 | 2.83 | 2.53 |
| Option 2 | 2.97 | 2.68 |

## 11.2. Power Module

As previously specified in subsection 11.1.1, in order to ensure that the solar panels and the power module are compatible it is best to select a power module from the same company from which the solar panels are. In addition, the power module should be able to handle the input current and voltage from the panels as well as the output power buses and include sufficiently powerful batteries. Since the solar panels are from ISIS it is best to also select the ISIS power module, since satisfies all of the requirements and ensure compatibility. In addition, the module works with different interfaces, namely UART(RS232) and I2C, which allows for a bigger design space for the OBC. There are 3.3 V and 5 V regulated buses, as well as an unregulated bus. There is also the possibility for a daughter board which allows for a custom bus as well as it would enable ISIS AntS2.0 interface and ISIS solar panel data interface and readout. The power module consists of a two Li-Ion cell battery pack, which can provide 20 W over 5 V and store up to 6400 mAh [6]. Each battery has an integrated protection circuit module, which prevents over-current, over-charging and over-discharging. Furthermore there is an option whose batteries store 12800 mAh, however, such storage is required during the mission.

## 11.3. Electric Block Diagram

The electrical block diagram displays the electrical equipment of the system. It shows the power interactions within the satellite such as the power provision, power conversions and the batteries. In Figure 11.1, the necessary power for every system can be seen as well as the required voltage. Both the telemetry and the OBC require a 3.3 V regulator and the payload and ADCS require a 5 V regulator. The electric heater is not included in the block diagram since

[5] https://bhanderi.dk/research/publications/bhanderi_earth_albedo_model.pdf [Retrieved on 18-06-2019]
[6] https://www.isispace.nl/product/ieps-electrical-power-system/ [Retrieved on 18-06-2019]

it is internal to the electric module. Furthermore, the power provided by the panels, which is depicted on the diagram, shows the optimal power that a panel can produce with no losses and a zero degrees incidence angle. In addition one of the side panels would produce less since the aperture for the payloads would be on that side. The ADCS components are coupled together to a 1.4 W consumption as currently the individual consumption of the components is unknown.

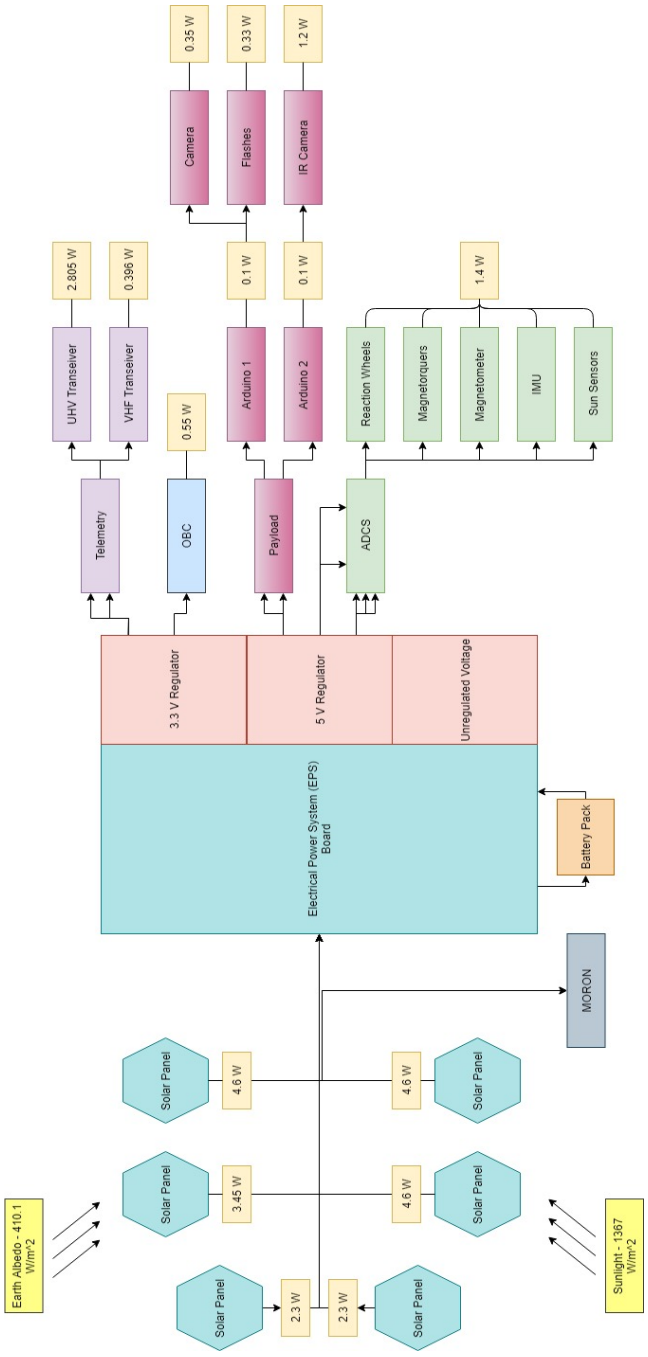


Figure 11.1: Electric block diagram of the satellite

## 11.4. Verification

Every commercial off the shelf component such as the solar panels listed in Table 11.1 and the electrical module described in section 11.2 is verified and validated in accordance to the Qualification Engineering Module. Furthermore, all tests that are performed: functional, vibration,

mechanical shock, thermal cycling and thermal vacuum, follow the ESA standard, namely the ECSS-E-ST-10-03C and the GEVS: GSFC-STD-7000A.

In order to verify that the EPS is compatible with all the other systems and that it provides the necessary power, an EPS model is created. The model is created such that every power consuming system is represented by a class. The simulation represents an orbit or several consecutive orbits so that the state of the battery and the power consumption are tracked. Code coverage is preformed and optimized as it lowers the chances of unforeseen bugs. Not only would the tests and calculation be performed for values within daylight but also for the boundary conditions where states change and at the end of each orbit to evaluate the state of the system. In addition, in order to verify the model as well as to double check the power budget a second power model is developed. The models are developed independently, employing different methods, while also using the same inputs. The resulting values for the calculations are within 1.5%, which indicate that the models are correct.

## 11.5. Fail-Safe

In order to avoid single point of failure, fail-safe cases are developed. The three main cases that affect the EPS and would not cause immediate End-of-Mission (EoM) that have to be investigated are if the payload, ADCS or battery fail.

### 11.5.1. Payload Power Protection

One of the main features of the concept of modularity and plug-and-play is that if the payload fails it should not affect the satellite bus, and by extension the EPS, in any way. Therefore, when system components are integrated the power protection of the payload should be handled separately from the other systems. The voltage regulators and the power lines' protection would have independency and a failure would only result in loss of payload.

### 11.5.2. ADCS Failure

In case of a failure in the ADCS, the Space Truck would start tumbling freely in space. When a cuboid-shaped satellite tumbles freely in space the usual method to estimate the illuminated area is to divide the total area covered by solar panels by four[42]. Therefore the satellite would enter in a back-up power mode. In it the power generated is highly limited. Instead of almost 3 W, the solar panels would be able to generate approximately 1.97 W, when the albedo takes effect and 1.82 W when it does not. In this case the power budget and duty cycle of the system would be updated such that the satellite would be still operative.

### 11.5.3. Battery Failure

The on-board battery pack serves two purposes: it provides power during eclipse and it is necessary to reach peak power. On one hand, if the battery fails, the following cycle would be repeated every orbit due to the fact that during eclipse there would be no power: the satellite enters safe mode as there is no power supplied to the OBC and as a result everything is turned off. The watchdog will not be serviced, meaning it would try to turn the OBC back on. It would keep doing so until the OBC is back on and services the watchdog. This would happen when the solar panels provide enough power again. Therefore, if the battery fails to fulfill its first purpose, it would not result in EoM. On the other hand, battery failure would mean that the system would not be able supply enough power to transmit. The transmitter requires approximately 2.8 W, whereas the system would produce 3 W, while the OBC and ADCS are also working, which means that there would be not enough power. In order to avoid single point of failure, the communication system is designed such that it has a micro-controller, which would allow the system to continue working independently, when everything else is turned off. This would allow the satellite to send its status to the ground station and in turn be able to receive a duty cycle which would be able to facilitate the communication system power consumption.

# 12
# Thermal Control System

To design the thermal control system, it is important to know the thermal requirements of the spacecraft. These are thus presented in section 12.1. To then do the initial estimates for the thermal control system, a highly simplified model is made. This model is discussed in section 12.2. The thermal model is used to determine the coatings that are required to maintain the Space Truck's temperature within its design limits. Note that the battery may require an electrical heater to maintain its temperature above its minimum operational temperature. However, whether or not it is actually required is not yet conclusively shown. The results of the thermal model are presented in section 12.3. The final design of the thermal control system is then presented in section 12.4. Note that as most COTS come with integrated temperature sensors or the option to have them, temperature sensors are not considered. If a module is selected that does not come with an integrated temperature sensor, sensors will be considered during the detailed design phase.

## 12.1. Thermal Requirements

To get an idea of the thermal range within which the thermal control system must maintain the spacecraft's temperature, the operational temperature ranges for the different subsystems has been determined. The results are summarized in Figure 12.1. It can be seen that the temperature range that is compatible with all subsystems is between -10 $°C$ and 40 $°C$. To determine the design range, 10 $°C$ is subtracted from either end of the range. This is consistent with standard practices[42]. The design range is then from 0 $°C$ to 30 $°C$. This range is indicated in Figure 12.1 by two red lines.

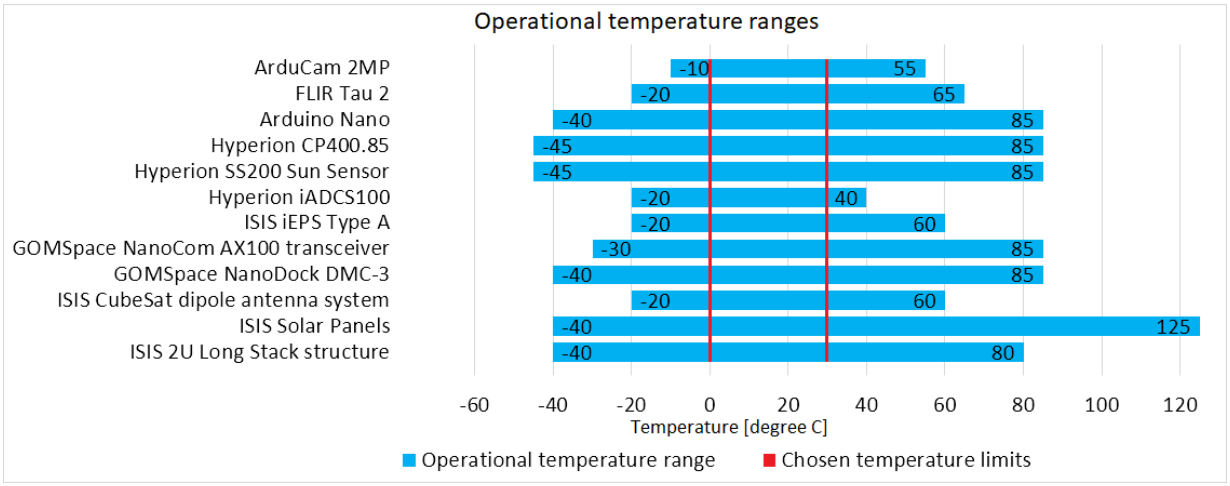


Figure 12.1: The thermal operational ranges of the different subsystems

## 12.2. Preliminary Thermal Model

The thermal model is made up of two parts, the thermal environment the spacecraft is in and the spacecraft itself. The thermal environment is discussed in subsection 12.2.1 and the model

of the spacecraft is presented in subsection 12.2.2. The two parts are combined in subsection 12.2.3. The verification of the thermal model is discussed in subsection 12.2.4.

### 12.2.1. The Thermal-Radiation Environment

The heat fluxes in and out of the spacecraft are visualized in Figure 12.2. The main heat flows are the direct solar flux received, the solar flux that gets reflected by the Earth (albedo), the IR radiation emitted by the planet and the radiation emitted by the satellite itself. Additionally, the spacecraft also dissipates heat internally, $Q_{internal}$, due mainly to electrical heat losses.

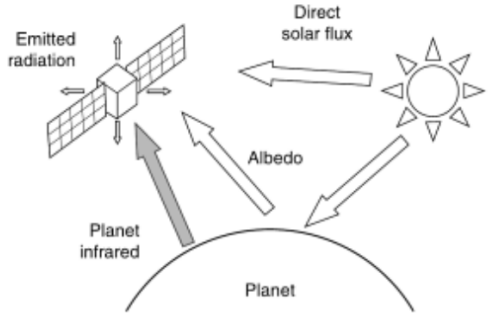


Figure 12.2: The thermal environment of the spacecraft [27]

The direct solar flux, $G_s$, is given to vary between 1321.6 $W/m^2$ and 1412.9 $W/m^2$ depending on the position of Earth along its orbit [27]. For the preliminary thermal model, the mean value of 1367.25 $W/m^2$ is used.

The albedo radiation, $G_A$, is dependent on the solar flux and the albedo coefficient, $a$. The albedo coefficient for Earth can vary between 0.05 and 0.95, depending on the surface/cloud coverage below the spacecraft. For the preliminary thermal model, the albedo is assumed to be 0.3, the mean value for Earth [27].

The IR radiation, $q_I$, at the Earth's surface is given to be between 216 $W/m^2$ and 258 $W/m^2$ [42]. For the preliminary thermal model the average value of 237 $W/m^2$ is used.

### 12.2.2. The Spacecraft Thermal Model

For the preliminary thermal model, the spacecraft is modelled as a solid block with uniform temperature and specific heat capacity. Each surface of the spacecraft is characterized by its area, absorptivity and emissivity.

The specific heat capacity, $c$, is approximated using the values for aluminum, copper and FR4 (the material the PCB's are made of). This is done as these are the main contributors to the spacecrafts mass and thus the spacecraft's heat capacity. The heat capacity of aluminum can be approximated to be 910 $J/kg \cdot K$, that of copper to be 390 $J/kg \cdot K$[1] and that of FR4 to be 1200 $J/kg \cdot K$[2]. To determine how these values should be combined to get an estimation of the total specific heat capacity of the spacecraft, it is important to note that the estimation should be conservative. As the specific heat acts as a damper for the temperature variation, a higher specific heat will result in a smaller temperature range experienced by the spacecraft. Thus, to keep the heat capacity estimate conservative, it is taken to be lower than is likely the case for the final spacecraft. To combine the heat capacities of the individual materials, approximate mass fractions are used for aluminum and FR4. The rest of the mass fraction is assumed to be made up of copper. This is done as copper has the lowest specific heat capacity of the main contributors to the mass. Thus, the resulting specific heat capacity will be lower than is likely the case for the real spacecraft. The structure will be made out of aluminum and have a mass of about 248 $g$, the PCB's are assumed to make up about 212.8 $g$ (this takes into account 7 10cmx10cmx0.16cm boards which is the approximate amount needed) and the rest of the mass is assumed to be made up of copper. Using these values, the spacecraft's overall specific heat capacity can be approximated to be 511 $J/kg \cdot K$.

[1] https://www.engineeringtoolbox.com/specific-heat-metals-d_152.html [Retrieved on 4-06-2019]
[2] http://www.akemalhammar.fr/online/cond_pcb.html [Retrieved on 21-05-2019]

From the CubeSat specifications, the areas of the spacecraft's surfaces can be determined [11]. The area of the top and bottom surfaces (+Z and -Z faces) are known to be 0.01 $m^2$ from the CubeSat specifications. For a 2U CubeSat as currently under consideration, the sides (+X, -X, +Y and -Y faces) have an area of approximately 0.0213 $m^2$.

The absorptivity and emissivity of the surfaces is dependent on their coating and these are thus the main parameters which are changed to suit the thermal needs of the spacecraft.

The spacecraft model is implemented in code by dividing up the spacecraft into its surfaces, each having an area, absorptivity, emissivity and a normal vector. The angle between the normal vector of the surface and the incident radiation can then be used to calculate the projected area which will then be used to calculate the effective radiation hitting the surface.

### 12.2.3. Combining the Thermal Environment and the Spacecraft Thermal Model

The main part of combining the thermal environment with the spacecraft thermal model is to determine the heat absorbed by each surface. The model uses the normal vector and area of each surface and the vector of the incoming radiation to determine the effective area exposed to radiation. This area, along with the optical properties of the surface, can then be used to determine the absorbed heat. The equations for the absorbed heat are taken from SMAD [42] along with the equation for heat emitted by the spacecraft. Note that in the thermal model, the calculation of heat absorbed/emitted is done for each surface individually.

For the incident radiation it is assumed that the radiation is collimated. This is an accurate representation of the solar flux hitting the spacecraft due to the spacecraft's distance to the Sun. For the radiation coming from the Earth, however, this is not a very accurate representation due to the close proximity of the spacecraft to the planet. When this assumption is made, the surfaces of the spacecraft that are parallel to the axis connecting the Earth's center with the spacecraft's center do not receive radiation while in reality they would. The result is that less radiation is absorbed in the simulation then in reality and the spacecraft will be simulated at a lower temperature then it would be in reality.

For the internally dissipated heat it is assumed that the spacecraft consumes all the produced power as heat and that the power consumption is constant throughout the orbit.

It is also important to note that not all solar radiation hitting the spacecraft will be absorbed as heat. Some of the radiation will be converted into electrical energy by the solar panels and thus not contribute to the absorbed heat.

The equilibrium temperature for a given position and orientation of the spacecraft can then be calculated by equating the absorbed heat with the emitted heat and solving for the spacecraft temperature [42]. However, a more accurate representation of the spacecraft in orbit may be obtained by determining the heat absorbed at each point along the orbit. Then, for a begin temperature calculate the emitted heat using the current spacecraft temperature. The net output heat, Q, can then be determined which can be used in Equation 12.1 to determine the change in temperature [42]. Note that in Equation 12.1, dt is the time it takes for the spacecraft to go from one point in the orbit to the next. This procedure can be repeated for each point along the orbit to give an estimate for the temperature variation.

$$dT = \frac{Q \cdot dt}{m \cdot C} \tag{12.1}$$

### 12.2.4. Verifying the Preliminary Thermal Model

To verify the thermal model, first, the implementation of the surfaces was checked. This was done by calculating the effective area of each surface being radiated with the incoming radiation coming from different directions and with the spacecraft at different orientations. The effective areas were then calculated by hand using calculus and compared with those calculated by the thermal model. All values were verified, indicating that the calculations for the effective radiated areas are correct.

The implementation of the absorbed radiation was tested by calculating the absorbed radiation by hand using the equations presented in [42]. These values are then compared with the ones produced by the thermal model. Some initial mismatches were found but these were quickly resolved.

The implementation of the heat capacity can be checked by increasing and decreasing the heat capacity of the spacecraft. If the heat capacity increases, the temperature variations decrease and vise versa. When this test is performed on the thermal model, the expected behaviour is observed.

## 12.3. Preliminary Results for the Thermal System

As calculating the temperature of the spacecraft for every possible orbit is impossible, only the extreme cases are considered. The extreme cases for the orbital altitudes are 300 $km$ for the lowest altitude and 700 $km$ for the highest. Note that for this analysis the altitudes from section 5.1 were used as opposed to those of section 5.5. This is as this analysis was done before the orbital characteristics were revised. The extreme cases for the sun exposure of the satellite are for when the spacecraft is continuously exposed to sunlight and for when the spacecraft is in an equatorial orbit where the eclipse time is longest. The resulting extreme cases are then the following:

- The first situation is when the spacecraft is in an equatorial orbit at an altitude of 300km. The spacecraft is oriented with one of the long edges pointing toward the sun as described in subsection 11.1.2 under option 2.
- The second situation is the same as the first one, except that the spacecraft is orbiting at an altitude of 700km.
- The third situation is when the spacecraft is orbiting in a polar orbit where the plane of the orbit is perpendicular to the axis connecting the Earth and Sun such that the spacecraft is continuously exposed to solar radiation. The spacecraft will never be in this type of orbit permanently. However, this situation is still analyzed because it is an extreme case, i.e., the maximum temperature will be experienced in this situation. The spacecraft is orbiting at an altitude of 300km. The spacecraft is oriented towards the Sun in the same way as in situation 1 and 2.
- The fourth situation is the same as the third one, except that the spacecraft is orbiting at an altitude of 700km.

For each of these situations, the day and eclipse times are only dependent on the altitude of the spacecraft. The values for the day and eclipse times can be obtained from Table 5.1.

These situations cover the extremes of what the spacecraft is going to encounter in normal operation and are thus sufficient for the preliminary thermal analysis.

The absorptivity and emissivity of the surfaces are determined based on the properties of the materials used on the outside and there layout. The materials on the outside of the spacecraft are the solar cells, the black anodized aluminum which the rails are made out of and the aluminized kapton that covers the rest of the outside surfaces. The absorptivity and emissivity of the solar cells are assumed to be 0.91 and 0.86 respectively[3]. The absorptivity and emissivity of the black anodized aluminum are assumed to both be 0.88[25]. The absorptivity and emissivity of the aluminized kapton are 0.14 and 0.12 respectively. To determine the average absorptivity and emissivity of each distinctive side, the properties of each material can be averaged using the area fraction of the material on each side as weights. The resulting properties of the three distinctive sides are presented in Figure 12.3.

[3] `http://cubesat.wikidot.com/the-technology-of-solar-cells` [Retrieved on 10-06-2019]

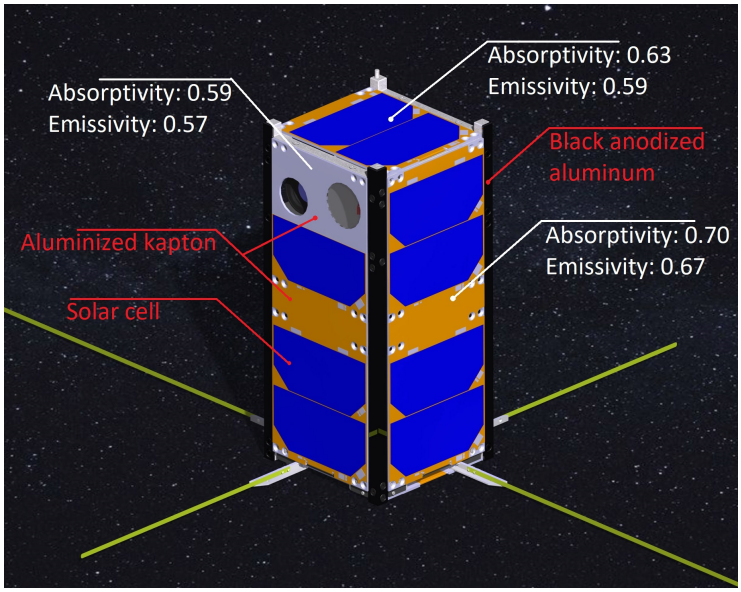


Figure 12.3: The three distinctive types of sides of the spacecraft. In white, the relevant optical properties of the respective surface are given. The elements that make up the surface are given in red

Running the simulations produces the minimum and maximum temperatures given in Table 12.1. These values can then be compared to the design limits of the individual subsystems given in section 12.1.

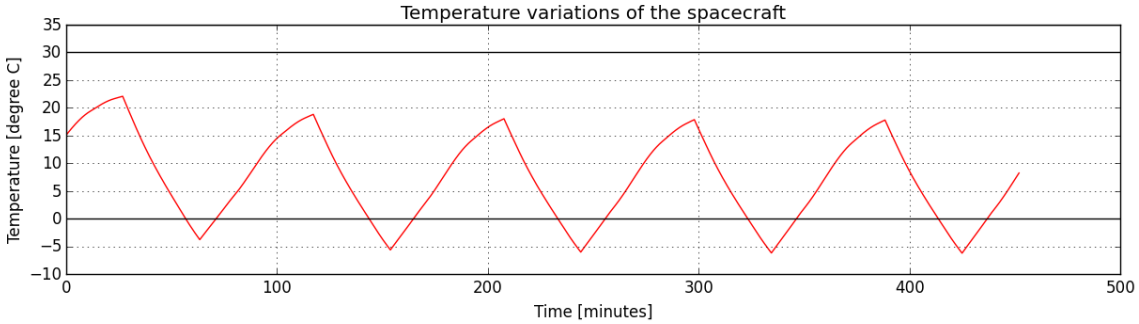


Figure 12.4: The simulated temperature variations of the spacecraft in an equatorial orbit at 300km altitude. The design temperature range is indicated by two solid, horizontal lines

Table 12.1: The results for the preliminary thermal model

| Situation | Altitude [km] | Orbit type | Min. temperature [°C] | Max. temperature [°C] |
|---|---|---|---|---|
| 1 | 300 | Equatorial | -6.33 | 17.9 |
| 2 | 700 | Equatorial | -5.13 | 19.4 |
| 3 | 300 | Polar (continuous Sun exposure) | 30.4 | 31.5 |
| 4 | 700 | Polar (continuous Sun exposure) | 29.5 | 30.5 |

It can be seen that the temperature limits are not met. However, the lower limit is exceeded by only 6.33 $^{\circ}C$ and the upper limit is exceeded by only 1.5 $^{\circ}$. This is considered not to be an issue as the specific heat was taken lower than it will probably be for the real spacecraft. Thus, the simulated temperature limits are lower/higher than they will likely be in reality. Also, as it is the ADCS and the ArduCam that drive the design temperature range, only these components might not meet there temperature requirements. Measures can be taken to ensure

that these components do not exceed their operational range. These measures are discussed in section 12.4.

## 12.4. Final Thermal Control System Design

The thermal control system will for the majority consist of coating on the outside of the spacecraft. These are made up of predominantly solar cells, aluminized kapton and black anodized aluminum as shown in Figure 12.3. If during a more detailed analysis it is found that the temperature of some components is higher than their operational range, the relevant components can be equipped with a small heat sink that conducts the heat away from them. If the temperature is found to be too low, the component can be equipped with an electrical heater.

As the battery is likely to require a electric heater, but this heater is, as of now, not yet sized, the heater is assumed to use about 0.37 $Wh$ per orbit. This is equal to a continuous heater power of 0.25 $W$ which is similar to what other CubeSats use. The ISIS Space iEPS Type A comes with an integrated electrical heater that is controlled by the on-board microcontroller.

The mass of the thermal system consists of the mass of the thermal coatings and the potentially used heat sinks.

# 13
# Command and Data Handling

This chapter discusses the decisions and considerations made in determining a suitable On-Board Computer (OBC) for the spacecraft, intra-spacecraft communication structure and methods of communication for intra-spacecraft communications.

## 13.1. Requirements for the System

The requirements for the CDH system can be found in Requirements. Summarised, the main criteria are:

1. Communicate with the ADCS, Power, Comms and Payloads
2. Capabilities to schedule tasks in advance
3. Process the data acquired from spacecraft systems and then use it/send it on to the relevant system
4. Have a safe mode and be able to enter it

All designs considered will incorporate these requirements.

## 13.2. OBC Options

Potential CDH systems are summarized in Table 13.1. All options have been thought of with consideration given to the requirements in chapter 4 and technical realities discussed in section 13.4.

The OBC from Hyperion BV is physically smaller than most of the other options available. It is still a very powerful option and has flight heritage. Another options for the OBC is the ISIS (Innovative Solutions In Space) on-board computer. The third option is the Beagle Board Back (BBB) on a PC/104 board from Pumpkin Space. This was considered a more ”powerful”option than the ISIS board. Finally, the fourth option is the OBC from Endurosat, which is the cheapest option. Given the price, it was thought of that two of these boards could be put in one satellite for redundancy. This OBC also has built-in 3-axis accelerometers with easy connection of temperature sensors, sun sensors and magnetotorquers possible.

Table 13.1: On-Board Computer Options

| | ISIS On-Board Computer | Pumpkin Space MBM2 | Endurosat On-board computer | Hyperion CP400.85 Processing Platform |
|---|---|---|---|---|
| Processor | ARM9 400MHz processor | AM3358BZCZ100 1GHz | ARM Cortex M7 216MHz processor | ARMv7-A 500 MHz |
| Operating System | FreeRTOS or kubOS Linux | Linux Debian | Not specified | Linux based |
| RAM (volatile memory) | 64MB | 512MB DDR3L | 2MB | 512MB |
| Interface Protocols | I2C, SPI, UART | I2C, UART, USB, and 10/100 Ethernet | CAN, I2C, SPI, UART | I2C, SPI, USB, UART on a companion board |
| Non-volatile memory | 2x SD card slots (up to 32GB) | 4GB eMMC internal storage with SD card slot | 2MB | 512 MB with optional 7.5GB extra on companion board |
| Mass | 94g | 70.7g | 58g | 7g |
| Dimensions | 96 x 90 x 12.4 mm3 | 96 x 93 x 19.6 mm3 | 90.2 x 95.9 x 15.4 mm3 | 50 x 20 x 8.2mm |
| Power Consumption | 0.4 W | 1.5-2.5W | 0.5 W | 0.55 W |
| Cost | 4400 Euros | 4950 Euros | 2900 Euros | Not specified |

### 13.2.1. Trade-Off

For each of the design options as discussed in chapter 6, an OBC is considered and deemed suitable for a concept. However it was confirmed that the Hyperion CP400.85 would be sponsored by Hyperion Technologies leading to a significant decrease in considered cost and enables a high degree of customization. Compared to the other options, this is a very capable board with a low mass, sufficient processor and in-budget power consumption. This OBC also supports a variety of protocol interfaces through its companion board and supports the BUS protocol chosen in section 13.4.

## 13.3. Payload Controller Selection

In chapter 9, the payload architecture was described, which is designed such that each payload module has its own controller. The function of this controller is to facilitate operations between the Space Truck's OBC and the instrumentation of the payload. In this section, a suitable micro controller will be chosen for this purpose.

There are different micro controllers available, in various sizes and performance brackets. The choice of trade-off candidates was done considering the following:

- Common Availability: Widely used micro controllers are desired, as they are designed to work in many different applications, are well documented, and are generally easy to develop for.
- Size: The current available space for payload is quite limited.
- Flight Heritage: Given the tight development timeline of the project, testing time will be limited. Flight proven hardware reduces testing time and improves the design.
- Power Required: Limited power is available for the payloads, the lower the power required the better.

Given these considerations,trade-off candidates were chosen. Two of these are higher in complexity, allowing for a larger variety of payload instrumentation, but being more demanding on the rest of the satellite. The other two are less complex and more efficient, but more limited in performance too. The four trade-off candidates are:

1. Arduino Nano

2. ”Blue Pill”/”Black Pill”, also known as STM32F103
3. Raspberry Pi Zero
4. PocketBeagle

Despite all being micro controller boards, these options still have many significant differences. Therefore, before a trade-off was performed, in-depth research was done on each board. The information was gathered under five headers, namely: Physical properties, Power, Performance, Ease of implementation and Reliability. The result of this is in Table 13.2.

Table 13.2: Specifications of payload micro controller trade-off candidates

| Criterion | Sub-criterion | Arduino Nano | STM32F103 | Raspberry Pi Zero W | PocketBeagle |
|---|---|---|---|---|---|
| Physical Properties | Mass [grams]<br>Size [mm]<br>Operation Voltage [V] | 7<br>45 x 18<br>3.3, 5 | 12<br>57 x 24.4<br>3.3, 5 | 9<br>65 x 30 x 5<br>5 | 10<br>55 x 35<br>5 |
| Power | Power Consumption [W] | 0.1 | 0.2 | 0.9 | 0.75 |
| Performance | I/O Pins<br>Flash memory<br>RAM<br>Processor<br>Supported Protocols<br>Clock Speeds | 23<br>32k<br>2k<br>ATmega328P<br>SPI,UART,I²C<br>16 MHz | 32<br>64k<br>20k<br>STM32<br>SPI,UART,I²C,CAN<br>72 MHz | 40<br>SDHC up to 32 GB<br>512M<br>ARM11<br>USB,UART,I²C,SPI<br>1000 MHz | 44<br>SDHC up to 32 GB<br>512M<br>ARM Cortex A8<br>USB,I²C,UART,SPI,CAN<br>1000 MHz |
| Ease of Implementation | Platform Prevalence<br>Mounting holes | Common<br>Yes | Uncommon<br>Blue: No - Black: Yes | Common<br>Yes | Uncommon<br>No |
| Reliability | Flight heritage<br>Op. Temperature Range | Multiple instances<br>-40, +85 | At least one instance<br>-40, +85 | At least one instance<br>-40, +85 | At least one instance<br>-40,+90 |

Next, a trade-off was performed, with the five groupings of Table 13.2 used as trade-off criteria. However, three changes were made to the sub-criteria:

- The operational temperature range was removed, as it is almost identical for all candidates.
- Operational voltage was removed. Since the power system is able to supply both 3.3V and 5V, there is no preference for any board in this category.
- The processor row has been removed, as the performance of the processor will be assessed based on both clock frequency and flight heritage status.

The resulting trade-off can be found in Figure 13.1. Each micro controller criterion was graded on a scale from 1 (very bad) to 5 (very good), within the context of the mission. For clearance reasons, physical size is considered to be very important (25%). There is a distinct benefit in a micro controller being smaller than 50 mm in size, as it will be able to fit on its side inside a payload compartment. This is visualized in Figure 13.2. Power consumption is also taken with a weight of 25%, as available power is small. Performance is weighed at 20%. Lastly, ease of implementation and reliability have been considered with a weight of both 15%.

| Criterion | Weights | Arduino Nano | STM32F103 | Raspberry Pi Zero | PocketBeagle |
|---|---|---|---|---|---|
| **Physical Properties** | **0.25** | **1.25** | **0.80** | **0.60** | **0.60** |
| Mass | 0.20 | 5 | 4 | 4 | 4 |
| Size | 0.80 | 5 | 3 | 2 | 2 |
| **Power** | **0.25** | **1.00** | **1.00** | **0.50** | **0.50** |
| Power Consumption | 1.00 | 4 | 4 | 2 | 2 |
| **Performance** | **0.20** | **0.62** | **0.76** | **0.98** | **0.98** |
| I/O Pins | 0.20 | 4 | 4 | 5 | 5 |
| Flash memory | 0.10 | 3 | 3 | 5 | 5 |
| RAM | 0.10 | 2 | 3 | 4 | 4 |
| Supported Protocols | 0.50 | 3 | 4 | 5 | 5 |
| Clock Speeds | 0.10 | 3 | 4 | 5 | 5 |
| **Ease of implementation** | **0.15** | **0.60** | **0.53** | **0.60** | **0.38** |
| Common system | 0.50 | 4 | 3 | 4 | 3 |
| Mounting holes | 0.50 | 4 | 4 | 4 | 2 |
| **Reliability** | **0.15** | **0.60** | **0.45** | **0.45** | **0.45** |
| Flight heritage | 1.00 | 4 | 3 | 3 | 3 |
| | | **4.07** | **3.54** | **3.13** | **2.91** |

| Legend | |
|---|---|
| 1 | very bad |
| 2 | bad |
| 3 | acceptable |
| 4 | good |
| 5 | very good |

Figure 13.1: Trade-off of the payload micro controller candidates

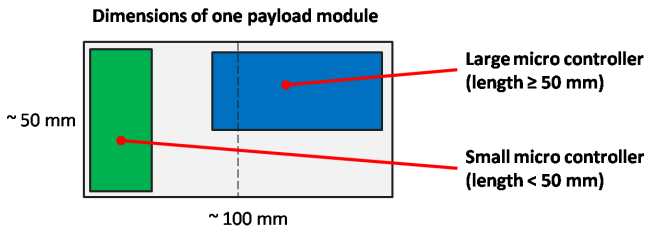


Figure 13.2: Placement advantages of micro controllers with a length smaller than 50 mm

From the trade-off, the Arduino Nano emerges as the best choice. While less powerful than other options, its size, low power requirements, and flight heritage makes it stand out.
The Arduino Nano however comes with only 32 kilobytes of flash storage. This means high data rate and resolution sensors like e.g. video cameras may not be supported. Whilst 32 kilobyte storage is substantial for use within CubeSats, it cannot be guaranteed that this is always enough. As a recommendation, when detailed software development starts, an educated estimate must be made to ensure that 32k worth of storage is enough. If not, there are three options:

1. Add a storage expansion chip, which are commercially available for Arduino-like boards.
2. Choose another ATmega-based micro controller with more storage, such as the ATmega256x. This keeps the controller architecture constant, which simplifies integration.
3. Choose another micro controller with more storage. This provides more freedom, but also requires significantly more integration effort in terms of software development and testing.

In addition, space-saving coding techniques may be applied to minimize code size.

## 13.4. Protocol Selection

For intra-spacecraft communication, a communication bus protocol must also be chosen. Ideally, the same protocol can be used for all systems to simplify the design and integration. From Figure 13.3, it can be seen that $I^2C$ and UART are the most common protocols within the chosen subsystem components.

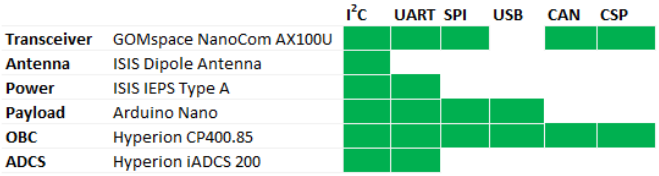


Figure 13.3: Inventory of every subsystem, and the communication protocols that are natively supported by each

However, there are other aspects to consider and therefore the subsystem will be taken as criterion in the protocol trade-off. Firstly, there is the matter of choosing between a half-duplex or full duplex connection. For some connections, such as the connection between OBS and the transceiver, it is preferable to have a full duplex connection, so that data can be transferred both ways without interfering. Secondly, there is the number of lines to consider. Some protocols require more data lines than others, requiring more space to implement. For mass and clearance reasons, lower is better. Thirdly, there is software overhead required to consider. Finally, there is reliability, which for this analysis was split up into flight heritage, error checking capability, and line redundancy.

With these criteria, a trade-off was performed, the details of which can be found in Figure 13.4. The CAN and CSP protocols were withheld from the trade-off, because their subsystem compatibility was too poor. Instead, several line configurations (RS, Recommended Standards) for UART were included in the trade-off. The trade-off was performed using the same grading scheme as for the payload controller trade-off.

| Criterion | Weights | RS232 | RS485 | RS422 | I2C | SPI |
|---|---|---|---|---|---|---|
| **Performance** | **0.1** | **0.4** | **0.4** | **0.4** | **0.2** | **0.4** |
| Full duplex | 1 | 4 | 4 | 4 | 2 | 4 |
| **Physical Size** | **0.2** | **0.8** | **0.8** | **0.6** | **0.8** | **1** |
| Amount of lines | 1 | 4 | 4 | 3 | 4 | 5 |
| **Software** | **0.15** | **0.75** | **0.6** | **0.75** | **0.45** | **0.6** |
| Software overhead | 1 | 5 | 4 | 5 | 3 | 4 |
| **Reliability** | **0.3** | **0.84** | **1.20** | **1.20** | **0.78** | **0.78** |
| Error checking | 0.2 | 4 | 4 | 4 | 2 | 3 |
| Flight heritage | 0.2 | 4 | 4 | 4 | 5 | 4 |
| Line redundancy | 0.6 | 2 | 4 | 4 | 2 | 2 |
| **Compatibility** | **0.25** | **1** | **1** | **1** | **1.25** | **0.75** |
| Subsystem Compatibility | 1 | 4 | 4 | 4 | 5 | 3 |
| | | **3.79** | **4.00** | **3.95** | **3.48** | **3.53** |

| Legend | |
|---|---|
| 1 | very bad |
| 2 | bad |
| 3 | acceptable |
| 4 | good |
| 5 | very good |

Figure 13.4: Trade-off of the protocol candidates.

From Figure 13.4 can be seen that RS-485 and RS-422 surface as best choices. After consulting with industry experts, RS-485 was chosen definitively because of its reported more common occurrence and compatibility with commercially off-the-shelf CubeSat parts. The ISIS antenna, based on its datasheet, cannot talk over UART with RS-485, and as such will need its own I2C connection. However, since this line is presumed to only relay antenna deployment commands, this is considered a surmountable obstacle.

## 13.5. Intra-Spacecraft Communications

The connections between hardware components can be seen in Figure 13.5. As RS-485 was chosen for the electrical interface with a UART data interface for the OBC communications with all subsystems, there will need to be five lines between the OBC and a subsystem. In total, 15 pin connectors on the OBC board for this, configured according to the respective standards. As UART was chosen, the clock rate of each peripheral does need to be specified pre-launch. The EPS and antenna deployment are the only systems which do not support differential communication protocols (i.e. RS-485), therefore a different protocol must be used. The EPS does support I2C and RS-232, UART. As the rest of the data transmitted will be using UART, it will be easier to keep this protocol the same for all systems, therefore RS-232 will be used for the EPS-OBC connection. For the ISIS antenna, it supports I2C for deployment, therefore I2C will be used for that particular system.

## 13.6. Software

All software design will be done in the next phase of the project (see chapter 21). To aid in the design for the code, the Functional Flow Diagram in section 15.3 provides a good overview of all the functions the code needs to be written for.

## 13.7. Sensitivity Analysis

Compared to other systems, the sensitivity of the CDH system to changing external parameters, such as orbital height is very little. Different OBC choices also have little impact on the overall system performance as the required processing power for this mission is not significant to what all OBC options listed in Table 13.1 can provide. As the current OBC companion board has support for a multitude of computer bus protocols, there will not be a challenge for physically incorporating a new protocol resulting from a protocol re-selection or a SC subsystem change. The choice of micro-controller is more susceptible to change as the available power and mass for that system is tight, however other micro-controllers also meet the requirements for the system.

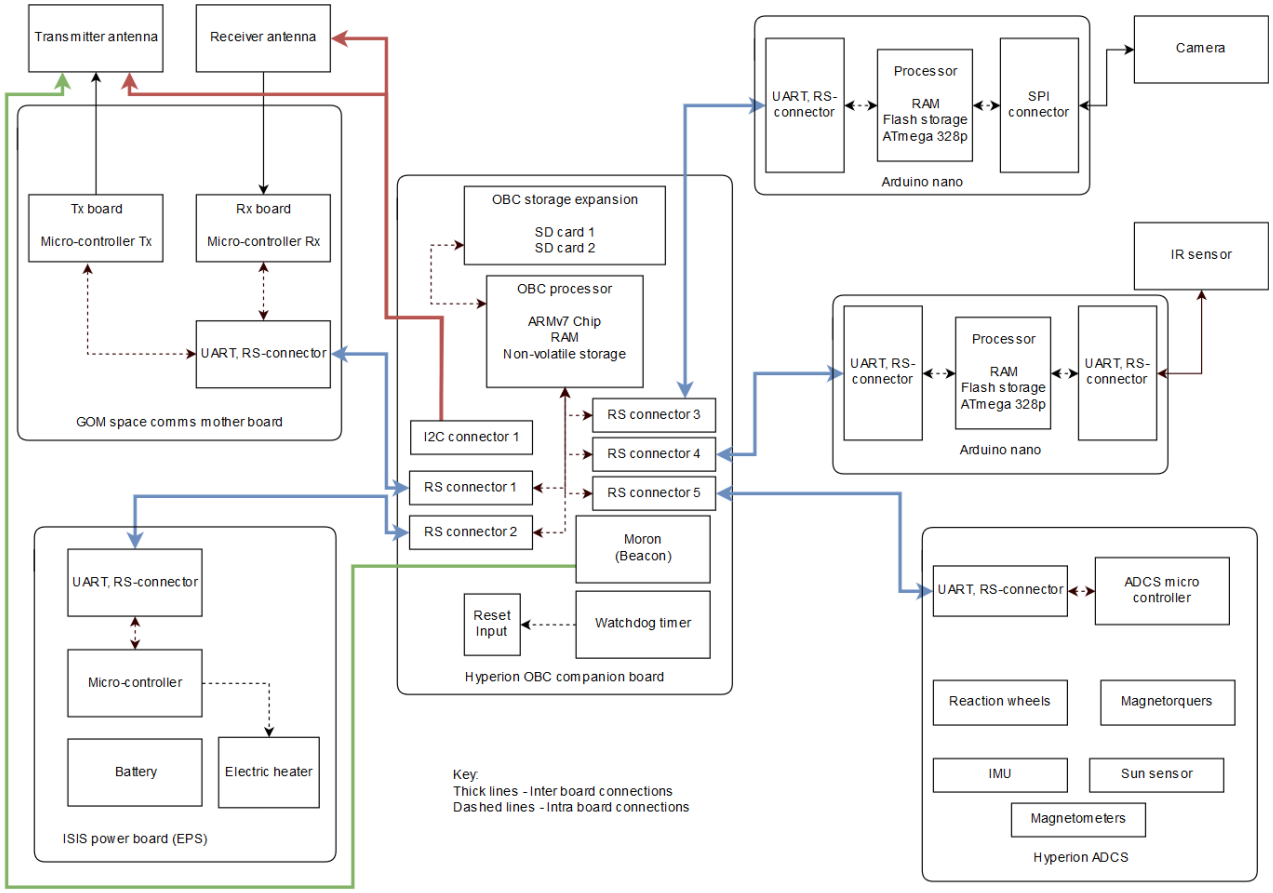


Figure 13.5: Hardware connection and communication block diagram showing all inter- and intra-board communication (UART RS-485/232 (blue), $I^2C$ (red), direct beacon line (green), intra-board communication (black))

# 14

# Attitude Determination and Control

For the attitude determination and control system a Hyperion ADCS module and additional components are selected (section 14.1 and section 14.2. Following from this, an estimate on the worst-case disturbances is evaluated and the control characteristics of the reaction wheels and magnetotorquers are determined (section 14.3). Finally the control modes for the ADCS are presented (section 14.4). In section 14.5, the sensitivity analysis in discussed.

## 14.1. Concepts and Hyperion Sponsorship

From the concept trade-off of the satellite a simplex, passive ADCS is preferred. However, as the payload is chosen to provide images of earth, a high degree of pointing stability is required. During the trade-off procedure one of the project sponsors Hyperion Technologies BV approached the design team offering a fully sponsored, active ADCS. This ADCS is able to provide high pointing accuracy while being highly mass and power efficient.

Furthermore, the resulting cost benefits and availability of components and infrastructure in Delft were some of the main considerations that led to the ADCS being changed to an active, integrated ADCS. Throughout the subsequent design integration, Hyperion has proven to be very reliable and responsive to relevant design questions. Another factor taken into account is the capability of the ADCS which leads to stabilize and maneuver the satellite.

It should be stated however, that information on economic value and reliability (e.g. Technology-Readiness-Level (TRL) and component reliability) is limited. If the system would not be sponsored, it might be infeasible due to certain payload and budget considerations. This should be taken into account for successive missions of the Space Truck concept.

## 14.2. Trade-Off

For the Hyperion iADCS 200 which is the sponsored version two configuration choices need to be discussed: The ADCS allows the implementation of a star tracker (STR) and reaction wheels (RW) which are not considered in the concept trade-off. Apart from these components the ADCS further includes: 1 Inertial Measurement Unit (IMU), 1 Magnetometer (MTM), 3 Magnetotorquers (MTQ) and sun sensors. The STR has a best case 2-axes pointing knowledge (PK) of 30 arc seconds [1] and the sun sensors a 2-axes PK of at minimum 1° (under 45° incidence angle) [2].

### 14.2.1. Star Tracker

A star tracker is able to significantly improve PK in sunlight and especially in eclipse. Furthermore, if used in combination with sun sensors, magnetometers and gyroscopes redundancy is added to the system. One downside of the star tracker is that it increases complexity of the ADCS in terms of controlling and hardware. In addition, the measuring time of the star sensor is usually between 0.1 and 0.2 s [1] while for a sun sensor it can be as low as 0.01 s [2]. This means for a star tracker a gyroscope is required to maintain high accuracy over a longer period of time requiring additional power. As the STR is very sensitive it needs to be constantly pointed away from the sun and the earth making pointing maneuvers more complicated or accepting

[1] https://hyperiontechnologies.nl/products/st200-star-tracker/ [Retrieved on 21-06-2019]
[2] https://hyperiontechnologies.nl/products/ss200/ [Retrieved on 21-06-2019]
[3] https://hyperiontechnologies.nl/products/iadcs100/ [Retrieved on 21-06-2019]

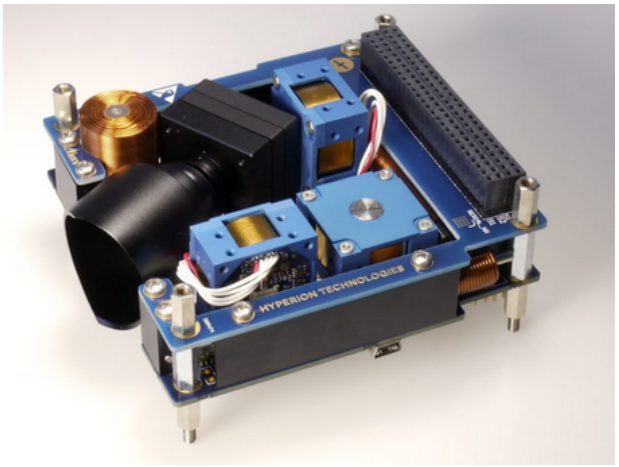


Figure 14.1: Hyperion iADCS 100 with STR and RWs [3](precessor of the sponsored system)

momentary unavailability during maneuvering. Due to this effect CubeSat requires additional sun sensors which can take over.

Moreover, the slew rates that can be achieved during active tracking are limited, meaning during initial tumbling the STR may not be usable. Finally, the accuracy achieved without the star tracker can be sufficient for the payload considered for the Space Truck leading to a considerable decrease in power consumption. This leaves the STR as a less desired option for the ADCS.

### 14.2.2. Reaction Wheels

Reaction wheels (RWs) have the ability to provide very accurate pointing and turning maneuvers. This is due to the fact that the delivered torque is independent of orientation or orbital position compared to e.g. magnetotorquers (MTQs). They can also provide higher angular accelerations to the satellite if required.

The disadvantages of having reaction wheels are that they can induce jitter (uncertainty in rotation axis) and vibrations in your satellite which may need to be accounted for in certain sensor measurements/calibrations e.g gyroscope noise environment [42]. Furthermore, if used for high accuracy pointing, reaction wheels need to be desaturated regularly, meaning the excess momentum is dumped, which increases power consumption. Moreover, RWs consist of moving parts meaning they introduce complexity and are subject to mechanical wear.

All of these points need to be accounted for during orbital maneuvering, however for pointing the satellite it is a lighter and less complex option than e.g. control momentum gyros. Moreover, they allow motion with degree accuracy compared to MTQs which are simpler but need more time for attitude corrections which is likely to cause problems with camera pointing. Considering the favored payload options the use of RWs may be unavoidable as they generally provide better pointing stability than MTQs and can be easily integrated in the provided ADCS.

## 14.3. Control Behaviour and Validation

In this section the ADCS usage is validated by making a first-order worst case disturbance computation and a simplified estimate on the achievable rotation rates of the RWs.

### 14.3.1. Disturbance and Actuation Model

Disturbance torques in orbit have 4 possible sources: Solar radiation, earth magnetic field (EMF) disturbance, atmospheric drag and gravity gradient. For CubeSats in LEO orbit drag and magnetic disturbance torques are usually dominating. Gravity gradient is small if the difference between the maximum and minimum moments of inertia $I_z - I_y$ is small (relevant for long boom structures). As the gravitational force ($3\mu/2R^3$) decreases with altitude, elongated satellites tend to align their axis of minimum inertia with gravity direction ($\theta \rightarrow 0$) [42].

Solar radiation and atmospheric drag are both considered pressure forces caused by photons or gas molecules colliding with the spacecraft [10] on a certain projected area ($A_r, A_s$). Drag depends mainly on orbital velocity (V) and atmospheric density ($\rho$), while solar radiation depends on solar radiation flux ($F_s/c$) and reflectivity of the satellite (q). The angle $\varphi$ is the Sun incidence angle. The torque is caused by geometric deviations in the center of mass position [42] ($c_p - c_m$). Magnetic disturbance torque is caused by Eddy currents (electric induction) (D) inside the satellite which induces a magnetic dipole producing a torque [10].

For the disturbance model, the drag and magnetic field are modelled with the method described by Wertz and Larson in SMAD [42]. For the other disturbances, values from literature are assumed. This method provides a simplified first order estimation for the disturbance torques in orbit which is implemented under the following assumptions.

- Earth is spherical with homogeneous gravity field.
- Satellite can be modelled as a homogeneous cuboid.
- The drag is estimated at worst-case density (increasing the mean amplitude by a factor of 2.6 at 300 km and 10 at 700 km [4]) [42].
- The drag coefficient $C_D$ is independent of spacecraft orientation (varies between 2 and for 4 depending on orientation) [33].
- Reference velocity and area are maximized for worst-case.
- The magnetic field is caused by a constant dipole M and is a function of dipole distance R and latitude $\lambda$ only (effects of time and ascending node neglected).
- The angle between magnetic field vector and dipole of the satellite is 90°.
- GaAs solar panels have a reflectivity of about 30 % without coatings [34].

$$T_a = \frac{1}{2}\rho C_D A_r V^2 \left(c_p - c_m\right) \tag{14.1}$$

$$T_m = D\frac{M}{R^3}(2 - cos(\lambda)) \tag{14.2}$$

$$T_g = \frac{3\mu}{2R^3}\left|I_z - I_y\right| \sin(2\theta) \tag{14.3}$$

$$T_s = \frac{F_s}{c} A_s (1+q)\left(c_p - c_m\right)\cos\varphi \tag{14.4}$$

The computed disturbance torques for the considered altitude range can be seen in Table 14.1. For a more detailed outline of the variables and their assumed values, please refer to the previous (mid-term) report [13]. It is stated in SMAD that for LEO orbits magnetic and drag disturbances are usually dominating which is true for 300 and 500 km, while for 700 km, magnetic disturbance is still dominating. The verification of the results is performed with the default calculations from [42]. During this step it was found that a slightly different value for the magnetic dipole strength was used for different versions of SMAD [23, 42] leading to a difference of about 2 % for the magnetic field assumption (for the calculation a value of $7.8 \cdot 10^{15}$ $Tm^3$ is used). For the worst case offset a value of 5 cm (along $z$-axis) is assumed [11].

For the torque estimations of the MTQs the Equation 14.2 is utilized, while for the RWs some simple kinematic relations are utilized.

RWs and MTQs both change the angular momentum of the satellite which is defined as the product of mass moment of inertia I and the angular rate $\omega$. A change in angular momentum is usally achieved by a torque T that acts for a time $\Delta t$. The RW when speeding up induce an (ideally) equal and opposite torque to the satellite.

$$I_2\omega_2 = I_1\omega_1 + \sum T\Delta t \tag{14.5}$$

[4] Due to time constrains the previous orbital design range of 300-700 km was assumed in stead of 300-600 km. Since the a larger design space is considered, the system will not be under designed

Table 14.1: Worst case disturbances against altitude for 2U CubeSat for considered orbits (numbers given in nNm)

| | 300 km | 500 km | 700 km |
|---|---|---|---|
| Drag | 4570 | 260 | 25 |
| Magnetic | 4200 | 3850 | 3530 |
| Gravity | 12.5 | 11.5 | 10.6 |
| SRP | 8 | 8 | 8 |

### 14.3.2. Control and Stability Characteristics

From the equations described in subsection 14.3.1 an initial estimate on the slew rates, momentum and angular acceleration of the satellite can be created. Furthermore, the minimum time to turn a certain angle can be computed using the assumption that one wheel is constantly accelerated and then decelerated again. The control characteristics for the RWs can be found in Table 14.2. The values are representative for the smallest available RWs, which were found to be sufficient to provide accurate pointing for the CubeSat. The calculations were verified by hand-written calculations. The axes of reference for the maneuvers are specified in Figure 14.2.

Table 14.2: Slew rates, MMOI, angular acceleration and minimum slew time for RW and CubeSat [5]

| | RW | S/C (x,y-axis) | S/C (z-axis) |
|---|---|---|---|
| $\omega_{max}$ [rpm] | 10000 | 1.57 | 3.94 |
| MMOI $[kgm^2]$ | $1.64 * 10^{-6}$ | $1.04 * 10^{-2}$ | $4.17 * 10^{-3}$ |
| $\dot{\omega}_{max}[rad/s^2]$ | 53.05 | $8.35 * 10^{-3}$ | $2.01 * 10^{-2}$ |
| slew time 90° [s] | - | 13.7 | 8.7 |
| slew time 180° [s] | - | 19.4 | 12.3 |

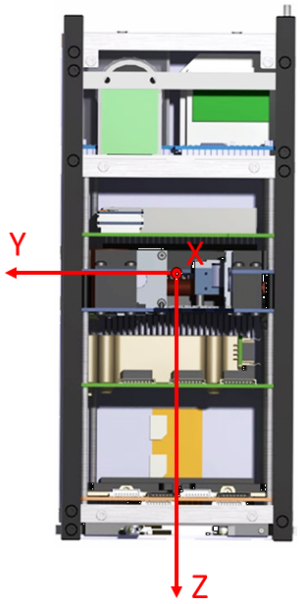


Figure 14.2: Reference/Body coordinate system for the Space Truck

For the MTQs the maximum slew rates and accelerations are more difficult to determine as they depend on orbital altitude and latitude. As the satellite needs to pass over Delft the inclination needs to be between 52 and 128 °. The altitude range as mentioned before is 300 - 700 km. In Figure 14.3 the simplified magnetic field is shown for different altitudes and longitudes

[5]Information for RWs provided by Hyperion Tech. (https://hyperiontechnologies.nl/products/[Retrieved on 21-06-2019])

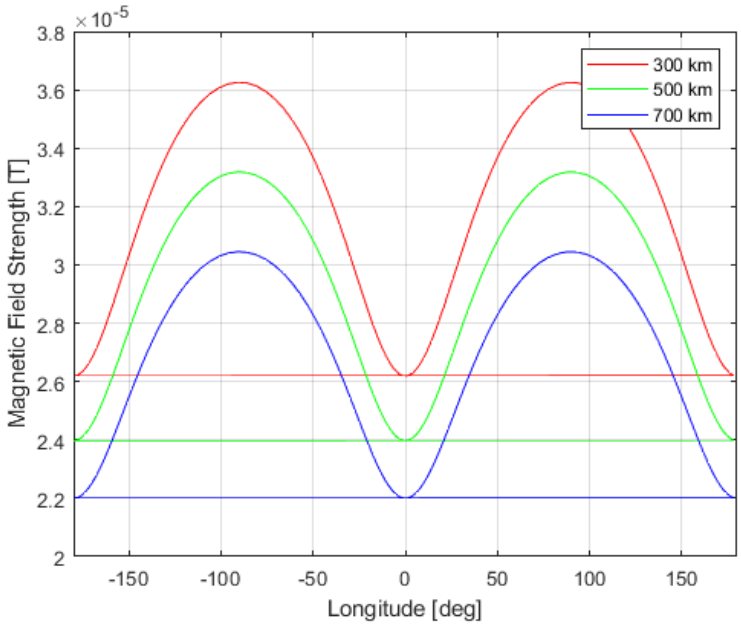


Figure 14.3: Simple Dipole Magnetic field model for 52° inclination

in a 52° inclination orbit. It can be observed that the Magnetic field strength decreases by about 16 % from 300 to 700 km.

One MTQ induces a magnetic dipole moment of about $0.1 - 0.2Am^2$ (nominally) [6] meaning the maximum control torque is proportional to the internal magnetic field of the satellite and the angle between the S/C magnetic field and the EMF. This means the achievable torques can range between 0 (fields aligned) and about $10\mu Nm$ (300 km and 90°) for one MTQ. This is significantly less than the RW torque of about $87\mu Nm$.

However, one important distinction is that RWs have a limited momentum change they can provide, while MTQs can provide continuous torque. Furthermore, the MTQs also facilitate a boost mode which increases the induced dipole moment to $0.25Am^2$ (z-axis) and $1Am^2$ (x,y-axis). This means an achievable maximum torque of about 40 $\mu Nm$. This however consumes additional power and is likely not feasible for disturbance balancing.

At altitudes around 300 km the maximum assumed atmospheric drag and magnetic disturbances occur. For this case, to achieve stability over a period of time, a combination of MTQ and RW operations would be required. In addition for certain orientations where attitude cannot be maintained either free tumbling or changes in orientation are required. This can be achieved by using the magnetic disturbance as a damping mechanism against the drag.

Another strategy would be to reduce the effective distance $c_p - c_m$ (see section 15.2) for drag in the most critical direction. This could significantly decrease the worst-case assumed drag disturbance torque ensuring better maneuverability of the satellite. If a lower orbit should be chosen where both drag and magnetic disturbance are significant, the significance of these torque reduction techniques can be analysed in more detail.

### 14.3.3. Model Review

For the model dipole, the EMF is only varying with latitude and altitude. However, if more accurate EMF models are considered other factors need to be taken into account which change the field magnitude and direction significantly. The first factor is that the magnetic field poles are not aligned with the geographic poles but deviates by about 10° [9]. This mainly affects the amplitude of the maxima for a given inclination.

Another factor is that the EMF is asymmetric this due to charged particle interactions caused by solar radiation and solar wind [3]. As these interactions are a function of time, the magnetic

[6] Information for MTQ (`https://hyperiontechnologies.nl/products/mtq200/`[Retrieved on 23-06-2019])

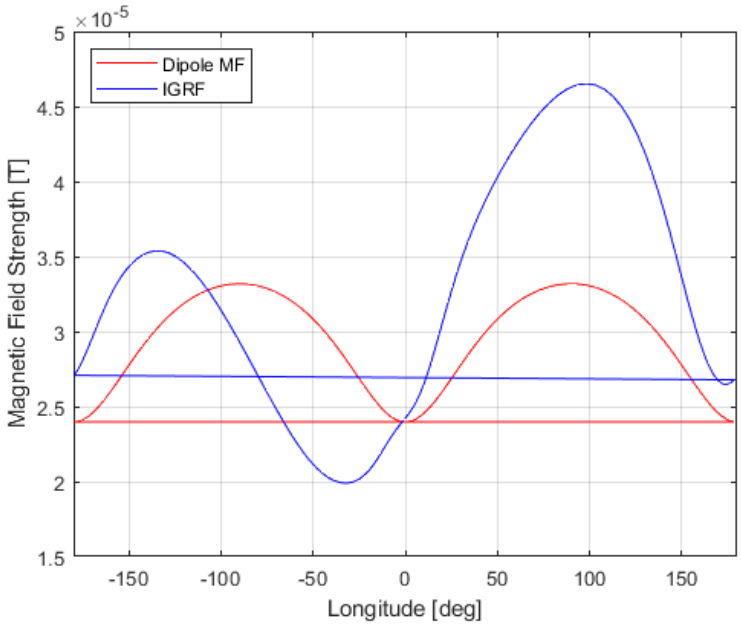


Figure 14.4: Dipole and IGRF Magnetic Field (500 km, 52 deg inclination) [Data for the 01.01.2015]

field magnitude also changes with time. Furthermore, the overall field strength decreases continuously over time. This means both the ascending node and the mission time are crucial factors for an accurate estimate of the EMF.

For an impression on the impact of these factor an international geomagnetic reference field (IGRF) [7] model is used utilizing data from an undisturbed orbital propagator[8]. This IGRF computation relates to the dipole model for a default orbit (h = 500 km, i = 52 °, Ω = 0 ° [9]), as seen in Figure 14.4. The asymmetry of the EMF can be clearly observed for the IGRF for positive and negative longitudes of the orbit.

It can be observed that the asymmetry of the magnetic field has a significant impact on its local magnitude. This needs to be accounted for the MTQs as the accuracy of the initial estimate is in the order of about 35% which is also highly dependent on solar activity. The considered time frame for the IGRF denotes a maximum solar activity which compresses the magnetic field increasing its magnitude in LEO.

In terms of drag modelling, the highest uncertainties are present for the atmospheric density, drag coefficient and orbital velocity. In the upper layers of the atmosphere the density becomes highly sensitive to all types of disturbances e.g. solar activity, magnetic field fluctuations and local atmospheric composition [33]. The uncertainty in density increases with increasing altitude. This makes it very difficult to estimate the worst-case density the satellite experiences in its lifetime.

For the drag coefficient the uncertainties result from surface-particle interactions as well as geometry of the satellite. As the $C_D$ is usually averaged uncertainties for specific orientations can be more significant than others [33]. For the model a circular Kepler orbit was assumed which introduces velocity uncertainties due to gravity effects but also atmospheric winds and other interactions can cause deviations in orbital velocity [33].

As estimating the accuracy of the drag model is not trivial the worst case estimation is deemed to be sufficient at this design stage. To optimize the ADCS performance either detailed analysis or in-situ demonstration may be required.

[7] https://nl.mathworks.com/matlabcentral/fileexchange/34388[Retrieved on 13-06-2019]
[8] https://nl.mathworks.com/matlabcentral/fileexchange/69439[Retrieved on 13-06-2019]

## 14.4. Control Operations for ADCS

The ADCS has 5 main operational modes which can be seen in Figure 15.5, Figure 15.6 and 15.7. The ADCS is semi-autonomous meaning it can perform certain operations like momentum dumping and detumbling without input from the OBC. When sun pointing is required the ADCS receives a command from the OBC, checks if the sun is in view and if so switches to sun pointing. A similar procedure is applied for target pointing except that the ADCS requires a reference orientation or target to point to. Different ADCS modes are visualized in the functional flow diagrams presented in section 15.3.

The target pointing mode can have two different objectives; the first one is payload operation while second one involves increased satellite drag to accelerate de-orbiting if necessary. De-orbiting will be applied mainly after the end of the primary mission as it increases the wear on the RW if they should be required. The information on which objective is needed is provided by the OBC, while the target orientation is in the reference memory of the ADCS. If pointing is not required anymore the OBC sends a command that resets the ADCS into momentum dumping and idle condition.

In idle condition the system performs self-diagnosis and switches to detumbling or RW momentum dumping if required. During nominal operation the ADCS operates a control loop which checks for complete sensory input at certain time intervals. When sensor reference,e.g. due to collision, is lost the ADCS switches into emergency mode. In emergency mode the system runs diagnosis and tries to redetermine its attitude. Momentum dumping can be enable/disabled through the OBC by a simple logical switch.

For pointing operations two additional submodes can be defined as disturbance balancing and slew maneuvering. Usually both modes are required for pointing. During balancing the reference orientation is kept constant for a time set by the OBC, while for maneuvering the ADCS turns the SC towards a specified attitude.

## 14.5. Sensitivity Analysis

For the ADCS the following error sources are considered:

- Actuator malfunction
- Sensor malfunction
- Software malfunction
- Interface malfunction

Malfunctioning of components can have multiple consequences including loss of performance, erroneous data output and/or loss of interface communication.

The malfunctioning of an actuator for example could lead to decrease in pointing accuracy and reduced actuation (by 60 - 95 %) for a RW , while a MTQ malfunction could result in difficulties with momentum dumping, higher power consumption as RWs might have to be used. Furthermore, if a de-orbiting mode is implemented, it can induce a lot of wear to the RW when they are used, which would decrease the effective lifetime of the ADCS. It should be considered that for the actuators sometimes experimental values were used and there might be some reduction of performance in orbit. This was assumed a negligible issue as the primary mission life of the satellite is comparably short but it might have effects on the de-orbiting performance of the SpaceTruck.

In terms of sensors, electrical or mechanical defects of a gyroscope or one sun sensor may occur. For the sun sensor the data of the remaining sun sensors would be utilized. This could lead to a significantly reduced PK for certain orientations. This could be compensated by the gyroscopes for short-term measurements (a few minutes) without significant PK loss. The malfunction of a gyroscope can be compensated as long as all sun sensors are operating. A higher update rate of the other sensors would be required and the PK in eclipse would be reduced, these effects however are not deemed mission critical. In case of multiple sensor failure the usage of the on-board camera as an additional sensor may have to be considered. The MTM is the least likely to fail as it is a very simple mechanism. However, it is very sensitive

to magnetic disturbances of the satellite and has to be updated with sun sensor data to provide sufficient accuracy [1].

The most likely form of software malfunction is assumed to be a bit-flip in the data readings. This should first of all not cause the ADCS break-down. If a significant deviation in data is detected the ADCS micro controller should check for the next data input. If the error keeps occurring, the ADCS is going to enter emergency mode as then it is likely that there is a more serious issue. In emergency mode the ADCS is going to perform self-diagnostics and may enable external debugging. Interface malfunctioning should be avoided as communication between OBC and ADCS is mission-critical. This risk can be mitigated by e.g. keeping data communication to a minimum and introducing multiple lines.

Spacecraft induced attitude uncertainties are assumed to be most significant for the MTM (uncorrected dipole moment). These would however only have a strong performance effect if elliptical orbits or insufficient momentum dumping are considered (see MTQ malfunction) [19].

Another disturbance source is the momentum stored in the RWs. During idle condition and sun-pointing, RWs can be considered to be non-active. Their use should be limited to stabilizing the spacecraft with very high precision during target-pointing. Depending on orbit momentum dumping may be applied on a more or less regular bases where the change in rotational stiffness of the satellite needs to be considered [42].

# 15
# System Integration

In this chapter, the integrated system is presented. In section 15.1, an overview of the final design is given. In section 15.2, the layout of the spacecraft is presented. In section 15.3 and section 15.4 the functional flow diagram and functional breakdown structure of the Space Truck are given respectively.

## 15.1. System Characteristics

The resource budgets for the final design are presented in subsection 15.1.1. The performance analysis is given in subsection 15.1.2.

### 15.1.1. Resource Budgets

The resource budgets of the final design are given in Table 15.1 through Table 15.3.

The mass budget is given in Table 15.1. The mass for the beacon is included in the mass of the OBC adapter board as it will be integrated on this board. The 51 $g$ reserved for adapter boards is for the adapter board for the transceiver modules. However, it is notable that the OBC adapter board will most likely be custom made. Considering this, it may be worthwhile to integrate the transceiver modules on the OBC adapter board.

As the final orbit is not known yet, the total available power is based on the worst case orbit for the power budget. This corresponds to an equatorial orbit at 300 $km$ as for this orbit, the eclipse time is longest relative to the total orbital period. The mean power generation is then 2.83 $W$. The corresponding total energy available is about 4.26 $Wh$ per orbit. To make the power budget, the power consumption is split up into different parts. The two main parts are for the spacecraft in eclipse and for the spacecraft in the sun exposed part of the orbit. During both of these parts, the receiver is assumed to be on which is equivalent to the receiver always being on. This is done as the receiver, once powered on, is never turned off. During the eclipse, the OBC and ADCS are assumed to be idling as the spacecraft is assumed to do the payload operations during the sun exposed part of the orbit. Also, during eclipse the heater is assumed to be on as some components might get too cold during the eclipse. For the sun exposed part of the orbit, the OBC is assumed to be under nominal load. This is as the payload is likely to be run during this part of the orbit and running the payload might require some OBC processing. Also the ADCS is assumed to be under nominal load as the spacecraft will be pointed towards the sun/payload target during this part of the orbit. In addition to these basic power requirements, a 58.2 $s$ period is assumed where the spacecraft turns. This corresponds to three 180 ° turns for the worst case turning scenario as presented in Table 14.2. This is done as the spacecraft is likely to have to turn when it comes out of eclipse to point towards the sun. Then two turns are assumed for the spacecraft to point towards a target and back. 180 ° was assumed as that is the most the spacecraft would ever have to correct. The part for transmitting data is assumed to be 15 minutes (900 $s$) which was found to be a good compromise between available transmitting time and available payload power. The power available for the payload is then 1 $W$ for 0.5 $h$, i.e., 500 $mWh$ per orbit. Not that if the payload would not require the available power, it could be used to increase the transmitting time or vice versa. Table 15.4 summarizes these blocks. The power budget is then based on this power distribution. The final power budget is given in Table 15.2.

A stack height budget has been given instead of a volume budget. This is as a CubeSat mostly consists of different components stacked on top of one another and it thus makes more

sense to divide up the stack height itself instead of the volume. The stack height available in the chosen structure is 14.45 $cm$. Note that this is only the height of the stack rods and does not include the height of the payload compartment. As a result, the payload does not need to be taken into account in the height budget. Also the antenna is not taken into account in the height budget as it can be mounted on the outside of the structure. As the OBC and the beacon are integrated on the OBC adapter board, they are not included in the height budget either. Also the communications system is not included as it is integrated on the adapter board. The height of the connectors has been included in the height of the relevant subsystems. The final stack height budget has been given in Table 15.3.

Table 15.1: The mass budget for the final design of the Space Truck. The greater the contribution to the total mass, the darker the cell is colored

| Mass budget | | |
|---|---|---|
| | Nominal [g] | Margin [g] |
| ADCS | 370 | 76 |
| Structures | 198 | 50 |
| Payload | 500 | 0 |
| Thermal | 50 | 50 |
| Comms | 134 | 0 |
| Power | 675 | 0 |
| C&DH | 7 | 8 |
| Cabling/ conncectors | 31 | 0 |
| OBC adapter board | 100 | 20 |
| Beacon | 0 | 0 |
| Adapter boards | 51 | 0 |
| System margin | | 180 |
| Nominal total | | 2116 |
| Margin total | | 204 |
| Nominal + margin total | | 2320 |
| Total | | 2500 |

Table 15.2: The power budget for the final design of the Space Truck. The greater the contribution to the total mass, the darker the cell is colored

| Power budget | | |
|---|---|---|
| | Nominal [mWh] | Margin [mWh] |
| ADCS | 1294 | 0 |
| Payload | 500 | 0 |
| Thermal | 371 | 0 |
| Comms | 1298 | 0 |
| Power | 0 | 0 |
| C&DH | 737 | 0 |
| OBC adapter board | 0 | 0 |
| Beacon | 10 | 0 |
| Adapter boards | 0 | 0 |
| System margin | | 50 |
| Nominal total | | 4210 |
| Margin total | | 0 |
| Nominal + margin total | | 4210 |
| Total | | 4260 |

Table 15.3: The height budget for the final design of the Space Truck. The greater the contribution to the total mass, the darker the cell is colored

| Stack height budget | | |
|---|---|---|
| | Nominal [cm] | Margin [cm] |
| ADCS | 3.4 | 0 |
| Structures | 0 | 0 |
| Payload | 0 | 0 |
| Thermal | 0.5 | 0 |
| Comms | 0 | 0 |
| Power | 2.7 | 0 |
| C&DH | 0 | 0 |
| OBC adapter board | 1.6 | 0 |
| Beacon | 0 | 0 |
| Connectors | 0 | 0 |
| Spacing | 2.5 | 0.5 |
| Adapter boards | 1.6 | 0 |
| System margin | | 1.65 |
| Nominal total | | 12.3 |
| Margin total | | 0.5 |
| Nominal + margin total | | 12.8 |
| Total | | 14.45 |

Table 15.4: The duration that each subsystem is on and how much power each subsystem consumes during this period

| Description | Duration [s] | Power consumption [W] | | | | | |
|---|---|---|---|---|---|---|---|
| | | ADCS | CDH | Thermal | Rx | Tx | Payload |
| Night cycle | 2191.64 | 0.56 | 0.4 | 0.61 | 0.396 | - | - |
| Day cycle | 3230.84 | 1.04 | 0.55 | - | 0.396 | - | - |
| Maneuvering | 58.2 | 3.64 | - | - | - | - | - |
| Transmission | 900 | - | - | - | - | 2.805 | - |
| Payload functionality | 1800 | - | - | - | - | - | 1 |

### 15.1.2. Performance Analysis

The main capability of the satellite is taking visible light and infrared pictures. The visible light camera has a resolution of 2 megapixels. The satellite can send these images at a bit rate of 19200 bps, which is quite high for a 2U CubeSat. The system also has a capable attitude control

with 1.57 rpm rotational rate around x and y axes, 3.94 rpm rotational rate around z axis and a pointing accuracy of at least 5°. Considering these parameters and the high performance 500 MHz OBC, quite some headroom is left for potential payloads that have higher demands than the camera experiments for this mission.

Table 15.5: System Characteristics of the Satellite

| | | | | | |
|---|---|---|---|---|---|
| Total Mass [g] | 2500 | Rotational Rate x,y-axis [rpm] | 1.57 | Operating System | LINUX based |
| Power Generate [W] | - | Rotational Rate z-axis [rpm] | 3.94 | Ground Station | TU Delft |
| Size | 2U | Slew Time 180 deg x,y-axis [sec] | 19.4 | Launcher | TBD |
| Down Link Data Rate [kB/s] | 19.2 | Slew Time 180 deg z-axis [sec] | 12.3 | Altitude [km] | 300-600 |
| Up Link Data Rate [kB/s] | 9.6 | Memory Storage | 2 SD expandable + 0.5 Gb internal | Inclination [degree] | 50-130 |
| Contact Time [min] | 4-5 | Processor | 500 MHz ARMb7 | Resolution Camera [MP] | 2 |
| Pointing Accuracy [degree] | 1-5 | RAM [MB] | 512 | Resolution IR Camera [MP] | - |

## 15.2. Spacecraft Layout

The positioning of the subsystems in the satellite is shown in Figure 15.1. The payload is at the top of the spacecraft, as is foreseen for the ISIS 2U Longstack structure. The subsystem that is placed closest to the payload is the on-board computer. This is done to minimize cabling, as cables must run to both Arduino Nanos sitting in the payload bay. The communication to the other subsystems is done through the stack pins that connect the subsystems.

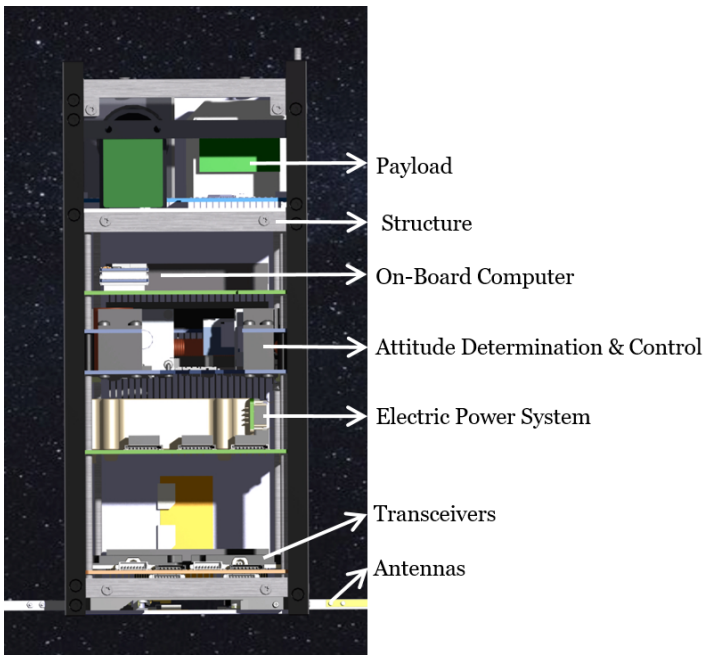


Figure 15.1: Layout of the Space Truck. The layout of the payload is shown in detail in Figure 9.6

The ADCS is placed most centrally of all systems for two reasons. Firstly, it is the heaviest of all subsystems and therefore placing it in the center of the spacecraft decreases the difference between the geometric center and center of gravity which is desirable to minimize disturbance torques. Secondly, if jitter is present in any of the reaction wheels, the effect on the spacecraft is reduced by placing the reaction wheels close to the center of gravity.

The EPS (electric power system) is placed furthest from the payload and the on-board computer. This decreases the risk of possible damage to these subsystems in case of a battery failure. Since the ADCS is considered a non-critical subsystem, it is acceptable to have it next to the battery.

Finally, the transceivers are placed at the bottom of the spacecraft, adjacent to the antennas. This minimizes the cable length between the two subsystems to achieve the lowest noise and error rate possible during transmission and reception. The antennas are placed at the bottom of the satellite to reduce interference from other subsystems and because there is space for the transceivers.

There is 37 mm of room between the electric power system and the transceivers. This is an asset for the future of the Space Truck since other subsystems can be added in future versions. In the current iteration of the satellite, the extra room can be used in order to shift the EPS so that the center of gravity is perfectly calibrated in the geometric center of the satellite and aerodynamic and solar pressure disturbance torques are negated around one axis.

## 15.3. Functional Flow Diagram

The functionality of the spacecraft can be divided into four modes; the initialization mode, the idle mode, the nominal mode and the safe mode. The complete functional flow diagram is given in Figure 15.2 through Figure 15.7.

The initialization mode is entered on system startup. Each subsystem will initially function independently while seeking to connect to the OBC. The OBC will meanwhile be looking to connect to attached subsystems. Once the subsystems establish a connection with the OBC, they switch over to idle mode. The OBC will be trying to establish connections for a set amount of time. Once this time has expired, the OBC will go through deployment checks. The OBC will go into idle mode once the deployment checks all return positive. Also the beacon is activated during the initialization mode. Once activated, it can not be stopped or interacted with. The beacon is only shown in the initialization part of the functional flow diagram, but do note that it keeps running for the entire lifetime of the spacecraft. The functional flow diagram for the initialization mode is given in Figure 15.2 and Figure 15.3.

During the idle mode, the spacecraft will be doing basic tasks like gathering housekeeping data and maintaining the power system. Besides this, the spacecraft will be listening for ground station inputs and checking for scheduled tasks. If a task is received or scheduled, the OBC will send the subsystems involved in the task their respective commands. The subsystems that are not involved in the task will just remain in their idle mode. This way, the power consumption can be kept at a minimum. The functional flow diagram for the idle mode is given in Figure 15.4 and Figure 15.5.

Each subsystem has a nominal mode. During this mode, the functions that are not running on a semi-permanent basis will be executed. For example, the communications system will always be listening. The nominal mode for the communications system includes transmitting of data. Note that when a subsystem enters their nominal mode, the idle mode is not completely shut down. Only the branch that triggered the nominal mode will be exited while the other functionality described in the idle mode will keep running. The functional flow diagram for the initialization mode is given in Figure 15.6 and Figure 15.7.

In safe mode, only the essential functions are operational. The spacecraft will check its own status and transmit that status periodically. The spacecraft will be waiting for ground station input. Once it receives this input, it will act upon it accordingly. After the input command has been executed, the spacecraft will check if the error that triggered the safe mode has been resolved. If it has, the spacecraft performs checks on all connected subsystems. If this is cleared, the spacecraft will wait for ground station input to return to idle mode. The reasoning behind this is that this way, the engineers on the ground get a chance to look at the housekeeping data to make sure everything is running as expected. This way, the spacecraft can't accidentally go back to idle mode if it has an undetected error. The functional flow diagram for the safe mode is given in Figure 15.7.

During all the modes, the basic houskeeping functionality of checking temperatures, maintaining the power system and listening for ground station inputs are maintained.

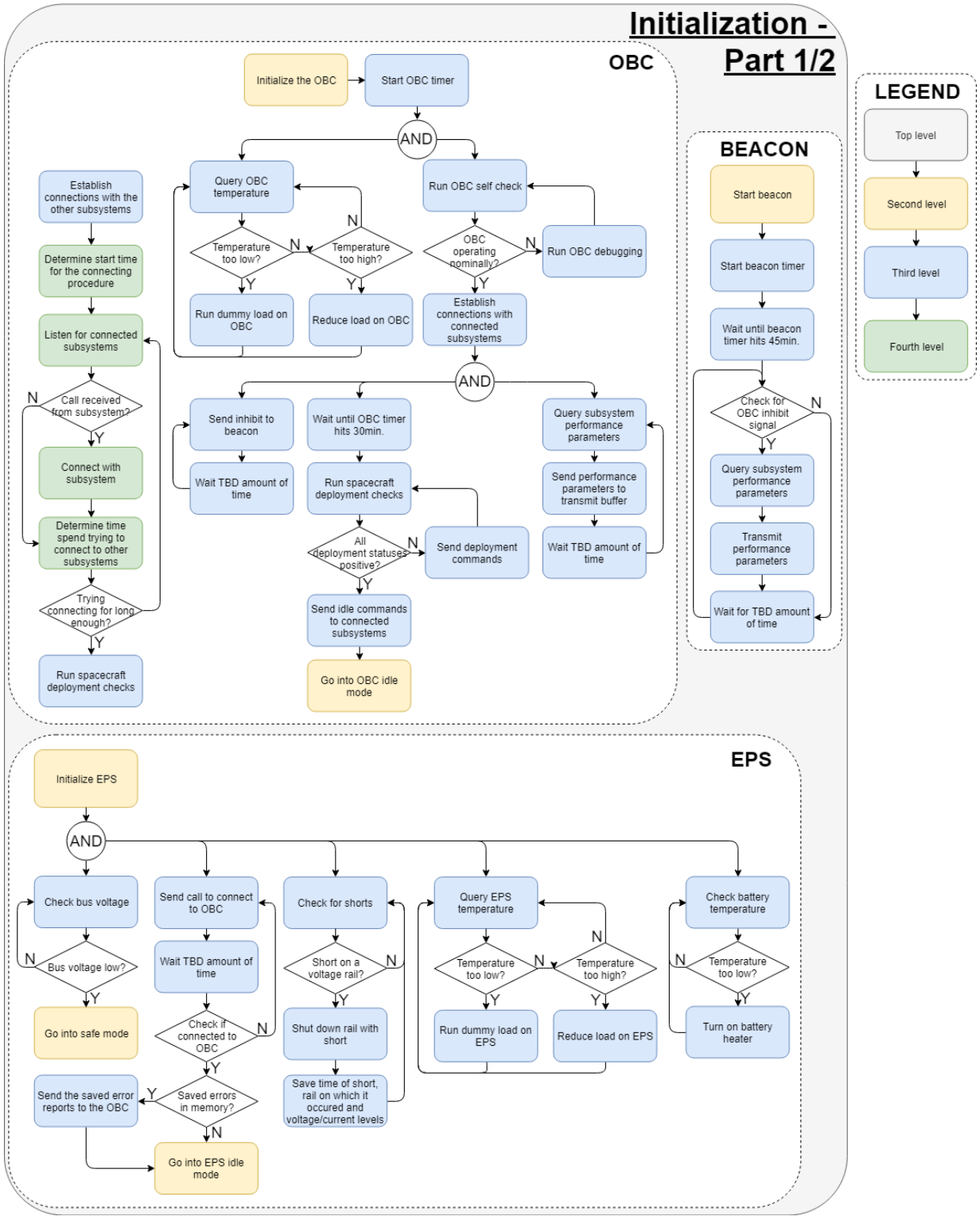


Figure 15.2: The first half of the initialization mode part of the functional flow diagram

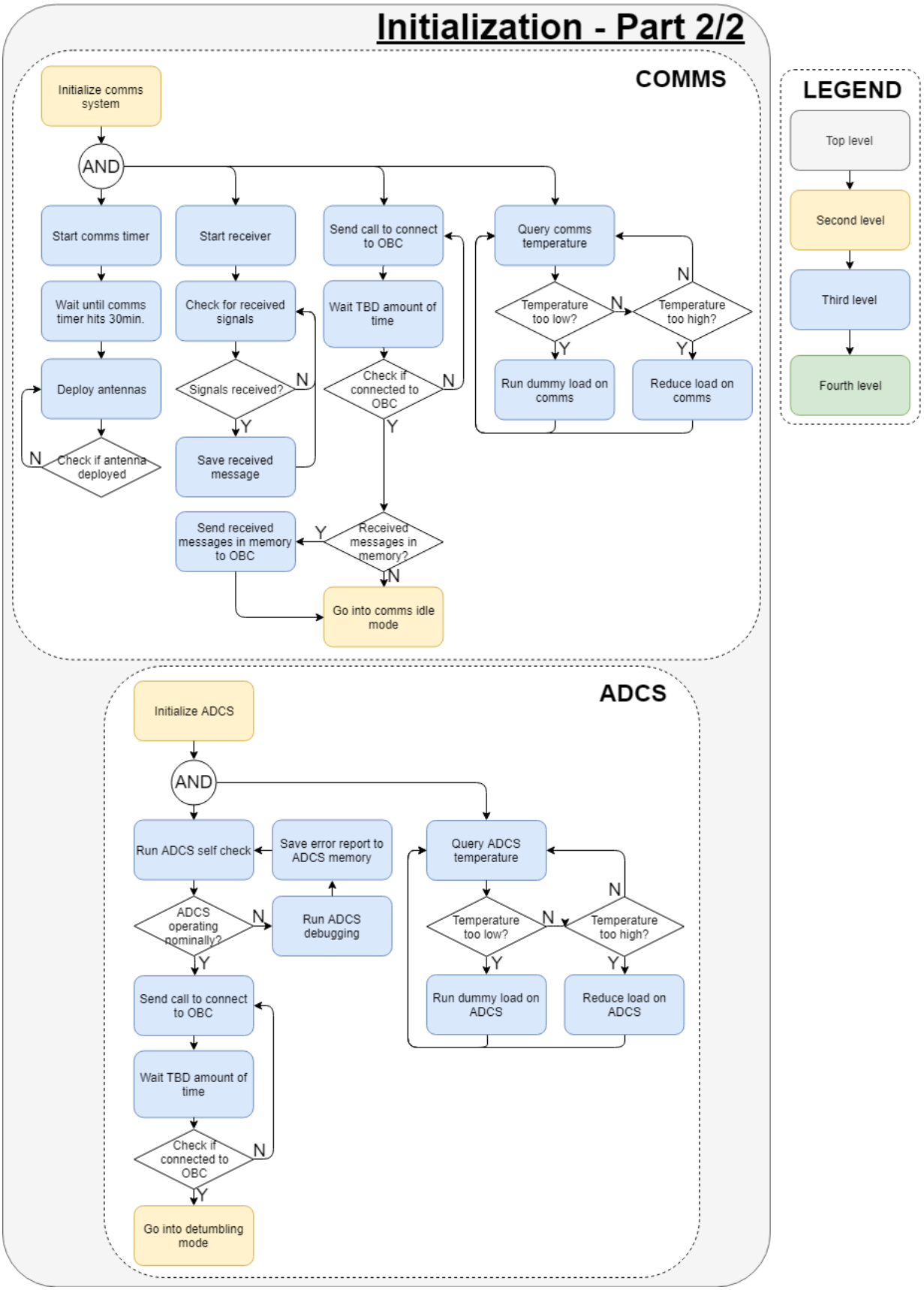


Figure 15.3: The second half of the initialization mode part of the functional flow diagram

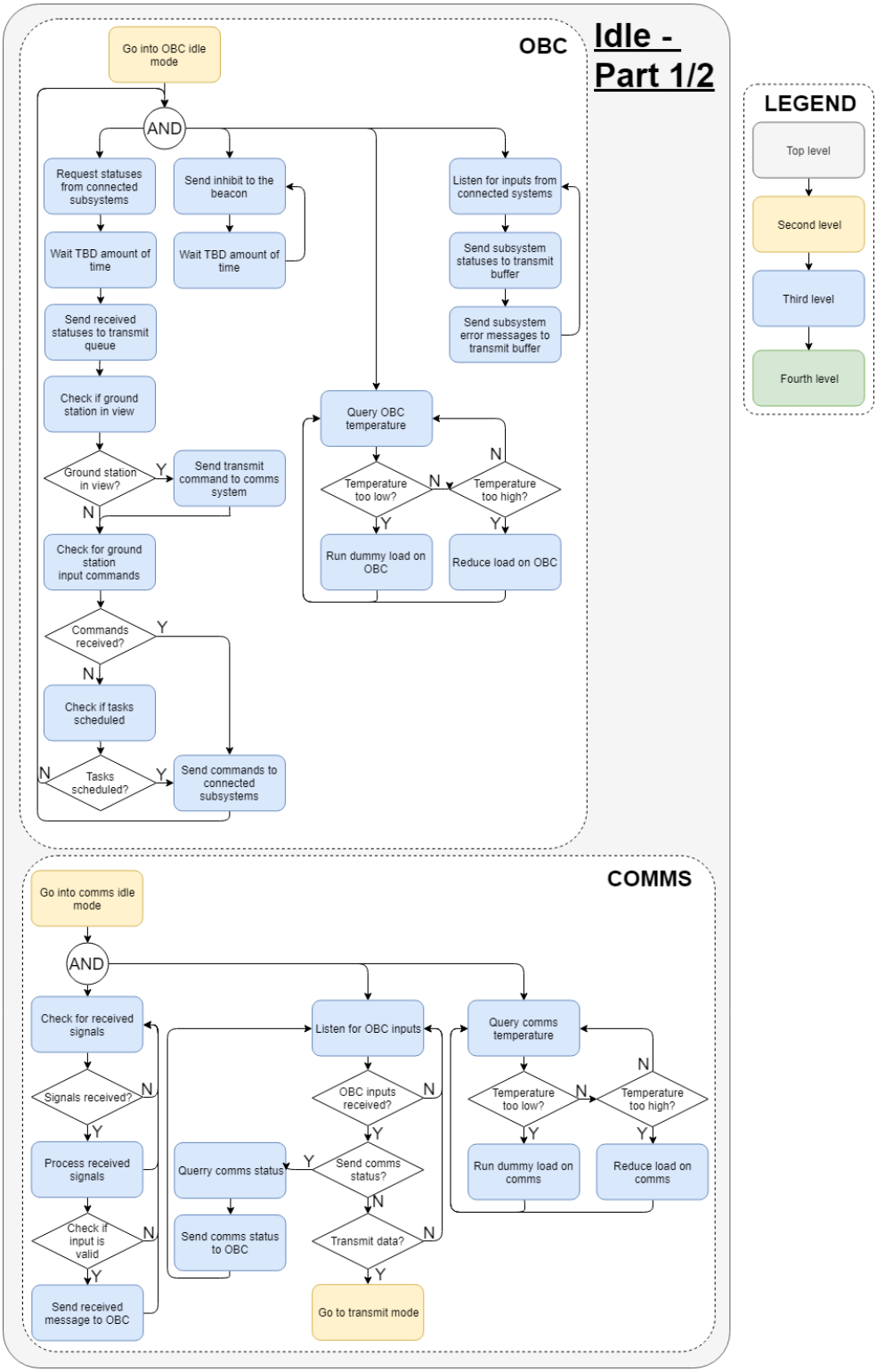


Figure 15.4: The first half of the idle mode part of the functional flow diagram

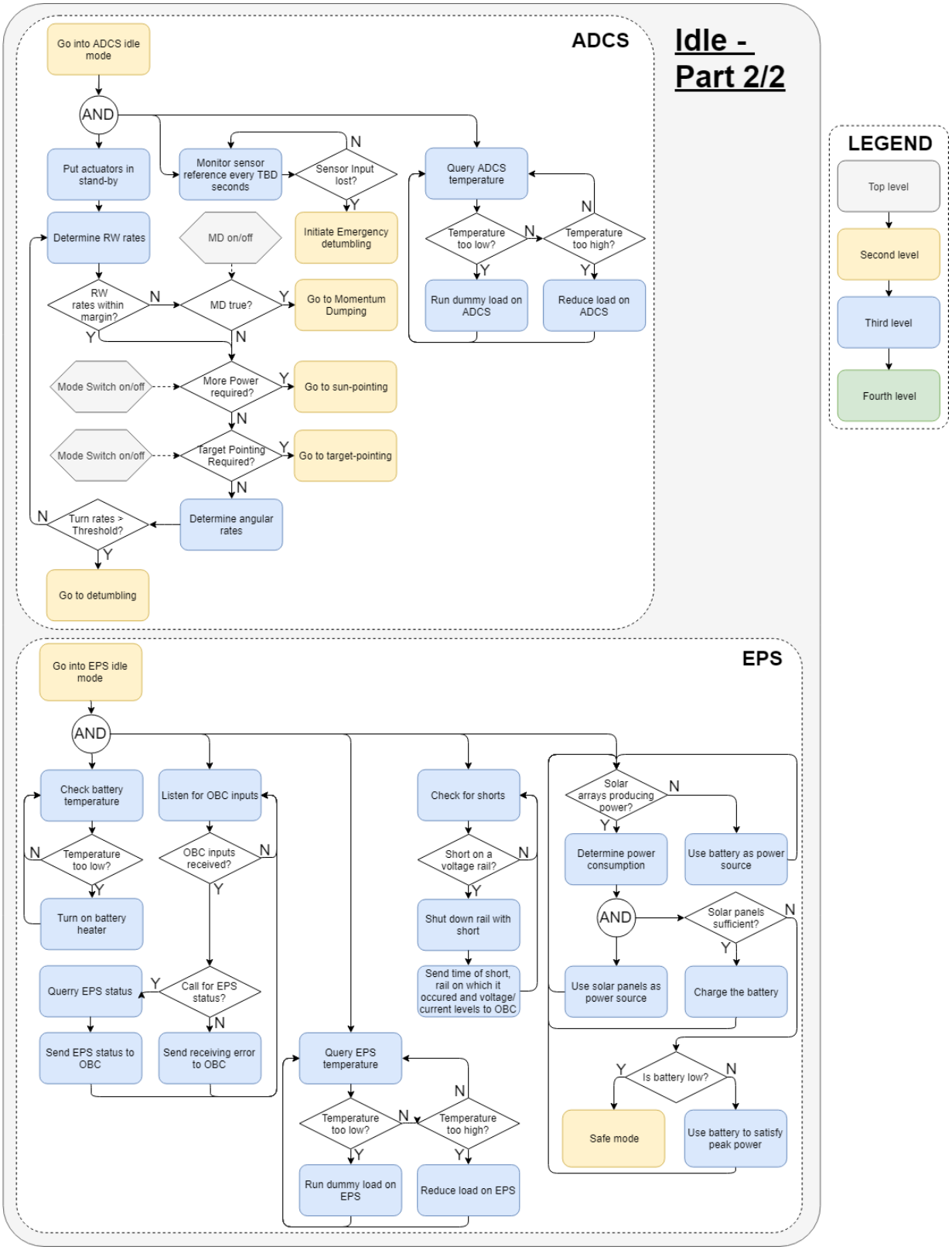


Figure 15.5: The second half of the idle mode part of the functional flow diagram

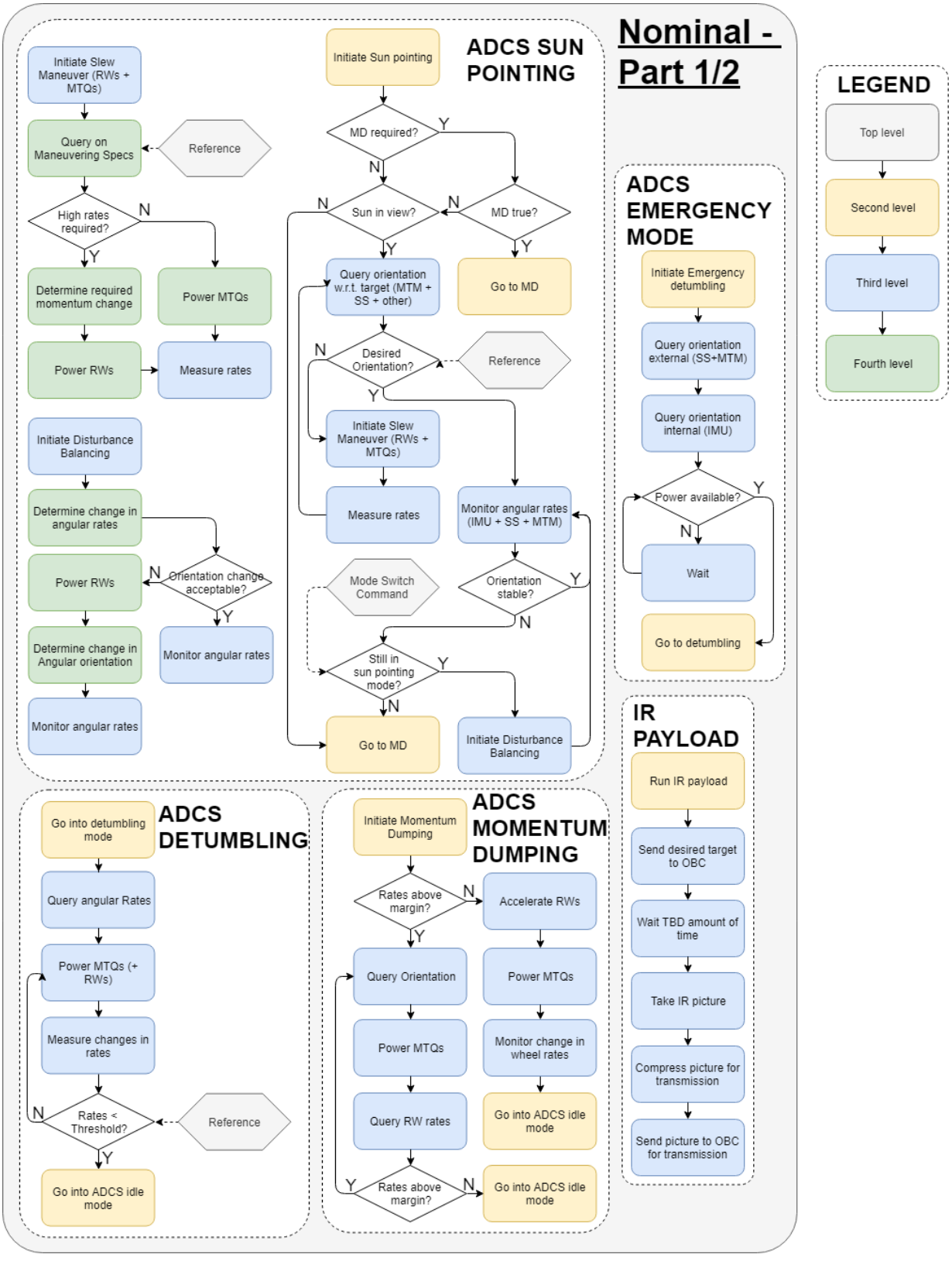


Figure 15.6: The first half of the nominal mode part of the functional flow diagram

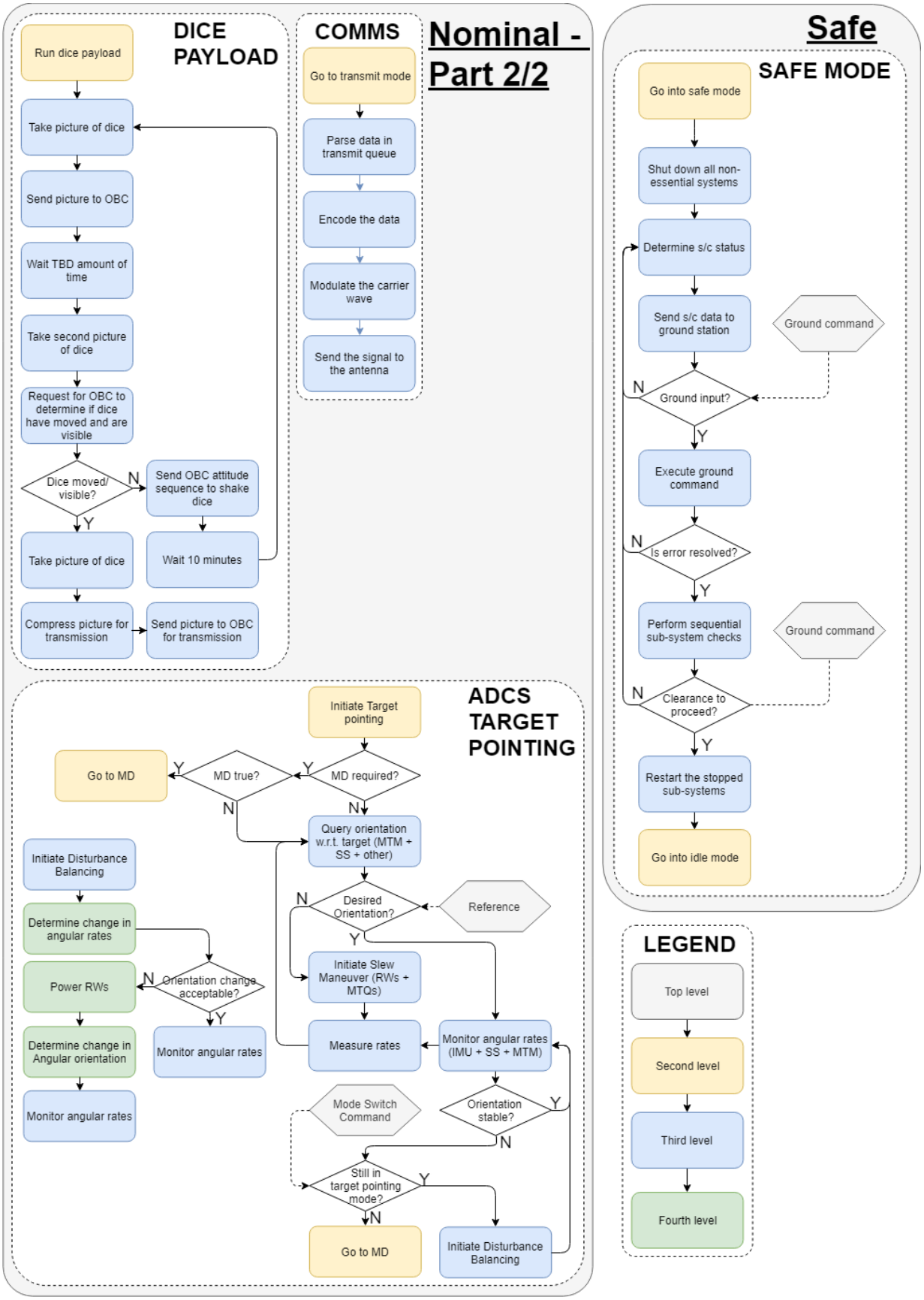


Figure 15.7: The second half of the nominal mode part of the functional flow diagram along with the safe mode

# 15.4. Functional Breakdown Structure

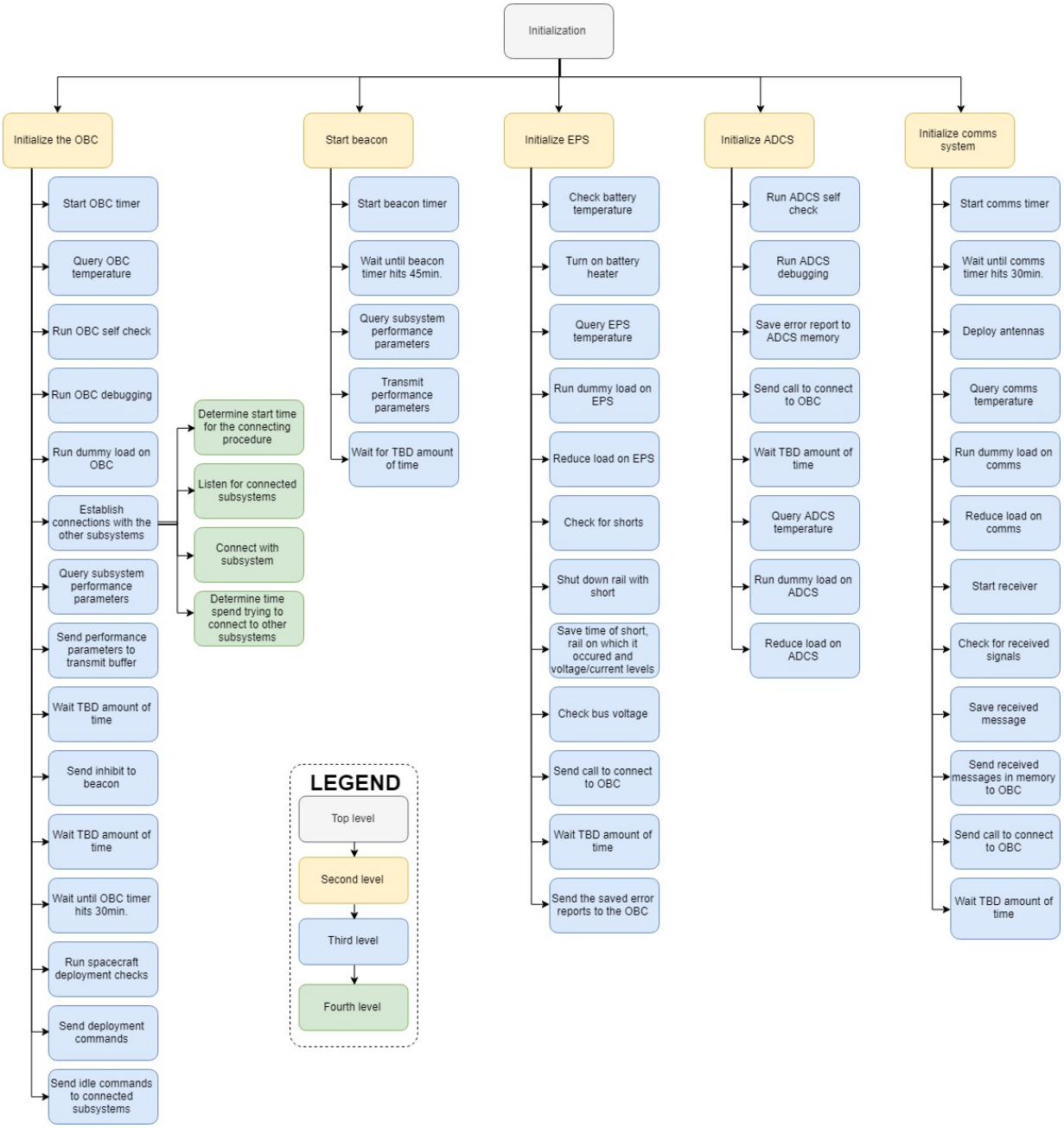


Figure 15.8: The initialization mode, part of the functional breakdown structure

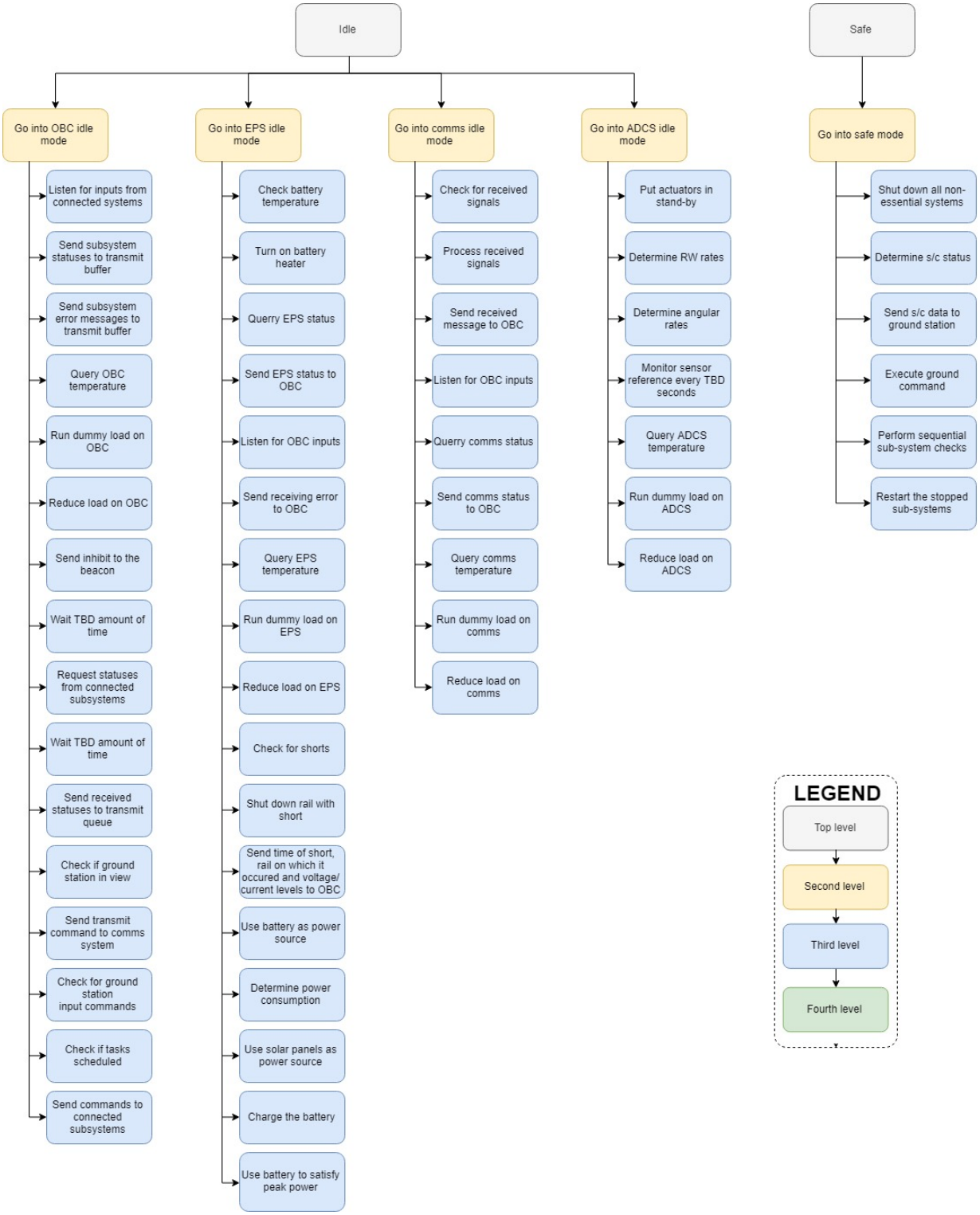


Figure 15.9: The idle and safe modes, part of the functional breakdown structure

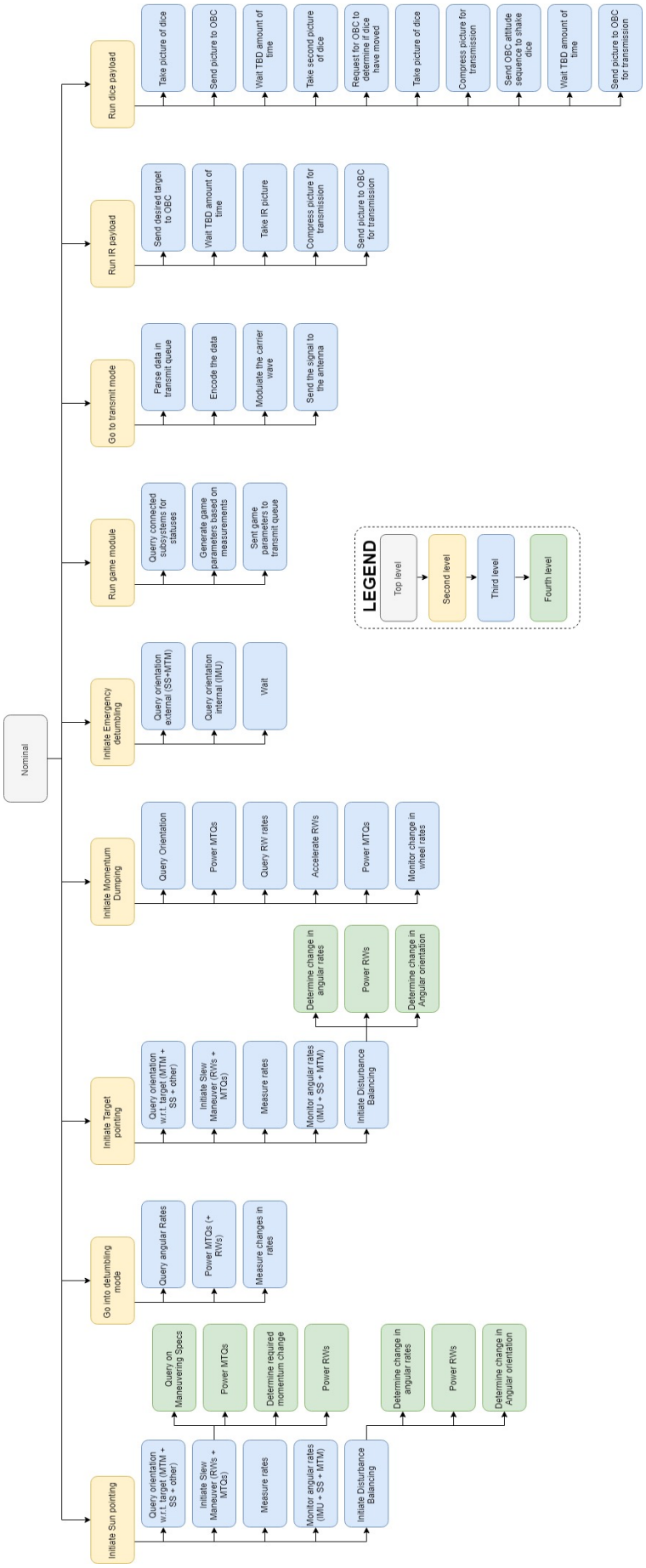


Figure 15.10: The nominal mode, part of the functional breakdown structure

# 16
# Risk Management

Risk is the possibility for a negative event occurring in the future. It is defined by two characteristics: the likelihood of the event and its consequence. The objective of risk management is to identify, analyse and mitigate all possible negative events that can occur resulting in mission failure. As the objective of the project is to design an 'Ultra-Reliable Space Truck', the focus on reliability cannot be overemphasised.

This chapter covers the approach taken to identify, analyze and mitigate risks. This approach includes study of in-orbit spacecraft and CubeSat failures for insights into different types of failure modes. Risk identification, analysis and mitigation strategies are presented for the design. Both, risks that appear as consequence of, or risks that have been mitigated because of design choices are discussed. The initial risks are mapped in terms of likelihood and consequence in a risk map. The change in these risks as a result of risk mitigation is shown in a post-mitigation risk map.

## 16.1. Approach

This section explains the approach taken to manage risks that present along with the design choices. It is first important to understand the types of failures that can occur in a spacecraft. A study of general spacecraft failures and another one, specific to CubeSat failures have been analysed to get some insights. This is explained in section 16.2. Next part of the chapter is about risk identification, analysis and mitigation. Fault tree analysis (FTA) is used for risk identification in this project. It is an analytic technique in which the worst negative event which is in this case, a complete mission failure or Loss Of Mission (LOM) can be linked to faults and failures occurring in subsystems and components. LOM is defined as failure of spacecraft to facilitate any of the payload experiments. The system is then analysed to find all possible ways LOM can occur. Failures in system, subsystem, components or parts can also lead to partial mission failure which is defined as mission degradation. The fault tree is a graphical model of various sequential or parallel combination of events/faults resulting in LOM or mission degradation. These faults can be associated with many contributing factors such as subsystem failure, human error, software failure, or other events. It has to be understood that failure of design to reach product realization also leads to LOM. FTA helps identify faults/events that have the most severity, and along with the probability of such an event occurring, a risk map can be developed. This in return can be used to make a risk mitigation plan.

From the fault tree analysis done during the previous design phase[13], all subsystems were found to be critical paths of failure, as in a complete subsystem failure could lead to LOM. Therefore each subsystem is analysed separately in section 16.3. This can be used to find critical subsystems and components. The sub-events contributing to LOM can be assessed in terms of the probability of it occurring. This can be used working up to the probability of the main event (LOM) occurring. For example, reliability of subsystems and components from statistics from previous missions and that provided by manufacturers can be used to calculate the reliability of the system itself. Using statistical data of spacecraft mission failures, potential risks can also be identified. A survey of general spacecraft failures and another specific to CubeSats have been analysed for the same reason.

Once the risks have been identified, their likelihood and consequence can be estimated. A score from 1 to 3 is defined for both these criteria. It can be seen in Table 16.1. The total risk score for a particular risk is calculated by multiplying its likelihood and consequence (high

risks are shown as red and low risks as green). Depending on the score, mitigation strategies can be planned. Once the risks have been mitigated, their risk score changes. Both the initial risk and how it changes after mitigation has been shown in the risk map and post-mitigation risk map in the last chapter.

Table 16.1: Likelihood and consequence score

| Score | Likelihood | Consequence |
|---|---|---|
| 1 | Not likely | No or minimum consequence |
| 2 | Likely | Mission degradation |
| 3 | Very likey | Loss of mission |

## 16.2. Spacecraft and CubeSat Failure Statistics

From a study of 156 in-orbit spacecrafts failures that occurred between 1980 – 2005[40], source of failures along with the failure rate have been listed in Table 16.2. The chance that these failures can lead to LOM or mission degradation has also been listed. For example, failures occurring in AOCS (Attitude and Orbital Control System) system as a whole accounts for 32% of all failures. The percentage that a failure in AOCS subsystem has lead to LOM is 30%, and similarly 25% of the time it has led to mission degradation. About 45% of the time, this has not affected the mission because most spacecrafts have redundant or high grade components, given that chance of failure in this particular subsystem is high. These numbers give a qualitative idea about the possible failures that could occur in spacecrafts, as this data does not reflect CubeSat failures particularly. Failures in the power subsystem are mostly attributed to solar arrays. Only 20% of the time a failure in power subsystem has not affected the mission, and about 45% of the time it has lead to LOM. In CDH and TTC subsystems control processors have the highest failure recorded. For this reason, most missions carry redundant processors. Mechanical systems such as thermal control, radiation shields and structure of the spacecraft and payloads have been grouped together, with payload failure as the highest record. Failure in this group has lead to LOM 52% of times, as most missions are considered a failure if the payload has failed. Some failures in subsystems cannot be attributed to a particular component or source due to lack of information from both CubeSat developers and the telemetry system. This is grouped under unknown category within the subsystems.

From a study of cubesat failures by M. Swartwout[38], the events contributing to LOM can be seen in Figure 16.1. He also found that 59% of all launches of CubeSats in the period 2000–2012 were successful. About 10% of the missions failed because of launch failure. This shows the risk of LOM even before deployment of satellite. This gives a better idea about failures related to CubeSats. About 45% of the time, no contact could be established with the CubeSat after a failure had occurred. No particular subsystem or failure type could be assigned to this category because of the lack of telemetry data. It was noticed that most missions in this category were university led with lower budgets in both cost and time. It was also mentioned that many university missions did not go through vigorous testing at system level even though many tests were conducted at subsystem and component level. In spacecraft systems, sometimes unforeseen design errors do not manifest themselves until integration and system level test phase [29]. This highlights the importance of system level testing. The use of COTS component that were not fully developed for space application (for temperature ranges and radiation levels) is related to a large amount of failures in the history of the CubeSat. This attributes to failures that cannot be accounted for or are unforeseen. The size and mass restriction of CubeSats allow very little redundancy in terms of parts or components. EPS and TTC subsystems account for 33% of failures. Solar arrays, batteries and electronic circuit damage due to radiation or short circuit leads to most of the failures in this category. About 2% of the time, failure was due to collision with space debris.

Table 16.2: In-orbit spacecraft failure analysis(1980-2005)[40]. The colours used to show critical subsystems can be compared only within the column and for component failure percentage, within each subsystem(Red to yellow to green - high to low failure rate, vice versa for success rate)

| Subsystem | LOM % | Mission degradation % | Success % | Source of failure | | Failure % | Subsystem level failure % |
|---|---|---|---|---|---|---|---|
| AOCS | 30 | 25 | 45 | Propulsion | Thrusters | 4,5 | 32 |
| | | | | | XIPS | 3,2 | |
| | | | | | Oxidiser tank | 0,6 | |
| | | | | | Fuel tank | 2,6 | |
| | | | | Control | CMG | 1,3 | |
| | | | | | Reaction wheels | 1,9 | |
| | | | | | Momentum Wheels | 3,2 | |
| | | | | Sensors | Gyroscope | 5,4 | |
| | | | | Electronics | | 0,6 | |
| | | | | Software | | 1,3 | |
| | | | | Environment | | 1,6 | |
| | | | | Unknown | | 5,8 | |
| Power | 45 | 35 | 20 | Generator | Solar array | 13,2 | 27 |
| | | | | | Fuel cells | 0,8 | |
| | | | | Storage | Batteries | 5,9 | |
| | | | | Distribution | Converter | 0,8 | |
| | | | | | Regulator | 0,8 | |
| | | | | | Amplifier | 1,4 | |
| | | | | | Bus | 1,4 | |
| | | | | Unkown | | 2,7 | |
| CDH & TTC | 33 | 26 | 41 | Communication | Antenna | 4,6 | 27 |
| | | | | | Transponder | 3,8 | |
| | | | | | GPS | 0,5 | |
| | | | | Electronics | | 4,6 | |
| | | | | Software | | 1,9 | |
| | | | | OBC | Control processor | 7,0 | |
| | | | | | Computer reset | 1,9 | |
| | | | | Unkown | | 2,7 | |
| Mechanical, Payload & others | 52 | 24 | 24 | Structure | | 2,4 | 14 |
| | | | | Payload | | 7,7 | |
| | | | | Tether | | 1,5 | |
| | | | | Docking | | 0,7 | |
| | | | | Unknown | | 1,7 | |

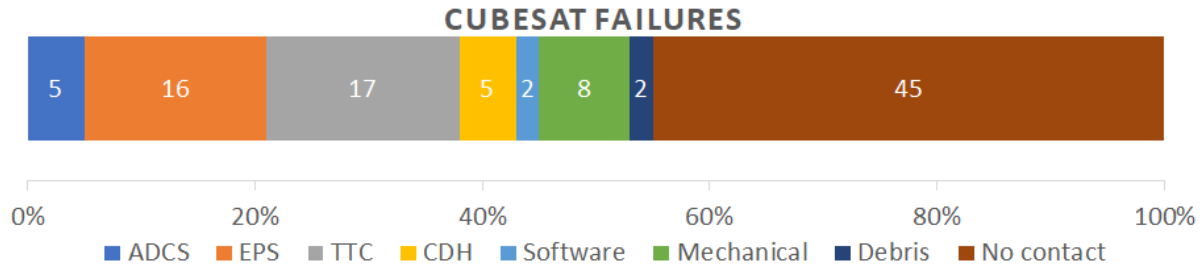


Figure 16.1: Causes of in-orbit CubeSat mission failures(2000-2012)[38]

## 16.3. Risk Analysis and Mitigation

In this section, along with insights from the failure studies, risks are identified using the FTA. Each subsystem is looked into specifically for risky components and parts. Each design choice comes with a risk and in some cases performance has to be traded for a low risk component, like the choice of non-deployable solar panels over deployable ones. Sometimes, a better system demanding more power and space is selected to avoid a particular risk like in case of TTC system. Some of the risks for the CubeSat are system level and others are specific to parts and components. The FTA is broken down for general system and individual subsystem failures. Each of these risks are given an identity number so as to be traceable in the risk map and for future uses. The failures are scored in terms of Likelihood (L) and Consequence (C) to arrive at the risk score which is the multiple of likelihood and consequence. The rationale for the L and C scores are explained for each failure. For each risk, a mitigation idea or strategy is put forth. The risk is then re-evaluated in terms of their likelihood and consequence after risk-mitigation and a new risk score is defined. Each risk is then depicted in the risk map and the post-mitigation risk map.

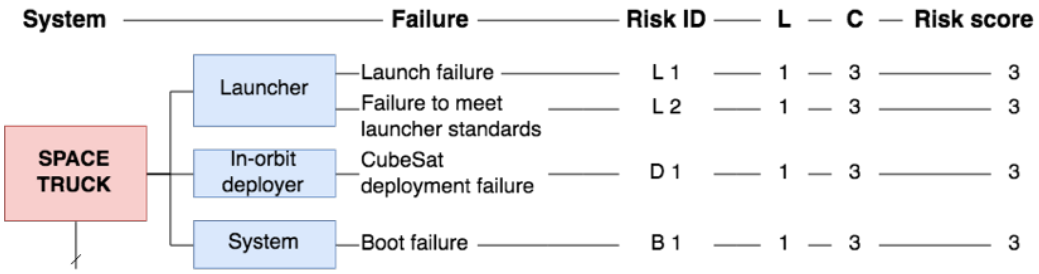


| Risk ID | Risk score | Rationale | Mitigation | L | C | Risk score |
|---|---|---|---|---|---|---|
| L 1 | 3 | About 10% of CubeSats (2002-2012) failed because of launch failure. Launching it again would need more time and budget, meaning VSV wont be able to send it on their 75th year anniversary. | Generally not much can be done about launch failures, though launchers can be analyzed using statistics to identify ones with high success rate. | 1 | 3 | 3 |
| L 2 | 3 | Launcher standards can be overlooked easily, though very unlikely. This would cost more time and money. | Enough time and budget must be allocated for testing procedures. A compliance matrix must be made to check if the CubeSat meets all launcher requirements and standards. | 1 | 1 | 1 |
| D 1 | 3 | This is a not very likely since most deployer pods have been flight proven. | Deployment pods with most flight heritage and success rate must be selected. | 1 | 3 | 3 |
| B 1 | 3 | This could happen if the complete system booting protocol is dependent on either a timer, ground command, or any single initiation process. If for example, the timer fails and no other means to boot the satellite has been set, it could mean LOM. | Multiple boot sequence initiations for different scenarios should be pre-programmed. An option use ground command for booting must also be included, given that the TTC system switches on independently of the CDH and that it can be used to boot the system. This would mean even if boot failure occurs, if it can be reinitiated successfully, there is no consequence. | 1 | 1 | 1 |

Figure 16.2: FTA and system level risk analysis and mitigation

### 16.3.1. EPS

Deployable solar panels pose as a risk due to failure prone deployment systems. If a cubesat has other sensors behind the deployable panels, it can be assumed that this failure mode can lead to mission degradation, if not LOM. It was decided to keep the design simple, therefore use non-deployable solar panels. Radiation damage to batteries can cause out-gassing or explosion in which case it can be assumed that the battery has failed.

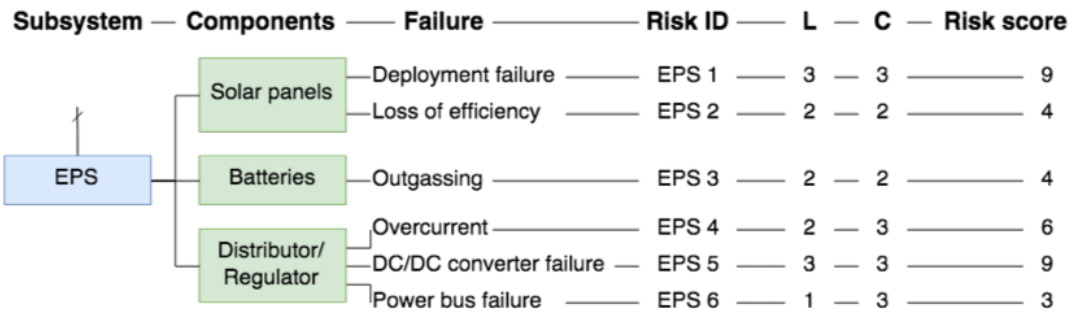


| Risk ID | Risk score | Rationale | Mitigation | L | C | Risk score |
|---|---|---|---|---|---|---|
| EPS 1 | 9 | Solar panel deployment uses burn wire similar to antenna. For the same reasons explained earlier for the TTC system, this can happen. Deployment systems also have moving mechanical parts, this adds to the risk of failure. Deployable solar panels are used in missions that need high power and its failure would mostly lead to LOM. | Non deployable solar panels have been selected for this CubeSat in order to avoid this risk completely. | 1 | 1 | 1 |
| EPS 2 | 4 | Solar panels degrade over time, but higher radiation dose can pace this process. Efficiency can also be miscalculated and the actual power available may not close the power budget. | Use of cover glass for solar panels depending on orbital conditions, and mission duration. If the mission duration is too short compared to the degradation rate of the solar panels given that it provides the necessary power till the EOL, no risk exists. However a higher safety margin can be taken so as to account for this risk. | 1 | 2 | 2 |
| EPS 3 | 4 | Batteries have very low thermal and radiation range within which it can operate, compared to most other components. They also degrade over time due to thermal and radiation cycling. Loss of batteries would mean non-operational spacecraft during eclipse and also lower peak power depending on the power generation system. | For longer missions, enough radiation and thermal shielding must be provided. Higher safety margin must be assumed while making the thermal model. This would reduce the likelihood of failure. | 1 | 2 | 2 |
| EPS 4 | 6 | Depending on the architecture of the EPS, this could be a issue. Watchdogs and other overcurrent systems exist but it can be said with certainty that if these fail, a complete subsystem can be damaged. | Overcurrent protection must be provided for all subsystems on both ends of the power lines. Fuse must be added to critical paths. Sneak circuit analysis must be done to find latent circuits, which could cause a short-circuit. This reduces both likelihood and consequence. | 1 | 2 | 2 |
| EPS 5 | 9 | This is one of the most failure prone components in a EPS system. This component matches the power a particular subsystem needs in terms of voltage. A failure could potentially damage the subsystem or at the least disconnect it from power. | Multiple DC/DC converters in a parallel architecture will make this a non-SPOF (Single Point Of Failure). This could mean lot of heat is generated at these nodes, the thermal control model must take this into account. The power budget must also account for loss of power in the form of heat. | 3 | 1 | 3 |
| EPS 6 | 3 | This is not very likely as power buses are tested multiple times, but the consequence can be that one or many subsystems are disconnected from power leading to LOM. | Redundant powerlines must be added for critical paths. This would reduce the consequence of such a failure. | 1 | 2 | 2 |

Figure 16.3: FTA of EPS and subsystem/component level risk analysis and mitigation

### 16.3.2. TTC

Initially a half duplex telecommunication system was to be used for the TTC, which uses a Rx/Tx switch to alternate between transmitting and receiving using the same antenna. Other than the fact that the CubeSat is not ready to receive commands at all times, a failure in the switch could leave the telecommunication system in one of the two modes(receiving or transmitting) or lead to a complete failure of the TTC. It was decided to use a full duplex system with two transceivers (which can function as a transmitter or receiver) with dedicated antennas in order to avoid the risk. If two different frequency bands could be used for the two transceivers, each of which can potentially be used as a half duplex system, it provides for redundancy in case one of them failed.

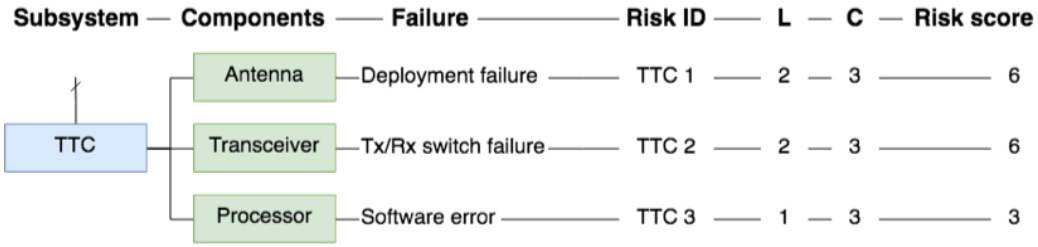


| Risk ID | Risk score | Rationale | Mitigation | L | C | Risk score |
|---|---|---|---|---|---|---|
| TTC 1 | 6 | This could happen if the capacitor meant to provide high burst of power to the burn wire fails, or if the power available during the burn sequence is less than the needed power. This could happen if the batteries are completely drained due to long storage before launch. | The CubeSat must be programmed to use burn sequence once the required power is available. At least one way to verify the deployment must be included. An option to reinitiate this using ground command as a last resort must be incorporated into design. This would reduce the consequence of deployment failure as it can be reinitiated. | 2 | 1 | 2 |
| TTC 2 | 6 | This switch alternates the transceiver between listening and sending mode. It could be damaged if there is impedance mismatch between the connector and transmitting/receiving power. | End-to-end testing to ensure communication system functions properly. Use of a full duplex system provides redundancy in case of a failure. This reduces its likelihood and consequence. | 1 | 2 | 2 |
| TTC 3 | 3 | Though it is not very likely, a unexpected software error can leave the satellite with no ability to make contact with ground. | End-to end testing. A simulator must be developed and revised to test and maintain the software before, during and after field testing. A way to reinstall or update the software must be included. If major bugs can be eliminated, the consequence of a software error can be reduced. | 1 | 2 | 2 |

Figure 16.4: FTA of TTC system and subsystem/component level risk analysis and mitigation

### 16.3.3. ADCS

The integrated ADCS system selected for this CubeSat comes with an option to include a star tracker. These are used in missions that require a high pointing knowledge. They are very sensitive to light, therefore cannot be pointed at the sun or earth as the high intensity light can damage the sensors. In order to avoid this, the layout/configuration of the star tracker with respect to other subsystems, sensors, instruments, etc and the attitude control algorithm, must be designed such that the star tracker never points at the sun/earth through out the mission duration. Since the mission does not require high pointing knowledge, the star tracker is not used which also reduces design complexity.

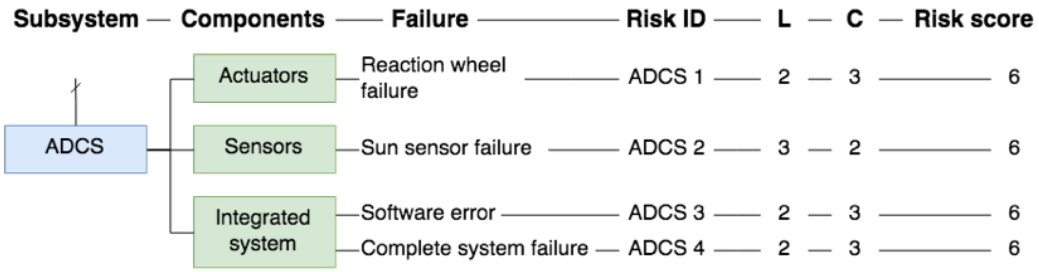


| Risk ID | Risk score | Rationale | Mitigation | L | C | Risk score |
|---|---|---|---|---|---|---|
| ADCS 1 | 6 | Mechanical moving parts have higher failure rate than other components. Loss of an actuator would mean less or no control along at least one axis, this could lead to LOM. | The selected ADCS system has both reaction wheels and magnetorquers. Reaction wheels provide better control that magnetorquers but incase of failure, the CubeSat can still be controlled with a lower pointing accuracy. | 2 | 2 | 4 |
| ADCS 2 | 6 | Sun sensors are likely to fail easily, but many satellites use sun sensors for coarse attitude determination. There are generally other sensors for fine tuning. | Redundant sun sensors need to be incorporated in the design. | 3 | 1 | 3 |
| ADCS 3 | 6 | The system selected for this mission has in the past failed due to software issues, but it can be fixed if identified early. | A simulator must be developed and revised to test and maintain the software before, during and after field testing. An option to update and reinstall the software from memory, in case of failure must be included. This would reduces both the probability and consequence of such a failure. | 1 | 2 | 2 |
| ADCS 4 | 6 | Integrated ADCS for CubeSats are new and have low TRL. It can be assumed that though not very likely, a complete failure can lead to LOM. | Complete system test after integration can to a certain extent reduce this risk. This would predict if such a failure is possible and if so, a way to minimize its likelihood can be found. Worst case scenario, a different ADCS can be selected. | 1 | 3 | 3 |

Figure 16.5: FTA of ADCS and subsystem/component level risk analysis and mitigation

### 16.3.4. CDH

The command and data handling subsystem can be considered the brain of the satellite as it handles the working of all other subsystems and makes critical decisions based on pre-programmed logic. It can be assumed that in case of a centralised command centre, failure of this subsystem can leave the satellite completely unusable. For the same reason, much effort is made by CDH manufacturers to make it highly reliable. Some of the decisions made regarding the selection of data protocol was to use one type so as to keep the architecture simple as long as all subsystems support the protocol. In any case the CDH system selected during the trade-off comes with an option to configure the pins in the PC104 as per subsystem requirements and also add protocol converters in case a subsystem has a unsupported communication protocol.

### 16.3.5. Thermal Control System

The thermal model made for the CubeSat suggest that with the current configuration and orbit, most subsystems have thermal operational limits higher than the expected thermal variations except for the battery. The EPS system selected for the cubesat comes integrated with active thermal control for the batteries. This system keeps the batteries above the lower threshold and switches off power to and from the battery if the temperature goes above its higher threshold. In general failure of battery due to higher temperature is very unlikely given that it is a integrated part of the EPS made for space application.

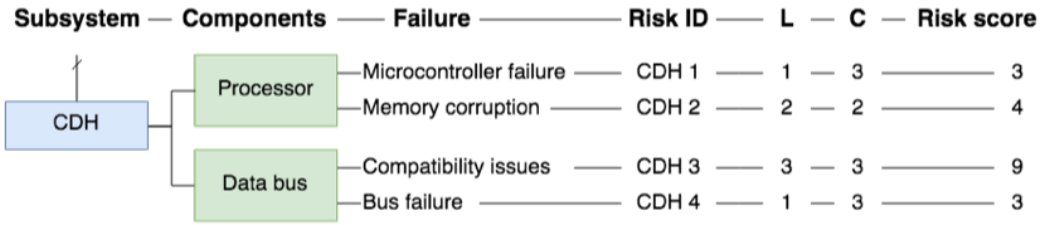


| Risk ID | Risk score | Rationale | Mitigation | L | C | Risk score |
|---|---|---|---|---|---|---|
| CDH 1 | 3 | Unlikely because they are made for space environment and are generally rad-hard. Nevertheless its failure can lead to LOM. | Given that it is a low risk, radiation shielding must suffice. Carrying redundant processors can resolve this issue completely. | 1 | 1 | 1 |
| CDH 2 | 4 | This can happen due to radiation, most times these can be fixed if identified early. | Debugging mechanisms must be incorporated to identify and resolve this at the earliest. An option to reset the memory must also be present. The likelihood remains the same but since it can be fixed, the consequence is minimized. | 2 | 1 | 2 |
| CDH 3 | 9 | Different subsystems have different protocols and the CDH must be compatible with all of them. Mismatches if identified at design stages can be fixed. After complete integration, this could extend the launch and testing schedules and would cost more. | Flatbed and overall complete system testing after integration, running all possible scenarios that can happen during the life of the CubeSat. This reduces the likelihood of compatibility issues. | 1 | 3 | 3 |
| CDH 4 | 3 | Bus lockups are common in some satellites depending on the type of protocol used, but do not have major consequences except for reset or slow functioning. A complete bus failure is unlikely but depending on the type of protocol selected, and bus architecture, its possible to have no communication with some subsystems if not all. | Overall system testing including thermal and radiation cycle tests. If the CubeSat can be directed to safe-mode when a bus lockup is identified, then the consequence can be managed. | 1 | 2 | 2 |

Figure 16.6: FTA of CDH system and subsystem/component level risk analysis and mitigation

### 16.3.6. Payload

The concept for the primary school payload involves carrying two rubber dice in a free floating manner inside a cylindrical enclosure. Though the mass of both the free floating dice is less than a gram compared to the mass of the spacecraft($2.5kg$), the behaviour of free floating objects in launch conditions cannot be modelled at this stage. With launch, vibration and shock tests, one can predict the feasibility of this payload. An option to keep the dice docked using some sort of mechanism which can release them once the CubeSat is in orbit is one way to mitigate this risk. This not only adds to the complexity of the design but also brings in new risks. In any case if the payload does not pass these tests, a backup option is provided in subsection 9.3.6.

The high school payload is a IR camera operational within aircraft altitudes($11km$). This camera has no space heritage and therefore the reliability of this payload cannot be predicted. Most issues with sensors in space has to do with degradation due to UV radiation. The lens can be UV coated to reduce the risk of sensor damage.

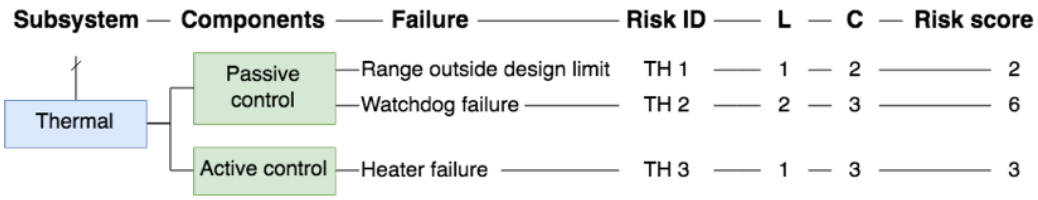


| Risk ID | Risk score | Rationale | Mitigation | L | C | Risk score |
|---|---|---|---|---|---|---|
| TH 1 | 2 | The thermal model for the CubeSat is made based on simplifications which may not match reality. Though not very likely, the actual environment might be different than the one designed for. Unless the range is completely off, some components may have to be operated only during favorable conditions leading to degradation of mission. | Higher safety margin for thermal model and thermal vacuum testing. | 1 | 1 | 1 |
| TH 2 | 6 | Watchdogs work based on information provided by sensors and/or estimates made using housekeeping data. Noise in the data can trigger watchdog operations when not needed and vice-versa. | Electromagnetic compatibility testing reveals sources of noise within the CubeSat. Methods to quantify and filter noise from housekeeping data must be incorporated. This reduces the likelihood of such a failure. | 1 | 3 | 3 |
| TH 3 | 3 | Active thermal control is used in components with minimum threshold range such as batteries. Such components are generally critical to the mission. | Running dummy loads on components produce heat. This is one way to keep the components above the lowest operating temperature limit. This can reduce the consequence of this failure mode. | 1 | 2 | 2 |

Figure 16.7: FTA of Thermal control system and subsystem/component level risk analysis and mitigation

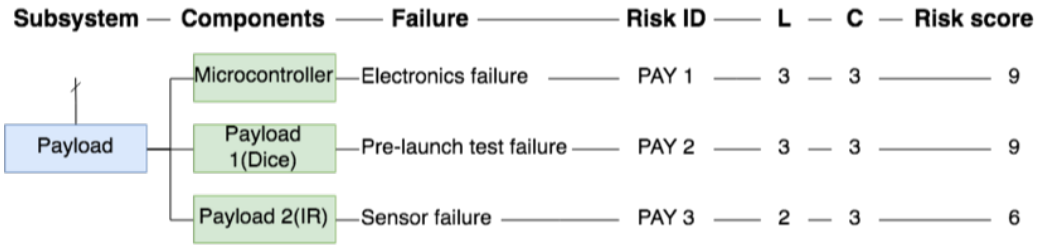


| Risk ID | Risk score | Rationale | Mitigation | L | C | Risk score |
|---|---|---|---|---|---|---|
| PAY 1 | 9 | The microcontroller selected for this mission is Arduino Nano, which is not made for space applications. The electronics can be more susceptible to damage due to radiation and thermal cycling. Failure of this means payload sensors cannot be used which is seen as LOM. | If radiation proves to be a major issue after radiation testing for the microcontroller, radiation shield must be incorporated. Though the likelihood and consequence of this failure mode cannot be analyzed with certainty before testing, it can be assumed that the risk is reduced overall. | 2 | 2 | 4 |
| PAY 2 | 9 | In case of the payload with free floating dice, the CubeSat meeting all the standards as per launch requirements cannot be predicted before a complete system test. If it fails to meet these requirements, the payload cannot be used in the mission. | A backup option of a payload without free floating bodies is provided in case it fails pre-launch tests. | 1 | 1 | 1 |
| PAY 3 | 6 | The IR sensor selected for the second payload, is meant to be used within 11km altitude. Though the main issue with these sensors in a space environment, has to do with radiation and thermal cycling, its working capability cannot be predicted with certainty. Unusable payload would also mean LOM. | Thermal vacuum, thermal cycling tests and radiation testing will be enough to predict the working of this sensor in space. Use of UV coated lens can reduce the degradation of the sensor due to UV. | 2 | 2 | 4 |

Figure 16.8: FTA of payload module and component level risk analysis and mitigation

## 16.4. Risk Map

Once the risks have been identified and analysed, preventive measure and strategies can be adopted to reduce it. In spite of all measures, risks remain and in some cases the measures to reduce the probability of failure can be introduced and in others the consequence of an inevitable risk can be reduced.. Knowledge of risk provides an opportunity to avoid problems. It is a continuous effort as risk changes constantly and must be evaluated at every phase of the mission starting from development, through testing and deployment, and finally during lifetime of system. Some of the mitigation processes need to be addressed at the very beginning phase of the project. Some recommendations in risk mitigation has to do with overall system tests and use of low risk components. For example, structural deformation due to vibrations and launch loads can only be avoided if a thorough vibration test is conducted after complete integration of the CubeSat. Failure of electronics due to radiation and thermal loads can be avoided by using proper radiation and thermal shields and radiation-hardened components. These strategies change the risks involved and a post-mitigation risk map can thus be created.

In Figure 16.9, most of the risks reduce as a consequence of mitigation. Risk of launch and in-orbit CubeSat deployer failure cannot be mitigated at this stage of the project. The post-mitigation risk map is qualitative with respect to how much each risk reduces as a result of the respective mitigation approach undertaken.

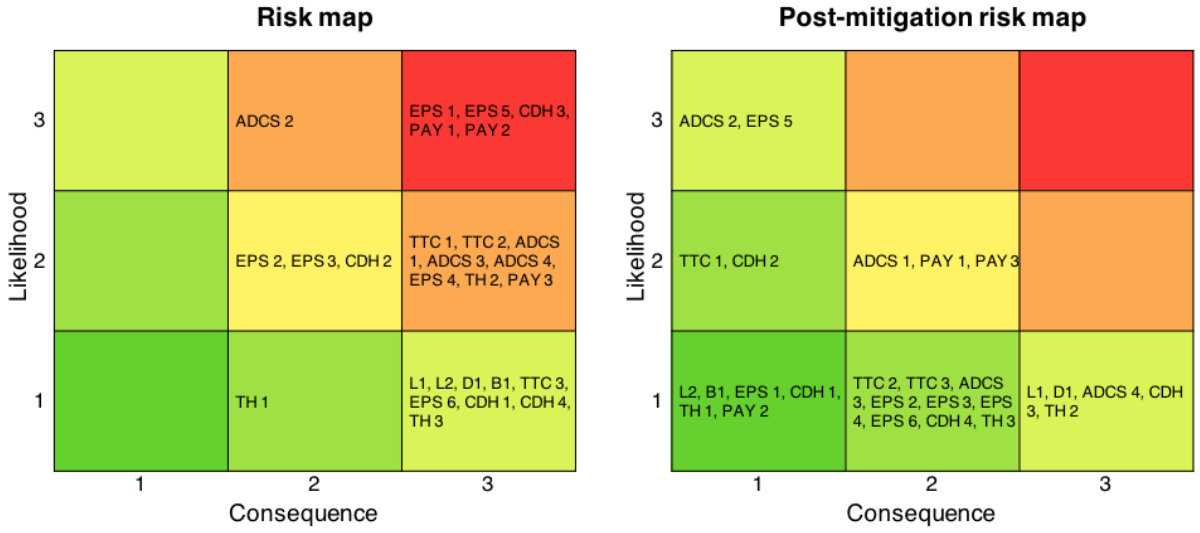


Figure 16.9: Risk map and Post-mitigation risk map

# 17

# Compliance Matrix

This chapter goes over all the requirements found in chapter 4 and evaluates to see if the design meets all the specified requirements.

| Requirement | Compliant Design? | Comments |
|---|---|---|
| SC-GEN-1010 | YES | |
| SC-GEN-1020 | NO | We have hardware/components which have not flown before, namely the payload module components |
| SC-GEN-1040 | YES | |
| SC-GEN-1050 | YES | |
| SC-GEN-1060 | YES | |
| SC-GEN-1070 | YES | |
| SC-GEN-1080 | - | To be provided by launch provider |
| SC-GEN-1090 | NO | Including extra design from the VSV next year, certification will start around May 2020 |
| SC-GEN-1100 | - | Can not be certain until detailed CAD files are obtained from suppliers |
| SC-GEN-1110 | - | Can not be certain until detailed CAD files are obtained from suppliers |
| SC-GEN-2010 | YES | |
| SC-GEN-2030 | YES | The payloads themselves are capable of withstanding the radiation |
| SC-GEN-2040 | - | To be demonstrated during software testing |
| SC-PMS-1010 | YES | |
| SC-PMS-1020 | YES | |
| SC-PMS-1030 | YES | |
| SC-PMS-1040 | YES | |
| SC-PMS-1050 | YES | |
| SC-PMS-1060 | - | System design not fully known as it is COTS |
| SC-PMS-1070 | - | Will be fulfilled during mission |
| SC-PMS-1080 | YES | |
| SC-PMS-1090 | YES | |
| SC-PMS-1100 | YES | |
| SC-STR-1010 | YES | |
| SC-STR-1020 | YES | |
| SC-STR-1030 | YES | |
| SC-STR-1040 | YES | |
| SC-STR-1050 | YES | |
| SC-STR-1060 | YES | |
| SC-STR-1070 | YES | |
| SC-STR-1080 | YES | |
| SC-STR-1090 | YES | |
| SC-STR-1100 | YES | |
| SC-ADCS-1010 | YES | |
| SC-ADCS-1020 | YES | |

| | | |
|---|---|---|
| SC-ADCS-1030 | YES | Different times may also be chosen after further design depending on the SC opperation |
| SC-ADCS-1040 | YES | |
| SC-ADCS-1050 | YES | |
| SC-ADCS-1060 | YES | |
| SC-ADCS-1070 | YES | |
| SC-ADCS-1080 | YES | |
| SC-ADCS-1090 | YES | |
| SC-ADCS-1100 | - | This is software-dependant which will be done by the VSV |
| SC-COM-1010 | YES | |
| SC-COM-1020 | YES | |
| SC-COM-1030 | YES | |
| SC-COM-1040 | YES | |
| SC-COM-1050 | YES | |
| SC-COM-1070 | YES | |
| SC-COM-1080 | YES | |
| SC-COM-1090 | YES | |
| SC-COM-1100 | YES | |
| SC-COM-1110 | YES | |
| SC-COM-1120 | YES | |
| SC-COM-1130 | YES | |
| SC-COM-1140 | - | This is software-dependant which will be done by the VSV |
| SC-COM-1150 | YES | |
| SC-COM-1160 | YES | |
| SC-THRM-1010 | YES | |
| SC-THRM-1020 | YES | |
| SC-THRM-1030 | YES | |
| SC-THRM-1040 | YES | |
| SC-THRM-1050 | YES | |
| SC-CDH-1010 | YES | |
| SC-CDH-1020 | YES | |
| SC-CDH-1030 | YES | |
| SC-CDH-1031 | YES | |
| SC-CDH-1032 | YES | |
| SC-CDH-1033 | YES | |
| SC-CDH-1034 | YES | |
| SC-CDH-1035 | YES | |
| SC-CDH-1036 | YES | |
| SC-CDH-1040 | YES | |
| SC-CDH-1060 | YES | |
| SC-CDH-1070 | YES | |
| SC-CDH-1080 | YES | |
| SC-CDH-1090 | YES | |
| SC-CDH-1100 | YES | |
| SC-CDH-1110 | - | This is software-dependant which will be done by the VSV |
| SC-CDH-1120 | - | This is software-dependant which will be done by the VSV |
| SC-CDH-1130 | - | This is software-dependant which will be done by the VSV |
| SC-CDH-1140 | - | This is software-dependant which will be done by the VSV |
| SC-CDH-1150 | - | This is software-dependant which will be done by the VSV |
| SC-CDH-1160 | - | This is software-dependant which will be done by the VSV |
| SC-PAY-1010 | YES | |
| SC-PAY-1020 | YES | |
| SC-PAY-1030 | YES | |
| SC-PAY-1040 | YES | |
| SC-PAY-1050 | YES | |
| SC-PAY-1060 | YES | |

| | | |
|---|---|---|
| SC-PAY-1070 | YES | |
| SC-PAY-1080 | YES | |
| SC-PAY-1090 | YES | |
| SC-PAY-1100 | YES | |
| SC-PAY-1130 | YES | |
| SC-PAY-1140 | YES | |
| SC-PAY-1150 | YES | |
| SC-PAY-1160 | YES | |
| SC-PAY-1170 | - | To be provided by launch provider |

# 18

# Reliability, Availability and Safety Characteristics

This chapter addresses three parameters that are very important for every aerospace product, reliability, availability and safety. Measures are taken in order to improve the characteristics for all three.

## 18.1. Reliability

Besides the payload, the Space Truck is comprised of all commercial off-the-shelf (COTS) components. All of these are expected to be fully developed and flight proven before the Space Truck launch, substantially increasing the reliability of the mission.

Two reliability issues can be identified for the design: The payload as well as the interfacing of the subsystems. If it is decided that the dice concept is used for the payload, several structural elements need to be designed and tested by the team. It is possible that despite rigorous testing and design a problem is overlooked and a structural element fails during launch.

The electronics that are planned for the payload (Arduino Nano, Arducam and FLIR Tau 2) are not designed for space, which is a further issue for reliability. However all of them have at least partial flight heritage meaning it is more crucial to test the complete payload configuration instead of the individual electronics. In order to make the design as reliable as possible, the configuration is tested for launch loads, thermal cycling, radiation and vacuum, as described section 21.3. Despite testing, as with the structural elements, this is a reliability concern.

Finally, the reliability of the interfacing between the different components is a further area that must be treated carefully. By carefully and methodically performing flat bed testing together with experts who know of common issues that come up, this reliability issue can be mitigated.

For a further analysis of the risks associated with the mission, see chapter 16.

## 18.2. Availability

As mentioned previously all bus components are COTS meaning they can be easily manufactured and are compatible. Moreover, all parts and test facilities for the satellite subsystems are provided by companies in Europe, most of them in the Netherlands. This allows for shorter ways of transportation and enables close cooperation between the different parties. Additionally, through sponsorships the companies are motivated to provide high engagement and active support towards the project. In addition the commercial space market is moderate in size meaning that most of the companies, especially in the Netherlands stand in regular contact with each other. This can speed up communication significantly.

Even though the payload is not COTS, space-proven materials and electrical components are used which can be easily implemented. The certification tests could be provided by multiple companies, accelerating the process.

## 18.3. Safety

The safety during launch is ensured through the satellite being held in the launch pod, being physically detached from the launch vehicle. Moreover, system operation is disabled while the Space Truck is in the launch pod. This is mainly to ensure there is no signal interference for the launch vehicle. Satellite ejection is performed by simple mechanical devices and employing

no explosive charges. During production and assembly appropriate safety measures should be applied and use of hazardous chemicals should be avoided.

In the orbital planning phase if available, the orbit can be selected to minimize possibility of collision with large orbital debris. Besides this, for collision avoidance de-orbiting also needs to be considered. De-orbiting of the satellite reduces the risk of collision after the mission life of the satellite and prevents the creation of additional space debris. A more detailed analysis about orbital lifetime can be found in section 5.4.

Insurance for the satellite also need to be taken into account as usually the liability for a satellite relates to the country it is operated from, in this case the Dutch government. This means the satellite has to be insured for its mission duration. This is applied to cover the potential damage the satellite may cause while it is operational.

# 19

# Operations and Logistics

The operating logic behind the Space Truck project is different from the current market for CubeSats. For a generic CubeSat developer the payload objective is usually defined first and then the bus is designed to provide the best possible performance for the payload. Some developers also design a CubeSat bus that could accommodate payloads within a certain resource budget. The idea behind the Space Truck differs from both the above mentioned cases by allowing for a separate development of bus and payload. It can also accommodate more than 1 payload hence the name Space Truck. This is depicted in Figure 19.1.

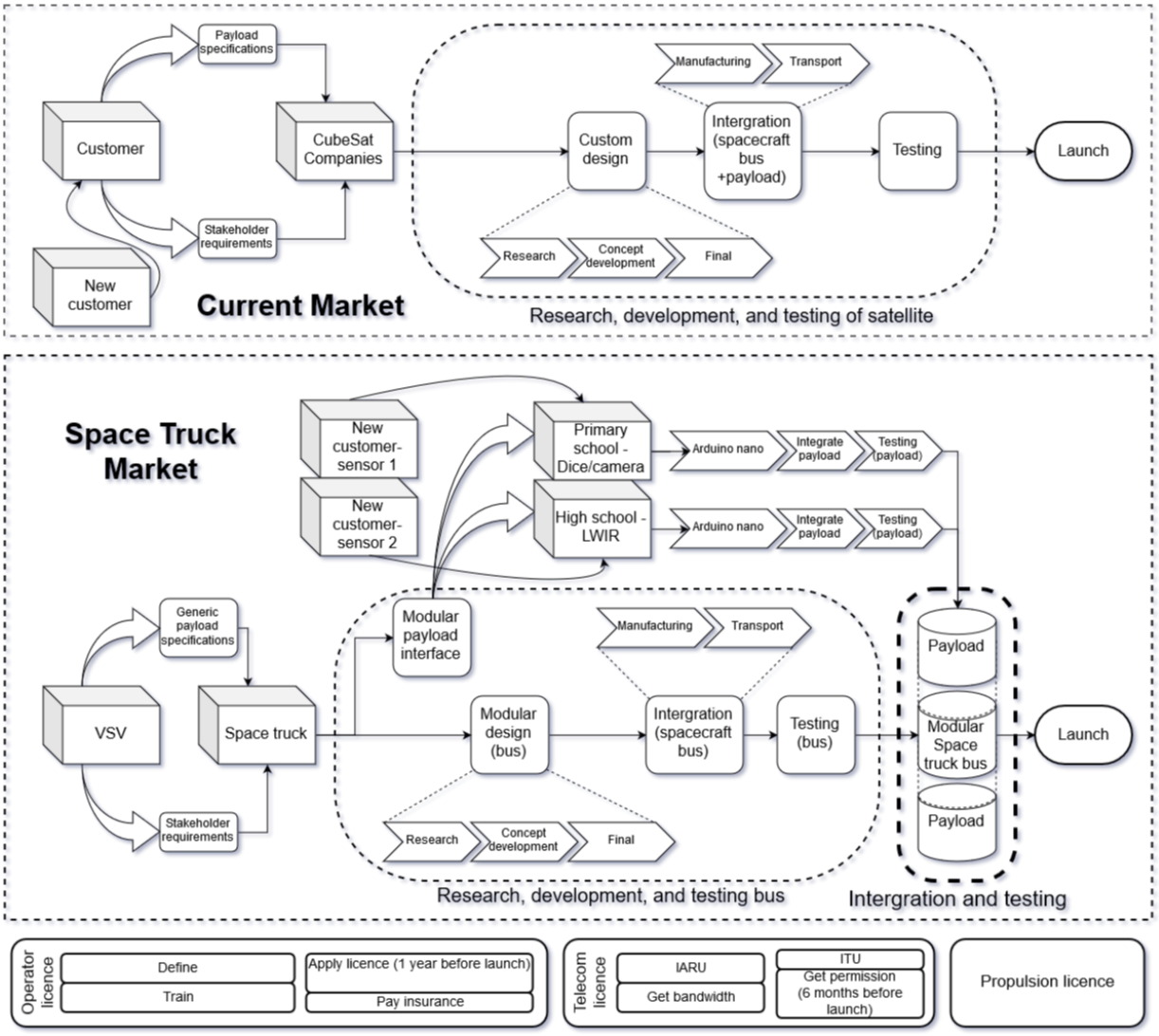


Figure 19.1: Space Truck market operations and licence acquisition

It takes about a year of intense auditing of an organisation to acquire a licence, which allows to operate the Space Truck. Since ISIS, AMSAT and TU Delft possess a licence to operate a CubeSat, it is possible for one of them to own the Space Truck in order to significantly save valuable certification time. A telecom licence combines acquiring a permission from the International Telecommunication Union (ITU) and the International Amateur Radio Union (IARU), which is for an allocation of bandwidth. The process takes at least six months and therefore needs to be commenced as soon as possible if required. Since an amateur radio frequency is used for telecommunication, it is not possible to have a paid engineer do the Space Truck's operations. In addition, the use of propulsion system in CubeSats requires a licence. However, as there are no requirements for an orbit control, there is no propulsion system required on-board.

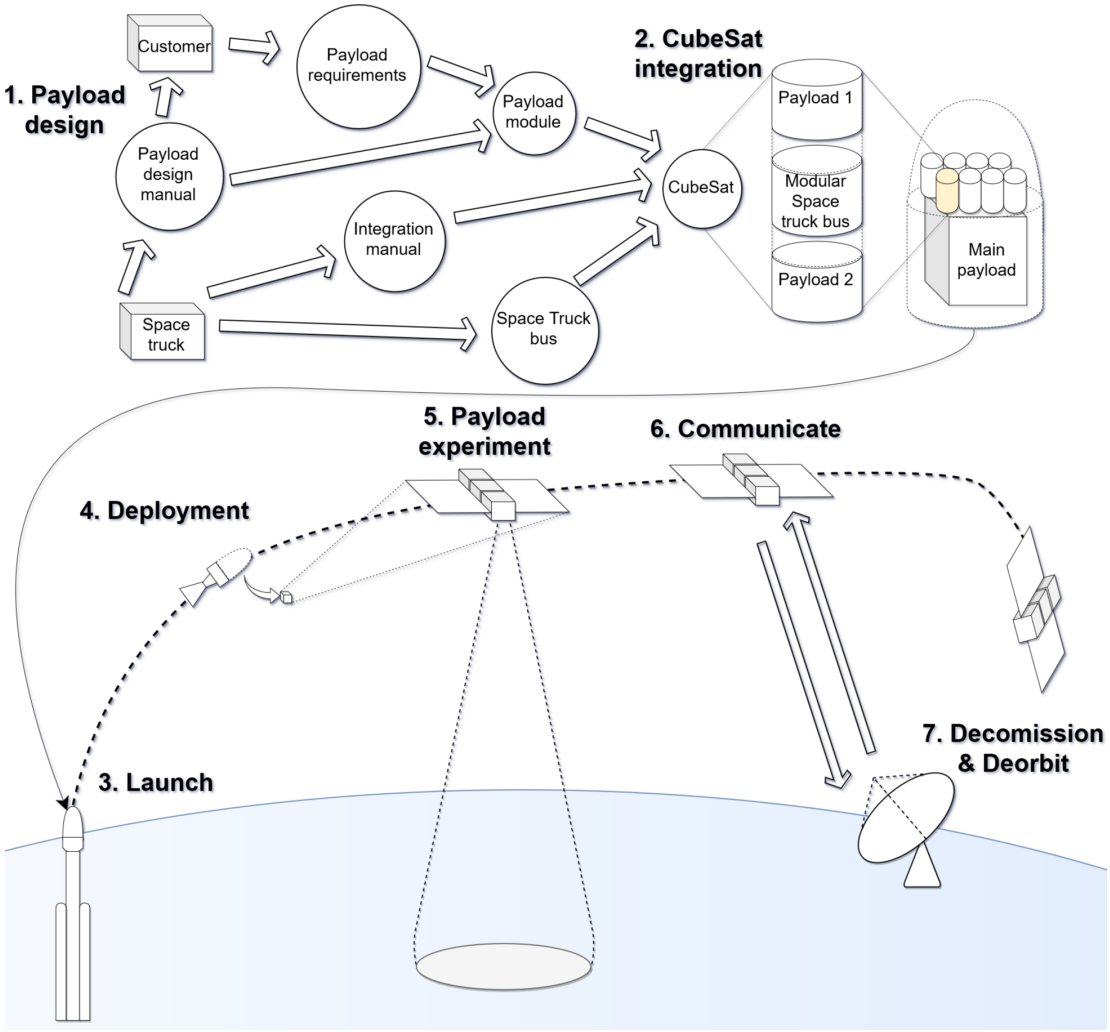


Figure 19.2: Mission logistics

The payload module includes an Arduino Nano to which the sensors are connected. The idea is that if this setup works on the first Space Truck, the concept can be repeated as long as the sensors or instruments to be carried by the Space Truck are compatible with Arduino nano or a similar logic controller. A payload development manual will be created which would be both understandable and easily implementable by high school students and school personal. It will provide all the necessary details from supported platforms to testing of the payload module. The payload could be tested by the use of a personal computer connected to an Arduino nano for operations. In short, once the Space Truck has been developed, modular payloads, which would be designed and developed by students could be integrated though a simple mechanical and electrical interface such as a Arduino nano. A final system level testing will be performed

before launch. Since the Space Truck is developed and produced first, new customers would need to develop their payloads within its constraints. The payload design will be extensively supported by the Space Truck provider.

The complete mission logistics on a higher level is shown in Figure 19.2 and the Space Truck logistics in Figure 19.3. Additional information on testing facilities can be found in Table 21.1. The Space Truck transmits telemetry as a beacon package which can be received by radio amateurs all around the world as specified in chapter 10. The data from the payloads are transmitted mainly while pass over the Netherlands. If the data volume is too high to be transmitted in one pass, it can be done over multiple passes. Command uplink to the satellite is facilitated by the TU Delft ground station providing full ground support for the Space Truck.

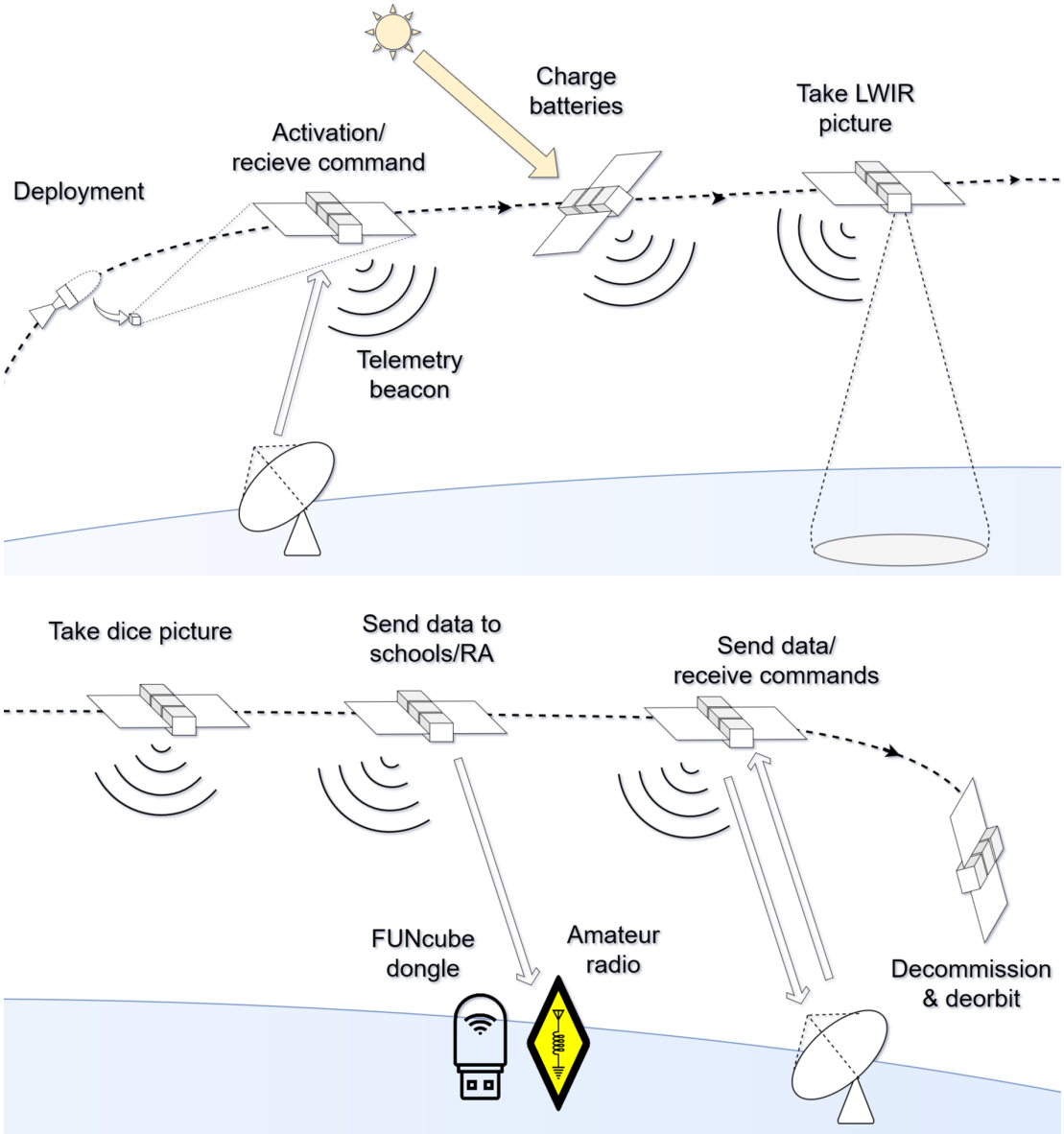


Figure 19.3: Space Truck logistics

# 20

# Sustainable Development Strategy

In this chapter, the sustainable development strategy, which addresses both the sustainability of the design as well as the way the product contributes to sustainability, is outlined.

## Design Reusability

The first way in which sustainability is incorporated in the project is by creating a flexible design. The Space Truck is meant to be a reliable device, and one that can facilitate a multitude of different payloads, in a variety of orbits. This means that the design is reusable, as the Space Truck can be used for different missions, not just for one specific use case. This reusability has a two-fold impact on sustainability. Firstly, it will reduce design and testing efforts of potential future Space Truck missions, leading to reduced waste. Secondly, it may also open an extra avenue for companies or educational institutions that are thinking of designing a satellite for a mission that a Space Truck could also perform. These parties may then decide to fly an already existing Space Truck, rather than designing their own, and so development and testing efforts are significantly reduced.

Moreover, the connection between bus and payload has been designed to facilitate the Plug and Play (PnP) concept. The payload modules feature a commonly available micro controller from the Arduino family, which can interact with the On-Board Computer (OBC) on the Space Truck. This makes developing new payloads accessible to not just companies, but potentially anyone who has experience with such a micro controller. The On-Board software design also reflects this. A more in-depth discussion about this can be found in chapters 9 and 13. Designing the satellite bus with this PnP concept in mind contributes to the reusability and versatility of the overall design.

## Component Selection

Secondly, the design implementation itself should be sustainable as well. To a large extent, this is done by using commercial off-the-shelf (COTS) components. The nanosatellite market has grown rapidly in recent years, which has resulted in there being one or more commercially available options for each subsystem of the Space Truck. Using these COTS components as much as possible has a number of benefits: Firstly, it saves on the design, manufacturing and testing of custom-made components, which reduces waste substantially. Additionally many of the companies are in Delft, and sourcing from them has the added benefit of saving on transportation, even if there is still some transportation involved in the fabrication of these components.

The Space Truck design outlined in this report implements this approach effectively. For both the satellite structure and many of its subsystems, locally sourced COTS options were chosen. In the current design, the only systems that implement custom hardware solutions are:

- Solar panels
- OBC adapter board
- Payload modules

However, it should be mentioned that the payloads themselves contain some COTS components as well, such as the micro controllers and cameras. More details can be found in chapter 9. Designing the product with this in mind ensures that testing efforts are minimized, as many of the COTS components have already been validated individually, thus reducing waste.

## Launch Vehicle

Thirdly, another approach towards sustainability can come from analysing the environmental impact the launch vehicle has, such as in its emission of greenhouse gases. This impact can then be offset, for example by reserving some of the available budget to take measures to nullify the effect. However, in the context of a single, 2.5 kg Space Truck, even the launch emissions are negligible. Therefore, these options are not further examined at this design stage, but may be further explored during detailed design, when a launch vehicle has been selected, and its impact can be quantified.

## Orbital Lifetime Management

Lastly, end-of-life debris mitigation is another sustainability concern that was considered during design. The capability of the Space Truck design to deorbit itself was assessed. The current design concept of the Space Truck does not have orbital navigation capability, as budget constraints will not allow this. As a result, the Space Truck cannot deorbit itself using thrust.

However, by changing the ballistic properties of the Space Truck, its lifetime can be affected. Hence, the Space Truck design contains a deorbiting mode that utilizes this principle. At the end of its mission, the Space Truck can be turned such that the reference area with respect to the free stream is maximized. It can be shown that the drag area then increases from $0.02m^2$ to at most $0.02827m^2$. This results in increased drag, which in turn accelerates orbital decay. The impact of this was analyzed in chapter 5, where it can be shown that the deorbiting mode can affect the satellite lifetime substantially. However, the lifetime reduction varies with a number of parameters, such as altitude, and therefore the exact effect has to be further explored once a launcher is chosen.

Chapter 5 also outlines how the debris mitigation issue directly affected the design. Originally, the Space Truck was designed for an altitude for at most 700 km. After running orbit propagation simulations, it was found that the lifetime of the satellite would be much too long. Therefore, the design space was shrunk by moving this upper altitude limit from 700 km to 600 km. This affected the various subsystems accordingly.

In conclusion, this report contains several examples of where and how the chosen sustainable development approaches affect the design.

# 21
# Future Development Plan

This chapter reviews the next steps in the design, production and testing of the Space Truck satellite. As the purpose of this project is to have a flying CubeSat by the end of 2020, this chapter is intended to serve as a guide for the steps that still need to be taken.

## 21.1. Project Design and Development Logic

The Project Design and Development Logic (PP&D Logic) is made to show a logical order of activities that need to be performed after the DSE. An overview of the PD&D Logic can be found in Figure 21.1. The phase after the conceptual design is split up into 3 different parts: Transition, Detailed design and Test & Manufacturing. These three phases are put into a timeline, represented as a Gantt chart that can be found in Appendix C. More details for the transition phase can be found in this section. The Detailed Design and Test & Manufacturing phases are described in more detail in section 21.2 and section 21.3 respectively.

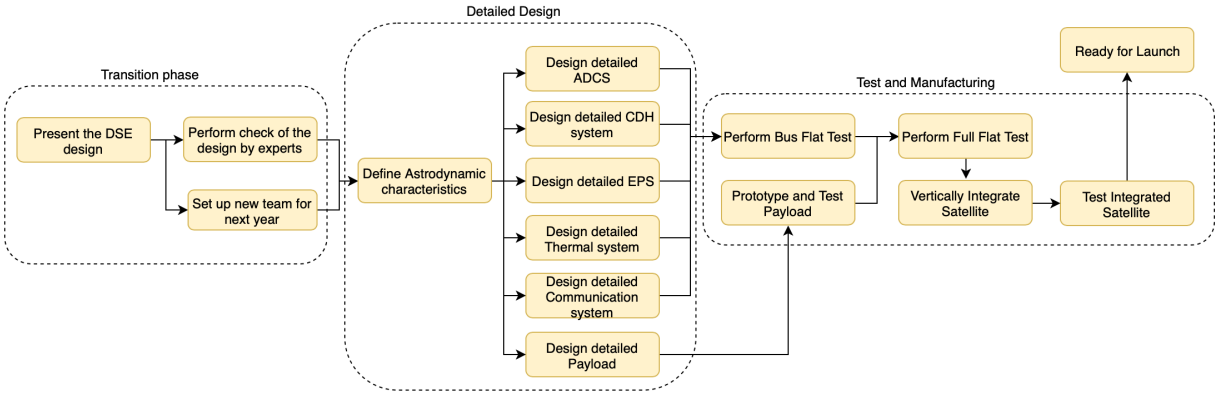


Figure 21.1: Project Design & Development Logic overview

For the Project Design & Development Logic, the conceptual design group had close contact with the VSV, since they are setting up a committee for the next academic year to work further on this project. The committee will consist of 8 people, which will be the core team and work for approximately 20 hours per week. Additional to the core team, there will be a support team. An indication of the number of people that should be included in the support team is given. The larger groups are focused on engineering (Bus, Payload and Software & Communications). This is why there are more resources, in the form of support team members and internships, assigned to them. The educational department will focus on the implementation of the satellite in the the high school course and primary schools [28]. An overview of the layout of the team for next year is presented in Figure 21.2.

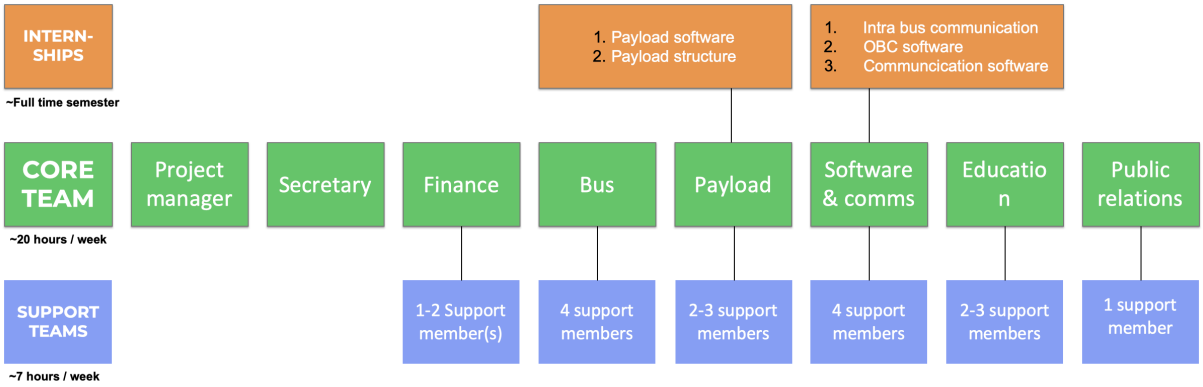


Figure 21.2: Overview of the team that will work on the project next year

Next to the Core and Support teams, student internships at the companies that sponsor this project can be utilized to design the non-COTS components of the satellite. The conceptual design group made a division on what subjects can be covered in these internships. Two internships are focused on designing the dice concept for the primary school module described in subsection 9.3.4. After the design review from the DSE, a decision might be made to discard the dice concept, then these internships would need to be re-assigned to optimize their value for this project. Some of the important design work that needs to be covered in the internships is shown in the following paragraphs.

### Payload Software

Payload software internship should focus on creating a simulation of the dice concept, which models the movement of the dice in space. It can also show the effect of using the ADCS to move the dice. In addition, the internship can also consist of programming the Arduino for each of the payload modules. After the precise schedule for the payload modules is known, it can be programmed onto the Arduinos.

### Payload Structure

In the payload structure internship, the support structures that were presented for the dice concept need to be further analysed. Modal analyses can be performed, as well as the sizing and analysis of the cut-outs, which are needed to attach the payload modules to the satellite. In addition, an analysis of the structural quality of the Quartz to the aluminium connection, which is needed to attach the windows to the structure, needs to be performed.

### Intra-Bus Communication

The intra-bus communication internship focuses on the communication of the different subsystem between each other on a software level. The handling of the payload data should also be included into this internship.

### OBC Software

The software that will be present on the OBC needs to be written. This will likely require more work than can be done in one internship. However, the support team will be able to provide help.

### Communication Software

The decoding software for the up and down links needs to be written. In addition, the transceiver needs to be programmed and a command protocol needs to be developed. Due to the amount of work to be performed, the job might be split and tasks can be moved to the support and core team.

## 21.2. Detailed Design Phase

This section details additional design work which needs to be done to make sure the Space Truck can be launched by the end of 2020.

### 21.2.1. Astrodynamics

It is of utmost importance to have the launch orbit defined as early as possible. Both the power budget and the duty cycles depend heavily on the orbit. Defining the inclination and eclipse time would indicate precisely the amount of power that is generated during an orbit and would allow to define data transmission and payload operation times. The power model can be updated along the project, however, it can only be finalised when all of these are defined. After the orbit is selected, more simulations need to be done to define the final astrodynamic parameters for that orbit (including life time). Finally, a more precise sensitivity analysis can be performed for the selected orbit.

### 21.2.2. ADCS

The amount of work left for the design majorly depends on the sponsor Hyperion and it's procedures. The concepts of operations for the ADCS should be defined to sufficient level of detail to serve as a base for the software infrastructure of the ADCS. For this purpose the orientations of S/C for sun and target-pointing need to be defined with respect to the system reference frame. Once the operation concepts are defined, the operational modes, which are default or customized, can be selected. In the next step, the operational modes and logic are programmed by Hyperion.

As Hyperion has agreed to perform all necessary simulations on the ADCS themselves the design work on the ADCS can be concluded. These simulations should include control loops and data analysis for the ADCS processor as well as required magnetometer loads for disturbance balancing in orbit. In addition a better estimation of the achievable pointing accuracy is vital to the design. Once all crucial analysis is performed the operation scheduling can begin.

### 21.2.3. CDH System

The CDH system needs a lot of additional work done before it is flight ready. This is a challenge for aerospace students as a lot of it is programming and electronics related issues, which are not readily taught in the Aerospace Bachelor degree. It is advisable that people who apply have high personal interest/experience in these areas.

The first thing that can be determined is the BUS protocol implementation. In the design work, the DSE group determined that RS-422 using a UART protocol would be the most suitable for the CubeSat as it is full duplex and has a lot of redundancy. Talking to professionals at Hyperion Technologies, it was understood that there are some hardware incompatibilities of most COTS systems with RS-422, in that they do not support it. However, they often *do* support RS-485 using UART. 485 and 422 are similar to each other (485 is based off 422), but it is highly recommended to investigate the electrical differences in terms of voltages, how signals are sent, the hardware layout, ability to be used as a BUS (rather than a one-to-one connection) etc. From the DSE groups' understanding, the connections are very similar/the same, but different protocols cause a difference in programming requirements, cable requirements, number of UART connections available on the OBC companion board etc.

Secondly, the Software-Hardware communication needs to be written. No work has been done yet on how to get the code (which needs to be written) to talk to, get data from, and properly operate the hardware. Given the BUS protocol choice made (RS-422, which might be changed to RS-485), learn how to use those protocols with software and how to talk to hardware. Companies should be able to give pointers on that, as it is their hardware.

Finally, the software for the OBC needs to be written. No software has been written yet. The Hyperion OBC can ship with a Linux Debian OS, which should make programming, scheduling, and getting drivers easier. The software block diagram and functional flow diagram should give an idea of what needs to to be done in a very overall/holistic way. There is no doubt that as the design progresses, the scope of code to be written will expand. Make sure to at all steps write checks into the code to stop a bug happening and damaging the satellite.

### 21.2.4. Electric Power System

There are a number of things to be done to have the EPS ready for launch by 2020. First and foremost, detailed information of the EPS module, all of the components and their efficiencies is necessary. Obtaining it would allow more precise calculations and design of the system. In addition, the information is needed to prove that each voltage regulator has enough power lines and that the other systems are compatible with the EPS.

After that, creating a precise tumbling model is required. Currently there are calculations, which indicate that if the ADCS fails, the satellite would start tumbling and the power production would drop to 1.97 W. However, these calculations are based on a 20-year-old model and theory. Therefore, having a precise tumbling model would allow for a more detailed duty cycle in case of a failure of the ADCS.

### 21.2.5. Structures

In the further design of the structure, more advanced techniques should be applied in order to find the structural properties of the satellite. In order to find a more accurate model than the simple spring-mass model that has been used so far finite element methods should be used. Additionally, a more accurate computer model of the satellite should be created in order to predict exactly the center of gravity and mass of the satellite.

Additionally, the structure of the payload needs to be further designed and tested as explained in subsection 21.3.1. A concept has been created for the structure of the payload but the pieces have not been sized due to time constraints. A detailed analysis will also require finite element methods.

Finally, it is recommended to gain access to User's Manual of the Polar Satellite Launch Vehicle (PSLV). This is a likely launcher for the satellite. The natural frequency requirement that has been used for this launcher is 60 Hz from the reader of ADSEE-I, a TU Delft first year course. [44] However, other sources claim a primary frequency of 100 Hz along the longitundal axis [1]. If this is true, the design of the payload adapter plate must be reassessed and this frequency should be kept in mind for the design of other parts.

### 21.2.6. Thermal System

The overall temperature of the spacecraft has already been estimated. However, it is recommended to make a more detailed lumped-parameter thermal model of the spacecraft. This is to more precisely predict the temperature ranges of individual components and identify critical areas. The main areas of concern are the battery, the solar arrays and the transceiver modules.

For the battery, mainly the effectiveness of the electrical heater need to be investigated, i.e., whether or not the electrical heater included with the ISIS Space iEPS Type A is enough to keep the battery from undercooling. Also the power consumed by the electrical heater should be more accurately predicted to allow for more accurate sizing of the power system.

Considering that the solar panels are mounted on the outside and are directly exposed to sunlight, it should be investigated whether or not the solar panels will overheat/undercool. If the temperature of the solar arrays is predicted to be outside of their design range, thermal coating could be used on the back of the panels to change the panel thermal properties.

The transceiver modules, when transmitting, use a relatively large amount of power. Therefore it is recommended to investigate whether or not the transceiver modules will overheat or not. If they do, heat sinks should be included to radiate some of the heat away from the modules and into the side panels which will radiate the heat into cold space.

Also, as the Hyperion CP400.85 OBC does not come equipped with a temperature sensor, one will have to be integrated in the OBC adapter board. This needs to be taken into account during the design of the OBC adapter board.

### 21.2.7. Communication System

Once the transceivers are bought they need to be programmed with the desired settings. Their behaviour should be tested and determined. The communications link should be thoroughly tested on Earth by performing the full variety of operations. The exact contents, structure and

[1] https://davidpublisher.com/Public/uploads/Contribute/5615d0ec29987.pdf[Retrieved on 19-06-2019]

size of telemetry frames should be established and a precise transmission schedule should be formulated. Further, the telemetry decoding procedure has to be devised and specialized decoding software written. A detailed description as well as instructions on decoding the satellite telemetry have to be made available to the radio amateurs. The feasibility of a digipeater functionality should be more carefully assessed and, if possible, implemented. In that case a manual on digipeater use should also be made publicly available. Finally, the exact format of the satellite commands has to be established. One or more persons have to obtain a radio operator license and become trained in using the TU Delft ground station. These persons should then take on the responsibility of controlling the satellite.

### 21.2.8. Payload

After the final review of the DSE group, a group of experts will review the design that is presented. A development challenge in the design of the satellite currently is the dice concept for the primary school payload. Since this is not a COTS payload module, it will require more analysis, design and testing of this concept. The high school payload module will also require additional testing. Detailed design on the different components in the primary school module needs to be done (including the flash, the dice, camera + lens and the windows). The structural analysis of the primary school module and additional sizing of support structures should be performed. Next to the design of the payload modules, software need to be written for the Arduinos to implement the functions depicted in Figure 9.3.

## 21.3. Manufacturing, Assembly, Integration and Test

In this section, the overall philosophy of the Manufacturing, Assembly, Integration and Test (MAIT) phase will be described. After that, each phase is inspected in more detail.

During the beginning of the MAIT, there are two difficulties to be solved which can be done in parallel. One of these is the development of the payload. This is a module that has never been flown in space and therefore the structures must be rigorously designed and face tests like vibration and shock tests in order to verify them. The electronics (the Arducam, Thermal Imager and Arduino Nanos) which are not space graded must be proven to survive these tough mechanical environments as well as vacuum, radiation and thermal cycling tests.

The bus subsystems, unlike the dice concept, are already rigorously designed and tested for the space environment and by the time of launch all parts are expected to have flight heritage, proving their operability in space. The difficulties with these components are expected to lie in the interfacing between the components. In chapter 16, a paper is cited which states that the most common cause of failure in university satellites is a lack of system testing; components are often tested individually, but the interfacing is not tested seriously enough.

Once the subsystems have been tested together in a flat bed test and the payload has also been verified, they should be brought together and again, a flat bed test should be performed in which operations are simulated. Finally, the full system can be integrated vertically in the CubeSat format. After this is done, the final testing of the system can take place in which the full system is verified and qualified for flight. It is still to be decided by the VSV whether a different qualification and flight model will be built. This is a common practice but it also adds to the cost of the project, and since the goal is to have all parts sponsored, this may not be possible.

A top level flow chart of the MAIT process can be seen in Figure 21.3.

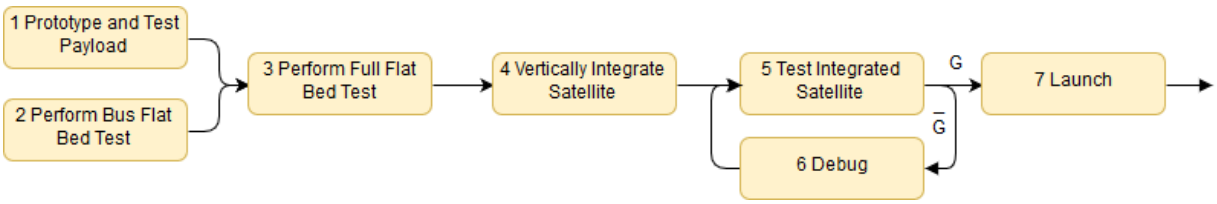


Figure 21.3: Top Level Flowchart of the MAIT Process

### 21.3.1. Prototyping and Testing the Payload

As mentioned above, it is very important to rigorously test the payload as not all components are commercial off the shelf and hence need to be verified for the space environment. Thus, it is recommended to prototype the payload and its structure as early as possible in order to begin payload testing before the bus is ready for space environment testing. Prototyping the payload can be further broken down into smaller blocks seen at the highest level of the flow chart in Figure 21.4. The different parts of the payload are labelled in Figure 9.6 for reference and engineering drawings of the structural elements to be manufactured are included in Appendix A.

The first step of prototyping is integrating and testing the thermal imagery camera. All the necessary components (the Arduino, instruments, lenses) are purchased and connected and it is tested if the camera can take images. Simultaneously, a test box can be manufactured, in which the instruments will be placed inside for testing. The test box is built around a mock structure which should not be larger than 1U and should simulate the ISIS 2U LS, described in chapter 8. Five 1U panels should be manufactured which simulate the solar panels. Holes must be cut out for the instrument apertures and a quartz window will be attached to the hole drilled in the dice compartments. Two of the side panels need to be attached to the side of the structure in this phase since the aluminium wall and the middle window, which form the compartment for the dice, need to be attached to them. This may be a permanent process, such as welding, as described in Table 9.3.4.

In the next phase of testing the payload concept, the full payload is integrated, which is visualized in Figure 21.5. The lens bracket, which stabilizes the lens during launch to minimize vibration, must be attached after the camera is attached to the structure since the camera cannot be placed if it is already attached. The Arduinos are placed, connected to their instruments and finally the dice are placed in their compartments and the mock solar panels are attached to close the box.

Finally, the payload can be tested. A full list of all tests that should be performed on the full satellite is given in subsection 21.3.5. Only the relevant tests are performed on the payload; these are mechanical as well as thermal cycling tests, vacuum and radiation testing. It is common to glue the components before performing mechanical testing so it is advised to perform these mechanical tests at the end. After each test, the payload should be inspected for structural damage and it should be checked whether pictures and thermal images can still be taken with the Arduinos. In the case of a failure, the payload may need to be redesigned and the relevant tests should be performed again.

### 21.3.2. Flat Bed Test of the Bus

In parallel with payload prototyping and testing, the bus subsystems such as the ADCS, Communications System and OBC can already be flat bed tested. In this phase the subsystems are acquired, placed on a table next to each other, connected electronically and it must be made sure that they interact in the expected manner. The different steps are outlined in Figure 21.6. First the different subsystems are tested and then they are brought together, and the full operations of the complete bus are simulated.

In order to test the EPS, the solar panels and battery are connected and it is made sure that the solar cells charge the battery and that the voltage and current readings are acceptable. The OBC is tested by connecting it to the PCB board that is designed for it and testing that it performs as expected. Once the OBC has been tested and is shown to function, it is connected to the ADCS and it is made sure that the two subsystems interface correctly, the ADCS has the required performance and operates correctly. The communication system is tested by first checking that the Gomspace transceivers can send and receive signals through the antennas with the expected performance. Then they are connected to the OBC and it is made sure that the OBC can also send and receive at the correct performance.

Finally, when all the subsystems have been tested they are all connected and a full flat-bed test is performed, by fully simulating operations.

### 21.3.3. Integration of Payload and Bus

Once the payload has been verified and the bus has also been proven to function together, one final step must be completed before integrating the satellite fully. A flat bed test should

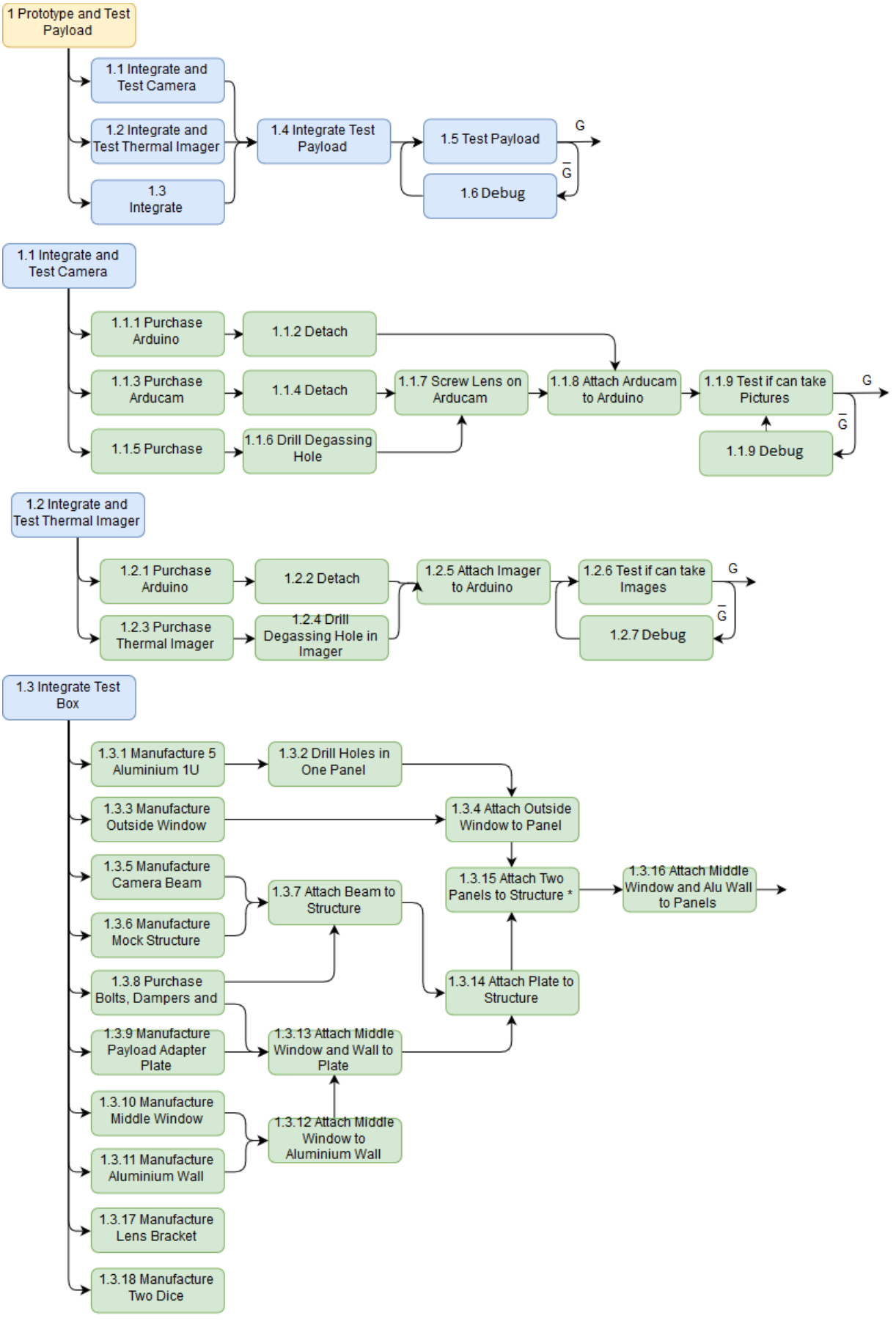


Figure 21.4: Flow Chart of the Prototype and Test Phase of the Payload (continued in Figure 21.5)

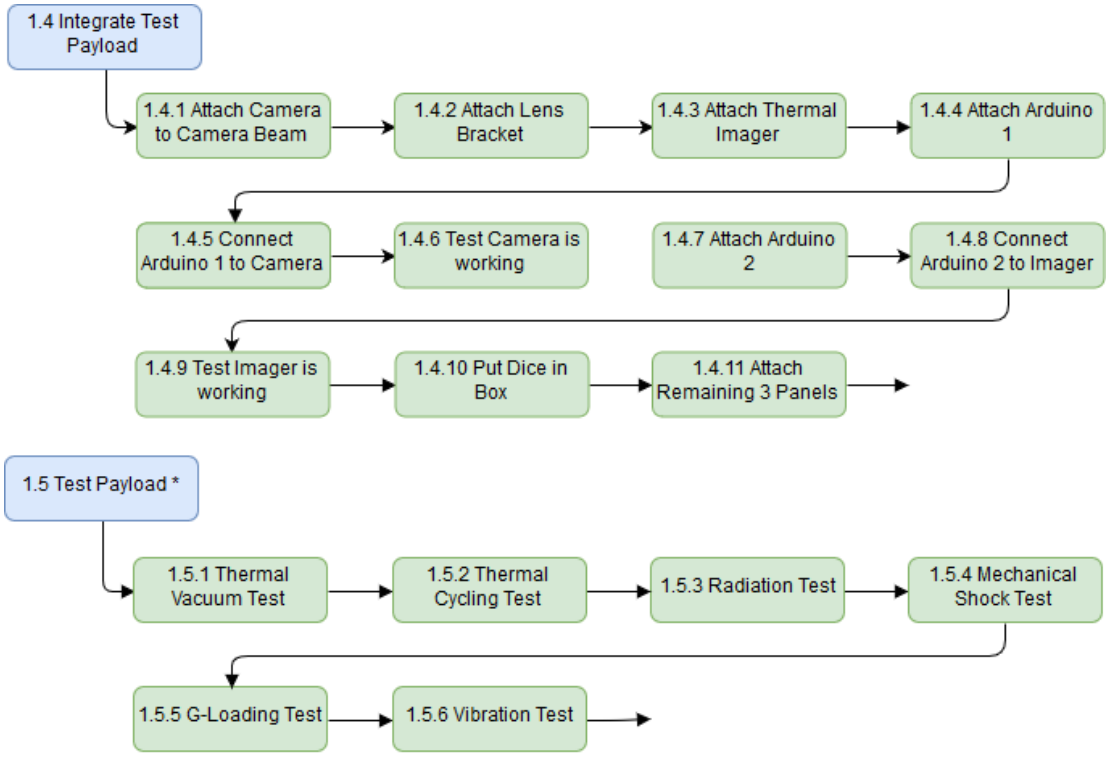


Figure 21.5: Flow Chart of the Prototype and Test Phase of the Payload (continued from Figure 21.4)

be performed including both the bus and the payload. This is represented in a flow chart in Figure 21.7. The interfacing of the Arduinos and the OBC as well as the EPS and the Arduinos and sensors need to be checked and operations should be simulated.

### 21.3.4. Vertical Integration of the Satellite

In order to vertically integrate the satellite, first the structure, spacers, nuts, bolts and dampers must be acquired. The structure is assembled and then the subsystems are slid on to the rods with spacers in between them in the required order as shown in Figure 15.1. The connections between the subsystems must also be established. When all of the subsystems are on the rods, the middle bulkhead is place on the rods and bolted in place. The payload can then be assembled on top of the bulkhead, similarly to how it was assembled during prototyping (subsection 21.3.1.) Difference are that the fully implemented structure and solar panels are used and the payload is connected to the bus.

After the payload is attached to the stack, the top bulkhead should be attached to the structure, the antennas should be connected to the transceivers and attached, and finally the remaining solar panels are bolted on to the structure.

### 21.3.5. Testing

Finally, the fully integrated system must be tested in order for it to be certified for flight. A full overview of the necessary tests along with a description and potential testing facilities is given in Table 21.1.

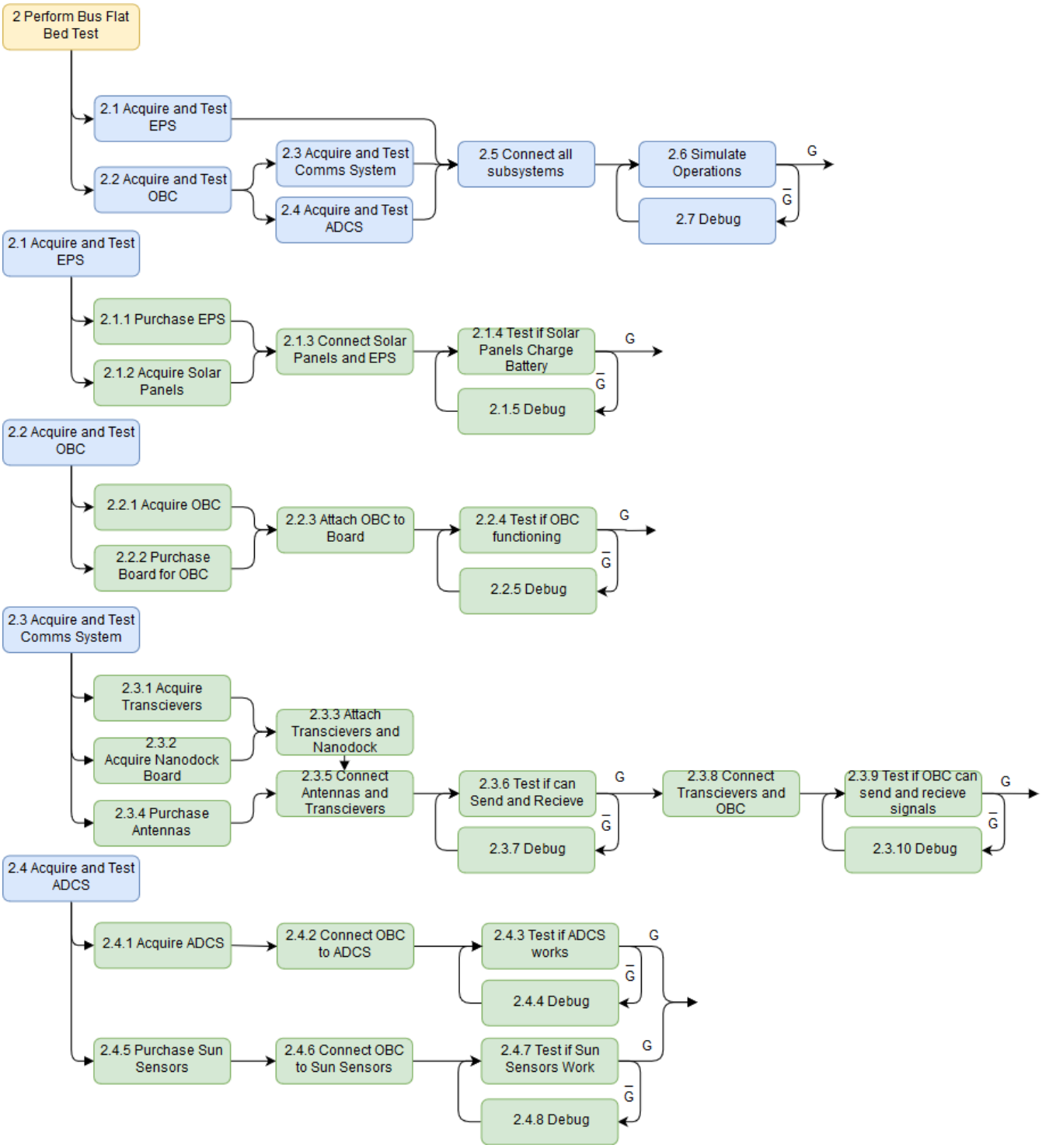


Figure 21.6: Flow Chart of the Flat Bed Test of the Bus Subsystems

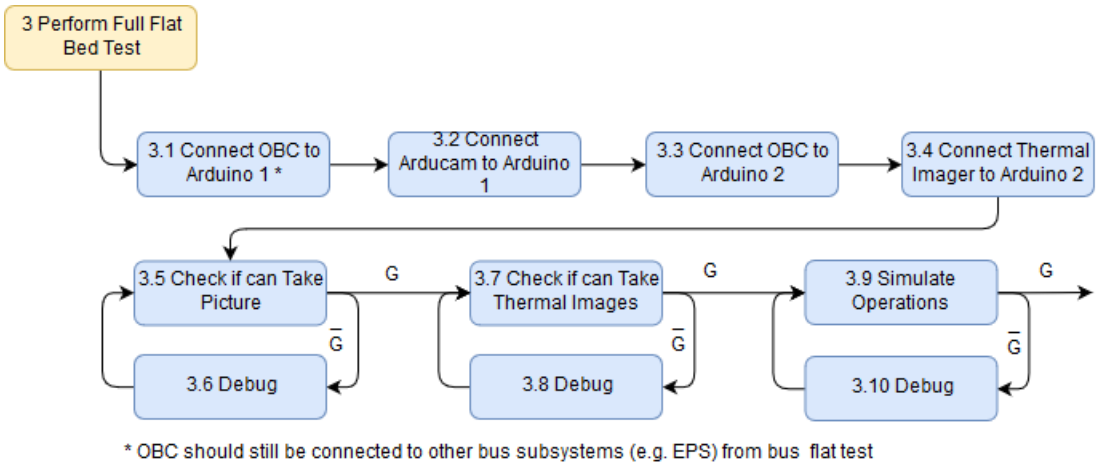


Figure 21.7: Flow Chart of the Flat Bed Test of the Bus with the Payload

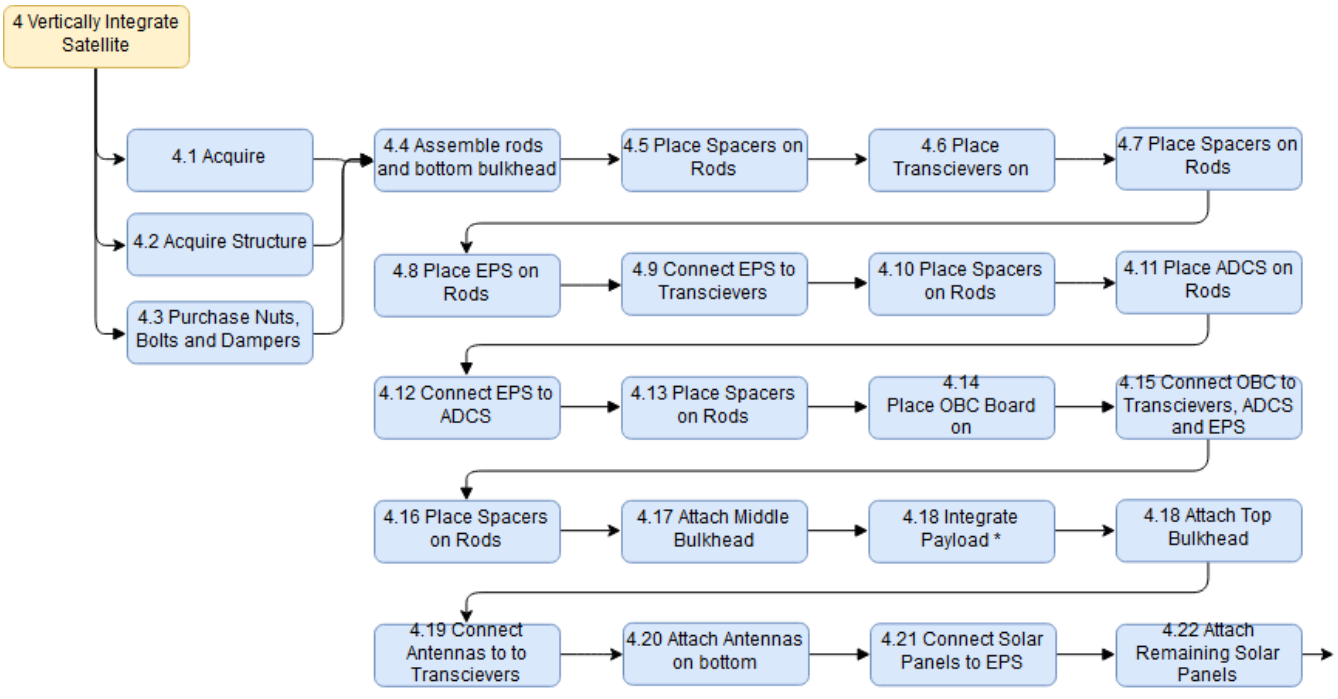


Figure 21.8: Flow Chart of the Vertical Integration of the Satellite

Table 21.1: The tests that are necessary in order to certify a cubesat for flight.

| Test | Potential Providers | Explanation |
|---|---|---|
| Vibration Test | ISIS | This test is used to verify the natural frequency of the cubesat, ensuring the vibration loads induced during launch do not destroy the satellite. |
| G-loading test | NLR, ESTEC | This test is to verify the satellite will withstand the loading forces it experiences during launch. |
| Mechanical shock test | ISIS | This test is to ensure the satellite can withstand the impulse loads associated with launching, such as state/faring separation. |
| Thermal vacuum test | ISIS | This test validates the satellite working in a vacuum. |
| Thermal cycling test | ISIS | This test verifies the spacecraft operating over the expected temperature ranges. |
| Radiation test | ESTEC | To verify if the satellite can operate nominally in the radiation environment it is exposed to. |
| End-to-end test | In-house | This test is to verify the entire communication system from the ground station-satellite works as expected. |
| EletroMagnetic Compatibility test | ISIS | This test it to make sure all electrical components are working together on the planned radio frequencies without any noise being produce by the spacecraft subsystems. |
| Bus surviveability test | In-house | To verify that spacecraft redundant systems and software fail-safes work as expected and maintain the spacecraft operation. |
| ADCS test | ISIS | This test is to verify and calibrate components related to the ADCS such as sun sensors, magnetometers, magnetourquers. |
| Deployment test | In-house | This test verifies that the deployment of the cubesat and its systems required for operation behave as expected such as antenna deployment. |

Table 21.2: A list of tests which are performed on cubesats prior to launch for the purposes of verifying flight readiness along with potential providers of such tests in the Netherlands

# 22

# Cost Breakdown

The cost breakdown for the Space Truck project is given in Figure 22.1. The first distinction, and the most important one, is between recurring costs and non-recurring costs. The reason that this distinction is so important is because the goal of the Space Truck is to be the first in a series of satellites. By keeping the one-time costs separate, one can more easily see what the long term costs are. These costs are then further broken down into there major parts.

The non-recurring costs are the costs for the facilities and the PR costs. The spacecraft only needs to be designed once and the development costs are, thus, also a one time cost. However, for developing the second satellite and the next in series, the design cost would be a recurring cost which would have to be taken into account. The facilities required to build the spacecraft also have to be established only once. One could argue that the PR costs are recurring, however, it is not yet known whether further PR will be required after the initial mission or not. Therefore the PR costs are taken into account separately.

The recurring costs are much more broad. The most obvious recurring costs are those for the individual components as the components, of course, can not be reused. Also the cost for the payload development is recurring considering it needs to be developed for each mission separately. As each mission needs to be tested in its final configuration, the testing costs apply to each mission individually. Manufacturing costs, operational costs, insurance and launch costs also apply to each mission individually.

The some of the values for the costs are given in Table 3.1.

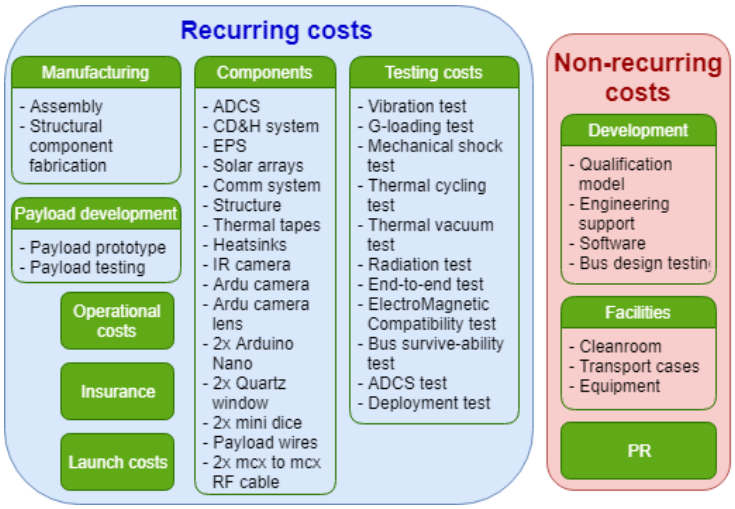


Figure 22.1: The cost breakdown structure for the post-DSE project activities

# 23
# Conclusion

As described before, this report is a product of a two-fold mission. First, it is the VSV's plan to launch an educational and commemorative CubeSat satellite in space in 2020. Their goal is to "*increase the general enthusiasm for technology and space travel among children*". They aim to achieve this goal by making the CubeSat carry two educational payloads, one directed at primary education, and the other at secondary education.
On the other hand, the mission of this DSE is a subset of VSV's mission, and concerns the preliminary design of this satellite and its payloads. Hence the project objective statement of this DSE is to *"design a mission that allows students to perform experiments in space by 2020"*.
A secondary objective of this project is, to design the satellite bus not just for this mission, but to design a reliable satellite bus that can support a variety of different payloads in a variety of LEO orbits.

At the end of this phase, it is important to assess whether both objectives, that of the VSV and that of the DSE, were achieved adequately. In this report, a design is made for a 2U CubeSat that can perform missions in space as high as 600 km above Earth's surface. It has active attitude control, which can be used to point the payloads, or point at the Sun, to increase available power on-board. It currently has a payload bay volume of half 1U, where multiple payloads may reside. These payload can connect to the satellite bus to receive power and gain access to the up and downlink to Earth. The hardware architecture and the choice of components of the satellite design reflect a purposefully simple design, given the ambitious timeline of the overarching project.

The payloads themselves are also designed. The primary school payload consists of a small experiment that will answer the question whether the game "rock-paper-scissors" can be played in space. The secondary school payload contains an infrared sensor that can be used to generate data for the students. The interaction between payload and spacecraft bus is of an accessible type, encouraging amateur and student interaction.

In conclusion, the outcome of this design phase aligns with the DSE project objective. The payload module implementation side is made accessible to students by its use of common protocols and hardware, and the overall design of the bus is kept simple, to make sure the development can be realized in time.

Regarding the VSV's mission, the Space Truck design is versatile, paving the way for future student CubeSat missions on the same platform, beyond the VSV's launch next year. This accessibility serves to involve children and young students with applications in space, nurturing within them an enthusiasm for space-related technology, and bringing outer space closer to them than ever before.

# Bibliography


[1] P. Appel. Attitude estimation from magnetometer and earth-albedo-corrected coarse sun sensor measurements. *Acta Astronautica 56*, Oct 2004.

[2] Gomspace Aps. *NanoCom AX100 Datasheet*, August 2016. Revision 3.3.

[3] W.I. Axford. The interaction between the solar wind and the earth's magnetosphere. *Journal of Geophysical Research*, 1962.

[4] Anna Case. Software defined radio methodologies for cubesat reliability. Technical report, Missouri University of Science and Technology, 2018.

[5] Anna Case and Kurt Kosbar. Communication systems for cubesat missions, 2018. ISSN 0884-5123. URL `http://hdl.handle.net/10150/631626`.

[6] A. Cervone. Lecture 09: Spacecraft telecommunications, September 2017. AE2111-II lecture notes.

[7] The Inter-Agency Debris Coordination Committee. Iadc space debris mitigation guidelines. Technical report, IADC, 2007.

[8] T. Krauthammer E. Ventsel. *Thin Plates and Shells. Theory: Analysis, and Applications*. CRC Press, 2001.

[9] E. Thebault et al. International geomagnetic reference field: the 12th generation. *Earth, Planets and Space*, 2015. doi: 10.1186/s40623-015-0228-95.

[10] J.R. Wertz et al. *Spacecraft Attitute Determination and Control*. D. Reidel Publishing Company, P. O. Box 17, Dordrecht, Holland, 1978.

[11] S. Lee et. al. *CubeSat Design Specification*. Cal Poly SLO, California, USA, 2014.

[12] T. Baldewijns et al. Baseline report dse group 4. Technical report, Delft University of Technology Faculty of Aerospace Engineering, 2019.

[13] T. Baldewijns et al. Midterm report dse group 4. Technical report, Delft University of Technology Faculty of Aerospace Engineering, 2019.

[14] S.C. Kenyon R.H. Rapp E.C. Pavlis F.G. Lemoine, N.K. Pavlis and B.F. Chao. New high-resolution model developed for earth's gravitational field. *Journal Of Geomagnetic Research, Vol. 79, No. 9*, 1998.

[15] Luxeon Flash. *Technical Datasheet DS49*, June 2004.

[16] FLIR. *FLIR Tau 2 Longwave Infrared Thermal Camera*, Spetember 2016.

[17] Stephen Frank and Don Hovey. Return on investment in education. a "system-strategy" approach to k-12 roi. 2014.

[18] N. Hamada G. Shabiralyani, K.S. Hasan and N. Iqbal. Impact of visual aids in enhancing the learning process case. *Education and practice*, 2015.

[19] T. Inamori, N. Sako, and S. Nakasuka. Compensation of time-variable magnetic moments for a precise attitude control in nano- and micro-satellite missions. *Advances in Space Research*, April 2011.

[20] ISO 22641:2012. Tm synchronization and channel coding. Standard, The Consultative Committee for Space Data Systems, July 2017.

[21] A. E. Hedin J. M. Picone and D. P. Drob. Nrlmsise-00 empirical model of the atmosphere: Statistical comparisons and scientific issues. *Journal Of Geomagnetic Research, Vol. 107, No. A12, 1468*, 2002.

[22] Raj Das John Mo and Sherman Cheung. *Demystifying Numerical Models*. Butterworth-Heinemann, 2018.

[23] J.J. Puschell J.R. Wertz, D.F. Everett. *Space Mission Engineering: The New SMAD*. Microcosm Press, 4940 W. 147th Street, Hawthorne, CA 90250 USA, 2011.

[24] B. Lange. The drag-free satellite. *AIAA Journal, Vol. 2, No. 9, 1590*, September 1964.

[25] J. M. Enoch V. Lakshminarayanan G. Li C. A. Macdonald V. N. Mahajan E. W. Van Stryland M. Bass, Dr. C. DeCusatis. *Handbook of Optics, Third Edition Volume I : Geometrical and Physical Optics, Polarized Light, Components and Instruments*. McGraw-Hill Education - Europe, New York, NY, United States, 2009.

[26] J. Maurer. Retrieval of surface albedo from space, 2002. URL `https://www2.hawaii.edu/~jmaurer/albedo/`.

[27] J. Meseguer, I. Pérez-Grande, and A. Sanz-Andrés. *Spacecraft thermal control*. Woodhead Publishing Limited, 80 High Street, Sawston, Cambridge CB22 3HJ, UK, 2012.

[28] Esero NL. *Satellieten en aardobservatie*, January 2016. Revision 1.1.

[29] U.S. Department of Defense. *Transition from Development to Production*, September 1985.

[30] Leveque K. Oltrogge D.L. An evaluation of cubesat orbital decay. *Annual AIAA/USU Conference on Small Satellites*, 2011.

[31] G. Swinerd P. Fortescue and J. Stark. *Spacecraft Systems Engineering, Fourth Edition*. John Wiley & Sons, Ltd., The Atrium, Southern Gate, Chichester, West Sussex, PO19 8SQ, United Kingdom, 2011.

[32] W. D. Pesnell and K. H. Schatten. An Early Prediction of the Amplitude of Solar Cycle 25. *Sol Phys*, 293:112, July 2018. doi: 10.1007/s11207-018-1330-5.

[33] D.M. Prieto, B.P. Graziano, and P.C.E. Roberts. Spacecraft drag modelling. *Aerospace Sciences*, 2016.

[34] M.K. Ray, S. Sasmal, and S. Maity. Improvement of quantum efficiency and reflectance of gaas solar cell. *International Journal of Engineering Research and General Science*, 2015.

[35] Glenn Robb. Circularly polarized antennas explained, without the math, 2017. URL `https://antennatestlab.com/wp-content/uploads/2017/09/CP-Explained-Without-Math.pdf`.

[36] J. Salem. Fused silica and other transparent window materials, 2016. URL "`https://ntrs.nasa.gov/archive/nasa/casi.ntrs.nasa.gov/20160010278.pdf`".

[37] D.S. Cooley J.J.K. Parker T.G. Grubb S.P. Hughes, R.H. Qureshi. Verification validation of the general mission analysis tool (gmat). Technical report, 2013.

[38] M Swartwout. The first one hundred cubesats: A statistical look. *JoSS*, 2:213–233, 01 2013.

[39] C. O. Asma T. Scholz and A. Aruliah. Recommended set of models and input parameters for the simulations of orbital dynamics of the qb50 cubesats. 2012.

[40] S Tafazoli. A study of on-orbit spacecraft failures. *Acta Astronautica - ACTA ASTRONAUT*, 64:195–205, 02 2009. doi: 10.1016/j.actaastro.2008.07.019.

[41] K. F. Wakker. *Fundamentals of Astrodynamics*. Institutional Repository Library, Faculty of Aerospace Engineering, Delft University of Technology, 2015.

[42] J.R. Wertz and W.J. Larsen. *Space Mission Analysis and Design*. Microcosm Press, 2377 Crenshaw Blvd., Suite 350, Torrance, CA 90501 USA, 1999.

[43] Emma Woodley. Practical work in school science-why is it important. *School Science Review*, 91(335):49–51, 2009.

[44] B.T.C. Zandbergen. *Aerospace Design & Systems Engineering Elements I Part I: Spacecraft (bus) Design and Sizing*. TU Delft Faculty of Aerospace Engineering, 2015.

# A

# Appendix A: Engineering Drawings

| No. | Name | Material |
|---|---|---|
| 1 | Payload Adapter Plate | Al 7075 or 6061-T6 |
| 2 | Camera Beam | Al 7075 or 6061-T7 |
| 3 | Middle Window | Quartz |
| 4 | Aluminium Wall | Al 7075 or 6061-T7 |
| 5 | Outside Window | Quartz |
| 6 | Solar Panel Cutouts | - |
| 7 | Lens Bracket | Al 7075 or 6061-T7 |

1

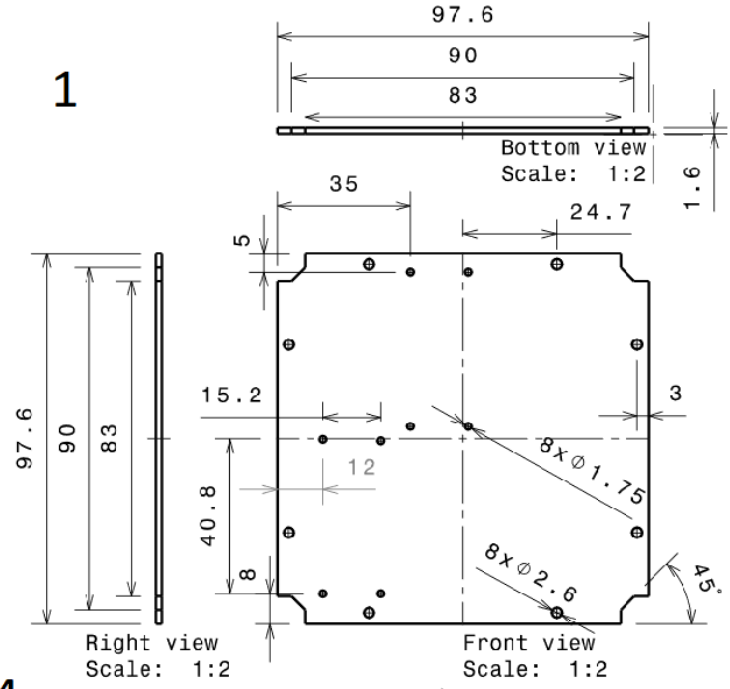


2

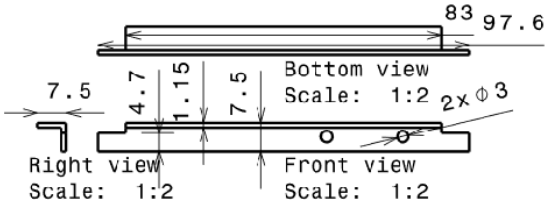


3

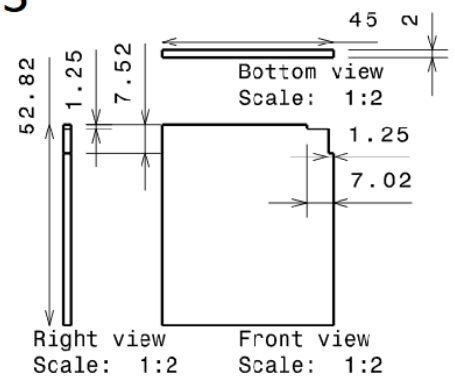


4

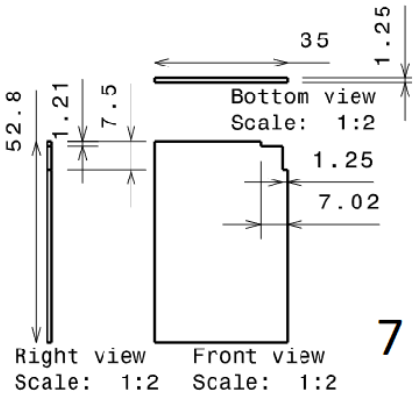


5

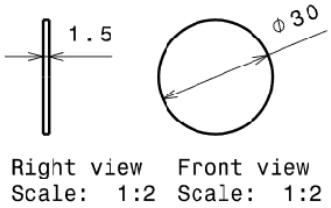


6

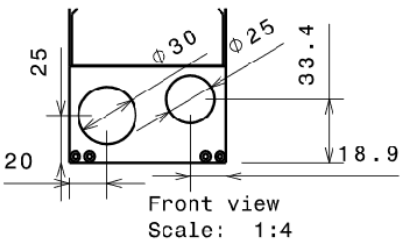


7

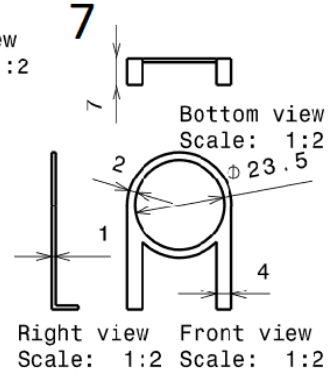

# B

# Appendix B: GMAT Simulation Input Parameters

Table B.1: Parameter configuration of the performed orbital lifetime simulations in GMAT

| | | |
|---|---|---|
| **Spacecraft Parameters** | | |
| State Type | Keplerian | |
| Dry Mass | 2.5 $kg$ | Upper mass limit as defined by requirements |
| $C_D$ | 2.2 | As GMAT takes one value for $C_D$, the most likely value was chosen. [30], [39] suggest using a $C_D$ of 2.2 for CubeSats. |
| $C_R$ | 1.8 | Default value |
| Drag Area | 0.02 $m^2$ | Approximate side panel area of a 2U CubeSat |
| SRP Area | 0.02 $m^2$ | Approximate side panel area of a 2U CubeSat |
| **Propagator Parameters** | | |
| Integrator | Prince-Dormand78 | The official GMAT documentation claims that the Prince-Dormand78 integrator is the best general purpose integrator in GMAT. The official V&V report of GMAT [37] also suggests that this integrator is slower, but substantially more accurate than many other Runge-Kutta methods. All simulations performed in this chapter use the default parameters. |
| Gravity Model | EGM-96 | According to [14], EGM-96 offers higher accuracy than the older JGM-2 and JGM-3 models. J-terms are calculated for 10 degrees, and up to 10 orders. |
| Atmosphere Model | MSISE90 | GMAT offers the MSISE90 and JacchiaRoberts models. Whilst both have been supplanted by NLRMSISE-00, [21] observes that MSISE90 is more accurate than JacchiaRoberts for LEO orbits between 400km and 800km. |
| Space Weather Predictions | | Predictions run up until June of 2044 (file last updated 06-02-2018) |
| Schatten Prediction | | Predictions run up until August of 2044 |
| SRP Model | Spherical (default) | Since SRP is an orbit disturbance of O(-6) [31], it is included in the model. Results may be improved by using a 3D model of a CubeSat, but this is left to a later design stage. |
| Third Bodies | Sol, Luna | According to [31], at 500km altitude, third body disturbances of Earth's moon O(-6) and Sol O(-7) dominate, all others are under O(-12). |

# C

# Appendix C: Gantt Chart

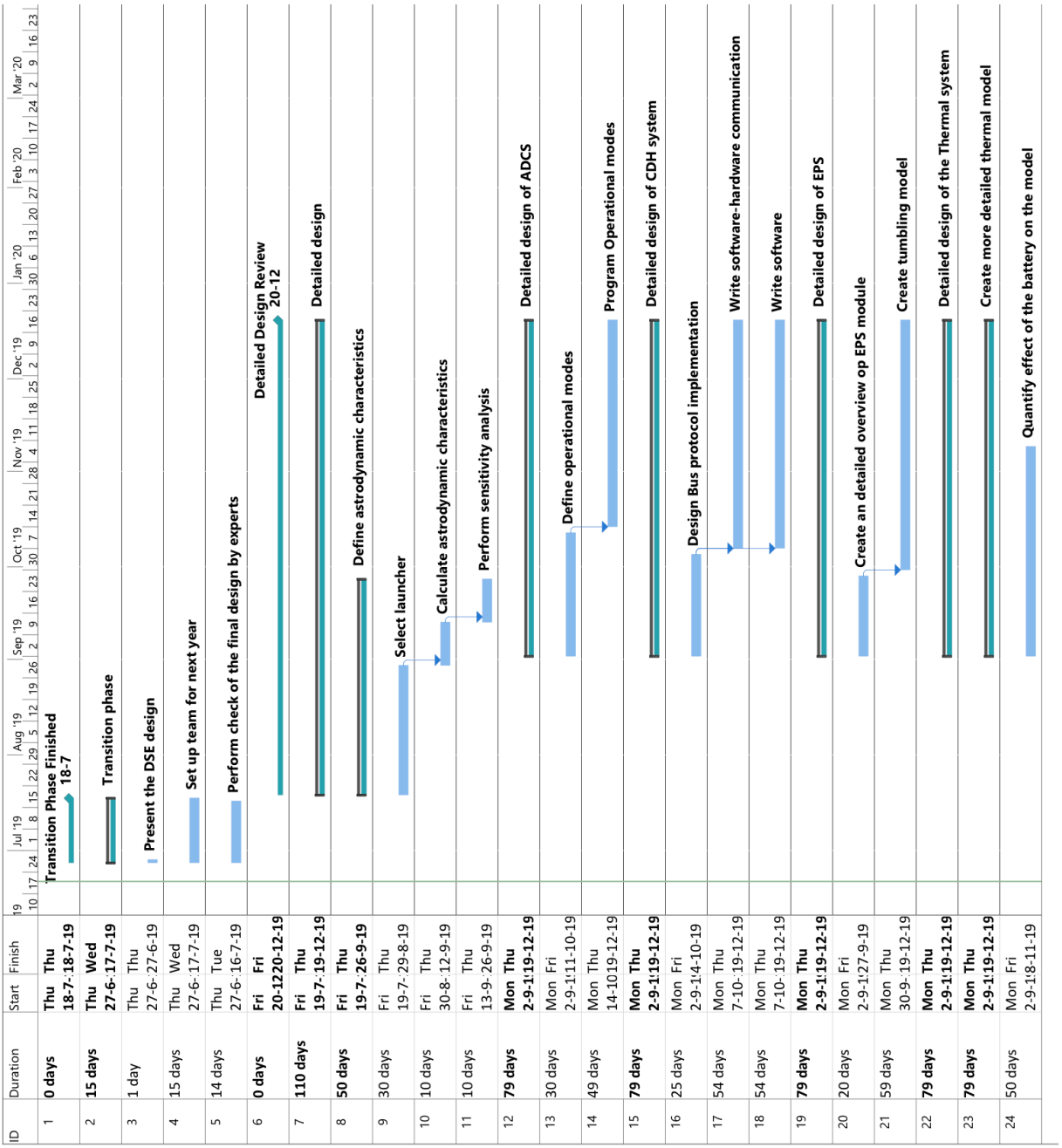


Figure C.1: Gantt Chart Number One

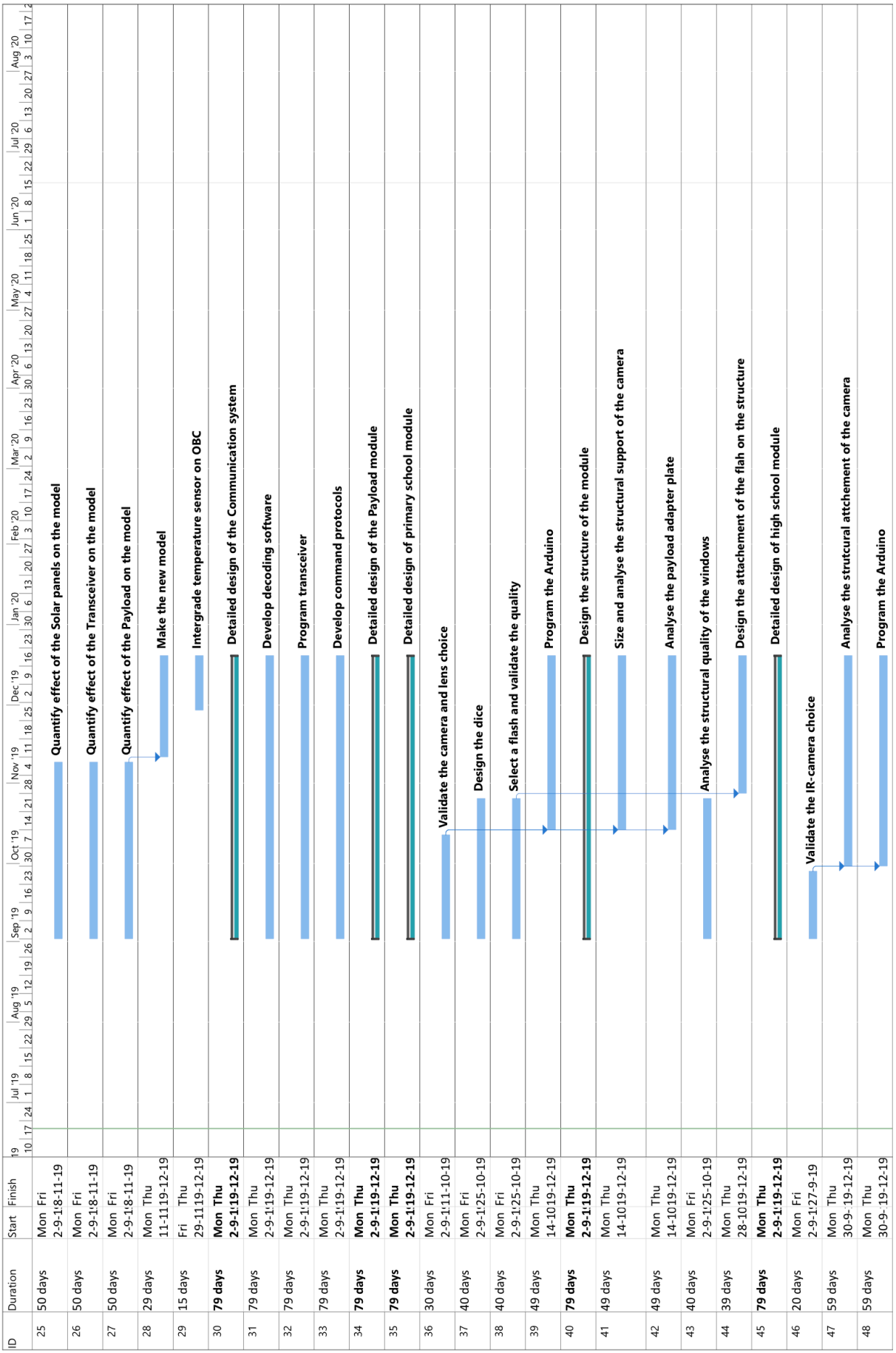


Figure C.2: Gantt Chart Number Two

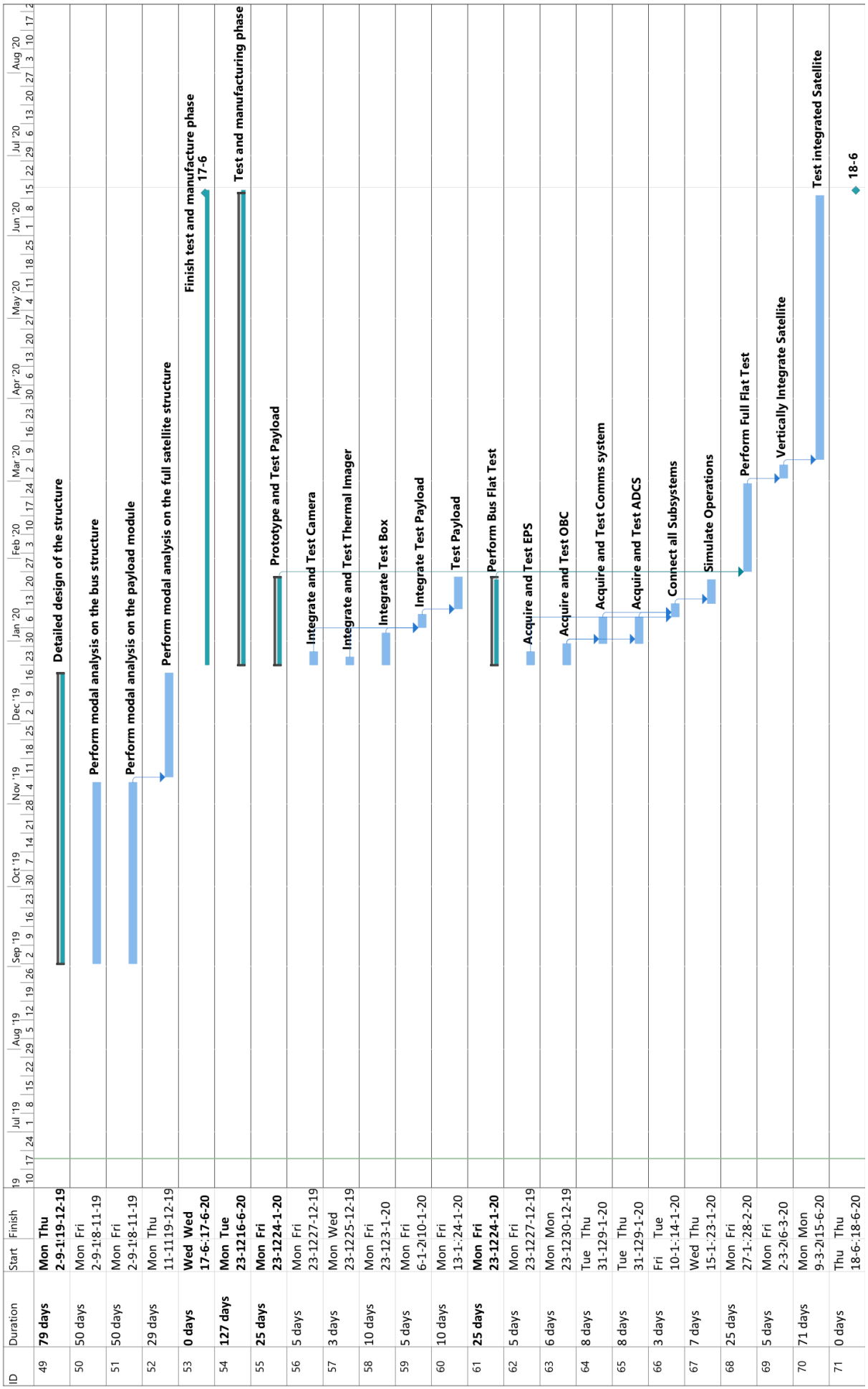


Figure C.3: Gantt Chart Number Three

D

# Appendix D: Individual Contributions

| Name | Work Division |
|---|---|
| Andrew | • 10 hours - Midterm Review Preparation<br>• 2 hours - Midterm Review Presentation<br>• 12 hours - Meetings + Meeting Preparation<br>• 6 hours - Latex and Documentation Management<br>• 50 hours - CDH Design Work/Research<br>• 6 hours - Requirements<br>• 6 hours - Compliance Matrix<br>• 12 hours - ROI<br>• 6 hours - Company Visits<br>• 6 hours - Report Proof Reading<br>• 1 hour - Personal Appendix<br>• 24 hours - Report Writing |
| Iliyan | • 6 hours - Report Feedback Implementation<br>• 2 hours - Acknowledgements<br>• 2 hours - Executive Overview<br>• 28 hours - Functional Flow Diagram<br>• 26 hours - Electric Power System<br>• 36 hours - Electric Power Model<br>• 10 hours - Electric Block Diagram<br>• 14 hours - Market Analysis<br>• 8 hours - System Integration<br>• 2 hours - Future Development Strategy<br>• 6 hours - Proofreading<br>• 8 hours - Meetings<br>• 4 hours - Company Visits |
| Johan | • 8 hours - Midterm Review Preparation<br>• 2 hours - Midterm Review Presentation<br>• 10 hours - Mission Patch Design<br>• 24 hours - Command and Data Handling design<br>• 8 hours - Midterm report feedback implementation<br>• 2 hours - 3D printing design<br>• 12 hours - Orbit simulations<br>• 4 hours - Astrodynamics stuff<br>• 40 hours - Reporting<br>• 12 hours - External Meetings<br>• 6 hours - Internal Meetings<br>• 8 hours - Sustainability Strategy<br>• 16 hours - Payload Conceptual Design<br>• 4 hours - Company Visits |

| | |
|---|---|
| Klaas | • 40 hours - Creating CATIA Model, Designing Parts, Creating Renders<br>• 24 hours - Structures Research<br>• 24 hours - Manufacturing, Assembly, Integration and Test Plans<br>• 24 hours - Writing<br>• 12 hours - Functional Flow Diagram and Defining Modes<br>• 8 hours - Meeting with 3D Printing Company, Preparing Parts for Printing<br>• 8 hours - Meetings<br>• 8 hours - Project Management Tasks |
| Mel | • 8 hours - Interface protocols - Research<br>• 16 hours - Risk management - Research<br>• 32 hours - Payload - Research and design<br>• 16 hours - Risk management - Analysis<br>• 24 hours - Risk management - Reporting<br>• 6 hours - Jury summary<br>• 16 hours - Payload design - Reporting<br>• 6 hours - Operations and logistics - Reporting<br>• 12 hours - Tutor/coach/vsv/experts Meetings<br>• 6 hours - Group meeting<br>• 2 hours - Company tour |
| Moritz | • 30 hours - Functional Flow ADCS modes<br>• 8 hours - Midterm Presentation and other Meetings<br>• 30 hours - Disturbance Modelling<br>• 16 hours - Actuator Modelling<br>• 40 hours - Modelling Research<br>• 30 hours - ADCS report writing<br>• 3 hours - Proofreading<br>• 2 hours - RAS characteristics |
| Simonas | • 55 hours - Communications protocols, data link research<br>• 50 hours - Report writing<br>• 20 hours - CubeSat communications operations research<br>• 15 hours - New antenna link budget calculations<br>• 10 hours - Design iteration, evaluation<br>• 8 hours - Midterm Presentation and other Meetings<br>• 2 hours - Documentation/Archive |
| Tim | • 10 hours - Midterm Presentation and other Meetings<br>• 35 hours - Preliminary design of the payload<br>• 35 hours - detailed design on the Primary School Module<br>• 16 hours - Design of the secondary payload<br>• 16 hours - Research future development plan<br>• 4 hours - Create Gantt chart<br>• 40 hours - Report writing (Payload section excl. the High School Module, Detailed design phase and PD&D Logic, executive overview of written parts)<br>• 12 hours - proofreading |

| | |
|---|---|
| Tuur | • 12 hours - Midterm peer review<br>• 50 hours - Making the functional flow diagram<br>• 16 hours - Updating the thermal model<br>• 8 hours - Research interface protocols<br>• 14 hours - EPS verification model<br>• 1 hours - Communication flow diagram<br>• 9 hours - Internal meetings<br>• 6 hours - External meetings<br>• 12 hours - Update resource budgets<br>• 2 hours - Cost breakdown<br>• 38 hours - Report writing |